厚生労働科学研究費補助金
難治性疾患克服研究事業

致死性骨異形成症の診断と予後に関する研究

平成２２年度　総括・分担研究報告書

研究代表者　澤井英明

平成２３（２０１１）年３月

厚生労働科学研究費補助金
難治性疾患克服研究事業

致死性骨異形成症の診断と予後に関する研究

平成２２年度　総括・分担研究報告書

研究代表者　澤井英明

平成２３（２０１１）年３月

厚生労働科学研究費補助金研究報告書目次

Ⅰ．総括研究報告

致死性骨異形成症の診断と予後に関する研究・・・・・・・・・・・・２
研究代表者　澤井英明（兵庫医科大学）

Ⅱ．分担研究報告

１．　全国調査による患者数等の疾患に関する基本的なデータの収集
・・・・・・・・・・・・・・・・・・・・・・・・・・・・・・１０
研究分担者　澤井英明、沼部博直、河井昌彦

２．　致死性骨異形成症の遺伝子診断に関する研究・・・・・・・２０
研究分担者　岡崎　伸

３．　致死性骨異形成症の遺伝子解析・・・・・・・・・・・・・・３０
研究分担者　長谷川奉延

４．　窒息性胸郭異形成症の遺伝子診断・・・・・・・・・・・・・３２
研究分担者　緒方　勤

５．　致死性骨異形成症の類似疾患の遺伝子診断に関する研究・・３７
研究分担者　池川志郎

６．　胎児超音波計測による長管骨長の基準値作成・・・・・・・４０
研究分担者　室月　淳、澤井英明、山田崇弘、堤誠司、佐藤秀平
篠塚憲男、高橋雄一郎、早川博生、夫　律子

７．　症例の収集と診断の支援システム構築・・・・・・・・・・・４３
研究分担者　室月　淳、澤井英明、山田崇弘、堤　誠司、
佐藤秀平、篠塚憲男、高橋雄一郎、早川博生、
夫　律子、岡本伸彦、鬼頭浩史、長谷川奉延、
河井昌彦、沼部博直、岡崎　伸、宮崎　治、緒方　勤、
池川志郎
研究協力者　西村　玄

８．　胎児ＣＴの実施のための撮影基準の作成・・・・・・・・・・４６
研究分担者　宮崎　治、澤井英明、室月　淳

Ⅲ．研究成果の刊行に関する一覧表
・・・・・・・・・・・・・・・・・・４９

Ⅳ．研究成果の刊行物・別冊
・・・・・・・・・・・・・・・・・・５５

Ⅰ．総括研究報告

厚生労働科学研究費補助金（難治性疾患克服研究事業）
総括研究報告書

致死性骨異形成症の診断と予後に関する研究

研究代表者　澤井英明　兵庫医科大学産科婦人科准教授

研究要旨

致死性骨異形成症 thanatophoric dysplasia は稀な先天性骨系統疾患で、2～5人／10万分娩程度とされる。しかし日本では正確な統計はなく、全国的な症例数の概略も不明である。またその名称の通り周産期致死性とされているが、学会等での報告によると長期の生存例が散見される。

そこで本研究事業の今年度の最重点項目として、全国の産科、小児科、整形外科のうち骨系統疾患の診断や母児の管理が可能と考えられる施設を対象に、全国調査（１次調査）として症例数とその予後についての概要の調査を実施した。産科108施設、小児科173施設、整形外科101施設から回答を得て、過去5年間に65症例が報告された。そしてそのうち周産期死亡を起こしたものは27例（54%）で、致死性という名称にもかかわらず、ほぼ半数は致死性ではなかった。出生直後からの適切な呼吸管理を実施すれば、半数近くが周産期死亡を起こさず、生存することが判明した。しかも1年以上の生存も15例と生産児（総数47例）の32%に達した。また致死性骨異形成症という名称については、産科と小児科では４割以上の医師が、不適切であると回答しており、今回の調査結果と合わせて、現状を反映しない疾患名の再検討の必要性を示唆した。

また今年度は次の研究を実施中である。１）胎児骨格異常の早期診断に必要な超音波検査の四肢長幹骨の正常値の日本人データは大腿骨と上腕骨しかないため、すべての四肢長幹骨について標準値作成プロジェクトを開始し、データ集積中である。２）胎児診断として３次元胎児ヘリカル CT は有用であるが、本法は胎児被爆、撮影条件、確定診断で重視すべき所見など、未解決の問題が山積している。放射線科医と技師で胎児 CT サブグループを結成し、撮影条件や症例数などの全国調査を実施中である。３）本疾患は FGFR3 遺伝子の突然変異による疾患で、遺伝子診断により確定診断できる。国内で遺伝子診断のできる体制の整備を行っている。４）胎児骨系統疾患に詳しい専門医のグループ「胎児骨系統疾患フォーラム」を基盤として、これまでの症例検討のまとめを作成すると同時に、胎児診断の基準を作成している。またウェブ上の症例診断支援システムを作成し効率的な疾患の診断を行い、臨床医を支援するシステムを構築中である。５）致死性骨異形成症についてのホームページを開設し、成果の社会還元を行っている。

研究分担者氏名　所属機関名及び所属機関における職名
室月　淳　宮城県立こども病院産科・部長
山田崇弘　北海道大学病院産科・助教
堤　誠司　山形大学医学部産科婦人科・助教
佐藤秀平　青森県立中央病院総合周産期母子医療センター産科・センター長
篠塚憲男　胎児医学研究所臨床研究・代表
夫　律子　クリフム夫律子マタニティクリニック・院長
高橋雄一郎　独立行政法人国立病院機構長良医療センター産科・医長
早川博生　春日井市民病院産婦人科・部長
長谷川奉延　慶応義塾大学医学部小児科学・准教授
河井昌彦　京都大学医学部附属病院小児科・准教授
沼部博直　京都大学大学院医学研究科社会健康医学系専攻医療倫理学・准教授
岡崎　伸　大阪市立総合医療センター小児神経内科・医長
岡本伸彦　大阪府立母子保健総合医療センター遺伝診療科・科長
鬼頭浩史　名古屋大学医学部附属病院整形外科・講師
宮崎　治　国立成育医療研究センター放射線診療部・医長
緒方　勤　国立成育医療研究センター研究所小児思春期発育研究部臨床・分子遺伝学・部長
池川志郎　理化学研究所ゲノム医科学研究センター・チームリーダー

A．研究目的

致死性骨異形成症 thanatophoric dysplasia: TD は線維芽細胞増殖因子受容体 3 (Fibroblast growth factor receptor 3: FGFR3)遺伝子変異によって生じる先天性骨系統疾患で、胎児は出生後早期に死亡するとされている。周産期致死性とされる骨系統疾患ではもっとも頻度が高いとされているが、日本では実際の患者数や出生頻度は不明である。また、その名称にもかかわらず実際には長期生存例の症例報告も散見される。

（１）全国調査による患者数等の疾患に関する基本的なデータの収集：

全国の医療機関の産科、小児科、整形外科のうち骨系統疾患の管理が可能と考えられる施設を対象に、全国調査（１次調査）として症例数とその予後についての概要の調査を実施し、患者数、周産期死亡率や出生後の児の生存の状況、そして長期生存の可能性を把握することを今年度の主たる目的とした。また実情と異なる可能性のあるその致死性骨異形成症という疾患名についての妥当性についての意見も聴取した。

致死性骨異形成症の分娩形式を決定するための正確な出生前診断の手法の確立と新生児管理に重要な予後の実際の情報が重要であることから、本年度には次のような研究も開始している。

（２）インターネット利用による胎児の骨系統疾患を診断支援するための症例検討システムの構築：

セキュリティの充実したウェブ閲覧型システムを構築して臨床医の診断の支援を行う。

（３）過去の症例検討のとりまとめ：

胎児骨系統疾患に詳しい各領域横断的専門医のグループ「胎児骨系統疾患フォーラム」でメールによる検討を行った骨系統疾患症例の整理と分析を行い、診断の指針の作成に役立つようにとりまとめる。

（４）妊娠期間中の胎児の診断指針の作成：

致死性骨異形成症の診断は出生後については、レントゲン所見と遺伝子診断による診断がほぼ確立している。したがって妊娠期間中に判明した骨格異常の胎児診断としてどのような所見に注目してどのような検査を行うべきかという指針の作成を行うために下記の事業を行う。

（ア）超音波検査：正常の胎児の四肢長幹骨の標準値作成プロジェクトを行って、日本人での標準値を得る。

（イ）胎児ＣＴ：全国調査を行って、胎児ＣＴの症例数の把握と、標準的な撮影方法と見方の指針の作成を行う。

（ウ）遺伝子診断：遺伝子診断により確定診断をできる体制づくりを支援する。

（５）地域診断支援システムの構築：日本全国を一定地域ごとに分担して胎児骨系統疾患の妊娠例に遭遇した産婦人科医から相談を受けられるような体制づくりを行い、臨床医療に成果を還元する。

（６）臨床医への情報提供：

所定の研究報告書を作成するのみならず、胎児骨系統疾患をまとめた書物を発刊して、臨床医に情報提供を行う。

（７）社会への還元：

公開シンポジウムの開催や致死性骨異形成症についてホームページによる情報発信を行って成果を社会に還元する。

Ｂ．研究方法

（１）全国調査による患者数等の疾患に関する基本的なデータの収集：

骨系統疾患の診断、児や母の管理が可能と考えられる施設として、総合周産期母子センターと地域周産期母子センター、大学病院の産科 381 施設、小児科 394 施設、整形外科 381 施設を対象にアンケート調査を行った。産科に対しては人工妊娠中絶を含めて、周産期の死産や生産の患児の状況を調査した。小児科に対しては出生児の予後の調査を重視して、出生直後の呼吸管理を中心とした介入的な処置により、その後の生命予後が改善されるかどうかも検討するために、より詳細な記録をとることとした。そして小児科については１年以上の長期生存例を経験している医師についてはインタビュー調査のための 2 次調査の依頼を行った。また整形外科については、本疾患が整形外科的管理を必要とするまで成長するかどうかを調査した。

（２）（３）（５）（６）（７）詳細はＣ．研究結果に記載した。

（４）妊娠期間中の胎児の診断指針の作成：

（ア）超音波検査：正常の胎児の四肢長幹骨の標準値作成プロジェクトとして研究分担者の産科医の所属する施設が中心となって、超音波検査の際に胎児の大腿骨、脛骨・腓骨、上腕骨、橈骨・尺骨の測定を行い、標準値を算出する。

（イ）胎児ＣＴ：全国調査として胎児ＣＴの撮影経験のある３施設の放射線科医・技師を中心に胎児ＣＴサブグループを結成し、撮影条件の調査用紙を作成し、全国の施設でこれまで胎児ＣＴの学会報告のある施設に対して、症例数の把握と撮影条件の調査を行う。

（ウ）遺伝子診断：関西と関東に各１施設の遺伝子診断が実施可能な施設を整備する。

（倫理面への配慮）

本研究においては、全体の研究計画について、研究代表者の所属する兵庫医科大学において倫理委員会の承認を得ている。また個別の研究分担者が行う研究については、診断指針の作成など全体の研究計画に承認されたことで十分と見なされる研究を除いて、各施設において倫理委員会の承認を得ている。

Ｃ．研究結果

全体像を図１に示す。

（１）全国調査による患者数等の疾患に関する基本的なデータの収集（図 2）：

全国調査を実施した施設のうち、産科　108 施設（回収率 28.3%）、小児科 173 施設　（回収率 43.9%）、整形外科 101 施設（回収率 26.5%）から回答を得た。過去 5 年間（2005.4～2010.9）の間に全症例数 72 例が報告され、内訳は産科 46 例、小児科 24 例、整形外科 2 例であった。うち重複（同じ症例が複数科から報告）が 7 例あることを確認

したため、実数としては65例であった。致死性骨異形成症は産科では骨系統疾患全体の中で最も頻度が高く、2番目の骨形成不全症の22例の2倍以上であった。また小児科においては2番目であったが、骨形成不全症2型の30例にほぼ並ぶ頻度であった。また小児科からは1年以上の生存例を経験している9施設からインンタビュー調査に同意するとの回答を得たため、次年度に2次調査として実施予定とした。

致死性骨異形成症の全症例65例（重複を除く独立した患者数）の亜分類は1型が38例、2型が8例、不明が19例（1型：2型≒5：1）で従来の報告と同じく1型が多い。性別については男児23例、女児35例、不明7例であった。遺伝子診断を実施されていたのは12例あり、9例でFGFR3遺伝子変異が検出されていた。また診断された時期については、55例は妊娠期間中に診断されていたが、10例は出生後の診断であった。

妊娠期間中のどの時期に診断されたかについては、妊娠初期（15例）、中期（23例）、後期（15例）に分散していた（不明2例）。妊娠の転帰（死産と生産）の週数も、妊娠29週以降で41週まで広い範囲に分布しており、特定の時期に集中していなかった。妊娠期間中に実施された検査とその所見としては、判明している46例の全例で超音波検査が実施されており、胎児CTも13例（28%）で実施されていた。検出された所見としては全例で四肢短縮が指摘されている。次いで胸郭低形成（90%）と大腿骨弯曲（65%）、巨大頭蓋（56%）、羊水過多（43%）が多く報告されている所見である。分娩形式は判明しているものについては、死産の3例は全例経腟分娩であったが、生産の28例では帝王切開が11例あり、約40%が帝王切開で出生していた。

全症例65例のうち、児が娩出後に実施された検査としては単純レントゲンが46例(71%)で実施されており、他には遺伝子検査(12%)があり、その他CTとMRIなどもあった。これらによる検査所見としては妊娠中の超音波検査と同様に四肢短縮（92%）、胸郭低形成（80%）とそれによる呼吸障害（65%）、大腿骨弯曲（69%）などがよく見られる所見であった。

妊娠の転帰で生産と報告された47例のうち、現在も生存しているのは16例（21%）であった。死亡の原因としては67%が呼吸不全で最も多かった。またこの生産47例のうち24例（51%）が周産期死亡に該当する出生後1週間以内に死亡しており、しかも死亡例はすべてが2日以内に死亡していた。そしてこの周産期死亡を超えて生存していた23例はすべてが最低60日以上(1年以上も15例で、うち10年以上も2例)も生存していた。しかもこの23例すべてが呼吸管理を実施されており、出生児は呼吸管理を実施すれば、61%が最低60日以上生存していることになる。反対に呼吸管理をしていないと全例が生後2日以内に死亡していた。

致死性骨異形成症という疾患名については産科医の43%、小児科医の45%が不適切と回答しており、重症骨異形成症などの名称が望ましいとしていた。

（２）インターネット利用による胎児の骨系統疾患を診断支援するための症例検討システムの構築：

システムは兵庫医科大学の協力により同大学にサーバーを設置して、運営することとし、システムの構築をすでに完了して、試行中である。今年度中にはウェブ上に匿名化して症例の経過と画像をアップして、専門家グループで討議して診断を支援するシステムが運用開始できる予定である。

（３）過去の症例検討のとりまとめ：

上記のウェブ上のシステム構築までの段階で全国の症例を検討した2,000通以上のメールの内容の解析と症例（108症例以上）の分析を行っている。

（４）妊娠期間中の胎児の診断指針の作成：

（ア）超音波検査については胎児の四肢長幹骨の標準値作成のためのデータ100症例以上の収集を目的として、宮城県立こども病院を中心に15施

設ほどで実施中（予定を含む）である。現時点では臨床研究としての倫理審査を申請中からすでに実施中の施設もあるが完了は来年度になる予定。

（イ）胎児ＣＴについては全国で胎児ＣＴを実施している施設17施設を対象に、詳細な胎児ＣＴの撮影条件とこれまでの撮影対象疾患を調査している（9施設からデータ回収済み）。現在データを解析中である。

（ウ）遺伝子診断は慶応大学と大阪市立総合医療センターにてFGFR3遺伝子診断が実施できるような体制を構築した。

（５）地域診断支援システムの構築：

研究班の研究分担者の属する施設を中心に、北海道、東北、東京、神奈川、東海、近畿、中国、四国においてほぼ中心的なセンター施設を選定した。九州地区を選定中であり、全国を網羅できる体制を今年度中に構築する予定である。

（６）臨床医への情報提供：

研究班でホームページ www.thanatophoric.com を作成し骨系統疾患の情報を提供し、診断や治療に取り組む産科医や小児科医などからの問い合わせを受け付ける体制を作った。すでに地域の病院（産科）から1件の問い合わせがあり、上記の地域診断支援システム(予定)に紹介して対応した。また12月12日(日)に本研究班会議と共催して、これらの医師を対象に第3回胎児骨系統疾患フォーラムを開催し、致死性骨異形成症を含めた胎児骨系統疾患の新生児管理について集中的な情報提供と討議を行った。

（７）社会への還元：

上記ホームページに患者家族向けの情報を提供している。また上記の第3回胎児骨系統疾患フォーラムにて一般参加者も対象とした公開講演会を開催した。

D．考察

（１）全国調査による患者数等の疾患に関する基本的なデータの収集：

過去5年間で65例の致死性骨異形成症の症例を確認した。これらは欧米で報告されている頻度1/20,000～50,000とすると、日本では年間50～20例程度となり、5年間で250～100例程度となる。研究班で把握した数値の5年間で65例は、調査の回答率と流産や死産では調査対象施設からはずれる可能性が高いことを考慮すると、日本でも同様の頻度であると推定できる。

また産科で診断される周産期死亡を起こしやすい重症の胎児骨系統疾患としては、骨形成不全症Ⅱ型の倍以上の頻度であり、一般的な認識以上に多いと考える。

診断基準の作成に重要な妊娠中の診断に寄与する所見としては、四肢短縮、大腿骨弯曲、胸郭低形成、羊水過多と巨大頭蓋が主たる所見である。大腿骨弯曲は四肢短縮の影響であり、胸郭低形成は胎児の嚥下障害を引き起こして、羊水過多になると考えられるので、事実上は四肢短縮、胸郭低形成と巨大頭蓋が妊娠中の胎児の致死性骨異形成症を診断する3つの主たる所見と言える。

致死性骨異形成症はその名の示すとおり、周産期致死と考えられており、本調査の結果では出生後に呼吸管理をしていない症例は全例が2日以内に死亡していた。しかし、出生直後に呼吸管理を行えば、ほぼ半数（23例／47例）が周産期死亡を起こさずに1週間以上生存し、しかもそれらの23例すべてが最低60日以上(1年以上も15例、うち10年以上も2例)も生存していた。これは非常に驚くべき数値であり、この疾患名が適切かどうかも問われる状況である。それはこの疾患名についての調査で、産科医や小児科医のほぼ半数が致死性骨異形成症という名称が適切ではないと回答していることや、本研究版のホームページに寄せられた患者家族からのメールでも、この疾患名について心を痛めているという意見があり、今後は疾患名の改訂の必要性も検討する必要があると考える。

（２）～（６）現在研究途上であり、それぞれ

の目的を達するために継続して行く予定である。

Ｅ．結論

日本で初めての致死性骨異形成症の全国調査を行い、過去５年間で65例のケースを確認した。その疾患名にもかかわらず、出生後の適切な呼吸管理を行うことで、長期生存が可能であることが判明し、出生直後の呼吸管理の実施の有無が生命予後に大きく影響することが判明した。

Ｆ．健康危険情報

特になし

Ｇ．研究発表

１．論文発表

室月淳：四肢骨格の超音波像－四肢長管骨が短いときに何を疑うか．臨床婦人科産科 2010. 64:612-617.

Nakashima Y, Haga N, Kitoh H, Kamizono J, Tozawa K, Katagiri T, Susami T, Fukushi J, Iwamoto Y. Deformity of the great toe in fibrodysplasia ossificnas progressiva. J Orthop Sci 2010. 15:804-809.

Dai J, Kim OH, Cho TJ, Schmidt-Rimpler M, Tonoki H, Takikawa K, Haga N, Miyoshi K, Kitoh H, Yoo WJ, Choi IH, Song HR, Jin DK, Kim HT, Kamasaki H, Bianchi P, Grigelioniene G, Nampoothiri S, Minagawa M, Miyagawa S, Fukao T, Marcelis C, Jansweijer MCE, Hennekam RCM, Bedeschi F, Mustonen A, Jiang Q, Ohashi H, Furuichi T, Unger S, Zabel B, Lausch E, Superti-Furga A, Nishimura N, Ikegawa S. Novel and recurrent TRPV4 mutations and their association with distinct phenotypes within the TRPV4 dysplasia family. J Med Genet 2010. 47:704-709.

Nishimura G, Dai J, Lausch E, Unger S, Megarbané A, Kitoh H, OH Kim, Cho TJ, Bedeschi F, Benedicenti F, Mendoza-Londono R, Silengo M, Schmidt-Rimpler M, Spranger J, Zabel B, Ikegawa S, Superti-Furga A. Spondylo-epiphyseal dysplasia, Maroteaux type (pseudo-Morquio syndrome type 2) and parastremmatic dysplasia are caused by TRPV4 mutations. Am J Med Genet. 2010. 152A:1443-1449.

Nishimura G, Dai J, Lausch E, Unger S, Megarban A, Kitoh H, Kim OH, Cho TJ, Bedeschi F, Benedicenti F, Mendoza-Londono R, Silengo M, Schmidt-Rimpler M, Spranger J, Zabel B, Ikegawa S, Superti-Furga A. Spondylo-epiphyseal dysplasia, Maroteaux type (pseudo-Morquio syndrome type 2), and parastremmatic dysplasia are caused by TRPV4 mutations. Am J Med Genet A. 2010. 152A:1443-1449.

Smits P, Bolton AD, Funari V, Hong M, Boyden ED, Lu L, Manning DK, Dwyer ND, Moran JL, Prysak M, Merriman B, Nelson SF, Bonaf L, Superti-Furga A, Ikegawa S, Krakow D, Cohn DH, Kirchhausen T, Warman ML, Beier DR. Lethal skeletal dysplasia in mice and humans lacking the golgin GMAP-210. N Engl J Med. 2010. 362:206-216,.

Dai J, Kim OH, Cho TJ, Schmidt-Rimpler M, Tonoki H, Takikawa K, Haga N, Miyoshi K, Kitoh H, Yoo WJ, Choi IH, Song HR, Jin DK, Kim HT, Kamasaki H, Bianchi P, Grigelioniene G, Nampoothiri S, Minagawa M, Miyagawa S, Fukao T, Marcelis C, Jansweijer MCE, Hennekam RCM, Bedeschi F, Mustonen A, Jiang Q, Ohashi H, Furuichi T, Unger S, Zabel B, Lausch E, Superti-Furga A, Nishimura G, Ikegawa S. Novel and recurrent

TRPV4 mutations and their association with distinct phenotypes within the TRPV4 dysplasia family. J Med Genet.2010. 47:704-709.

Yamada T, Nishimura G, Nishida K, Sawai H, Omatsu T, Kimura T, Nishihara H, Shono R, Shimada S, Morikawa M, Mizushima M, Yamada T, Cho K, Tanaka S, Shirato H, Minakami H. J Obstet Gynaecol Res. Prenatal diagnosis of short-rib polydactyly syndrome type 3 (Verma-Naumoff type) by three-dimensional helical computed tomography. 2010 .

Furuichi T, Dai J, Cho TJ, Sakazume S, Ikema M, Matsui Y, Baynam G, Nagai T, Miyake N, Matsumoto N, Ohashi H, Unger S, Superti-Furga A, Kim OH, Nishimura G, Ikegawa S. CANT1 mutation is also responsible for Desbuquois dysplasia, type 2 and Kim variant. J Med Genet. 2010.

Wada R, Sawai H, Nishimura G, Isono K, Minagawa K, Takenobu T, Harada K, Tanaka H, Ishikura R, Komori S. Prenatal diagnosis of Kniest dysplasia with three-dimensional helical computed tomography. J Matern Fetal Neonatal Med. 2011 Jan 20. [Epub ahead of print]

Watanabe A, Karasugi T, Sawai H, Naing BT, Ikegawa S, Orimo H, Shimada T. Prevalence of c.1559delT in ALPL, a common mutation resulting in the perinatal (lethal) form of hypophosphatasia in Japanese and effects of the mutation on heterozygous carriers. J Hum Genet. 2011 Feb;56(2):166-8. Epub 2010 Dec 23.

２．学会発表

１）河井昌彦　骨系統疾患の新生児管理について～致死性骨異形成症の新生児管理．第３回胎児骨系統疾患フォーラム　2010.12.12　大阪

２）須藤章　骨系統疾患の新生児管理について～在宅人工呼吸管理を行っている骨系統疾患２例（軟骨低発生症、屈曲肢異形成症）の経験　第３回胎児骨系統疾患フォーラム　2010.12.12　大阪

３）矢田有里、澤井英明、和田龍、田中宏幸、武信尚史、伊藤善啓、原田佳世子、池田ゆうき　出生前に胎児ヘリカルＣＴで診断し出生後に遺伝子変異を確認したⅡ型コラーゲン異常症　近畿産科婦人科学会　2010.11.7　京都

Ｇ．知的所有権の取得状況

1.特許取得

なし

2.実用新案登録

なし

3.その他

なし

Ⅱ．分担研究報告

厚生労働科学研究費補助金（難治性疾患克服研究事業）
分担研究報告書

全国調査による患者数等の疾患に関する基本的なデータの収集

研究分担者　澤井英明　兵庫医科大学（研究代表者）
　　　　　　沼部博直　京都大学
　　　　　　河井昌彦　京都大学
研究協力者　岡　要　京都大学

研究要旨

致死性骨異形成症は四肢短縮・著明な胸郭低形成による呼吸障害・大腿骨彎曲(Ⅰ型)・クローバー葉様頭蓋(Ⅱ型)を主徴とする先天性の骨系統疾患であり、米国の報告では出生１万あたりの有病率は 0.21～0.30 である。1967 年に“Thanatophoric (ギリシャ語で致死性を示す)”という表現を用いて初例が報告されて以来、患者は胸郭低形成による呼吸障害のため死産もしくは生後間もなく死亡するものと考えられてきた。これまで日本においては出生前から予後に及ぶ詳細な調査は行われておらず、本疾患についての情報は十分ではない。また近年では新生児呼吸管理の技術の進歩に伴い、長期生存の患者がしばしば報告され、「“致死性”骨異形成症」という疾患名称の妥当性について指摘されている。これらの背景から、全国質問紙調査により日本における致死性骨異形成症の概要と長期生存者の把握、また本疾患の医療に携わる臨床医が「致死性骨異形成症」という疾患名称についてどのように感じているか、臨床現場の意見を明らかにすることを本研究の目的とした。

全国の大学病院・総合周産期医療センター・地域周産期医療センター・こども病院の産科(381 施設)、小児科(394 施設)、整形外科(381 施設)の医師を対象に質問紙調査を実施した。患者調査は単純集計・クロス集計を、疾患名称に関する意見は帰納的分析を行った。

2005 年 4 月から 2010 年 9 月までに施設で診療した患者報告数は産科 53 例、小児科 30 例、整形外科 2 例であった。患者情報は 73 例が得られた。妊娠の転帰は母体保護法による人工妊娠中絶 15 例、死産 4 例、生産 51 例、不明 3 例であった。生産 51 例のうち 27 例は 2 日以内に死亡し、周産期死亡は 56%であった。呼吸管理実施例 24 例中 14 例は 1 年以上の生存であり、積極的呼吸管理には至らなかった 25 例は全例 2 日以内の死亡であった。疾患名称についての調査では産科・小児科では「妥当ではない」という回答の割合が 41%、45%と高く、整形外科では「わからない」という回答が 55%で半数を超えた。

本調査により致死性骨異形成症の出生前から予後に及ぶ情報が得られた。これらの情報は患者家族と医療者の話し合いの場において役立つことが期待される。疾患名称の妥当性の調査では、①医師の重篤性の捉え方による“致死性”の解釈の違い ②医師が感じる「伝

えにくさ」と「伝えやすさ」の両側面 ③患者家族に対する心理的な影響と配慮の必要性 ④周囲への影響 ⑤疾患名称変更に伴う問題 ⑥患者家族の視点の必要性 が明らかとなった。呼吸管理実施例では10年や23年という長期生存例もあり、今回の調査から得られた意見を踏まえ、“致死性”という用語を含まない疾患名称への変更も視野に入れた議論が今後、必要となるであろう。

A.研究目的

致死性骨異形成症Ｉ型/Ⅱ型（Thanatophoric dysplasiaⅠ/Ⅱ）は Fibroblast Growth Factor Receptor 3（*FGFR3*）遺伝子の点突然変異により発症し、四肢短縮・著明な胸郭低形成による呼吸障害・大腿骨彎曲(Ｉ型)・クローバー葉様頭蓋(Ⅱ型)を主徴とする先天性の骨系統疾患である1)。1967年Maroteauxらにより、生後数時間で死亡する四肢短縮症・小人症の一病型に対して、独立した疾患として“Thanatophoric (ギリシャ語で致死性を示す)”という表現を用いて最初に報告された2)。その報告以来、本疾患患者は胸郭低形成による呼吸障害のため死産もしくは生後間もなく死亡するものと考えられてきた3)4)5)。米国の調査では流産や死産を含む出生1万あたりの有病率は0.21～0.30と報告されている6)

日本におけるこれまでの調査では、出生1万に対する出生有病率は0.029と報告されている7)が、産科で流産や死産となった患者数は反映されていない。また出生前から予後に及ぶ詳細な調査は行われておらず、本疾患についての情報は十分ではない。

出生後の予後に関する詳細な情報がないにもかかわらず、現在も周産期致死と考えられているが、近年、新生児呼吸管理の技術の進歩に伴い、長期生存の患者がしばしば報告されている8)9)。それらの報告においては、“treatment decisions cannot be made based on etiologic diagnosis alone”，“What determines that a disorder lethal?” など、「“致死性”骨異形成症」という疾患名の妥当性も指摘されており、また長期生存が可能ならば“致死性”という言葉を疾患名称に入れることに対しては抵抗があるという専門家からの意見もある。疾患名称の変更については、これまでに「精神分裂病」について、医学的実体を十分に反映しておらず、スティグマを強化していたことなどを理由に変更の必要性が検討され「統合失調症」へと変更された経緯がある10)。

このような現状から日本における致死性骨異形成症の概要と長期生存者の把握は本医療にとって有用な情報となることが期待される。また致死性骨異形成症という疾患名称の妥当性についての調査は国内外で行われておらず、臨床医の意見を知ることは重要である。

なお本研究は平成22年度厚生労働科学研究費補助金による難治性疾患克服研究事業「致死性骨異形成症の診断と予後に関する研究」班の分担研究である致死性骨異形成症の現状ならびに疾患名称の検討に関する調査・研究の一部として資金を得て行った。

全国質問紙調査により致死性骨異形成症の概要（患者数・生存時間・臨床所見等）を明らかにすること、また本疾患の医療に携わる産科・小児科・整形外科の臨床医が「致死性骨異形成症」という疾患名称についてどのように感じているか診療現場の意見を明らかにすることを本研究の目的とした。本研究で収集される情報は、本疾患の周産期における遺伝カウンセリングを行う上でも有用な情報として活用することが期待できる。

B．研究方法

1. 対象施設

全国の大学病院 / 総合周産期医療センター / 地域周産期医療センター / こども病院■産科

(381 施設） ■小児科(394 施設） ■整形外科(381施設)を対象に実施した。

致死性骨異形成症は難治性疾患であり、患者は本疾患に対する専門性が高い病院で加療されていると考えられる。本疾患は早期では産科の胎児超音波検診の際に罹患を疑われる。地域の産科施設で胎児の四肢短縮が発見された場合には、確定診断や児・妊婦の周産期管理のため、そのほとんどが骨系統疾患の診療経験があり、新生児医療が可能である NICU が併設された病院へ紹介になると考え、上記の施設を選定した。診療科は産科、小児科、整形外科を調査対象に選定した。

2. データ収集項目

1）2005 年 4 月～2010 年 9 月まで(5 年 6 ヶ月間）に施設で診療した患者数

2）致死性骨異形成症の患者情報[基本属性、生存時間、臨床的事項（在胎期間、出生前後に実施した検査、臨床所見、合併症、呼吸管理法、経時的身体測定値など）]

3）“致死性骨異形成症”という疾患名称に対する産科・小児科・整形外科の臨床医の意見

3. 調査の概要

1）症例報告の文献8)9)11)や、「致死性骨形成症の診断と予後に関する研究」班に属する本疾患専門家の意見をもとに調査用紙を作成した。

2）調査用紙①～⑤[①調査依頼状 ②患者数調査票 ③患者情報（臨床的事項）調査票 ④インタビュー調査[長期生存者診療施設に対するインタビュー調査]依頼票 ⑤インタビュー調査同意書を2010 年 9 月 22 日に送付し、12 月初旬に再依頼状を送付のうえ、2010 年 12 月 31 日を締め切りとした。難治性疾患克服研究事業研究班として第二次調査(インタビュー調査)を今後実施予定のため④⑤の用紙を同封したが、本研究には含まない。

3）疾患名称についての調査は、「“致死性”骨異形成症という疾患名称についてどのように思われますか」という質問項目に対し、「妥当である」「妥当ではない」「わからない」「その他」の選択肢を設け、その理由を自由記載とした。全国調査は本疾患患者の受診が予想される施設を対象としているため、本疾患の医療に携わる医師からの意見が得られる機会と考え、上記の質問項目を調査票に併記し、全国調査に回答する医師から意見を得た

4. データ分析

1)患者情報の解析：単純集計、クロス集計、グラフ表示を用いて解析した。

2)自由記載の帰納的分析：

①記載内容の語彙を変えないよう、1 文に 1 つの意味が含まれるものを記録単位とした。

②記録単位を意味内容の類似性により分類、抽象化し、それらを示す適切な用語へと置き換え、サブカテゴリー、さらに上位のカテゴリーを構成した。

③質問に対する「その他」の意見は、個別性が高くカテゴリーとして集約されなかったため、回答者の記載の要約を結果とした。

①から③については妥当性を確保するため、内容分析の経験のある博士後期課程の学生 1 名と質的研究に造詣の深い教員 1 名の協力を得て、検討を重ねながら分析を行った。

5. 倫理的配慮

本研究は、京都大学大学院医学研究科・医学部及び医学部附属病院　医の倫理委員会の承認（承認番号 E963）を得て行った。

C．研究結果

1.回収率

2010年11月20日時点での回収率を以下に示す。3 科全体の回収率は 37.0%であった。

■産科　381 施設送付　127 施設回答
回収率 33.2%

■小児科　394 施設送付　186 施設回答
回収率 47.2%

■整形外科　381 施設送付　115 施設回答
回収率 30.2%

2. 患者数

2005年4月～2010年9月まで(5年6ヶ月間)の診療科別施設診療患者数を以下に示す。

■産科：53例　■小児科：30例　■整形外科：2例　(調査票分析による重複率：8.8%)

3. 患者情報[臨床的事項]調査の結果

患者情報[臨床的事項]調査では小児科25例、産科53例、整形外科2例の合計80例が得られた。生年、性別、アプガースコア、生存時間で重複例7例を抽出し、これらを除いた合計73例で解析を行った。その結果の一部をここに示す。

73例の性別は男性27例、女性38例、不明8例であった。致死性骨異形成症の病型[註1]はI型43例、II型8例、型不明22例であった。73例の妊娠の転帰は、母体保護法[註2]による人工妊娠中絶15例、死産4例、生産51例、不明3例であった。生産51例についての生存曲線を図1に示す。27例が2日以内の死亡であり、周産期死亡は56%であった。周産期以降（生後7日以降）の生存が24例あり、10年や23年という長期生存例の報告もあった。調査時点での死亡例(N=33)の死因は呼吸不全23例、心不全2例、イレウス・急性呼吸窮迫症候群1例、未回答7例であった。未回答7例においては6例に臨床所見として胸郭低形成、呼吸障害が認められ、7例とも2日以内の死亡であった。

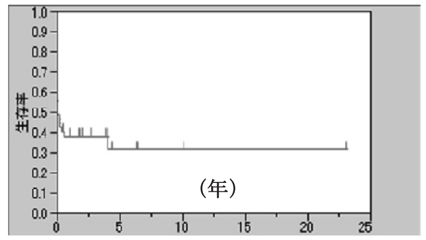

生存時間	リスク集合	死亡数	打ち切り
1(日)	51	24	0
2(日)	27	3	0
2(月)	24	3	0
4(月)	21	1	1
5(月)	19	0	1
6(月)	18	1	0
11(月)	17	0	1
1(年)	16	0	4
2(年)	12	0	4
3(年)	8	0	1
4(年)	7	1	2
6(年)	4	0	2
10(年)	2	0	1
23(年)	1	0	1

図 1：生産児(N=51)の生存曲線

本疾患患者は妊娠中に罹患を疑われることが多いが、22週未満診断例は19例あり、そのうち15例が母体保護法による人工妊娠中絶であった。22週以降の妊娠中の診断（疑い含む）は43例、出生後の診断は11例であった。遺伝学的検査は出生前に4例、出生後に7例実施されており、その結果は表1に示す通りである。生産児の分娩様式（産科のみ回答：N=31）では12例が帝王切開であり、適応理由は児頭骨盤不均衡(6例)や骨盤位(5例)の他、母の精神状態(罹患児の受け入れが出来ない)を理由とする例もあった。生産児51例（1例は所見不明のため50例で解析）の出生後の臨床所見を図2に示す。四肢短縮を全例に認め、胸郭低形成を90%、大腿骨彎曲を78%、前額部突出を70%に認めた。呼吸障害も高頻度(84%)に認めたが、生産児(N=51)のうち呼吸管理実施例24例中14例は1年以上の生存であり、その呼吸管理は気管切開7例、挿管6例、何らかの人工呼吸管理実施（詳細不明）1例であった。人工呼吸器についてはBiPAP(2相性陽圧呼吸)、DPAP（変換式陽圧呼吸)、

表1：遺伝学的検査の結果

遺伝子変異	N
c.742C>T p.Arg248Cys	3
c.1118A>G p.Tyr373Cys	3
c.1948A>G p.Lys650Glu	1
TDⅠ型*FGFR3*の点変異	1
変異見つからず	2
結果不明	1

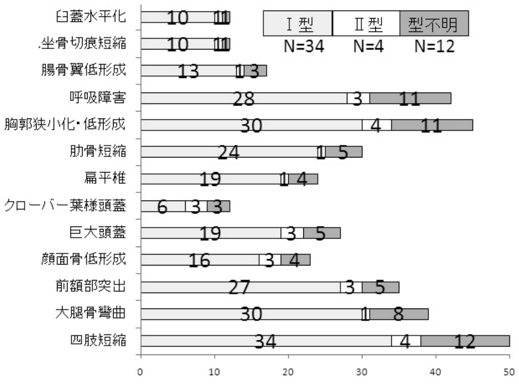

図2：出生後所見

[註1] 致死性骨異形成症はI型とII型に分類され、I型は大腿骨彎曲、著明な四肢長管骨の短縮、II型はクローバー葉様頭蓋、比較的まっすぐな大腿骨を特徴とする。

[註2] 不妊手術及び人工妊娠中絶に関する事項を定めること等により、母性の生命健康を保護することを目的とする法律。母体保護法の適応となる人工妊娠中絶は妊娠22週未満と制定されている。

SIMV（同調式間欠的強制換気）、HFO（高頻度振動換気）などであった。積極的な呼吸管理に至らなかった例[蘇生なし、もしくは口元酸素投与のみ]25例は全例2日以内に死亡していた。気管切開施行例は生後2か月～1年以内に切開術を施行されていた。家族の患児への愛着形成や受容が出来ずに、気管切開術施行に際して家族の同意を得るのに苦慮した例や、気管切開について家族の同意が得られないため挿管管理を続けている例も存在した。調査票回収の時点で生存の患者17例のうち、9例が入院管理、5例が在宅管理、3例が他施設転出であった。継続入院や施設転出のなかには、家族が患者の在宅受け入れが出来ていないためという理由も存在した。

4. 疾患名称について

疾患名称についてどのように感じているか、各科の回答の結果を図3に示す。回答数は産科110件、小児科164件、整形外科78件であった。産科、小児科では“致死性”骨異形成症という疾患名称について「妥当ではない」という回答の割合が41%、45%と高く、整形外科は「わからない」という回答が55%で半数を超えた。3科を比較すると、産科は他科に比べ「妥当である」の回答の割合が20%と多い結果であった。論文中の内容分析の結果の表記については、『カテゴリー』[サブカテゴリー]〈生データの要約〉を示している。それぞれの理由のカテゴリーを表2に示す。

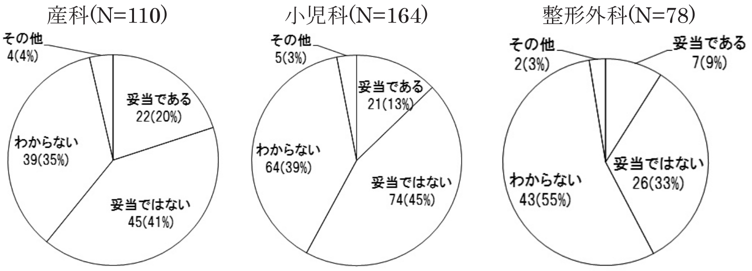

図3：疾患名称の妥当性について各科の回答

「妥当である」理由は、[概ね致死性である][自然経過（呼吸管理非実施）では致死性である]など『予後不良の病態と病名が一致』という理由が多く見られた。[実際に死亡例で家族に対し致死性であると説明ができた経験]など、患者家族にも『予後不良であることを疾患名から直感的に理解可能』と感じている医師もいた。

表2：各回答の理由【カテゴリー】

妥当である	
複数科	予後不良の病態と病名が一致
	予後不良（致死性）であることを疾患名から直感的に理解
	骨系統疾患国際分類の和訳である
産科	看取りという選択肢を提供しやすい
整形外科	一疾患一病名を原則とすべき
妥当ではない	
複数科	生存例の存在
	患者家族への心理的影響
	患者家族に対する配慮
	母親の児の受容に悪影響
	死、致死性という言葉自体が不適切
	個々の重篤の程度の違い
	家族への説明がしづらい
小児科	致死性という定義があいまいである
	実際の病態と名称のイメージとの乖離がある
	病態生理を示す病名が良い
	公費補助申請に不都合
	致死性とされると周囲の協力が得られにくい
	死亡が前提であり生前に診断できない印象がある
産科	出生前に致死性と診断できない
	この疾患に限り致死性とつけるのはどうか
	全ての骨系統疾患を致死性と呼ばない動向にある
	もともと人類を含むすべての生物はすべて致死性である
わからない	
複数科	経験がない
	疾患についての詳しい知識がない
	病態と相違ないが、表現としては考慮の余地がある
	他に適当な診断名が思いつかない
小児科	利点欠点がある
	自然歴を確認の上で名称の適切性を検討すべき
	長期生存でも合併症やADLが悪いのであれば名称は適切
産科	致死性であるかどうかは出生後に確認されるものである
	致死性という名称で説明した経験がない
整形外科	発症病理を示す病名が良い

「妥当ではない」理由の多くは[呼吸管理によって生命維持が可能である][現在の医療では致死とは限らない]など『生存例の存在』であった。[患者家族への衝撃が大きい][家族に希望を失わせる]〈22週以後に中絶が出来ない現状では母に対して絶望のみを与えてしまう〉という『患者家族への心理的影響』や、[家族向けへの病名としては適当でない]という『患者家族への配慮』も理由として多く見られた。また、〈一般の親に受け容れ難い病名で伝えにくい〉〈胎児超音波検査の説明の際に鑑別が必要な予後不良でない疾患の説明も同時に行わなければならない〉など、『家族への説明がしづらい』と感じている医師もいた。産科では胎内診断には限界があり、『出生前に致死性と診断できない』という出生前診断特有の問題が回答意見として見られた。小児科では〈致死性というと障

害者手帳などの公費申請の際に切られてしまう〉〈致死とされると周囲の協力が得られにくい〉など、生存患児を診る小児科医師が感じている、疾患名称が及ぼす患児のケア上の問題も明らかになった。

「わからない」の多くは経験や知識がないという理由であった。診療経験や知識がないため「わからない」を選択したが、〈致死性というと周囲の病気に対する理解を妨げる可能性がある〉など、妥当でない側面を認識している医師もいた。産科では[中絶されることが多く生児を知らない][経験は死産例のみである]ために『疾患についての詳しい知識がない』という意見や『致死性かどうかは出生後に確認されるものである』など、周産期を担当する診療科に特徴的な意見がみられた。また〈病態としては致死性であるが家族にとってはインパクトが強い〉という意見や、小児科に特徴的なものでは〈いかに重篤かを家族に理解頂けることは利点であるが、欠点として十分な医療がなされないまま亡くなってしまうケースがありそう〉〈致死性と言ったほうが親の覚悟はできる気がするが、逆に在宅ケア時にデイケアサービスなどの受け入れが悪くなる気がする〉など、疾患名の妥当である側面と妥当ではない側面の両方の意見を併記した回答も見られた。

「その他」の意見の要約は表 3 に示す通りである。

表 3 :「その他」の理由の記載内容

その他	
小児科	歴史の長い呼称なので十分な周知がなければ診療や統計などに混乱をきたす可能性がある。
	経験がなく専門家に検討してもらいたい。
	病態との相違はない。言葉の使い方に過敏ではないか。
	患者家族が負担感を感じているならば変更すべきであるが長期生存例が一部ならば妥当である。
産科	医学の進歩により今後検討されるべきである。
	ほとんどは早期死亡であり、致死性でもいいのかもしれない。世界的合意が必要な可能性があり、英語名から改称していく必要がある。
整形外科	新生児等を扱う小児科医師が担当すべき疾患である。

D．考察

1. 本調査の結果の活用が期待される場 ～家族との話し合いの情報源として～

本調査により、致死性骨異形成症の出生前の所見から予後に及ぶ情報を得ることができ、結果ではその一部を現状報告として示した。調査では家族が児の受容が出来ない例が報告され、患者の医療ケアに影響していた。このようなことから、本研究で収集された情報の活用が期待される場として以下の点について考察した。

重篤な障害をもった新生児の医療においては、児の治療方針の決定にあたり家族との話し合いが重要とされる。児にとって最善の利益となる決断が導き出されるためには、医療者と親の協働が不可欠であるからである。そして、その話し合いにおいては、「患者のためになるかを第一義とする」、治療方針の判断のために「正確な医学的情報がすべてに優先する」、「家族への医学的情報の最大限の提供と意見聴取」と心理的サポートが重要とされる[12)]。本疾患も患者の 85%は妊娠中に罹患を疑われており、出生前より児の治療方針について医療者と家族との話し合いの機会が設けられている。しかしこれまでは本疾患についての出生前から予後にわたる医学的情報が十分であったとは言えず、疾患名称についての調査においても、致死性骨異形成症という診断名だけで治療方針が決定され、児に十分な医療が提供されていない可能性が指摘された。

今後は本研究で収集された医療情報が、このような家族との話し合いの場において、具体性をもった話し合いの材料となり、家族が十分に納得のいく意思決定を援助することができると期待される。調査では家族のなかには、児の受容が出来ない例や、そのために気管切開の施行や在宅ケアに移行ができないという例も明らかになった。生存には呼吸管理が必要であるという結果からは、児の状態が落ち着いたあとには在宅ケアに向けた準備が必要であることを伝え、将来を見据えた話しあいを行うことも重要と考える。

2. 致死性骨異形成症という疾患名称に対する臨床医の意見

■医師の重篤性の捉え方による“致死性”の解釈の違い

疾患自体が致死性か非致死性かという点については、回答者により ①本疾患は致死性疾患である ②生存の可能性はあるが、生存のためには呼吸管理が必要とする病態は致死性である ③呼吸管理で生存可能ならば致死性ではない ④個々の重篤の程度には違いがあり一概に判断できない という4つの解釈が行われていた。②は生命予後も含めた解釈をしており、「その他」として記載されている意見と共に、名称の妥当性の検討には生存の可能性だけでなく長期予後やQOLを把握した上での解釈の必要性も示唆された。整形外科では診療の機会が乏しく、産科は診療経験が中絶例や死産例に限定されるという特徴的意見や、小児科が主体となり診療を行っている現状からは、生存患者を診療する機会や情報に触れる機会が、これらの解釈に影響する可能性があると考える。

■医師が感じる「伝えにくさ」と「伝えやすさ」の両側面

致死性という言葉は家族にとって受け入れ難く、医師自身が疾患名称を伝えにくいという困惑を感じていた。また本疾患に関わらず出生前診断には限界があり、産科医は不確実な診断による結果をどのように親に告知すべきか苦悩している[13)]。加えて本疾患では診断結果の説明の際に、鑑別すべき疾患として四肢短縮を示す他の予後不良ではない疾患（軟骨無形成症など）と致死性と言われる本疾患の説明を同時に行わなければならないというジレンマを感じている。一方で、予後不良と理解してもらいやすいことを理由に「妥当である」という回答も存在した。周産期医療において、医師は児が予後不良疾患であるという家族にとってのbad newsを伝えることに対して苦慮し、児の治療の差し控えを決定する場合には、倫理的ジレンマや葛藤を感じている[12)]。産科では致死性という言葉と看取りという選択肢を提供しやすいという意見が見られ、「致死性とされる疾患だから」と説明することで家族の納得が得られることに伝えやすさを感じていると考えられる。

■患者家族への心理的な影響と配慮の必要性

調査の結果では呼吸障害に対する呼吸管理実施により生存期間延長の可能性が示唆された一方、積極的な呼吸管理に至らなかった例では全例2日以内に死亡しており、重篤な疾患といえる。しかし、重篤さを表す言葉として致死性という言葉を使用することに対しては、多くの医師が妥当ではないと感じていた。致死性という言葉は、患者家族にとって、言葉から受ける印象が悪く、“ネガティブ”、“マイナス”、“ショッキング”などの心理的影響を与える可能性が考えられ、家族に対して十分な配慮を行う必要性がある。特に生存患者に対し致死性という言葉を使うことに対しては、医師自身も困惑を感じていた。

■周囲への影響

小児科からは、“致死性”という疾患名により在宅ケアに際して介護サービスの受託を拒否される可能性、周囲の協力が得られない可能性、祖父母の理解に悪影響を及ぼす可能性などが「妥当でない」とする回答理由として挙げられた。致死性という言葉がネガティブなイメージとして捉えられ、当事者に留まらず周囲にまで影響をもたらす可能性が示されている。生存者に対しても致死性という疾患名称が「死」を連想させ、容体の急変がおこる可能性を過度に危惧させるおそれもあると考える。本疾患は呼吸管理の必要性から出生後長期にわたる医療ケアや、将来的には在宅ケアを見据えた準備が必要になる。在宅ケアに移行した場合、患者家族にとってはサービスの利用や周囲の理解・協力が非常に重要であり、これらの意見は名称の妥当性を考える上でたいへん重要な視点と考える。

■患者家族の視点の必要性

本調査は医師を対象として行い、医師の視点か

らの意見を得たものである。名称変更を考慮するにあたり、実際に当事者である患者家族が疾患名称についてどう感じているかという患者家族の視点はたいへん重要である。患者家族が公開しているホームページ上では“「致死性」という病名が変わらない限り、本当の意味で私の気が休まることはないんだろうな…と思います”[註3]、米国の患者においても thanatophoric という言葉の意味が致死性であることを知り、“I think they should change the name to life bringing”[註4]など疾患名称に対する思いが見られる。患者家族からの意見聴取も、その調査自体が心理的負担になる可能性があるため倫理的配慮を含めた十分な検討が必要と考える。

■名称変更に伴う問題

疾患名称は国際名称や国際分類の和訳で制定されているため、名称変更により統計や診療に混乱をきたす可能性が考えられ、代替となる名称については熟慮する必要がある。また今後は関連学会が主体となり、名称変更に向けて議論をしていく必要もあると考える。

3. 研究の限界と今後の課題

本研究は調査法に以下の問題点や限界があり、患者数の推定はできない。①質問紙調査の際に患者がいない場合も“0”と記入し返送する旨を記載しなかった。②回収率が低い。通常第一次調査では患者数の調査に限定し回収率の向上を図る 14)が、本研究では患者数調査に加え患者情報(臨床的事項)調査と第二次調査(インタビュー調査)の依頼状を同時に送付したため、回答が煩雑な印象を与え、回収率の低下に影響したと考える。これらには事前に回避できた事項もあり、計画段階に深く考慮すべき点であった。骨系統疾患の鑑別診断には熟練を要するため、診断の正確性の担保については研究の限界である。研究班では診断基準の確立を目指すとともに、確定診断のための遺伝学的検査体制を整備している。

また今後の課題として、長期生存患者の人工呼吸管理状態の詳細や問題点、自然歴、QOL、精神発達面についての調査や、さらには長期にわたって患者のケアを行う家族に対する適切な支援を行うことを目的とした、患者家族が感じているケア上の不安や悩み、医療サービスの要望などについての調査も必要であると考える。これらについては、第二次調査(インタビュー調査)として実施することを検討している。

Ｅ．結論

全国質問紙調査により致死性骨異形成症の現状調査を行うとともに、臨床医が「致死性骨異形成症」という疾患名称についてどのように感じているかを調査・解析した。致死性骨異形成症という名称とは実情は異なり、出生直後に適切な呼吸管理が行えれば長期生存が可能であることが示された。しかし同時に出生直後に呼吸管理がなされていないと周産期死亡を起こす可能性が高いことも示された。これらの状況を総合的に判断し、疾患名が適切であるかどうかも含めて今後の研究を進めていくべきである。

参考文献

1)　西村玄: 骨系統疾患 X 線アトラス：遺伝性疾患の鑑別診断. 医学書院, 1993.

2)　成富研二: 先天性奇形症候群および遺伝性疾患データブック. 診断と治療社, 469-472, 2001.

3)　田中弘之: Achondroplasia group. 小児内科, Vol.36 増刊号, 76-78, 2004.

4)　澤井英明: Thanatophoric Dysplasia, type Ⅰ, typeⅡ. 小児内科, Vol.36 増刊号 300-303, 2004.

5)　澤井英明: 妊娠中にみつかる先天性四肢短縮症への対応と遺伝カウンセリング. 日本遺伝カウ

[註3] http://blog.goo.ne.jp/wsmayu0501/e/9c25486199c5aa7cb9187009da28e786

[註4] http://www.youtube.com/watch?v=R_Q92MC8plU

ンセリング学会誌，25，61-66，2004.

6） Waller DK, Correa A, Vo TM, Wang Y, Hobbs C, Langlois PH, Pearson K, Romitti PA, Shaw GM, Hecht JT：The population-based prevalence of achondroplasia and thanatophoric dysplasia in selected regions of the US. Am J Med Genet A. 2008；15；146A(18)：2385-9.

7） 城良二，君塚葵，柳迫康夫：骨系統疾患の出生有病率に関する全国調査．厚生科学研究費補助金（子ども家庭総合研究事業）研究報告書，4-8，1999.

8） Baker KM, Olson DS, Harding CO, Pauli RM：Long-Term Survival in Typical Thanatophoric Dysplasia Type 1. Am J Med Genet. 1997；70：427-436.

9） MacDonald IM, Hunter AG, MacLeod PM, MacMurray SB：Growth and development in thanatophoric dysplasia. Am J Med Genet. 1989；33：508-12.

10） 金吉晴：病名変更の意義と影響 Schizophrenia Frontier, Vol6, No.1, 38-41, 2005

11） Wilcox WR, Tavormina PL, Krakow D, Kitoh H, Lachman RS, Wasmuth JJ, Thompson LM, Rimoin DL：Molecular, radiologic, and histopathologic correlations in thanatophoric dysplasia. Am J Med Genet. 1998；78：274-81.

12） 田村正徳，玉井真理子：新生児医療現場の生命倫理．メディカ出版，2005.

13） 櫻井浩子，堀田義太郎：生存学研究センター報告10 出生をめぐる倫理-「生存」への選択．立命館大学生存学研究センター，2009.

14） 川村孝編：難病患者数と臨床疫学象把握のための全国疫学調査マニュアル第２版．厚生労働省難治性疾患克服研究事業 特定疾患の疫学に関する研究班，2006.

Ｇ．研究発表

１．論文発表

Yamada T, Nishimura G, Nishida K, Sawai H, Omatsu T, Kimura T, Nishihara H, Shono R, Shimada S, Morikawa M, Mizushima M, Yamada T, Cho K, Tanaka S, Shirato H, Minakami H. J Obstet Gynaecol Res. Prenatal diagnosis of short-rib polydactyly syndrome type 3 (Verma-Naumoff type) by three-dimensional helical computed tomography. 2010 .

Wada R, Sawai H, Nishimura G, Isono K, Minagawa K, Takenobu T, Harada K, Tanaka H, Ishikura R, Komori S. Prenatal diagnosis of Kniest dysplasia with three-dimensional helical computed tomography. J Matern Fetal Neonatal Med. 2011 Jan 20. [Epub ahead of print]

Watanabe A, Karasugi T, Sawai H, Naing BT, Ikegawa S, Orimo H, Shimada T. Prevalence of c.1559delT in ALPL, a common mutation resulting in the perinatal (lethal) form of hypophosphatasia in Japanese and effects of the mutation on heterozygous carriers. J Hum Genet. 2011 Feb;56(2):166-8. Epub 2010 Dec 23.

２．学会発表

１）河井昌彦　骨系統疾患の新生児管理について～致死性骨異形成症の新生児管理．第３回胎児骨系統疾患フォーラム　2010.12.12　大阪

２）矢田有里、澤井英明、和田龍、田中宏幸、武信尚史、伊藤善啓、原田佳世子、池田ゆうき　出生前に胎児ヘリカルＣＴで診断し出生後に遺伝子変異を確認したⅡ型コラーゲン異常症　近畿産科婦人科学会　2010.11.7　京都

Ｇ．知的所有権の取得状況

1. 特許取得

なし

2. 実用新案登録

なし

3. その他

なし

厚生労働科学研究費補助金（難治性疾患克服研究事業）
分担研究報告書

致死性骨異形成症の遺伝子診断に関する研究

研究分担者　岡崎　伸　大阪市立総合医療センター
研究協力者　玉川信吉　大阪市立総合医療センター

研究要旨
致死性骨異形成症の原因遺伝子であるFGFR3の遺伝子診断が、実施可能な施設は少ない。今回我々は、早期診断を可能とする為、自施設においてダイレクトシークエンス法による検査の構築を行った、FGFR3 の解析は既報の変異領域だけでなく、全エクソンについて解析が可能となるように準備した。

A．研究目的

致死性骨異形成症、唯一の原因遺伝子と考えられる FGFR3 の遺伝子診断が行える施設は少なく、現状では早期の遺伝子診断は困難である。我々は、迅速な遺伝子診断を実現するため、自施設内で実施可能なダイレクトシークエンス法による FGFR3 の全エクソン解析を構築し、また、院内倫理委員会において、遺伝子解析実施の審議を受け、遺伝子診断の体制を整えることを目的とした。

B．研究方法

NCBI ホームページから得た、FGFR3 の DNA 塩基配列 Reference　Sequence : NG__12632.1 から、FGFR3 のペプチドをコードするエクソンに対して 1～3 候補の Primer を設計し、コントロールＤＮＡを用いて、PCR 反応条件の検討をするとともに、シークエンシングが良好に実施できる Primer セットを選別した。

また、FGFR3 遺伝子解析の有用性を自施設である大阪市総合医療センターの倫理委員会にて説明し、遺伝子診断実施への審議を仰いだ。

（倫理面への配慮）

FGFR3 解析手順書を作成し、インフォームドコンセント確認方法、また、検体および報告書の匿名化を明記した。

C．研究結果

FGFR3 全エクソンを 10 領域に分け、PCR およびシークエンスを実施、10 領域すべてが、良好な検査精度と考えられる解析が確認できた。また、検討した条件から解析手順書を作成した。

平成 22 年 10 月の院内倫理委員会にて FGFR3 の遺伝子解析実施の許可を得た。

D．考察

遺伝子解析にあたっては、患者情報の保護、結果の管理、検体の管理など多くの注意事項がある。実際の運用にあたっては、想定外の事故等も考慮していく必要があると思われる。

Ｅ．結論

解析手順書の完成、院内倫理委員会の承認を得たことから、遺伝子診断開始の準備は、整ったと考えている。

Ｆ．健康危険情報

特記すべきことなし。

Ｇ．研究発表

１．論文発表	なし。
２．学会発表	なし。

Ｈ．知的財産権の出願・登録状況

１．特許取得	予定なし。
２．実用新案登録	予定なし。
３．その他	特記すべきことなし。

FGFR3　シークエンス解析手順書

平成 23 年 2 月 21 日　作成
小児神経内科　　　岡崎　伸
中央臨床検査部　　玉川　信吉

【はじめに、コンプライアンス】

遺伝子検査（生殖細胞系列）を実施する者は、以下の宣言、指針、ガイドラインを精読し、遵守したうえで検査にあたること。

・「ヒトゲノムと人権に関する世界宣言」（ユネスコ）

・「ヒト遺伝情報に関する国際宣言」（ユネスコ）

・「ヒトゲノム・遺伝子解析研究に関する倫理指針」（厚生労働省、文部科学省、経済産業省）

・「臨床研究に関する倫理指針」（厚生労働省）

・「遺伝学的検査に関するガイドライン」（各種関連学会）

・「遺伝カウンセリング・出生前診断に関するガイドライン」（日本人類遺伝学会）

・「遺伝性疾患の遺伝子診断に関するガイドライン」（日本人類遺伝学会）

【検査の注意事項】

1.分析にあたってはインフォームドコンセントの完了を文書にて確認すると。
また、インフォームドコンセント文書は決められた保管庫で管理すること。

2.検体は匿名記号（番号）により分析、保管すること。

3.報告は匿名記号（番号）によって行うこと。

【試薬】

主要な試薬を以下に示す。

名称	メーカー	Cat.No.
QIAamp DNA mini kit	QIAGEN	51304
Ampitaq Gold 360 Master Mix	Applied Biosystems （by life technologies）	439881
Distilled Water, Deionized, Sterile （以下 DDW と略）	ニッポンジーン	316-90101
QIAquick PCR Purification kit	QIAGEN	28104
Agencourt AMPure XP	BECKMAN COULTER	A63881
BigDye Terminator v3.1 Cycle sequencing kit	Applied Biosystems （by life technologies）	4337455
BigDye XTerminator 精製キット	Applied Biosystems （by life technologies）	4376486
3130 POP-7 ポリマー	Applied Biosystems （by life technologies）	4352759
10×Genatic Analysis Buffer with EDTA	Applied Biosystems （by life technologies）	402824

【機器】

主要な機器を以下に示す。

一般名称	機器名称・モデル	メーカー
サーマルサイクラー	Veriti 96-well サーマルサイクラー,0.2ml （以下 Veriti200 と略）	Applied Biosystems （by life technologies）
ボルテックスミキサー	Vortex GENIE 2	MS機器
キャピラリー電気泳動	3130 ジェネティックアナライザ	Applied Biosystems （by life technologies）

【分析手順】

　以下に操作の流れ（概略）を示す。
また、各操作の詳細は次項から記載する。

ー　操作の流れ　ー

1．DNA抽出

2．PCR（核酸増幅）

3．泳動と精製

4．DNA定量

5．サイクルシークエンシング

6．精製

7．ジェネティックアナライザーによる分析

8．データ解析

9．報告書作成

1. DNA抽出

EDTA 採血管により採血した全血を、QIAamp DNA mini kit によりDNA抽出を行う。詳細は試薬添付マニュアルにしたがい、Elution は 100μl の Buffer AE にて実施。

2. PCR

試薬は Ampitaq Gold 360 Master Mix を用い、各エクソンの Primer は SIGMA GENOSYS などのメーカーにて作成してもらう、Primer 一覧は次項に示す。試薬、サンプルの調整は以下のとおりとする。PCR は Veriti200 にて以下のとおりサイクル反応をおこなう

（反応液の調整）

	Exon2	その他の exon
Ampitaq Gold 360 Master Mix	12.5 μl	12.5 μl
360 GC enhancer	2.5 μl	—
50pmol/μl Forward primer	0.25 μl	0.25 μl
50pmol/μl Reverse primer	0.25 μl	0.25 μl
Template DNA (final concentration 50ng)	Variable (0.5～2 μl)	Variable (0.5～2μl)
DDW	Variable (to 25 μl)	Variable (to 25μl)
Total volume	25 μl	25 μl

（PCRの反応条件 全 exon 共通）

Step	Pre heat	PCR（35cycle）			1st hold	2nd hold
		Denature	Anneal	Extend		
Temp（℃）	95	95	60	72	72	4
Time	10min	15sec	30sec	1min	7min	∞

（各 exon の PCR 及びシークエンス primer）

対象 Exon	Primer 名称	配列	PCR Product 長
Exon2	FGFR3 2Fwd	TCTAACGAGCTGCCTTCCT	577bp
	FGFR3 2Rvs	CGAATAACAACAGCGGGAATC	
Exon3，4	FGFR3 3-4Fwd	ACTGCTGTGTCTGTAAACGG	806bp
	FGFR3 3-4Rvs	GGCATCTAGAGCCATGTCAG	
Exon5～7	FGFR3 5-7Fwd	TACACAGGACGGGAAACTGA	875bp
	FGFR3 5-7Rvs	CCCTAGACCCAAATCCTCAC	
Exon9	FGFR3 9Fwd	GTAACGACTCTGTCCCATGC	872bp
	FGFR3 9Rvs	CCGTAAGTCACAGGATTCCC	
Exon10	FGFR3 10Fwd	CTCTAGACTCACTGGCGTTA	572bp
	FGFR3 10Rvs	GTTCTGACTTCCACCAGCAT	
Exon11	FGFR3 11Fwd	ATGCTGGTGGAAGTCAGAAC	498bp
	FGFR3 11Rvs	CGTAAGGACGAAGAGTGTCA	
Exon12～14	FGFR3 12-14Fwd	CTCTTCGTCCTTACGAGCAG	914bp
	FGFR3 12-14Rvs	TCTTCATCACGTTGTCCTCG	
Exon15	FGFR3 15Fwd	CTGGACTACTCCTTCGACAC	509bp
	FGFR3 15Rvs	GACACGTACACGTCACTCTG	
Exon16，17	FGFR3 16-17Fwd	GACAACGTGATGAAGATCGCAG	834bp
	FGFR3 16-17Rvs	GTGGACGTCACGGTAAGGA	
Exon18，19	FGFR3 18-19Fwd	CAGGCTGTTCCCGAATAAGG	587bp
	FGFR3 18-19Rvs	ATCTGCACTGAGTCTCATGC	

3. 泳動と精製

PCR が正常に完了していたかを、3μl を用いて、2%アガロースゲル電気泳動でチェックする。チェック後、PCR 後反応液を精製する。反応数が少ない(8 個以内なら)場合は、QIAquick PCR Purification kit（QIAGEN）を使用。反応数が多い場合は、Agencourt AMPure XP（BECKMAN COULTER）を用いて精製を行う。操作法は各キットの取り扱い説明に従う、最後のエルーションは DDW で行う。

4. DNA定量

精製終了後の PCR 産物を 260nm にて吸光度測定、×50ng で DNA 定量。
10～20ng／μl になるよう必要におおじ DDW で希釈する。これを DNA template とする。

5. サイクルシークエンシング

サイクルシークエンシングは、機器は Veriti200 サーマルサイクラーを使用し、試薬は BigDye terminator v3.1cyclesequencing kit(Applied Biosystems)を用いる。反応液調整と反応条件は以下のとおり。

（反応液の調整、×8BigDye 法）

	Volume
DDW	Variable（to 20μl）
5×sequencing bufffer	3.5 μl
1.6pmol Fwd or Rvs primer	2 μl
V3.1 BigDye	1 μl
DNA template （final concentration 10～20ng）	Variable（0.5～3μl）
Total	20μl

（サイクルシークエンシング反応条件）

Step	Pre heat	Cycle sequencing(25cycle)			hold
		Denature	Anneal	Anneal/Extend	
Temp（℃）	94	96	50	60	4
Time	2min	10sec	5sec	2min30sec	∞

6. 精製

BigDye XTerminator 精製キットを用いて実施。

1)Xterminatorを室温に戻し、十分ボルテックスする。

2)先端をハサミで切り落としたチップで、Xterminator 7μlを8連PCRチューブにとる。

3)更に SAM溶液30μl を加える。

4)サイクルシーケンス反応液 1.5～2μlを加える

5)PCR チューブの蓋をしっかりと閉じ、プレート用アダプターを取りつけた Vortex GENIE2で最大パワー
で15分間ボルテックスする。

6)2500rpm、 2min遠心

7)上澄み 17μlをとりジェネティックアナライザーsample用PCRプレートに移す。

7. ジェネティックアナライザーによる分析

ジェネティックアナライザー3130（Applied Biosystems)を用い、ポリマーは、POP-7にて分析を開始する。

8. データ解析

データ解析用市販ソフト(日立 DNASIS)を用い、NCBI ホームページより得られた、Reference Sequence:
NG__12632.1を対照とし、変異の有無を確認する。

9. 報告書作成

パソコン用ワープロWordを用いて報告書を作成。患者の名前を記載せず、匿名番号によって、作成すること。また、FAXによる送信は禁止する。

厚生労働科学研究費補助金（難治性疾患克服研究事業）
分担研究報告書

致死性骨異形成症の遺伝子解析

研究分担者　長谷川奉延

研究要旨
骨レントゲン所見から胎児期に致死性骨異形成症(Thanatophoric dysplasia 以下 TD)と診断された4名でFGFR3遺伝子解析を行い、全例で既報変異を同定した。clover-leaf skull を認めないTDII型患者も存在するため、遺伝子解析による確定診断は有意義である。

共同研究者
慶應義塾大学医学部小児科高木優樹

A．研究目的

TD は著明な四肢短縮を認める致死性の先天性骨系統疾患である。TDは骨レントゲン所見から大腿骨の彎曲(telephone receiver様)が著明なI型と、頭蓋の変形(clover-leaf skull)が著明なII型とに分類される。TDの責任遺伝子はFGFR3であり、変異の陽性率は 90%と報告されている。また、I型、II型各々でFGFR3遺伝子変異のhot spotが異なる。本研究の目的は臨床的にTDと診断された患者のFGFR3遺伝子解析を行うことにより、1) 本邦におけるFGFR3遺伝子変異の陽性率を算出すること、ならびに 2)遺伝子型表現型を解明することである。

B．研究方法

研究の対象は骨レントゲン所見から胎児期にTDと診断され、家族から遺伝子解析の同意を得られた4名である。解析方法はPCR直接シークエンス法による遺伝子解析である。まずFGFR3遺伝子のTD hot spotを含むExon6,13,17を解析し、変異が陰性であれば全翻訳領域を解析した。

得られた結果より責任遺伝子変異の遺伝子型表現型関連の有無につき検討した。

(倫理面への配慮)

血液採取、遺伝子解析に関しては書面による同意を家族から得て行った。

C．研究結果

1)変異の陽性率:4 名中全例で遺伝子変異を同定した。同定された遺伝子変異の内訳は、R248Cが1名、S249Cが2名、K650Eが1名であった。なお、R248CおよびS249CはI型の、K650EはII型TDの既報かつhot spot変異である。

2)FGFR3遺伝子型表現型関連:R248CおよびS249C変異陽性の症例は3例とも著明な四肢の短縮、大腿の telephone receiver 様変形を認める典型的なI型TDであった。K650E 変異陽性の症例は著明な四肢短縮のため重度の骨系統疾患が疑われ 21 週で人工流産となったが、大腿の変形を認めず、clover-leaf skull も認めなかった。

Ｄ．考察

1)臨床的に TD と診断された症例では高率(4/4)で既報変異が同定される。新規変異は稀であるため、TD においてはまずは hotspot の解析のみで良い可能性が高い。

2)clover-leaf skull を認めない K650E 変異陽性患者の存在が証明された。同じ FGFR3 遺伝子変異による軟骨無形成症の重症型である SADDAN も著明な四肢短縮をきたすが、骨レントゲン上では clover-leaf skull の有無で II 型 TD との鑑別が行われる。SADDAN は新生児期の呼吸管理さえなされれば比較的予後は良好なため、両者の鑑別は極めて重要であり、遺伝子解析が唯一の鑑別手段となり得る。

Ｅ．結論

臨床的に TD と診断された症例では高率(4/4)で既報変異が同定される。clover-leaf skull を認めない TDII 型患者も存在するため、適伝子解析による確定診断は有意義である。

Ｆ．健康危険情報

なし

Ｇ．研究発表

１．論文発表

なし

２．学会発表

なし

Ｈ．知的財産権の出願・登録状況
（予定を含む。）

１．特許取得

なし

２．実用新案登録

なし

３．その他

なし

厚生労働科学研究費補助金（難治性疾患克服研究事業）
研究分担報告書

致死性骨異形成症の診断と予後に関する研究

窒息性胸郭異形成症の遺伝子診断

研究分担者　緒方　勤
国立成育医療研究センター研究所　分子内分泌研究部　部長

研究要旨

周産期致死性骨系統疾患の 1 つである窒息性胸郭異形成症（ASPHYXIATING THORACIC DYSTROPHY: ATD)について研究を行った。本疾患では、常染色体劣性疾患として発症する 3 つのタイプ(ATD1, ATD2, ATD3)の存在が知られ、ATD2 は第 3 染色体長腕に存在する IFT80 の変異により、ATD3 は第 11 染色体長腕に存在する DYNC2H1 の変異により発症する。われわれは、窒息性胸郭異形成症の 5 例において IFT80 の変異解析を終了し、DYNC2H1 の変異解析を行っている。その結果、IFT80 遺伝子変異解析を終了した 5 例中 1 例において、正常者には見られない第 4 エクソンのミスセンス変異（p.R113G）および第 4 イントロンの保存されたスプライスアクセプター部位の変異（IVS4-1G>C）が認められた。両親の解析により、第 4 エクソンのミスセンス変異は父親から、スプライスアクセプター部位の変異は母親から伝達されていることが判明した。患者は、重度の新生児期における呼吸困難の他に、眼間狭小、右外反肘と末節骨短縮を呈し、母親には病的表現型は見られなかったが、父親は軽度四肢短縮傾向と正常範囲の低身長傾向を呈していた。この結果は、窒息性胸郭異形成症が遺伝的異質性に富む疾患であること、また、AFT80 の遺伝子変異による ATD の頻度が高くないことを示唆する。さらに、患者・両親の表現型解析から、IFT80 の複合ヘテロ変異が胸郭低形成の他に顔貌や四肢・指趾の形成異常を生じること、IFT80 のヘテロ異常が骨の成長・形成に影響しうることを示唆するものである。このような症例の集積は、遺伝子型－表現型解析を通じて、各々の責任遺伝子変異による表現型スペクトラムの決定、変異遺伝子特異的合併症や長期予後の解明、現行治療法の効果の検討など、多くの有用なデータの構築に貢献すると期待される。

共同研究者
和田　友香（国立成育医療研究センター）

A．研究目的

窒息性胸郭異形成症 （ASPHYXIATING THORACIC DYSTROPHY: ATD）（短肋骨異形成症あるいは Jeune 症候群）は、周産期致死性骨系統疾患の 1 つであり、胸郭狭小と短い四肢などの外表奇形に骨盤，長管骨形成不全および腎，肝異形成を伴う遺伝性奇形

症候群である。発症頻度は10～13万人に一人の常染色体劣性遺伝疾患であり，その半数は乳幼児期に胸郭の低形成による呼吸不全で死亡する。また、幼児期以降に腎髄質嚢胞による腎機能不全により，透析導入となることも多い。

本疾患は､遺伝的異質性を伴う疾患であり、その発症には複数の責任遺伝子が関与する。現在少なくとも常染色体劣性疾患として発症する3つのタイプ(ATD1，ATD2，ATD3)の存在が知られている。そして、ATD2の責任遺伝子は第3染色体長腕に存在するIFT80であ

り、ATD3の責任遺伝子は第11染色体長腕に存在するDYNC2H1であることが判明している。一方、ATD1の責任遺伝子は第15染色体長腕にマップされているものの、未だ同定されていない。

本年度、われわれは、窒息性胸郭異形成症の5例においてIFT80の変異解析を終了し、DYNC2H1の変異解析を行っている。ここでは、その結果について報告する。

B．研究方法

・　症例：レントゲンならびに臨床的に窒息性胸郭異形成症と新省診断された5例を対象とした。代表的なレントゲン写真を図1に示す。

・　遺伝子解析：IFT80遺伝子の全19コードエクソンおよびDYNC2H1遺伝子の全89コードエクソンを直接シークエンス法で解析した。また、変異の確認は、サブクローニングを用いたシークエンスによった。同様に､DYNC2H1遺伝子の全89コードエクソンを解析中である。

（倫理面への配慮）

遺伝子解析にあたっては、ヒトゲノム・遺伝子解析研究に関する倫理指針を遵守し、検体の収集を含めた研究計画については、国立成育医療センター、および各検体の収集施設において予め倫理委員会の承認を得ている。検体は、書面によるインフォームド・コンセントを取得後に収集している。

C．研究結果

・　IFT80遺伝子変異解析:解析を終了した5例中1例において、正常者には見られない第4エクソンのミスセンス変異（p.R113G)および第4イントロンの保存されたスプライスアクセプター部位の変異（IVS4-1G>C）が認められた（図２）。両親の解析により、第4エクソンのミスセンス変異は父親から、スプライスアクセプター部位の変異は母親から伝達されていることが判明した。また、第16エクソンにp.Thr601Serという既報のミスセンス置換が認められた。

・　IFT80遺伝子変異陽性例の表現型：患者では、重度の新生児期における呼吸困難の他に、眼間狭小、右外反肘と末節骨短縮が認められた。現ザ、乳児期に達っしているが、腎機能障害が顕在化してきている。また、母親には病的表現型は見られなかったが、父親は軽度四肢短縮傾向と正常範囲の低身長傾向を呈していた。

・　DYNC2H1遺伝子変異解析：現在5例においてエクソン約1/3の解析を終了している。現在、変異は見られていない。

D．考察

窒息性胸郭異形成症5例中、1例においてIFT80の複合ヘテロ変異が同定された。この結果は、窒息性胸郭異形成症が遺伝的異質性に富む疾患であることに一致する。また、AFT80の遺伝子変異によるATDの頻度が高くないことを示唆する。4例においては、現在変異は同定されていない。DYNC2H1遺伝子変異が同定される可能性や、

未知の責任遺伝子変異の可能性が考えられる。

IFT80変陽性症例の表現型は、IFT80変異が胸郭低形成の他に、顔貌や四肢・指趾の形成異常を生じることを示唆する。さらに、保因者である父親の表現型は、世界で初めてIFT80のヘテロ異常が骨の成長・形成に影響しうることを示唆するものである。このような症例の集積は、遺伝子型－表現型解析を通じて、各々の責任遺伝子変異による表現型スペクトラムの決定、変異遺伝子特異的合併症や長期予後の解明、現行治療法の効果の検討など、多くの有用なデータの構築に貢献すると期待される。

Ｅ．結論

窒息性胸郭異形成症5例中、1例においてIFT80の複合ヘテロ変異が同定された。そして、遺伝子型－表現型解析から、IFT80複合ヘテロ変異が胸郭低形成の他に顔貌や四肢・指趾の形成異常を生じること、またヘテロ変異が軽度の骨成長・形成障害を招くことを示唆する。

Ｆ．健康危険情報

なし

Ｇ．研究発表

１．論文発表

1. Dateki S, Kosaka K, Hasegawa K, Tanaka H, Azuma N, Yokoya S, Muroya K, Adachi M, Tajima T, Motomura K, Kinoshita E, Moriuchi H, Sato N, Fukami M, Ogata T*. Heterozygous OTX2 mutations are associated with variable pituitary phenotype. J Clin Endocrinol Metab 95: (2): 756-764, 2010.

2. Dateki S, Fukami M, Uematsu A, Kaji M, Iso M, Ono M, Mizota M, Yokoya S, Motomura K, Kinoshita E, Moriuchi H, Ogata T*. Mutation and gene copy number analyses of six pituitary transcription factor genes in 71 patients with combined pituitary hormone deficiency: identification of a single patient with LHX4 deletion. J Clin Endocrinol Metab 95 (8): 4043-4047, 2010.

3. Kagami M, O'Sullivan MJ, Green AJ, Watabe Y, Arisaka O, Masawa N, Matsuoka K, Fukami M, Matsubara K, Kato F, Ferguson-Smith AC, Ogata T*. The IG-DMR and the MEG3-DMR at human chromosome 14q32.2: hierarchical interaction and distinct functional properties as imprinting control centers. PLoS Genet 6 (6): e1000992, 2010.

4. Yamazawa K, Nakabayashi K, Kagami M, Sato T, Saitoh S, Horikawa R, Hizuka N, Ogata T*. Parthenogenetic chimaerism/mosaicism with a Silver-Russell Syndrome-like Phenotype. J Med Genet 47 (11): 782-785, 2010.

5. Kato H, Yoshida R, Tsukamoto K, Suga H, Eto H, Higashino T, Araki J, Ogata T, Yoshimura K*: Familial cases of atypical clinical features genetically diagnosed as LEOPARD syndrome (multiple lentigines syndrome). Int J Dermatol 49 (10): 1146-1151, 2010.

6. Suzumori N*, Ogata T, Mizutani E, Hattori Y, Matsubara K, Kagami M, Suguhara-Ogasawara M. Prenatal diagnosis of paternal uniparental disomy 14: delineation of further patient. Am J Med Genet A 152A (12): 3189-3192, 2010.

7. Inoue H*, Kangawa N, Kinouchi A, Sakamoto Y, Kimura C, Horikawa R, Shigematsu Y, Itakura M, Ogata T, Fujieda

K. Identification and functional analysis of novel human growth hormone-releasing hormone receptor (GHRHR) gene mutations in Japanese subjects with short stature. Clin Endocrinol [Epub ahead of print] 2010 Nov 2 doi: 10.1111/j.1365-2265.2010.03911.x..

8. Yamazawa K, Nakabayashi K, Matsuoka K, Matsubara K, Hata K, Horikawa R, Ogata T*: Androgenetic/biparental mosaicism in a girl with Beckwith-Wiedemann syndrome-like and upd(14)pat-like phenotypes. J Hum Genet 56 (1): 91-93, 2011.

9. Inoue H*, Kangawa N, Kinouchi A, Sakamoto Y, Kimura C, Horikawa R, Shigematsu Y, Itakura M, Ogata T, Fujieda K. Identification and functional analysis of novel human growth hormone secretagogue receptor (GHSR) gene mutations in Japanese subjects with short stature. J Clin Endocrinol Metab 2010 Nov 17. [Epub ahead of print].

10. Dateki S, Fukami M, Tanaka Y, Sasaki G, Moriuchi H, Ogata T*. Identification of chromosome 15q terminal deletion with telomere sequences and its bearing on genotype-phenotype analysis. Endocr J (accepted).

11. Miyazaki O*, Nishimura G, Kagami M, Ogata T. Radiological evaluation of dysmorphic thorax in paternal uniparental disomy for chromosome 14. Ped Radiol (accepted).

12. Yamazawa K, Ogata T, Ferguson-Smith AC*: Uniparental disomy and human disease: an overview. Am J Med Genet C (Seminars in Medical Genetics) 154C (3): 329-334, 2010.

２．学会発表

Ｈ．知的財産権の出願・登録状況

１．特許取得

なし

２．実用新案登録

なし

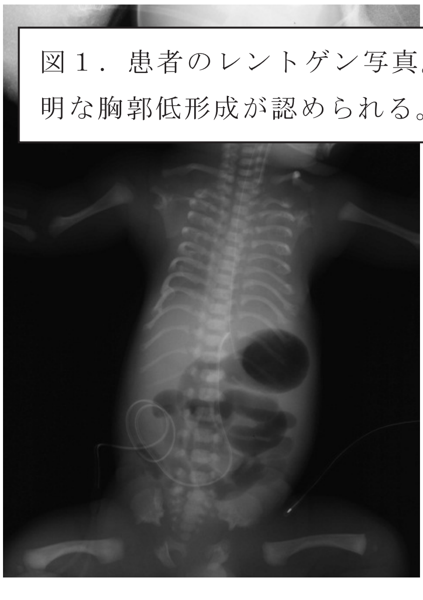

図１．患者のレントゲン写真。著明な胸郭低形成が認められる。

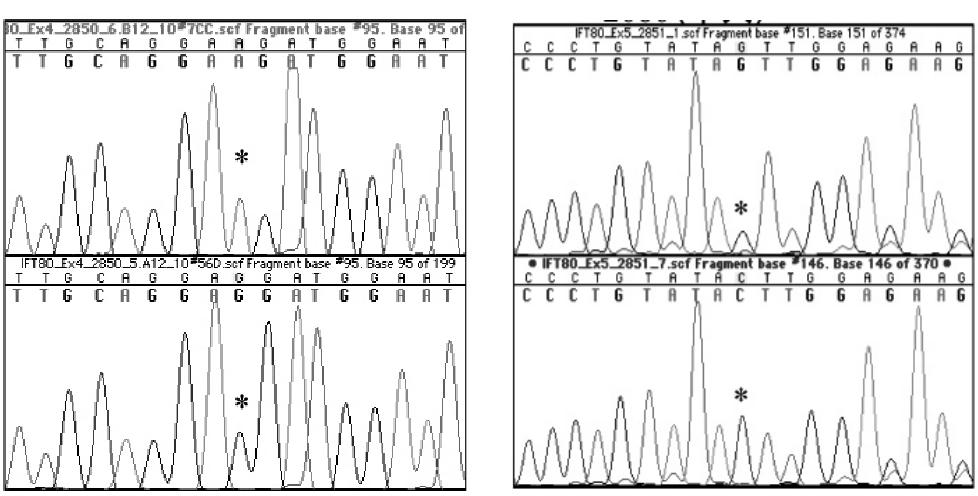

p.R113G

IVS4-1G>C

図 2.　IFT80 遺伝子の変異を示すクロマトグラム

厚生労働科学研究費補助金（難治性疾患克服研究事業）
研究分担報告書

致死性骨異形成症の類似疾患の遺伝子診断に関する研究

研究分担者　池川志郎
理化学研究所・ゲノム医科学研究センター
骨関節疾患研究チーム・チームリーダー

研究要旨

致死性骨異形成症には多くの類似疾患が存在し、正確な診断が困難で、確定診断のためには、遺伝子レベルでの診断システムを確立する必要がある。遺伝子診断システムの構築のために、致死性骨異形成症、及びその類似疾患のDNA解析を行なった。臨床家の協力の下に、致死性骨異形成症、及びその類似疾患の表現型の詳細なデータ（臨床像、X線像）とDNAを収集した。FGFR3を含む既知の疾患遺伝子に変異が疑われる場合は、それらの変異解析を行ない、変異が同定された患者については、表現型データとの対応を検討した。未知の疾患遺伝子が疑われる場合には homozygosity mapping などのゲノム解析を行った。その結果、致死性骨異形成症類似疾患のひとつ、Desbuquois骨異形成症の II型とその亜系であるKim型で、原因遺伝子CANT1を発見した。日本人には founder mutation があり、保因者頻度は700人に１人であることがわかった。致死性骨異形成症類似疾患の中には、保因者頻度がかなり高く、一般的な予想よりも発生頻度が高い疾患があり、胎児・新生児時の表現型データからは、鑑別診断は難しく、致死性骨異形成症の正確な診断のためには、類似疾患を含めた遺伝子診断法を確立する必要がある。

Ａ．研究目的

致死性骨異形成症は、多くの類似疾患が存在するため、正確な診断が困難である。確定診断のためには、遺伝子レベルでの診断システムを構築する必要がある。致死性骨異形成症の遺伝子診断法の確立のために、致死性骨異形成症、及びその類似疾患のDNA解析を行う。

Ｂ．研究方法

胎児骨系統疾患フォーラムを中心とする、臨床家の協力の下に、致死性骨異形成症、及びその類似疾患の表現型の詳細なデータ（臨床像、X線像）と genomic DNA を収集した。FGFR3 を含む既知の疾患遺伝子に変異が疑われる場合は、DNA sequence 解析をはじめとする遺伝子解析を行ない、変異の同定を試みた。変異が同定された患者については、表現型のデータとの対応を検討した。未知の疾患遺伝子が疑われる場合には、homozygosity mapping などのゲノム解析により、疾患遺伝子の同定を試みた。

（倫理面への配慮）

本研究の遂行にあったっては、ヒトゲノム・遺伝子解析研究に関する倫理指針（平

成13年3月29日文部科学省・厚生労働省・経済産業省告示第１号）に従っている。検体の収集を含めた研究計画については、理化学研究所、及び各検体の収集施設において予め倫理委員会の承認を得ている。検体は、書面によるインフォームド・コンセントを取得後に収集している。

Ｃ．研究結果

致死性骨異形成症の類似疾患のひとつである、Desbuquois骨異形成症の II型とその亜系である Kim 型で、CANT1 (calcium activated nucleotidase 1)遺伝子が、原因遺伝子であることを発見した (Furuichi et al. J Med Genet 2011)。日本には、古墳時代後期に韓国由来で伝達したと考えられる founder mutation があることがわかった(Dai et al. J Hum Genet, in press)。その保因者頻度は約750人に１人程度であった (Furuichi et al. J Med Genet 2011)。

Ｄ．考察

致死性骨異形成症の類似疾患の中には、保因者頻度がかなり高く、一般的な予想よりも、発生頻度が高い疾患がある事がわかった。胎児期､新生児時期の表現型の臨床像、X 線像のデータからは、それがいかに詳細なものであっても、致死性骨異形成症の診断、鑑別診断には多くの困難が伴い、類似疾患を正確に鑑別する事は困難であると考えられる。

Ｅ．結論

致死性骨異形成症の正確な診断のためには、遺伝子レベルでの診断法を確立する必要がある。

Ｆ．健康危険情報

なし

Ｇ．研究発表

１．論文発表

Furuichi T, Dai J, Cho TJ, Sakazume S, Ikema M, Matsui Y, Baynam G, Nagai T, Miyake N, Matsumoto N, Ohashi H, Unger S, Superti-Furga A, Kim OH, Nishimura G, Ikegawa S. CANT1 mutation is also responsible for Desbuquois dysplasia, type 2 and Kim variant. J Med Genet. 48(1):32-7. 2011.

２．学会発表

（招待講演のみ）

Ikegawa S. Genetic study of lumbar disc diseases. The 3rd Jishuitan Orthopedics Forum. Beijing. Apr. 24, 2010.

池川志郎. 遺伝学を用いた骨・関節疾患へのアプローチ. 第5回 Skeletal Research Meeting. 京都. 2010年6月12日.

池川志郎. ゲノムから疾患へ―ヒト遺伝学 (Human Genetics) を出発点とする疾患遺伝子と分子病態の解明. 京都大学再生医科学研究所 第 1 回生命医科学セミナー. 京都. 2010年9月7日.

池川志郎. ヒト遺伝学を出発点とする運動器疾患研究. 第 11 回運動器科学研究会. 軽井沢. 2010年9月10日.

Ikegawa S. Genomic study of bone and joint diseases using human and mouse genetics. 10th Annual meeting of the EAUHG (East Asian Union of Human Genetics Societies). Jinan. Oct. 8, 2010.

池川志郎. ゲノムから骨へ：ゲノム医科学による内軟骨性骨形成異常症の解明. 科学研究補助金　基盤 S「内軟骨性骨形成過程における転写制御ネットワークシステムの統合的理解」公開シンポジウム　:「内軟骨形成の制御機構とその破綻」. 吹田. 2011年1月21日

Ｈ．知的財産権の出願・登録状況
（予定を含む。）

１．　　特許取得
なし

２．　　実用新案登録
なし

３．その他

厚生労働科学研究費補助金（難治性疾患克服研究事業）
研究分担報告書

胎児超音波計測による長管骨長の基準値作成

（多施設共同観察研究）

研究分担者	室月　淳	宮城県立こども病院
	澤井英明	兵庫医科大学
	山田崇弘	北海道大学
	堤　誠司	山形大学
	佐藤秀平	青森県立中央病院
	篠塚憲男	胎児医学研究所
	高橋雄一郎	長良医療センター
	早川博生	春日井市民病院
	夫　律子	クリフム夫律子マタニティクリニック

研究要旨　超音波断層法による胎児の長管骨（すなわち大腿骨 femur、脛骨 tibia、腓骨 fibula、上腕骨 humerus、尺骨 ulna、橈骨 radius）の長さについての日本人の基準値をつくり、胎児骨系統疾患などの骨病変の診断に有用な基礎資料を作成する多施設共同研究である。なお大腿骨長については日本超音波医学会によりすでに基準値がつくられているが、それ以外の胎児の脛骨、腓骨、上腕骨、尺骨、橈骨の長さの基準値は、過去に海外では発表されており、本邦ではそれらが参考にされている。しかし長管骨の発達には人種差があり、日本人で決められた大腿骨長と欧米のそれを比べると、妊娠末期となると10mm 近い差が認められている。

胎児骨系統疾患は骨の全身の発達成熟に何らかの異常を呈する遺伝子病である。胎児骨系統疾患は、ほとんどが子宮内か出生直後に死亡する生命予後がきわめて悪いものから、成長後の低身長が唯一の症状である予後良好のものまで非常に多彩である。胎児期に骨短縮を認める疾患は100 種類以上あるといわれているが、ひとつひとつの疾患の発症頻度が低いため、胎児期に長管骨の短縮を認める場合、その診断に難渋することが多い。日本人胎児の長管骨の基準値を作成することにより、骨系統疾患の正確な診断の一助とする。

A．研究目的

胎児の長管骨、すなわち大腿骨 femur、脛骨 tibia、腓骨 fibula、上腕骨 humerus、尺骨 ulna、橈骨 radius の長さについての日本人の基準値をつくり、胎児骨系統疾患などの骨病変の診断の基礎資料を作成する。

大腿骨長（以下の図FL）については日本超音波医学会によりすでに基準値がつくられている。

それ以外の胎児の脛骨、腓骨、上腕骨、尺骨、橈骨の長さの基準値は、過去に Queenan (1980)、Farrant (1981)、Jeanty

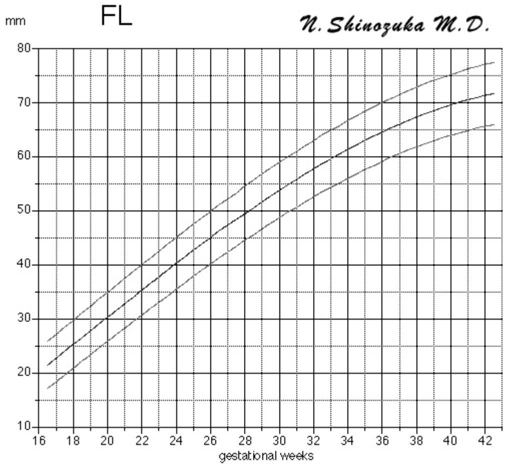

(1984)、Merz (1987)などが発表しており、本邦では今でもJeantyやMerzの値が用いられている。しかし長管骨の発達には人種差があるのは自然であり、日本人で決められた大腿骨長と欧米のそれを比べると、妊娠末期となると10mm近い差が認められている。実際にJenatyやMerzの基準値は、臨床上の印象よりかけ離れた評価が出てくることがしばしばである。

胎児骨系統疾患は骨の全身の発達成熟に何らかの異常を呈する遺伝子病である。胎児骨系統疾患は、ほとんどが子宮内か出生直後に死亡する生命予後がきわめて悪いものから、成長後の低身長が唯一の症状である予後良好のものまで非常に多彩である。胎児期に骨短縮を認める疾患は100種類以上あるといわれているが、ひとつひとつの疾患の発症頻度が低いため、胎児期に長管骨の短縮を認める場合、その診断に難渋することが多い。日本人胎児の長管骨の基準値を作成することにより、骨系統疾患の正確な診断の一助とする。

B．研究方法

試験タイプ：多施設共同観察試験

【対象】

1. 妊娠16週0日より妊娠40週6日まで
2. 16歳以上45歳未満
3. 単胎である
4. 妊娠初期にCRL計測により分娩予定日が決められている
5. 明らかな胎児奇形や発育遅延を認めない
6. 妊娠高血圧症や妊娠糖尿病などの母体合併症を認めない
7. 試験参加について本人から文書で同意が得られている

【方法】

1. 妊婦健康診査時に胎児の長管骨（大腿骨、脛骨、腓骨、上腕骨、尺骨、橈骨）の長さを計測して記録する。
2. 胎児期の長管骨はしばしば骨幹の部分しか骨化していない。その骨化部分を両端まで画面上に描出し、いちばん長いところを計測する。
3. 下腿の脛骨、腓骨、前腕の尺骨、橈骨は、それぞれ混同されて計測されることがあるので注意する。区別するために、最初に同一画面上に両方の骨を一緒に描出する。
4. 下腿では脛骨は腓骨より常に長い。腓骨は脛骨より外側に位置し、脛骨より若干薄く描出される。脛骨がより近位側に位置し、遠位側では脛骨、腓骨ともほぼ同じレベルにある。
5. 前腕では尺骨は橈骨より長い。尺骨はより近位側に位置し、より遠位側にあるのが橈骨である。
6. 長管骨の計測は画像に描出しやすい方で左右どちらでも構わない。胎児がうつ伏せか仰向けでない限り両側の長管骨をすべて描出することは難しいし、また時間的にも無駄である。
7. 胎児の計測データは、出生後に出生児の体重、身長、頭囲、腹囲のデータをあわせて事務局の宮城県立こども病院（室月　淳）に報告する。

（胎児）
妊婦
↓
ＩＣ（研究分担者）
↓
計測
↓
データ
↓
匿名化、本学のとりまとめ　澤井
↓
登録事務局
　～宮城県立こども病院～
↓
統計処理　～胎児医学研究所～
↓
公表

8.　統計処理などは共同研究者である胎児医学研究所・篠塚憲男に委託する。

【予定登録数と研究期間】
予定登録数：一施設100計測で合計1,000計測を目標とする。
予定研究期間：平成22年年6月（倫理委員会承認後）より平成23年3月31日。

宮城県立こども病院を中心に 15 施設ほどで実施中（予定を含む）である。現時点では臨床研究としての倫理審査を申請中からすでに実施中の施設もあるが完了は来年度になる予定。

【問い合わせ先】
適格基準など臨床的判断を要するもの：事務局（宮城県立こども病院　室月　淳）
記録用紙（CRF）記入など：胎児医学研究所（篠塚憲男）。
研究者などの登録など：事務局　宮城県立こども病院（室月　淳）。

Ｃ．研究結果
　研究実施中
Ｄ．考察
　研究実施中

Ｅ．結論
　研究実施中

Ｆ．健康危険情報
なし

Ｇ．研究発表
なし

Ｈ．知的財産権の出願・登録状況
（予定を含む。）
なし

厚生労働科学研究費補助金（難治性疾患克服研究事業）
研究分担報告書

症例の収集と診断の支援システム構築

研究分担者	室月　淳	宮城県立こども病院
	澤井英明	兵庫医科大学　（研究代表者）
	山田崇弘	北海道大学
	堤　誠司	山形大学
	佐藤秀平	青森県立中央病院
	篠塚憲男	胎児医学研究所
	高橋雄一郎	長良医療センター
	早川博生	春日井市民病院
	夫　律子	クリフム夫律子マタニティクリニック
	岡本伸彦	大阪府立母子保健総合医療センター
	鬼頭浩史	名古屋大学
	長谷川奉延	慶応義塾大学
	河井昌彦	京都大学
	沼部博直	京都大学
	岡崎　伸	大阪市立総合医療センター
	宮崎　治	国立成育医療研究センター
	緒方　勤	国立成育医療研究センター
	池川志郎	理化学研究所ゲノム医科学研究センター
研究協力者	西村　玄	東京都立小児総合医療センター

研究要旨　本研究は出生前に超音波検査で指摘された骨系統疾患疑いの胎児に対してどのように診断をアプローチし、その後の妊娠管理をどのように行い、分娩方式はどのようにして決定し、新生児管理に結びつけるかについて広範な専門集団が支援するシステムを構築するものである。具体的には１）インターネット利用による胎児の骨系統疾患を診断支援するための症例検討システムの構築、２）セキュリティの充実したウェブ閲覧型システムを構築して臨床医の診断の支援、３）過去の症例検討のとりまとめ、４）地域ごとの診断支援システムの構築、５）臨床医への情報提供、６）一般の妊婦や罹患児を持つ家族への情報提供といったシステム化されたフローを構築することである。

A．研究目的

本研究は出生前に超音波検査で指摘された骨系統疾患疑いの胎児に対してどのように診断をアプローチし、その後の妊娠管理をどのように行い、分娩方式はどのようにして決定し、新生児管理に結びつけるかについて広範な専門集団が支援するシステムを構築するものである。

B．研究方法

１）インターネット利用による胎児の骨系統疾患を診断支援するための症例検討システムの構築は、システムを兵庫医科大学の協力により同大学にサーバーを設置して、運営する。また専門システム開発業者とともにシステムの設計を行う。

２）上記システムを用いて、実際に臨床医から問合せのあった症例の検討を行う。

３）過去の症例検討のとりまとめは､」上記のウェブ上のシステム構築までの段階で全国の症例を検討した2,000通以上のメールの内容の解析と症例（108症例以上）の分析を行う。

４）地域ごとに胎児骨系統疾患に詳しい産科の専門家を配置し、地域の医療機関からの相談に乗る体制を構築する。

５）胎児骨系統疾患フォーラムと共同で臨床医への情報提供を目的に、講演会を開催し、またホームページでの情報提供を行う。

６）一般の妊婦や罹患児を持つ家族への情報提供をホームページを作成して行う。

C．研究結果

１）システムの構築をすでに完了して、試行中である。今年度中にはウェブ上に匿名化して症例の経過と画像をアップして、専門家グループで討議して診断を支援するシステムが運用開始できる予定である。

２）来年度から運用開始予定である。

３）過去の症例をとりまとめて日本周産期学会にて発表した。

４）研究班の研究分担者の属する施設を中心に、北海道、東北、東京、神奈川、東海、近畿、中国、四国においてほぼ中心的なセンター施設を選定した。九州地区を選定中であり、全国を網羅できる体制を今年度中に構築する予定である。

５）12月12日（日）に本研究班会議と胎児骨系統疾患フォーラムが共催して、一般臨床医を含めた医師を対象に第3回胎児骨系統疾患フォーラムを開催し、致死性骨異形成症を含めた胎児骨系統疾患の新生児管理について集中的な情報提供と討議を行った。

また、本研究班で致死性骨異形成症のホームページwww.thanatophoric.comを作成し骨系統疾患の情報を提供し、診断や治療に取り組む産科医や小児科医などからの問い合わせを受け付ける体制を作った。すでに地域の病院（産科）から1件の問い合わせがあり､上記の地域診断支援システム(予定）に紹介して対応した。

６）前記の第3回胎児骨系統疾患フォーラムにおいて一般市民を対象に公開講演会を開催した。

D．考察

本研究においては今年度で個別に体制はほぼ完成した。次年度からの運用においてはいかにこれらを有機的に結びつけて実施するかが鍵と考えられる。

E．結論

出生前に超音波検査で指摘された骨系統疾患疑いの胎児に対してどのように診断をアプローチし、その後の妊娠管理をどのように行い、分娩方式はどのようにして決定し、新生児管理に結びつけるかについて広範な専門集団が支援するシステムを構築した。

F．健康危険情報

なし

G．研究発表

なし

H．知的財産権の出願・登録状況
（予定を含む。）なし

厚生労働科学研究費補助金（難治性疾患克服研究事業）
研究分担報告書

胎児ＣＴの実施のための撮影基準の作成

研究分担者	宮崎　治	国立成育医療研究センター
	澤井英明	兵庫医科大学　（研究代表者）
	室月　淳	宮城県立こども病院
研究協力者	西村　玄	東京都立小児総合医療センター
	永松洋志	国立成育医療研究センター
	嶋田彩乃	国立成育医療研究センター
	堀内哲也	国立成育医療研究センター
	島貫義久	宮城県立こども病院
	佐々木清昭	宮城県立こども病院
	谷　千尋	広島大学
	木口雅夫	広島大学

研究要旨　胎児骨格 CT はここ数年行われるようになった新しい診断方法であるが、昨今 CT の X 線被ばくに対する問題意識が高まっている。そこで胎児 CT 検査に関する調査を施行することとした。胎児骨格 CT について、その施行頻度、適応、撮影方法、胎児被ばく線量などを調査し、本邦での胎児 CT の動向を知る必要がある。またその結果から胎児 CT 撮影方法の標準化が設定できることを目指している。この調査は無作為に医療施設に送るのではなく、本研究班の研究者や、胎児骨系統疾患ネットワーク、過去に国内の学会の抄録等を頼りに抽出した施設（参考資料：調査協力施設一覧）に依頼することで効率的にデータを収集し、解析する。

Ａ．研究目的

胎児ＣＴの実施は得られる情報が多い反面、被曝の問題が避けられない。今後胎児ＣＴが適正に実施されるために、現状の調査を行い、分析する。

Ｂ．研究方法

胎児 CT サブグループの長期的目的は２つあり、まず胎児 CT 撮影の後方視調査（平成 22 年）を行い、胎児 CT 撮影ガイドライン作成（平成 23 年）を行い、Diagnostic Reference Level(DRL)設定（平成 23 年）を行う。短期計画としては本年度に後方視サーベイ調査票を作成し、全国調査を実施する、回収、集計、解析を今年度中に行うこととした。

調査の対象医療機関は胎児骨系統疾患フォーラムと学会発表等から抽出した施設のうち調査協力に承諾が得られた１８施設に対してアンケートを送付した。

調査内容は３つのカテゴリーに分け、１）産科的総論：適応、倫理、informed concent

関連（澤井、室月）、２）CT 撮影・３D プロトコル技術（永松、嶋田、佐々木、木口）被ばく線量関連（堀内）、３）放射線診断結果、診断的価値（宮崎、島貫、谷）と分担した。

C．研究結果

研究実施中

D．考察

研究実施中

E．結論

研究実施中

F．健康危険情報

なし

G．研究発表

なし

H．知的財産権の出願・登録状況（予定を含む。）

１．　特許取得

なし

２．　実用新案登録

なし

３．その他

なし

Ⅲ．研究成果の刊行に関する一覧表

雑誌

発表者氏名	論文タイトル名	発表誌名	巻号	ページ	出版年
Dateki S, Kosaka K, Hasegawa K, Tanaka H, Azuma N, Yokoya S, Muroya K, Adachi M, Tajima T, Motomura K, Kinoshita E, Moriuchi H, Sato N, Fukami M, Ogata T*.	Hetero*zy*gous Or*X2* mutations are associated with variable pituitary phenotype	*J Clin Endocrin of Metab*	95 (2)	756-764	2010
Dateki S, Fukami M, Uematsu A, K‘iii M, Iso M, One M, Mizota M, Yokoya S, Motomura K, Kinoshita E, Moriuchi H, Ogata T*	Mutation and gene copy number analyses of six pituitary transcription factor genes in 7 1 patients with combined pituitary hormone deficiency: identification of a single patient with *LHX4* deletion	*J Clin Endocrin* M*etab*	95 (8)	4043-4047	2010
Kagami M, O'sullivan M J, Green AJ, Watabe Y, Arisaka 0, Masawa N, Matsuoka K, Fukami M, Matsubara K, Kato F, Ferguson-Smith AC, Ogata T	The IG-DMR and the *MEG3*-DMR at human chromosome 14q32.2: hierarchical interaction and distinct functional properties as imprinting control centers.	T *PLoS Genet*	6 (6)	100992	2010
Yamazawa K, Nakabayashi K, Kagami M, Sato T, Saitoh S, Horikawa R, Hizuka N, Ogata T	Parthenogenetic chimaerism/mosaicism with a Sliver-Russell Syndrome-like Phenotype.	*J Med Genet* 4 7	47(11)	782-785	2010
Kato H, Yoshida R, Tsukamoto K, Suga H, Eto H, Higashino T, Araki J Ogata T Yoshimura K	Familial cases of atypical clinical features genetically diagnosed as LEOPARD syndrome (multiple lentigines syndrome)	*Imt J Dermatol*	152A (1 2)	3189-3192	2010

Suzumori N*, Ogata T, Mizutani E, Hattori Y, Matsubara K, Kagami M, Sugiura-Ogasawara M.	Prenatal diagnosis of paternal uniparental disomy 14: delineation of further patient	*Am J Med Genet A*	152A	3189-3192	2010
Inoue H*, Kangawa N, Kinouchi A, Sakamoto Y, Kimura C, Horikawa R, Shigematsu Y, Itakura M, Ogata T, Fujieda K.	Identification and functional analysis of novel human growth hormone-releasing hormone receptor (*GHRHR*) gene mutations in Japnese subjects with short stature	*J Clin Endocrin of* M*etab*	NOV 17.	1365-2265	2010
Yamazawa K, Nakabayashi K, Matsuoka K, Matsubara K, Hata K, Horikawa R, Ogata T'	Androgenetic/biparental mosaicism in a girl with Beckwith-Wiedemann syndrome-like and upd(14)pat-like phenotypes	*J Hun Genet*	56 (1)	91-93	201 1
Dateki S, Fukami M, Tanaka Y, Sasaki G, Moriuchi H, Ogata T	Identification of chromosome 15q terminal deletion with telomere sequences and its bearing on genotype-phenotype analysis	*Endocr J* (accepted)			
Miyazaki 0*, Nishimura G, Kagami M, Ogata T	Radiologica1 evaluation of dysmorphic thorax in paternal uniparental disomy for chromosome 14.	*Ped Radiol* (accepted).			
Yamazawa K, Ogata T Ferguson-Smith AC	Uniparemtal disomy and human disease: an overview.	*Am J Med' Genet C* (Seminars in Medical Genetics)	154C (3)	329-334	2010
Furuichi T, Dai J, Cho TJ, Sakazume S, Ikema M, Matsui Y, Baynam G, Nagai T, Miyake N, Matsumoto N, Ohashi H, Unger S, Superti-Furga A, Kim OH, Nishimura G, Ikegawa S.	CANT1 mutation is also responsible for Desbuquois dysplasia, type 2 and Kim variant.	J Med Genet.	48(1)	32-37	2011

Wada R, Sawai H, Nishimura G, Isono K, Minagawa K, Takenobu T, Harada K, Tanaka H, Ishikura R, Komori S.	Prenatal diagnosis of Kniest dysplasia with three-dimensional helical computed tomography.	J Matern Fetal Neonatal Med.	Jan 20.	Epub ahead of print	2011
Watanabe A, Karasugi T, Sawai H, Naing BT, Ikegawa S, Orimo H, Shimada T.	Prevalence of c.1559delT in ALPL, a common mutation resulting in the perinatal (lethal) form of hypophosphatasia in Japanese and effects of the mutation on heterozygous carriers.	J Hum Genet.	56(2):	166-8.	2011
Yamada T, Nishimura G, Nishida K, Sawai H, Omatsu T, Kimura T, Nishihara H, Shono R, Shimada S, Morikawa M, Mizushima M, Yamada T, Cho K, Tanaka S, Shirato H, Minakami H.	Prenatal diagnosis of short-rib polydactyly syndrome type 3 (Verma-Naumoff type) by three-dimensional helical computed tomography.	J Obstet Gynaecol Res.	;37(2)	151-5.	2011
Sago H, Hayashi S, Saito M, Hasegawa H, Kawamoto H, Kato N, Nanba Y, Ito Y, Takahashi Y, Murotsuki J, Nakata M, Ishii K, Murakoshi Y	The outcome and prognostic factors of twin–twin transfusion syndrome following fetoscopic laser surgery.	Prenat Diagn.	30	1185-91	2010
Kitoh H, Kaneko H, Kondo M, Yamamoto T, Ishiguro N, Nishimura G.	Spondylometaphyseal dysplasia with cone-rod dystrophy.	Am J Med Genet A.	Mar 15.	Epub ahead of print	2011
Nakashima Y, Haga N, Kitoh H, Kamizono J, Tozawa K, Katagiri T, Susami T, Fukushi J, Iwamoto Y.	Deformity of the great toe in fibrodysplasia ossificans progressiva.	J Orthop Sci.	15(6)	804-9	2010

Nishimura G, Dai J, Lausch E, Unger S, Megarbané A, Kitoh H, Kim OH, Cho TJ, Bedeschi F, Benedicenti F, Mendoza-Londono R, Silengo M, Schmidt-Rimpler M, Spranger J, Zabel B, Ikegawa S, Superti-Furga A.	Spondylo-epiphyseal dysplasia, Maroteaux type (pseudo-Morquio syndrome type 2), and parastremmatic dysplasia are caused by TRPV4 mutations.	Am J Med Genet A.	152A(6):	1443-9.	2010

Ⅳ．研究成果の刊行物・別冊

Journal of Human Genetics (2011) 56, 166–168
© 2011 The Japan Society of Human Genetics All rights reserved 1434-5161/11 $32.00
www.nature.com/jhg

SHORT COMMUNICATION

Prevalence of c.1559delT in *ALPL*, a common mutation resulting in the perinatal (lethal) form of hypophosphatasia in Japanese and effects of the mutation on heterozygous carriers

Atsushi Watanabe[1,2], Tatsuki Karasugi[3], Hideaki Sawai[4], Banyar Than Naing[2], Shiro Ikegawa[3], Hideo Orimo[2] and Takashi Shimada[1,2]

Hypophosphatasia (HPP) is an inherited disorder caused by mutations in *ALPL* that encodes an isozyme of alkaline phosphatase (ALP), TNSALP. One of the most frequent *ALPL* mutations is c.1559delT, which causes the most severe HPP, the perinatal (lethal) form (pl-HPP). c.1559delT has been found only in Japanese and its prevalence is suspected to be high; however, the allele frequency of c.1559delT in Japanese remains unknown. We designed a screening system for the mutation based on high-resolution melting curve analysis, and examined the frequency of c.1559delT. We found that the c.1559delT carrier frequency is 1/480 (95% confidence interval, 1/1562–1/284). This indicates that ~1 in 900 000 individuals to have pl-HPP caused by a homozygous c.1559delT mutation. In our analysis, the majority of c.1559delT carriers had normal values of HPP biochemical markers, such as serum ALP and urine phosphoethanolamine. Our results indicate that the only way to reliably detect whether individuals are pl-HPP carriers is to perform the *ALPL* mutation analysis.

Journal of Human Genetics (2011) **56,** 166–168; doi:10.1038/jhg.2010.161; published online 23 December 2010

Keywords: *ALPL*; c.1559delT; perinatal form of hypophosphatasia; serum alkaline phosphatase; skeletal dysplasia; urine phosphoethanolamine

INTRODUCTION

Hypophosphatasia (HPP) is an inherited disorder characterized by defective mineralization of the bone and low activity of alkaline phosphatase (ALP; EC 3.1.3.1).[1,2] HPP is a clinically heterogeneous disease and classified into five forms according to severity and age of onset: perinatal (lethal), infantile (OMIM 241500), childhood (OMIM 241510), adult (OMIM 146300) and odontohypophosphatasia.[1] All forms of HPP display reduced activity of unfractionated serum ALP and the presence of either one or two pathologic mutations in *ALPL*, the gene encoding an ALP isozyme (TNSALP).

The perinatal (lethal) form of HPP (pl-HPP) is the most severe HPP with an autosomal recessive mode of inheritance. pl-HPP is more common in Japan than in other countries.[3] Parents of pl-HPP are heterozygous carriers of *ALPL* mutations. They show no clinical symptoms, but have reduced serum ALP activity and increased urinary phosphoethanolamine (PEA).[4–8]

ALPL is the only gene known to be associated with HPP.[1] More than 200 *ALPL* mutations have been described, accounting for most phenotype variabilities.[9] HPP is frequently caused by p.E191K and p.D378V in Caucasians,[1] whereas p.F327L[10] and c.1559delT[10,11] are more common in Japanese.[1] To date, c.1559delT has only been found in Japanese.[11] Some patients with pl-HPP are homozygous for c.1559delT, with parents who are heterozygous carriers for the mutation but with no evidence of consanguinity.[12,13]

To identify c.1559delT genotype and to examine its frequency in Japanese, we designed a screening system based on a high-resolution melting curve analysis.[14] In addition, we examined serum ALP activity and urine PEA in heterozygous c.1559delT carriers to determine whether these markers can identify the HPP carriers.

MATERIALS AND METHODS

This study was approved by the Institutional Genetic Research Ethics Committee at Nippon Medical School and RIKEN, Center for Genomic Medicine. Blood samples were collected under written informed consents from 3844 healthy Japanese without HPP and its related findings confirmed by orthopedic surgeons. Genomic DNA was extracted from peripheral blood leukocytes using standard protocols. The c.1559delT genotype screening was performed by the small amplicon genotyping method based on high-resolution melting curve

---

[1]Division of Clinical Genetics, Nippon Medical School Hospital, Tokyo, Japan; [2]Department of Biochemistry and Molecular Biology, Nippon Medical School, Tokyo, Japan; [3]Laboratory for Bone and Joint Diseases, Center for Genomic Medicine, RIKEN, Tokyo, Japan and [4]Department of Obstetrics and Gynecology, Hyogo College of Medicine, Nishinomiya, Japan

Correspondence: Dr A Watanabe, Division of Clinical Genetics, Nippon Medical School Hospital, 1-1-5 Sendagi Bunkyo-ku, Tokyo 113-8603, Japan.
E-mail: aw3703@nms.ac.jp

Received 17 October 2010; revised 23 November 2010; accepted 24 November 2010; published online 23 December 2010

analysis.[14] PCR primers for c.1559delT were designed to flank the mutation leaving only single base, including the mutation between the primers: 5′-TTTAAATTCTCGCGCTGGCCCTCTACCCC-3′ (forward) and 5′-TTTAAATTCCCTCAGAACAGGACGCTC-3′ (reverse). PCR conditions were as follows: initial denaturation at 95°C for 2 min, followed by 45 cycles at 94°C for 30 s and annealing at 67°C for 30 s. After PCR, high-resolution melting was performed in a 96-well plate LightScanner (Idaho Technology, Salt Lake City, UT, USA), which collected data from 55°C to 97°C at a ramp rate of 0.10°C sec^{-1}. The observed number of c.1559delT carriers was divided by the total number of individuals tested to determine the carrier frequency. Serum ALP activity and urine PEA were measured in c.1559delT-heterozygous parents of pl-HPP patients.

RESULTS

Three *ALPL* c.1559delT genotypes (wt/wt, wt/c.1559delT and c.1559delT/c.1559delT) were distinguished by the modified small amplicon genotyping method (Figure 1). A heterogeneous c.1559delT mutation (wt/c.1559delT) was detected in 8 of 3844 healthy Japanese subjects, indicating a carrier frequency of 1/480 in the Japanese population (95% confidence interval, 1/1562–1/284).

The numerical value of ALP activity and urinary PEA varied in heterozygous c.1559delT carriers in parents of perinatal HPP patients. The majority of heterozygous c.1559delT carriers had normal levels of both ALP activity (five out of six males and three out of four females) and urinary PEA (three out of six males and four out of five females) (Figure 2).

DISCUSSION

Based on our results, we estimated the frequency of c.1559delT-homozygous individuals (for example, those with pl-HPP) to be 1/900 000. Previous studies showed that all Japanese pl-HPP patients carried the c.1559delT mutation in at least one allele; half (10/20) were homozygous for c.1559delT and half (10/20) were compound heterozygous for c.1559delT,[9–13,15] which gives a pl-HPP prevalence of 1/450 000 for patients that are homozygous or compound heterozygous for c.1559delT mutation. The other common mutation on *ALPL* in Japan, p.F327L, is a mild allele whose product retained ~70% of its enzymatic activity. Patients compound heterozygous for c.1559delT and p.F327L are not associated with pl-HPP.[10]

Biochemical markers, serum ALP activity and urinary PEA levels fell within their normal ranges in the majority of the c.1559delT carriers examined in this paper, whereas heterozygous carriers of the severe forms in other *ALPL* mutations were reported to have reduced serum ALP activity and increased urinary PEA.[4–8] Some possible reasons why c.1559delT carriers display normal marker levels are as follows: the first is the protein properties caused by the different mutation positions. The c.1559delT mutation causes a frameshift downstream of codon L503, resulting in the elimination of the termination codon at 508 and the addition of 80 amino acids at the C-terminus. The mutant protein forms an aggregate that is polyubiquitinated and then degraded in the proteasome. However, the aggregates possess enzyme activity, and may, therefore, influence physiological processes before their destruction.[16] Second, serum ALP activity is affected by some other factors. The genetic modifier of ALP is reported to have a potential influence on serum ALP activity.[17] Total ALP value is also elevated by some environmental factors, in vitamin D deficiency[2] or in the third trimester of gestation by the increasing placental ALP, which is not affected by TNSALP.[18] Recently, it was shown that patients who are homozygous for the c.1559delT mutation differed in the severity of HPP, including both their symptoms and serum ALP activity.[15]

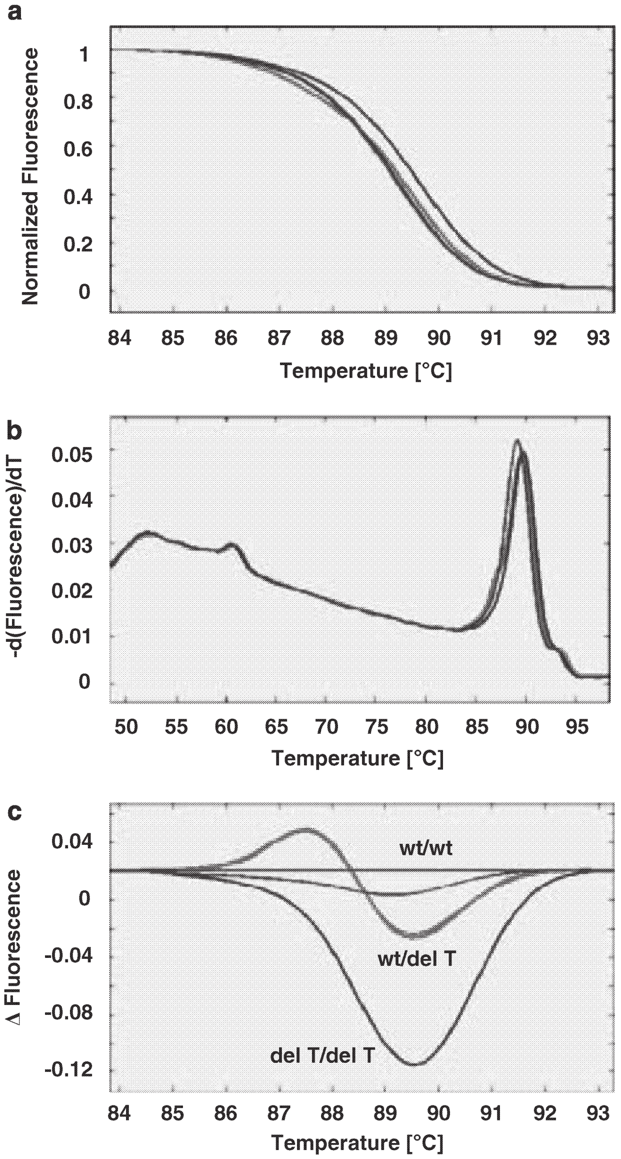

Figure 1 Identification of c.1559delT mutation in *ALPL* by small amplicon genotyping (SAG) method. (**a**) Normalized fluorescence plots. (**b**) d(fluorescence)/dT plot. (**c**) The corresponding fluorescence difference plots. Wild-type (wt/wt) samples are in gray; samples heterozygous for c.1559delT (wt/c.1559delT) are in red; and samples homozygous for c.1559delT (c.1559delT/c.1559delT) are in blue. The three genotypes were clearly distinguishable in the SAG method.

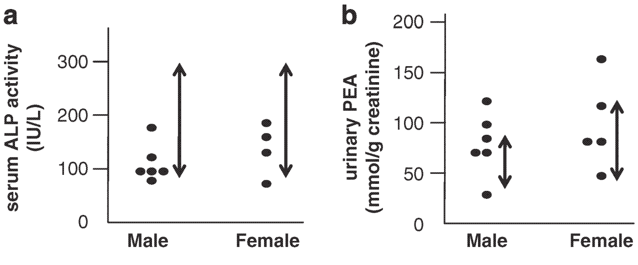

Figure 2 Biochemical marker levels in heterozygous carriers of the *ALPL* c.1559delT mutation. The serum ALP activity (**a**) and urinary PEA (**b**) levels in the majority of heterozygous carriers (wt/c.1559delT) fell within normal ranges (indicated by arrows).

Thus, the only way to reliably detect the pl-HPP carriers is to perform the *ALPL* mutation analysis. The small amplicon genotyping method in this study using the high-resolution melting curve analysis is a one-step, single-tube method for detection of specific mutations and faster, simpler and less expensive than the approaches requiring separations or labeled probes.[19]

The screening for c.1559delT in *ALPL* may be useful for diagnosis of pl-HPP in Japanese to provide optimum genetic counseling for fetal skeletal dysplasia. pl-HPP occasionally could not be diagnosed with sonographic examination in the first trimester because incomplete ossification is an usual finding at this stage of development.[20] To diagnose pl-HPP, collaborations between obstetricians and clinical geneticists are important and could provide support for parents of prenatal patients suspected of having skeletal dysplasia.

CONFLICT OF INTEREST

The authors declare no conflict of interest.

ACKNOWLEDGEMENTS

We wish to thank all the patients and family members who participated in this study, and all the clinicians for referring the families. We thank Hitomi Kondo for technical assistance. This work was supported by a Grant-in-Aid for Research on intractable disease from the Ministry of Health, Labour and Welfare of Japan (Project no. 095/2010).

---

1 Mornet, E. Hypophosphatasia. *Best Pract. Res. Clin. Rheumatol.* **22,** 113–127 (2008).
2 Whyte, M. P. Hypophosphatasia and the role of alkaline phosphatase in skeletal mineralization. *Endocr. Rev.* **15,** 439–461 (1994).
3 Satoh, N., Murotsuki, A. & Sawai, H. The birth prevalence rates for skeletal dysplasia in the registration system of the Japan Forum of Fetal Skeletal Dysplasia. *J. Jan. Perinat. Neonat. Med.* **45,** 1005–1007 (2009) (Japanese).
4 Gehring, B., Mornet, E., Plath, H., Hansmann, M., Bartmann, P. & Brenner, R. E. Perinatal hypophosphatasia: diagnosis and detection of heterozygote carriers within the family. *Clin. Genet.* **56,** 313–317 (1999).
5 Spentchian, M., Merrien, Y., Herasse, M., Dobbie, Z., Gläser, D., Holder, S. E. *et al.* Severe hypophosphatasia: characterization of fifteen novel mutations in the ALPL gene. *Hum. Mutat.* **22,** 105–106 (2003).
6 Zankl, A., Mornet, E. & Wong, S. Specific ultrasonographic features of perinatal lethal hypophosphatasia. *Am. J. Med. Genet.* **146A,** 1200–1204 (2008).
7 Sergi, C., Mornet, E., Troeger, J. & Voigtlaender, T. Perinatal hypophosphatasia: radiology, pathology and molecular biology studies in a family harboring a splicing mutation (648+1A) and a novel missense mutation (N400S) in the tissue-nonspecific alkaline phosphatase (TNSALP) gene. *Am. J. Med. Genet.* **103,** 235–240 (2001).
8 Mornet, E., Taillandier, A., Peyramaure, S., Kaper, F., Muller, F., Brenner, R. *et al.* Identification of fifteen novel mutations in the tissue-nonspecific alkaline phosphatase (TNSALP) gene in European patients with severe hypophosphatasia. *Eur. J. Hum. Genet.* **6,** 308–314 (1998).
9 The Tissue Nonspecific Alkaline Phosphatase Gene Mutations Database. http://www.sesep.uvsq.fr/03_hypo_mutations.php.
10 Michigami, T., Uchihashi, T., Suzuki, A., Tachikawa, K., Nakajima, S. & Ozono, K. Common mutations F310L and T1559del in the tissue-nonspecific alkaline phosphatase gene are related to distinct phenotypes in Japanese patients with hypophosphatasia. *Eur. J. Pediatr.* **164,** 277–282 (2005).
11 Orimo, H., Goseki-Sone, M., Inoue, M., Tsubakio, Y., Sakiyama, T. & Shimada, T. Importance of deletion of T at nucleotide 1559 in the tissue-nonspecific alkaline phosphatase gene in Japanese patients with hypophosphatasia. *J. Bone Miner. Metab.* **20,** 28–33 (2002).
12 Watanabe, A., Yamamasu, S., Shinagawa, T., Suzuki, Y., Takeshita, T., Orimo, H. *et al.* Prenatal genetic diagnosis of severe perinatal (lethal) hypophosphatasia. *J. Nippon Med. Sch.* **74,** 65–69 (2007).
13 Sawai, H., Kanazawa, N., Tsukahara, Y., Koike, K., Udagawa, H., Koyama, K. *et al.* Severe perinatal hypophosphatasia due to homozygous deletion of T at nucleotide 1559 in the tissue nonspecific alkaline phosphatase gene. *Prenat. Diagn.* **23,** 743–746 (2003).
14 Gundry, C. N., Dobrowolski, S. F., Martin, Y. R., Robbins, T. C., Nay, L. M., Boyd, N. *et al.* Base-pair neutral homozygotes can be discriminated by calibrated high-resolution melting of small amplicons. *Nucleic Acids Res.* **36,** 3401–3408 (2008).
15 Nakamura-Utsunomiya, A., Okada, S., Hara, K., Miyagawa, S., Takeda, K., Fukuhara, R. *et al.* Clinical characteristics of perinatal lethal hypophosphatasia: a report of 6 cases. *Clin. Pediatr. Endcrinol.* **19,** 7–13 (2010).
16 Komaru, K., Ishida, Y., Amaya, Y., Goseki-Sone, M., Orimo, H. & Oda, K. Novel aggregate formation of a frame-shift mutant protein of tissue-nonspecific alkaline phosphatase is ascribed to three cysteine residues in the C-terminal extension. Retarded secretion and proteasomal degradation. *FEBS J.* **272,** 1704–1717 (2005).
17 Kamatani, Y., Matsuda, K., Okada, Y., Kubo, M., Hosono, N., Daigo, Y. *et al.* Genome-wide association study of hematological and biochemical traits in a Japanese population. *Nat. Genet.* **42,** 210–215 (2010).
18 Whyte, M. P., Landt, M., Ryan, L. M., Mulivor, R. A., Henthorn, P. S., Fedde, K. N. *et al.* Alkaline phosphatase: placental and tissue-nonspecific isoenzymes hydrolyze phosphoethanolamine, inorganic pyrophosphate, and pyridoxal 5′-phosphate. Substrate accumulation in carriers of hypophosphatasia corrects during pregnancy. *J. Clin. Invest.* **95,** 1440–1445 (1995).
19 Vossen, R. H., Aten, E., Roos, A. & den Dunnen, J. T. High-resolution melting analysis (HRMA): more than just sequence variant screening. *Hum. Mutat.* **30,** 860–866 (2009).
20 Tongsong, T. & Pongsatha, S. Early prenatal sonographic diagnosis of congenital hypophosphatasia. *Ultrasound Obstet. Gynecol.* **15,** 252–255 (2000).

The Journal of Maternal-Fetal and Neonatal Medicine, 2011; Early Online, 1–4
© 2011 Informa UK, Ltd.
ISSN 1476-7058 print/ISSN 1476-4954 online
DOI: 10.3109/14767058.2010.545903

CASE REPORT

Prenatal diagnosis of Kniest dysplasia with three-dimensional helical computed tomography

RYU WADA[1], HIDEAKI SAWAI[1], GEN NISHIMURA[2], KAZUTOMO ISONO[3], KYOKO MINAGAWA[3], TAKASHI TAKENOBU[1], KAYOKO HARADA[1], HIROYUKI TANAKA[1], REIICHI ISHIKURA[4], & SHINJI KOMORI[1]

[1]*Department of Obstetrics and Gynecology, Hyogo College of Medicine, Nishinomiya-shi, 663-8501 Japan,* [2]*Department of Pediatric Imaging, Tokyo Metropolitan Children's Medical Center, Fuchu-shi, 183-8561 Japan,* [3]*Department of Pediatrics, Hyogo College of Medicine, Nishinomiya-shi, 663-8501 Japan, and* [4]*Department of Radiology, Hyogo College of Medicine, Nishinomiya-shi, 663-8501 Japan*

J Matern Fetal Neonatal Med Downloaded from informahealthcare.com by 210.190.246.185 on 01/21/11
For personal use only.

Abstract

Objective. Fetal three-dimensional helical computed tomography (3D-CT) has attracted attention in the diagnosis of fetal skeletal dysplasias because of limited diagnostic capabilities of standard ultrasonography to delineate the skeleton. Here we report the first instance of diagnosing Kniest dysplasia with 3D-CT.

Methods. Fetal 3D-CT was performed for a fetus at 28 weeks' gestation after ultrasonography at 24 weeks had shown moderate shortening of the limbs, mild narrow thorax, and polyhydramnios. The imaging parameters were set so as to reduce estimated fetal irradiation dose to 12.39 mGy of the CT dose index volume and 442 of the dose length product.

Results. Fetal 3D-CT revealed dumbbell-shaped femora and platyspondyly with coronal cleft of the lumbar vertebral body. This warranted a diagnosis of Kniest dysplasia and corresponded well with postnatal radiographic findings. In retrospect, however, spinal deformation was somewhat underestimated due to image smoothing associated with image processing in 3D-CT. Genetic testing for *COL2A1* confirmed Kniest dysplasia; i.e., a *de novo* mutation of A–C transversion at the splice acceptor site of the 3′ end of intron 16.

Conclusions. The combined use of 3D-CT with ultrasonography is a power tool for the prenatal diagnosis of congenital skeletal dysplasias.

Keywords: *Kniest dysplasia, skeletal dysplasia, helical CT, three-dimensional, prenatal diagnosis*

Introduction

Kniest dysplasia (OMIM 156550) is an autosomal dominant (AD) skeletal dysplasia characterized by characteristic mid-face hypoplasia and distinctive skeletal changes, including dumbbell deformity of the long bones and platyspondyly with coronal clefts [1]. The exact incidence remains to be determined. The disorder is caused by a heterozygous mutation of the type II collagen gene (*COL2A1*), however, most cases are attributed to sporadic mutations. Reports on the prenatal diagnosis of Kniest dysplasia have been very limited.

The routine use of ultrasonography in obstetric management has apparently increased occasions of encountering fetal skeletal dysplasias. The technical development of ultrasonography has continuously improved the diagnostic accuracy for these disorders *in utero* [2]. However, a precise diagnosis is not necessarily warranted by ultrasonography alone; thus, guidelines for the prenatal diagnosis of fetal skeletal dysplasias have emphasized combined use of multi-modalities, including *in-utero* radiography, fetal magnetic resonance imaging (MRI), three-dimensional ultrasonography, and genetic testing [3]. Recently, fetal three-dimensional helical computed tomography (3D-CT) has been introduced as a powerful tool for the prenatal diagnosis of skeletal dysplasias [4–6]. Accurate diagnosis accomplished with fetal 3D-CT has been shown to help perinatal management and genetic counseling.

We report here on the first case in which fetal 3D-CT warranted a prenatal diagnosis of Kniset dysplasia caused by a *de novo COL2A1* mutation. Fetal ultrasonography at 24 weeks' gestation did not provide optimal images for the definitive diagnosis, while fetal 3D-CT at 28 weeks' gestation did. The diagnosis was postnatally confirmed on radiological and molecular grounds.

Case report

A 23-year-old Japanese primigravida was referred at 24 weeks' gestation because of fetal limb shortening found with ultrasonography. Fetal parameters measured by ultrasonography were biparietal diameter (BPD) 64.4 mm (−0.2 SD), femoral length (FL) 32.6 mm (−3.8 SD), humeral length

Copyright Informa Healthcare 2010
Not for Sale or Commercial Distribution
Unauthorized use prohibited. Authorized users can download, display, view and print a single copy for personal use.

(Received 2 December 2009; revised 23 June 2010; accepted 19 November 2010)

Correspondence: Hideaki Sawai, Department of Obstetrics and Gynecology, Hyogo College of Medicine, 1-1 Mukogawa-cho, Nishinomiya-shi, 663-8501 Japan. Tel: +81-798-45-6481. Fax: +81-798-46-4163. E-mail: sawai@hyo-med.ac.jp

J Matern Fetal Neonatal Med Downloaded from informahealthcare.com by 210.190.246.185 on 01/21/11
For personal use only.

(HL) 30.5 mm (-4.5 SD), fetal trunk area (FTA) 35.9 cm^2, and estimated fetal body weight (EFBW) 756 g (-1.2 SD). The fetal thorax was deemed to be slightly hypoplastic. An amniotic fluid index (AFI) exceeding 27 cm constituted the diagnosis of polyhydramnios at 24 weeks' gestation. Other findings, including abnormal facial and head profiles with a short and flat nose, did not help make the diagnosis definite. The limb shortening was not so severe as to consider a lethal skeletal dysplasia [7], and the overall ultrasonographic findings strongly indicated a diagnosis of achondroplasia. However, polyhydramnios at 24 weeks' gestation was considered uncommon in achondroplasia. Thus, fetal 3D-CT was planned to obtain further information. We also offered chromosomal analysis by amniocentesis to the couple, but they did not agree with genetic examination.

At 28 weeks' gestation, fetal 3D-CT was performed after informed consent. Fetal 3D-CT images were obtained using a 16 slice scanner (SOMATOM Sensation 16-Slice Cardiac CT Scanner; Siemens) with 12.39 mGy of the CT dose index volume (CTDIvol). CT images were obtained using volume rendering with three-dimensional reconstruction (3D-VR) and maximum intensity projection (MIP). The 3D-VR images showed platyspondyly, limb shortening, and a dumbbell appearance of the tubular bones (Figure 1a). MIP images revealed a coronal cleft of the 4th lumber vertebral body and facilitated identification of the dumbbell deformity (Figure 1b, c). Given these findings, a diagnosis of Kniest dysplasia was the most plausible diagnosis. Since Kniest dysplasia is not associated with bone fragility or macrocephaly, we concluded that the vaginal delivery would be possible and safe for the fetus, and the couple also agreed this decision. We then repeated amniocentesis with withdrawal of amniotic fluid to reduce polyhydramnios.

A female neonate was vaginally delivered following spontaneous onset of labor pain at 37 weeks' gestation. Birth weight was 2863 g and length 40.8 cm. Apgar score at 5 min was 6, but the newborn progressed quickly to respiratory distress requiring intubation, and then artificial ventilation was carried out for 10 days. Physical findings included a flat mid-face, depressed nasal bridge, micrognathia with cleft palate, and micromelia. Hearing impairment was noted later on brainstem auditory evoked response. The radiological findings were identical with those on the previous fetal 3D-CT; i.e., broad thorax, platyspondyly, dumbbell appearance of the long bones, coronal cleft of the 4th lumber vertebral body and broad ilia with hypoplasia of the basilar portion (trefoil-shaped pelvis) (Figure 2a, b). However, flat and deformed vertebral bodies with anterior wedging were severer than expected based on the fetal 3D-CT imaging. A diagnosis of Kniest dysplasia was made, but dyssegmental dysplasia Rolland–Desbuquois type was not completely excluded. Genetic testing for *COL2A1* revealed a *de novo* mutation of A–C transversion in the splicing acceptor site of intron 16 (Figure 3) and confirmed the diagnosis of Kniest dysplasia.

Discussion

Ultrasonography has played a central role in the prenatal diagnosis of skeletal dysplasias in the second or third trimesters of pregnancy. However, conventional two-dimensional ultrasonography has provided limited diagnostic success, with only 50–68% of cases being accurately diagnosed [7,8]. The accuracy may decline when we have to address a very rare disorder with no family history [9]. A systemic approach to the fetal skeleton with conventional ultrasonography enables one to identify shortening and/or curvature (bowing) of the limbs, bone fractures, thoracic

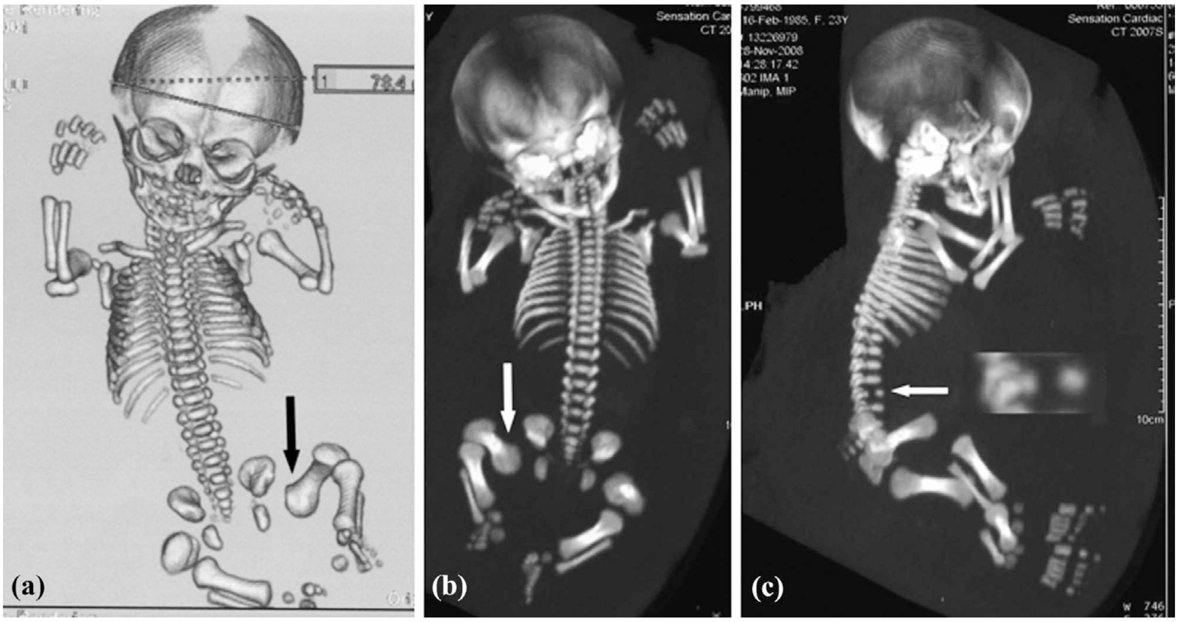

Figure 1. Images of helical CT of the fetus. (a) Frontal image of 3D-VR showing platyspondyly, shortness of the limbs and dumbbell appearance (an arrow) of tubular bones. (b) Frontal image of MIP showing prominent broad metaphyses (an arrow) resulting from splaying, which strongly suggested a diagnosis of Kniest dysplasia. (c) Lateral image of MIP showing coronal cleft in the 4th lumber vertebral body (an arrow) and prominent broad metaphyses. Magnification of the coronal cleft is shown to the right of the arrow.

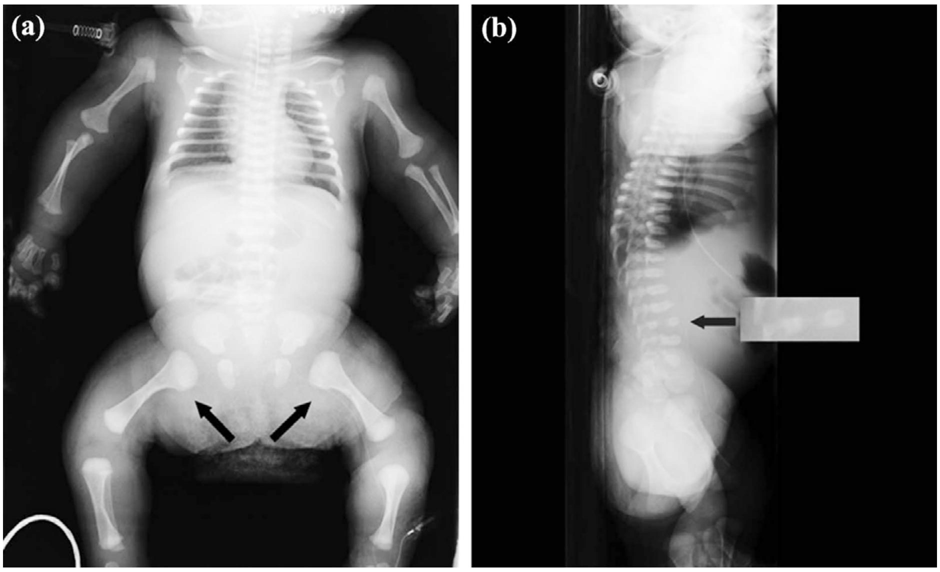

Figure 2. Standard radiographs after birth. (a) Frontal image showing relative broad thorax, platyspondyly, shortness of the limbs, short femora and dumbbell appearance (an arrow) of tubular bones, and broad ilia with hypoplasia of basilar portion (trefoil-shaped pelvis). (b) Lateral image showing prominent splaying of metaphyses of femora, coronal cleft in the 4th lumber vertebral body (an arrow). Magnification of the coronal cleft is shown to the right of the arrow.

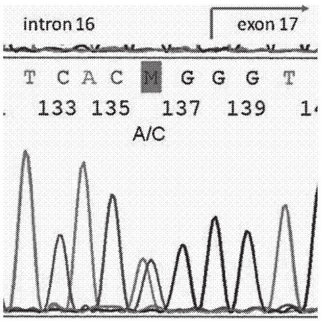

Figure 3. Sequencing analysis of the *COL2A1* gene showing AG to CG mutation in the splicing acceptor site of intron 16. In the absence of this mutation, exon 17 would start at the next codon G (blue arrow).

hypoplasia, presence of scapulae and clavicles, and decreased bone density (hypomineralization) in fetal skeletal dysplasias [10]. However, certain anatomical parts, such as the vertebral column and pelvic bones are difficult to evaluate, and several specific findings, such as stippled epiphyses, may be overlooked [9]. In the present case, ultrasonography displayed only moderate shortening of the limbs, mild thoracic hypoplasia, and abnormal facial profiles and we were not able to make a definitive diagnosis of Kniest dysplasia.

There have been very few reports on prenatal diagnosis of Kniest dysplasia. Only three cases have been reported in the literature [11–13]. Bromley et al. first reported the prenatal sonographic features of an affected fetus in the second trimester, but did not reach a diagnosis of Kniest dysplasia [11]. The diagnostic difficulty was attributed to the incomplete development of the skeletal alterations of the disorder in the second trimester, other than slightly short long bones. Kerleroux et al. also described the difficultly of making an antenatal diagnosis of Kniest dysplasia particularly because the disorder is similar to spondyloepiphyseal dysplasia congenita [12]. Cuiller et al. employed not only standard ultrasonography but also 3D ultrasonography, and they were able to conclude that the fetus had a severe, but non-lethal, skeletal dysplasia, most probably Kniest dysplasia, based on their findings with 3D ultrasonography [13]. However, they also commented on the diagnostic limitation of conventional ultrasonography.

As in the present case, abnormal facial and head profiles with a short and flat nose, no frontal bossing, normal BPD, and mild to moderate shortening of the limbs are common ultrasound findings of Kniest dysplasia in previous reports. By contrast, straight or bent long bones, absence or presence of polyhydramnios, and normal to mild hypoplastic thorax are variable among reported cases. To ascertain the diagnosis of Kniest dysplasia, it is necessary to rely on the skeletal hallmarks of the disorder; i.e., coronal clefts, platyspondyly, severe metaphyseal flaring (a dumbbell-shaped appearance) of the long bones, and broad ilia with hypoplasia of the basilar portion (trefoil-shaped pelvis). In our case, we were able to identify a coronal cleft on the fetal 3D-CT, which pointed to a diagnosis of Kniest dysplasia. Coronal clefts are observed not only in Kniest dysplasia (63%) but also in other bone dysplasias; e.g., in atelosteogenesis (88%), chondrodysplasia punctata (79%), dyssegmental dysplasia (73%), and short rib polydactyly syndrome (73%) [14]. However, 3D-CT clearly delineated other skeletal hallmarks of Kniest dysplasia and eventually led to a definitive diagnosis. In general, ultrasonography often fails to identify platyspondyly even when the examination was conducted with experienced ultrasound operators [10]. Identification of coronal clefts of the vertebral body and exact assessment of pelvic deformity may also be beyond the diagnostic capability of ultrasonography.

We have already reported on the usefulness of fetal 3D-CT, where based on short limbs, hypoplastic lung and macrocephaly, it was possible to diagnose thanatophoric dysplasia [6]. Fetal 3D-CT can also identify fetal skeletal dysplasias more

J Matern Fetal Neonatal Med Downloaded from informahealthcare.com by 210.190.246.185 on 01/21/11
For personal use only.

accurately (73–94%) than standard ultrasonography [8,9]. MIP and 3D-VR are the image-processing techniques most commonly used current 3D-CT imaging. As shown in Figure 1, 3D-VR is helpful in observing the global structure of the skeleton. On the other hand, MIP is useful in precise observation of each bone. In our case, MIP imaging was similar to postnatal radiographs (Figures 1b and 2a). The use of both techniques is recommended since this result in exquisite imaging and reliable interpretation. Two-dimensional multiplanar reformatted imaging (MPR) may also be done to preclude overlooking subtle changes in a fetus. However, we have to emphasize that image smoothing associated with image processing may underestimate certain skeletal changes, such as deformity of the vertebral bodies, as exemplified in our case.

In the present case, we needed to make a differential diagnosis between Kniest dysplasia and dyssegmental dysplasia Rolland–Desbuquois type both prenatally and postnatally. Dyssegmental dysplasia is an autosomal recessive (AR) disorder caused by mutations of the perlecan gene. The radiological hallmarks, including platyspondyly with multiple coronal clefts and dumbbell-shaped tubular bones, overlap with those of Kniest dysplasia. Yet, coronal clefts are more severe in dyssegmental dysplasia than those in Kniest dysplasia [1]. In addition, the vertebral bodies in dyssegmental dysplasia are often irregular in shape and size, the finding of which is termed anisospondyly. In our case irregularly shaped vertebral bodies were somewhat prominent. Since differential diagnosis between dyssegmental dysplasia and Kniest dysplasias is important for genetic counseling because of different modes of inheritance (AR *vs.* AD), we performed a molecular analysis to detect mutations in *COL2A1* in the present child. Heterozygous mutations of *COL2A1* cause several clinical entities collectively termed type II collagenopathies, including Kniest dysplasia, Stickler dysplasia type 1, and spondyloepiphyseal dysplasia with variable severity [15]. Most cases of Kniest dysplasia are caused by exon skipping due to splice-site mutations in the triple helical region of *COL2A1* [15]. The mutation of A–C transversion in the splicing acceptor site of intron 16 found in the present patient was novel and presumed to cause exon 17 skipping (Figure 3).

In conclusion, we have reported a sporadic case of Kniest dysplasia successfully diagnosed *in utero* with fetal 3D-CT. The diagnosis was confirmed by genetic testing after birth. Fetal 3D-CT is a powerful tool in the diagnosis of fetal skeletal dysplasias when ultrasound diagnosis is inconclusive. In addition to the 3D-VR technique commonly utilized with 3D-CT, the MIP technique is essential to evaluate anatomical details in congenital skeletal dysplasias.

J Matern Fetal Neonatal Med Downloaded from informahealthcare.com by 210.190.246.185 on 01/21/11
For personal use only.

Acknowledgements

The authors acknowledge Dr. Osamu Miyazaki for suggestion of the parameters description of fetal 3D-CT and Dr. Jun Murotsuki for arrangement of discussion. The authors thank Gregory H. Smith for helping in the preparation of this manuscript.

Declaration of interest: This report is supported by Grant-in-aid for Scientific Research from the Ministry of Health, Labour and Welfare of Japan, H22-Nanchi-Ippan-046.

References

1. Spranger JW, Brill PW, Poznanski AB. Bone dysplasias: an atlas of genetic disorders of skeletal development.2nd ed. Oxford: Oxford University Press; 2002. pp 38–40, pp 155–159.
2. Krakow D, Alanay Y, Rimoin LP, Lin V, Wilcox WR, Lachman RS, Rimoin DL. Evaluation of prenatal-onset osteochondrodysplasias by ultrasonography: a retrospective and prospective analysis. Am J Med Genet A 2008;146:1917–1924.
3. Krakow D, Lachman RS, Rimoin DL. Guidelines for the prenatal diagnosis of fetal skeletal dysplasias. Genet Med 2009;11:127–133.
4. Bonnefoy O, Delbosc JM, Maugey-Laulom B, Lacombe D, Gaye D, Diard F. Prenatal diagnosis of hypochondroplasia: three-dimensional multislice computed tomography findings and molecular analysis. Fetal Diagn Ther 2006;21:18–21.
5. Miyazaki O, Nishimura G, Sago H, Watanabe N, Ebina S. Prenatal diagnosis of chondrodysplasia punctata tibia-metacarpal type using multidetector CT and three-dimensional reconstruction. Pediatr Radiol 2007;37:1151–1154.
6. Tsutsumi S, Sawai H, Nishimura G, Hayasaka K, Kurachi H. Prenatal diagnosis of thanatophoric dysplasia by 3-D helical computed tomography and genetic analysis. Fetal Diagn Ther 2008;24:420–424.
7. Schramm T, Gloning KP, Minderer S, Daumer-Haas C, Hörtnagel K, Nerlich A, Tutschek B. Prenatal sonographic diagnosis of skeletal dysplasias. Ultrasound Obstet Gynecol 2009;34:160–170.
8. Ruano R, Molho M, Roume J, Ville Y. Prenatal diagnosis of fetal skeletal dysplasias by combining two-dimensional and three-dimensional ultrasound and intrauterine three-dimensional helical computer tomography. Ultrasound Obstet Gynecol 2004;24:134–140.
9. Cassart M, Massez A, Cos T, Tecco L, Thomas D, Van Regemorter N, Avni F. Contribution of three-dimensional computed tomography in the assessment of fetal skeletal dysplasia. Ultrasound Obstet Gynecol 2007;29:537–543.
10. Dighe M, Fligner C, Cheng E, Warren B, Dubinsky T. Fetal skeletal dysplasia: an approach to diagnosis with illustrative cases. Radiographics 2008;28:1061–1077.
11. Bromley B, Miller W, Foster SC, Benacerraf BR. The prenatal sonographic features of Kniest syndrome. J Ultrasound Med 1991;10:705–707.
12. Kerleroux J, Roux MS, Cottin X. The difficulty of prenatal diagnosis of Kniest's disease. A propos of a case simulating congenital spondylo-epiphyseal dysplasia. J Gynecol Obstet Biol Reprod (Paris) 1994;23:69–74.
13. Cuillier F, Cartault F, Chaitali Shah, Lemaire P, Alessandri JL. Kniest syndrome. Internet. 2004. In: The Fetus net. Electronic Citation. http://www.thefetus.net/page.php?id=1397 via the INTERNET. Last accessed 2 December 2009.
14. Westvik J, Lachman RS. Coronal and sagittal clefts in skeletal dysplasias. Pediatr Radiol 1998;28:764–770.
15. Nishimura G, Haga N, Kitoh H, Tanaka Y, Sonoda T, Kitamura M, Shirahama S, Itoh T, Nakashima E, Ohashi H, Ikegawa S. The phenotypic spectrum of COL2A1 mutations. Hum Mutat 2005;26:36–43.

RIGHTSLINK

THE JOURNAL OF
Obstetrics and Gynaecology Research

The official Journal of Asia and Oceania Federation of Obstetrics and Gynaecology
Japan Society of Obstetrics and Gynecology

doi:10.1111/j.1447-0756.2010.01324.x

J. Obstet. Gynaecol. Res. 2010

Prenatal diagnosis of short-rib polydactyly syndrome type 3 (Verma-Naumoff type) by three-dimensional helical computed tomography

Takahiro Yamada[1], Gen Nishimura[2], Keiichiro Nishida[3], Hideaki Sawai[4], Tokuhiko Omatsu[5], Taichi Kimura[6], Hiroshi Nishihara[6], Rina Shono[1], Shigeki Shimada[1], Mamoru Morikawa[1], Masato Mizushima[1], Takashi Yamada[1], Kazutoshi Cho[1], Shinya Tanaka[6], Hiroki Shirato[5] and Hisanori Minakami[1]

Departments of [1]Obstetrics and Gynecology, [5]Radiology, and [6]Molecular and Cellular Pathology, Hokkaido University Graduate School of Medicine, Sapporo, [2]Department of Radiology, Tokyo Metropolitan Kiyose Children's Hospital, Kiyose, [3]Department of Human Morphology, Okayama University Graduate School of Medicine and Dentistry, Okayama, and [4]Department of Obstetrics and Gynecology, Hyogo College of Medicine, Nishinomiya, Japan

Abstract

We present a case of short-rib polydactyly syndrome (SRPs) type 3 in which accurate prenatal diagnosis was feasible using both ultrasonography and 3D-CT. SRP encompass a heterogeneous group of lethal skeletal dysplasias. However, the phenotypes overlap with those of nonlethal skeletal dysplasias (i.e. Ellis-van Creveld syndrome and Jeune syndrome). As accurate prenatal diagnosis of SRP is helpful for parents, we used 3D-CT in the early third trimester to examine a fetus suggested to have phenotypes of 'short-rib dysplasia group' on ultrasonography. 3D-CT showed mild modification of the vertebral bodies, small ilia with horizontal acetabula and triangular partial ossification defects, and subtle metaphyseal irregularities of the femora. These CT findings and an extensive literature search regarding the phenotypes of various diseases categorized as short-rib dysplasia group led to a correct prenatal diagnosis of SRP type 3. This case exemplified the usefulness of 3D-CT for the precise prenatal diagnosis of skeletal dysplasias.

Key words: 3D-CT, asphyxiating thoracic dystrophy, Jeune syndrome, prenatal diagnosis, short-rib polydactyly syndrome.

Introduction

Short-rib polydactyly syndromes (SRPs) encompass a heterogeneous group of lethal skeletal dysplasias that are inherited in an autosomal recessive manner. SRPs are classified into four types: type 1 (Saldino-Noonan; OMIM 263530), type 2 (Majewski; OMIM 263520), type 3 (Verma-Naumoff; OMIM 263510), and type 4 (Beemer-Langer; OMIM 269860). Nosology and Classification of Genetic Skeletal Disorders: 2006 Revision lists these disorders as 'short-rib dysplasia (with or without polydactyly) group'.[1] The constellation of a severely narrow thorax, short limbs, and polydactyly allows prenatal diagnosis of SRPs with fetal ultrasonography. However, the phenotypes of SRPs overlap with those of nonlethal, but occasionally semilethal, skeletal dysplasias that belong to the short-rib dysplasia group (i.e. Ellis-van Creveld syndrome [EvC]; OMIM 225500]) and asphyxiating thoracic dystrophy ([ATD] Jeune syndrome; OMIM 208500). Recent reports have suggested the usefulness of three-dimensional helical computed tomography (3D-CT) in the differential diagnosis of skeletal disorders.[2] Here, we report a fetus with SRP type 3 diagnosed prenatally

---

Received: August 10 2009.
Accepted: February 5 2010.
Reprint request to: Dr Takahiro Yamada, Department of Obstetrics and Gynecology, Hokkaido University Graduate School of Medicine, N15W7 Kita-ku, Sapporo 060-8638, Japan. Email: taka0197@med.hokudai.ac.jp

© 2010 The Authors
Journal of Obstetrics and Gynaecology Research © 2010 Japan Society of Obstetrics and Gynecology

Table 1 Differential diagnosis and comparison between results of ultrasound, three-dimensional computed tomography (3D-CT), and postnatal examination of the fetus in the present case

	Present case				SRP1	SRP3	SRP2/4	ATD	EvCD
	Prenatal		Postnatal						
	Ultrasonography	3D-CT	Radiograph	Phenotype					
Head and face									
Macrocephaly	++	++	++	++	+	+	+	–	–
CNS abnormalities	–	NA	NA	–	+	+	+	–	+
Cleft lip	–	NA	NA	–	–	–	++	–	+
Shortened frenula	Unclear	NA	NA	++	++	++	++	–	+
High clavicles	Unclear	++	++	++	++	++	++	++	++
Bones									
Short limb	++	++	++	++	++	++	+	+	+
Polydactyly	++	++	++	++	++	++	++	+	++
Narrow thorax with short rib	++	++	++	++	++	++	++	+	+
Hypoplasia of tibia	–	–	–	–	–	–	++	–	–
Flaring of the metaphyses	+	++	++	++	–	++	–	–	–
Irregularity of the metaphyses	Unclear	+	+	+	+	+	–	+	–
Pointed metaphyses	Unclear	–	–	–	++	–	–	–	–
Spondylar dysplasia	Unclear	+	+	+	+	+	–	+	–
Hypoplasia of iliac bones	Unclear	++	++	++	++	++	–	++	++
Other organs									
Congenital heart defect	–	NA	NA	–	+	+	–	–	++
Renal abnormalities	–	NA	NA	+	+	+	+	+	–
Genital abnormalities	++	NA	NA	++	++	++	+	–	–

++, prominent; +, present; –, absent. CNS, central nervous system; NA, not applicable. This table is made based on findings of previous reports.[3,4,10,11]

based on fetal ultrasonography and additional 3D-CT. The present case represents another example indicating the powerful capability of 3D-CT in the prenatal diagnosis of fetal skeletal dysplasias.

Case Report

A 23-year-old primigravida was referred for further investigation of fetal short limbs at 28 weeks of gestation. She was in a non-consanguineous marriage and had neither relevant medical history nor significant family history. Ultrasonography of the fetus revealed a narrow and small thorax covering only the dorsal part of the viscera, short femora of 30 mm (–7.26 SD), short humeri of 29 mm (–6.27 SD), mild ulnar deviation of the hands, short digits, bilateral postaxial polydactyly in the hands and feet, and long biparietal diameter (BPD) of 79.0 mm (+2.7 SD) suggestive of macrocephaly. Bilateral renal dysplasia and penile hypoplasia were also suspected. The volume of amniotic fluid was normal. These findings suggested a lethal or semilethal skeletal dysplasia classified as belonging to the short-rib dysplasia group shown in Table 1. After obtaining informed consent, computed tomography (CT) was performed at 33 weeks of gestation with a 64-detector row CT scanner (Aquilion64; Toshiba Medical Systems, Tokyo, Japan) with the following parameters: collimation, 0.5 mm; peak tube potential, 100 kVP; gantry rotation time, 0.75 s; beam pitch, 53; and tube current between 260 and 335 mA using an automatic tube current modulation technique. The volume CT dose index (CTDIvol.) was 21.5 mGy. The data from the CT scanner were stored and transferred onto a workstation (ZIOSTATION; Ziosoft, Tokyo, Japan). Multiplanar reconstruction (MPR) and 3D reconstruction by shaded surface display (SSD) images of fetal bones were created and reviewed interactively on the workstation. They provided additional information, including high-rising clavicles, mild modification of the vertebral bodies, subtle metaphyseal irregularities of

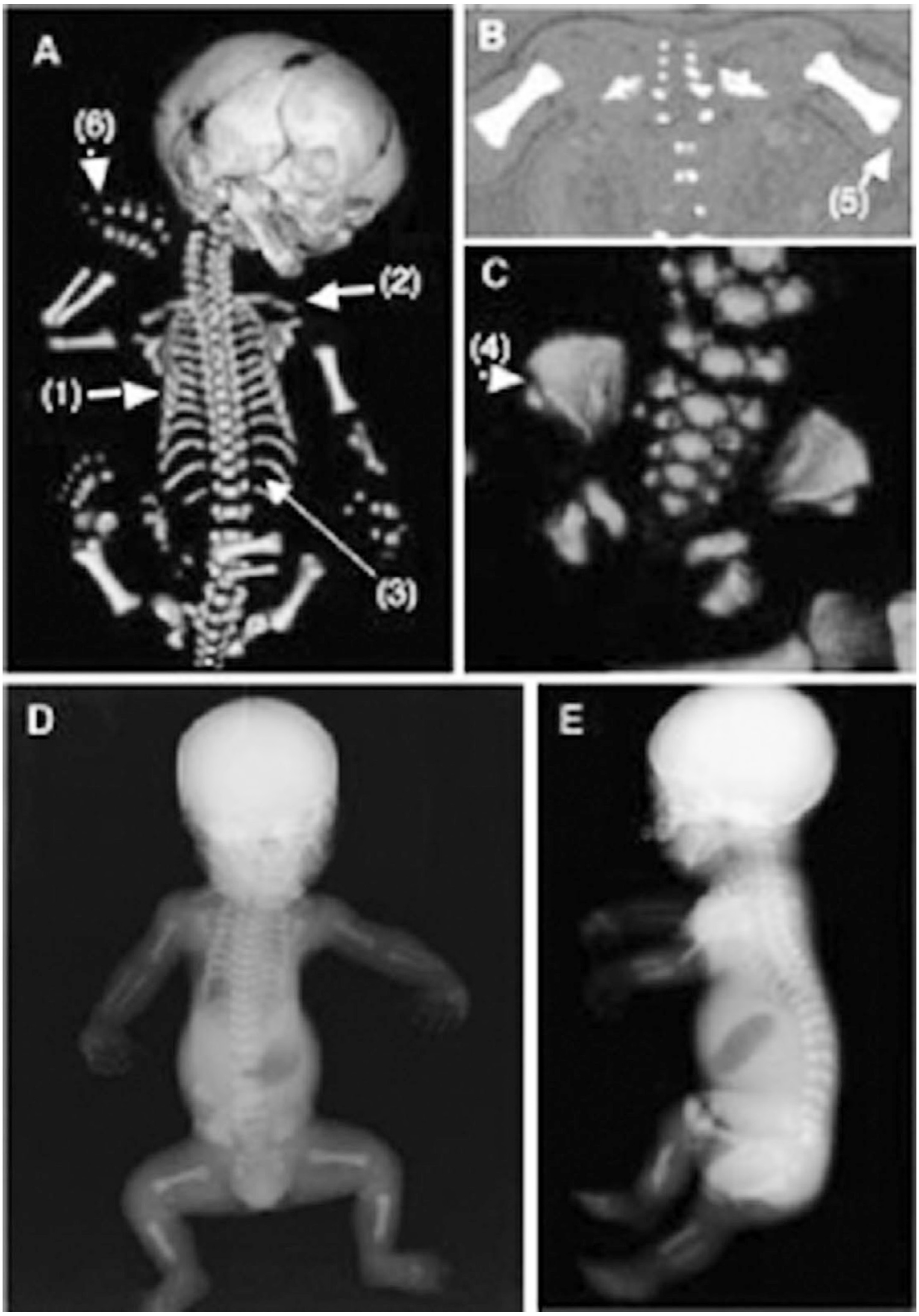

Figure 1 (a–c) Fetal computed tomography (CT) showed a narrow thorax (1), high-rising clavicles (2), mild modification of the vertebral bodies (3), small ilia with horizontal acetabula and triangular ossification defects at the inferior aspect of the lateral iliac margin (4), subtle metaphyseal irregularities of the femora (5), and brachydactyly with postaxial polydactyly (6). (d,e) Radiological findings on postnatal radiographs were identical to those of fetal CT.

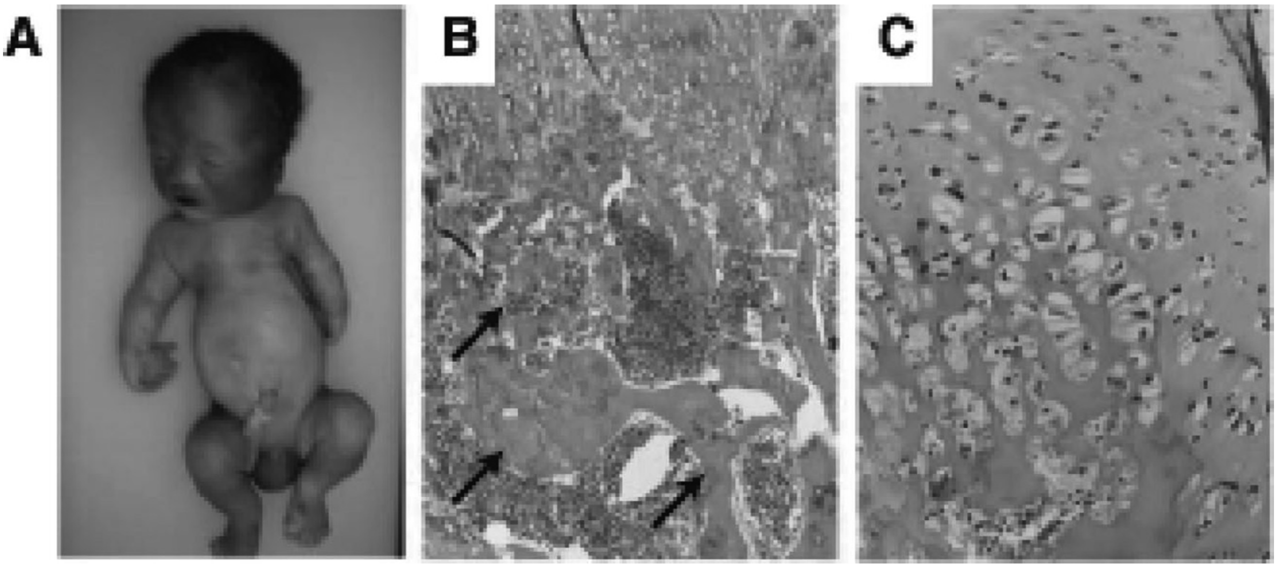

Figure 2 (a) Macroscopic view of the infant. The infant had macrocephaly, shortened frenula, club hands, polydactyly in the bilateral hands and feet, a bell-shaped narrow thorax, protruding abdomen, hypoplasia of the bilateral kidneys, bilateral dilated ureter, hydropic scrotum, and absent penis. (b,c) Histological findings of growth plate cartilage at costochondral junction. (b) There was loss of columnization with irregularly dispersed hypertrophic cells. The numbers of resting and hypertrophic chondrocytes were markedly reduced in some areas. Calcified cartilage islands (arrow). (c) Irregularly dispersed hypertrophic cells hypertrophic chondrocytes with PAS-stained cytoplasmic inclusion bodies in chondrocytes. HE stain (b). PAS stain (c). Original magnification ×50 (b), ×200 (c).

the femora, and hypoplasia of iliac bones (Fig. 1a,b,c). The acetabular roofs were horizontal and arched with triangular ossification defects at the inferior aspect of the lateral iliac margin (Fig. 1c). After 3D-CT, a diagnosis of SRP type 3 was made prenatally based on Table 1. The parents chose cesarean section even after receiving full information regarding SRP type 3, and a male infant weighing 2328 g was delivered (Fig. 2a). The infant died of respiratory failure 3 h after birth. The skeletal manifestations on postmortem radiographs corresponded to those seen on 3D-CT (Fig. 1d,e; Table 1).

Macroscopic pathological examination at autopsy showed lung hypoplasia (left lung, 7.6 g; right lung, 10.0 g; lung/body weight ratio, 0.75%), hypoplasia of the bilateral kidneys, bilateral dilated ureter, hydropic scrotum, and absent penis (Fig. 2a). Chromosomal analysis using cultured lymphoblasts from cord blood showed a normal 46,XY karyotype.

Histological examination of growth plate cartilage at the costochondral junction revealed reduced numbers of resting and hypertrophic chondrocytes, a disorganized hypertrophic zone with loss of columnization, residual cartilaginous nests in the metaphyseal trabeculae, and PAS-positive intracytoplasmic inclusion bodies. Dispersed hypertrophic chondrocytes were separated by the normal cartilaginous matrix, but not by the fibrous tissue. Notably, calcified cartilage islands were observed in the metaphyseal trabeculae, and some were continuous with the physis through a narrow bridge (Fig. 2b,c). All of these histological findings were consistent with those of SRP type 3.[3–5]

Discussion

Measurement of fetal size, including femoral length, is currently a routine practice in obstetrics, facilitating identification of skeletal dysplasias with short limbs. Once limb shortening is identified, the subsequent diagnostic task involves assessment of the thorax to ascertain the presence or absence of thoracic hypoplasia, which allow determination of the clinical outcome of the fetus. Disorders that belong to the short-rib dysplasia group constitute a considerable portion of cases of skeletal dysplasia with thoracic hypoplasia. Prenatal diagnosis of short-rib dysplasia group using ultrasonography is feasible.[6–9] In the present case, the ultrasonography findings, including visceral anomalies, favored a diagnosis of SRP. However, detection of subtle skeletal abnormalities is generally difficult with ultrasonography. Additional information on subsequent 3D-CT and MPR, including mild spondylar dysplasia, subtle metaphyseal changes, and irregular ossification defects in the outer iliac margin, eventually led to a diagnosis of SRP type 3 in this case.

Differential diagnosis between SRP, ATD, and EvC is difficult.[10,11] Antenatal diagnosis of SRP subtypes also appears difficult as there have been reports of common abnormalities, such as macrocephaly and polydactyly, as shown in Table 1. However, meticulous formulation of imaging findings on ultrasonography and 3D-CT helped in the prenatal diagnosis of SRP type 3 in the present case (Table 1). 3D-CT is particularly useful to delineate the axial skeleton. Although 3D image reconstruction tends to conceal fine bone details, such as mild metaphyseal dysplasia, this drawback was compensated by MPR (Fig. 1b). We evaluated the general skeletal structures first by 3D image reconstruction, and then examined the fine bone details by MPR, in which we were able to view any 2D images of bones as MPR and 3D images without rescanning independent of the fetal presentation.

The histological observations in the present case supported the suggestion that ATD type 1 and SRP type 3 may belong to the spectrum of the same pathogenetic entity.[3–5] In fact, mutations of *DYNC2H1* have recently been reported as a common cause of ATD and SRP3.[12] However, mutations of *IFT80* have also been reported as a cause of ATD, indicating genetic heterogeneity.[13]

In summary, the present case further exemplified the diagnostic capability of precise prenatal diagnosis of skeletal dysplasia. As shown in Table 1, meticulous interpretation of ultrasonography and CT imaging findings enabled us to subclassify SRP. To our knowledge, this is the first report of prenatal diagnosis in this group using 3D-CT.

References

1. Superti-Furga A, Unger S, The Nosology Group of the International Skeletal Dysplasia Society. Nosology and classification of genetic skeletal disorders: 2006 revision. *Am J Med Genet A* 2007; **143**: 1–18.
2. Cassart M, Massez A, Cos T *et al*. Contribution of three-dimensional computed tomography in the assessment of fetal skeletal dysplasia. *Ultrasound Obstet Gynecol* 2007; **29**: 537–543.
3. Yang SS, Langer LO Jr, Cacciarelli A *et al*. Three conditions in neonatal asphyxiating thoracic dysplasia (Jeune) and short rib-polydactyly syndrome spectrum: a clinicopathologic study. *Am J Med Genet Suppl* 1987; **3**: 191–207.
4. Erzen M, Stanescu R, Stanescu V *et al*. Comparative histopathology of the growth cartilage in short-rib polydactyly syndromes type I and type III and in chondroectodermal dysplasia. *Ann Genet* 1988; **31**: 144–150.
5. Hentze S, Sergi C, Troeger J *et al*. Short-rib-polydactyly syndrome type Verma-Naumoff-Le Marec in a fetus with histological hallmarks of type Saldino-Noonan but lacking internal organ abnormalities. *Am J Med Genet* 1998; **80**: 281–285.
6. Meizner I, Barnhard Y. Short-rib polydactyly syndrome (SRPS) type III diagnosed during routine prenatal ultrasonographic screening. A case report. *Prenat Diagn* 1995; **15**: 665–668.
7. Hill LM, Leary J. Transvaginal sonographic diagnosis of short-rib polydactyly dysplasia at 13 weeks' gestation. *Prenat Diagn* 1998; **18**: 1198–1201.
8. den Hollander NS, Robben SG, Hoogeboom AJ *et al*. Early prenatal sonographic diagnosis and follow-up of Jeune syndrome. *Ultrasound Obstet Gynecol* 2001; **18**: 378–383.
9. Viora E, Sciarrone A, Bastonero S *et al*. Three-dimensional ultrasound evaluation of short-rib polydactyly syndrome type II in the second trimester: a case report. *Ultrasound Obstet Gynecol* 2002; **19**: 88–91.
10. Golombeck K, Jacobs VR, von Kaisenberg C *et al*. Short rib-polydactyly syndrome type III: comparison of ultrasound, radiology, and pathology findings. *Fetal Diagn Ther* 2001; **16**: 133–138.
11. Spranger JW, Brill PW, Poznanski A (eds). *Bone Dysplasias*, 2nd edn. München: Oxford University Press: 2002; 15–21, 125–138.
12. Dagoneau N, Goulet M, Geneviève D *et al*. DYNC2H1 mutations cause asphyxiating thoracic dystrophy and short rib-polydactyly syndrome, type III. *Am J Hum Genet* 2009; **84**: 706–711.
13. Beales PL, Bland E, Tobin JL *et al*. IFT80, which encodes a conserved intraflagellar transport protein, is mutated in Jeune asphyxiating thoracic dystrophy. *Nat Genet* 2007; **39**: 727–729.

© 2010 The Authors

Heterozygous Orthodenticle Homeobox 2 Mutations Are Associated with Variable Pituitary Phenotype

Sumito Dateki, Kitaro Kosaka, Kosei Hasegawa, Hiroyuki Tanaka, Noriyuki Azuma, Susumu Yokoya, Koji Muroya, Masanori Adachi, Toshihiro Tajima, Katsuaki Motomura, Eiichi Kinoshita, Hiroyuki Moriuchi, Naoko Sato, Maki Fukami, and Tsutomu Ogata

Department of Endocrinology and Metabolism (S.D., N.S., M.F., T.O.), National Research Institute for Child Health and Development, and Division of Ophthalmology (N.A.) and Department of Medical Subspecialties (S.Y.), National Children's Medical Center, Tokyo 157-8535, Japan; Department of Pediatrics (S.D., K.M., E.K., H.M.), Nagasaki University Graduate School of Biomedical Sciences, Nagasaki 852-8501, Japan; Department of Pediatrics (K.K.), Kyoto Prefectural University of Medicine, Graduate School of Medical Science, Kyoto 602-8566, Japan; Department of Pediatrics (K.H., H.T.), Okayama University Graduate School of Medicine, Dentistry, and Pharmaceutical Sciences, Okayama 700-8558, Japan; Division of Endocrinology and Metabolism (K.M., M.A.), Kanagawa Children's Medical Center, Yokohama 232-8555, Japan; and Department of Pediatrics (T.T.), Hokkaido University School of Medicine, Sapporo 060-8638, Japan

Context: Although recent studies have suggested a positive role of *OTX2* in pituitary as well as ocular development and function, detailed pituitary phenotypes in *OTX2* mutations and *OTX2* target genes for pituitary function other than *HESX1* and *POU1F1* remain to be determined.

Objective: We aimed to examine such unresolved issues.

Subjects: We studied 94 Japanese patients with various ocular or pituitary abnormalities.

Results: We identified heterozygous p.K74fsX103 in case 1, p.A72fsX86 in case 2, p.G188X in two unrelated cases (3 and 4), and a 2,860,561-bp microdeletion involving *OTX2* in case 5. Clinical studies revealed isolated GH deficiency in cases 1 and 5; combined pituitary hormone deficiency in case 3; abnormal pituitary structures in cases 1, 3, and 5; and apparently normal pituitary function in cases 2 and 4, together with ocular anomalies in cases 1–5. The wild-type Orthodenticle homeobox 2 (OTX2) protein transactivated the *GNRH1* promoter as well as the *HESX1*, *POU1F1*, and *IRBP* (interstitial retinoid-binding protein) promoters, whereas the p.K74fsX103-OTX2 and p.A72fsX86-OTX2 proteins had no transactivation functions and the p.G188X-OTX2 protein had reduced (~50%) transactivation functions for the four promoters, with no dominant-negative effect. cDNA screening identified positive *OTX2* expression in the hypothalamus.

Conclusions: The results imply that *OTX2* mutations are associated with variable pituitary phenotype, with no genotype-phenotype correlations, and that *OTX2* can transactivate *GNRH1* as well as *HESX1* and *POU1F1*. (***J Clin Endocrinol Metab* 95: 756–764, 2010)**

Pituitary development and function depends on the spatially and temporally controlled expression of multiple transcription factor genes such as *POU1F1*, *HESX1*, *LHX3*, *LHX4*, *PROP1*, and *SOX3* (1, 2). Whereas mutations of some genes (*e.g. POU1F1*) result in a relatively characteristic pattern of pituitary hormone deficiency, those of other genes (*e.g. HESX1*) are associated with a wide range of pituitary phenotype including combined pi-

---

ISSN Print 0021-972X ISSN Online 1945-7197
Printed in U.S.A.
Copyright © 2010 by The Endocrine Society
doi: 10.1210/jc.2009-1334 Received June 23, 2009. Accepted November 9, 2009.
First Published Online December 4, 2009

Abbreviations: CGH, Comparative genomic hybridization; CPHD, combined pituitary hormone deficiency; EPP, ectopic posterior pituitary; FISH, fluorescence *in situ* hybridization; HD, homeodomain; IGHD, isolated GH deficiency; IRBP, interstitial retinoid-binding protein; MLPA, multiplex ligation-dependent probe amplification; NMD, nonsense mediated mRNA decay; OTX2, orthodenticle homeobox 2; PH, pituitary hypoplasia; SOD, septooptic dysplasia; TD, transactivation domain.

tuitary hormone deficiency (CPHD), isolated GH deficiency (IGHD), and apparently normal phenotype. However, because mutations of these genes account for a relatively minor portion of patients with congenital hypopituitarism (2, 3), multiple genes would remain to be identified in congenital hypopituitarism.

Orthodenticle homeobox 2 (*OTX2*) is a transcription factor gene primarily involved in ocular development (4). It encodes a paired type homeodomain (HD) and a transactivation domain (TD) and produces two functionally similar splice variants, isoform-a (GenBank accession no. NM_21728.2) and isoform-b (NM_172337.1) with and without eight amino acids because of alternative splice acceptor sites at the boundary of intron 3 and exon 4 (5). To date, at least 10 pathological heterozygous *OTX2* mutations have been identified in patients with ocular malformations such as anophthalmia and/or microphthalmia (6, 7). Ocular phenotype is highly variable, ranging from anophthalmia to nearly normal eye development, even in patients from the same family. Furthermore, most patients also exhibit brain anomaly, seizure, and/or developmental delay.

Recent studies have indicated that *OTX2* is also involved in pituitary development and function. Dateki *et al.* (8) showed that *OTX2* is expressed in the pituitary and has a transactivation function for the promoters of *POU1F1* and *HESX1* as well as the promoter of *IRBP* (interstitial retinoid-binding protein) involved in ocular function and that a frameshift *OTX2* mutation identified in a patient with bilateral anophthalmia and partial IGHD barely retained the transactivation activities. Subsequently a missense *OTX2* mutation with a dominant-negative effect and a frameshift *OTX2* mutation with loss-of-function effect were identified in CPHD patients with and without ocular malformation (9, 10).

However, detailed pituitary phenotypes in *OTX2* mutation-positive patients as well as other possible *OTX2* target genes for pituitary development and function remain to be determined. Here we report five new patients with *OTX2* mutations and summarize clinical findings in *OTX2* mutation-positive patients. We also show that *OTX2* is expressed in the hypothalamus and has a transactivation function for the promoter of *GNRH1*.

Patients and Methods

Patients

We studied 94 Japanese patients consisting of: 1) 16 patients with ocular anomalies and pituitary dysfunctions accompanied by short stature (<−2 SD) (six with anophthalmia and/or microphthalmia and CPHD, five with anophthalmia and/or microphthalmia and IGHD, three with septooptic dysplasia (SOD) and CPHD, and two with SOD and IGHD) (group 1); 2) 12 patients with ocular anomalies whose pituitary functions were not investigated (one with bilateral microphthalmia and short stature, one with bilateral optic nerve hypoplasia and short stature, and 10 with anophthalmia and/or microphthalmia and normal stature) (group 2); and 3) 66 patients with pituitary dysfunctions but without ocular anomalies (five with IGHD and 61 patients with CPHD) (group 3). No demonstrable mutation was identified for *HESX1* in patients with SOD, *GH1* and *HESX1* in patients with IGHD, and *POU1F*, *HESX1*, *LHX3*, *LHX4*, *PROP1*, and *SOX3* in patients with various types of CPHD (2). All the patients had normal karyotype.

Primers and probes

The primers and probes used in this study are shown in Supplemental Table 1, published as supplemental data on The Endocrine Society's Journals Online web site at http://jcem.endojournals.org.

Sequence analysis of OTX2

This study was approved by the Institutional Review Board Committee at National Center for Child Health and Development. After obtaining written informed consent, the coding exons 3-5 and their flanking splice sites were PCR amplified using leukocyte genomic DNA samples of all 94 patients and were subjected to direct sequencing on a CEQ 8000 autosequencer (Beckman Coulter, Fullerton, CA). To confirm a heterozygous mutation, the corresponding PCR products were subcloned with TOPO TA cloning kit (Invitrogen, Carlsbad, CA), and normal and mutant alleles were sequenced separately.

Prediction of the occurrence of aberrant splicing and nonsense mediated mRNA decay (NMD)

To examine whether identified mutations could cause aberrant splicing by creating or disrupting exonic splicing enhancers and/or splice sites (11, 12), we performed *in silico* analyses with the ESE finder release 3.0 (http://rulai.cshl.edu/cgi-bin/tools/ESE3/esefinder.cgi) for the prediction of exonic splice enhancers and with the program at the Berkeley Drosophila Genome Project (http://www.fruitfly.org/seq_tools/splice.html) for the prediction of splice sites. We also analyzed whether identified mutations could be subject to NMD on the basis of the previous report (12, 13).

Deletion analysis

Multiplex ligation-dependent probe amplification (MLPA) was performed for *OTX2* intragenic mutation-negative patients as a screening of a possible microdeletion affecting *OTX2*. This procedure was performed according to the manufacturer's instructions (14), using probes designed specifically for *OTX2* exon 4 together with a commercially available MLPA probe mix (P236) (MRC-Holland, Amsterdam, The Netherlands) used as internal controls. To confirm a microdeletion, fluorescence *in situ* hybridization (FISH) was performed with a long PCR product for *OTX2* (a 6096 bp segment from intron 2 to exon 5) together with an RP11-566I2 BAC probe (14q11.2; Invitrogen, Carlsbad, CA) used as an internal control. The probe for *OTX2* was labeled with digoxigenin and detected by rhodamine anti-digoxigenin, and the control probe was labeled with biotin and

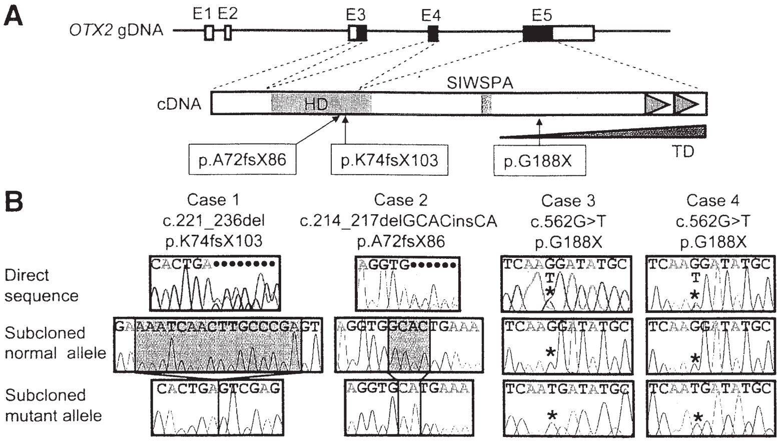

FIG. 1. Sequence analysis in cases 1–4. A, The structure of *OTX2* (the isoform-b) and the position of the mutations identified. The *black* and *white boxes* on genomic DNA (gDNA) denote the coding regions on exons 1-5 (E1-E5) and the untranslated regions, respectively. *OTX2* encodes the HD (a *blue region*), the SIWSPA conserved motif (an *orange region*), and the two tandem tail motifs (*green triangles*). The TD (a *gray triangle*) is assigned to the C-terminal side; deletion of each tail motif reduces the transactivation function, and that of a region distal to the SIWSPA motif further reduces the transactivation function. In addition, another TD may also reside in the 5′ side of the HD (17). The three mutations identified in this study are shown. B, Electrochromatograms showing the mutations in cases 1–4. Shown are the direct sequences and subcloned normal and mutant sequences. The deleted sequences are shaded in *gray*, and the inserted sequence is highlighted in *yellow*. The mutant and the corresponding wild-type nucleotides are indicated by *red asterisks*.

detected by avidin conjugated to fluorescein isothiocyanate. To indicate an extent of a microdeletion, oligoarray comparative genomic hybridization (CGH) was carried out with 1×244K human genome array (catalog no. G4411B; Agilent Technologies, Palo Alto, CA), according to the manufacturer's protocol. Finally, to characterize a microdeletion, long PCR was performed with primer pairs flanking the deleted region, and a long PCR product was subjected to direct sequencing using serial sequence primers. The deletion size and the junction structure were determined by comparing the obtained sequences with the reference sequences at the National Center for Biotechnology Information Database (NC_000014.7; Bethesda, MD), and the presence or absence of repeat sequences around the breakpoints was examined with Repeatmasker (http://www.repeatmasker.org).

Functional studies

Western blot analysis, subcellular localization analysis, DNA binding analysis, and transactivation analysis were performed by the previously reported methods (8) (for details, see Supplemental Methods). In this study, we used the previously reported expression vector and fluorescent vector containing the wild-type *OTX2* cDNA; the probes with the wild-type and mutated OTX2 binding sites within the *IRBP*, *HESX1*, and *POU1F1* promoter sequences; and the luciferase reporter vectors containing the *IRBP*, *HESX1*, and *POU1F1* promoter sequences (8). We further created expression vectors and fluorescent vectors containing mutant *OTX2* cDNAs by site-directed mutagenesis using Prime STAR mutagenesis basal kit (Takara, Otsu, Japan), and constructed a 30-bp probe with wild-type (TAATCT) and mutated (TGGGCT) putative OTX2 binding site within the *GNRH1* promoter sequence and a luciferase reporter vector containing the *GNRH1* promoter sequence (−1349 to −1132 bp) by inserting the corresponding sequence into pGL3 basic. The *GNRH1* promoter sequence was based on the report of Kelley *et al.* (15). Transfections were performed in triplicate within a single experiment, and the experiment was repeated three times.

PCR-based expression analysis of *OTX2*

Human cDNA samples were purchased from CLONTECH (Palo, Alto, CA) except for leukocyte and skin fibroblast cDNA samples that were prepared with Superscript III reverse transcriptase (Invitrogen). PCR amplification was performed for the cDNA samples (0.5 ng), using the primers hybridizing to exon 3 and 4 of *OTX2* and those hybridizing to exons 2/3 and 4/5 (boundaries) of *GAPDH* used as an internal control.

Results

Identification of mutations and substitutions

Three novel heterozygous *OTX2* mutations were identified in four cases, *i.e.* a 16-bp deletion at exon 4 that is predicted to cause a frameshift at the 74th codon for lysine and resultant termination at the 103rd codon (c.221_236del16, p.K74fsX103) in case 1; a 4-bp deletion and a 2-bp insertion at exon 4 that is predicted to cause a frame shift at the 72nd codon for alanine and resultant termination at the 86th codon (c.214_217delGCACinsCA, p.A72fsX86) in case 2; and a nonsense mutation at exon 5 that is predicted to cause a substitution of the 188th glycine with stop codon (c.562G>T, p.G188X) in two unrelated cases (3 and 4; Fig. 1). In addition, heterozygous missense substitutions were identified in patient 1 (c.532A>T, p.T178S) and patient 2 (c.734C>T, p.A245V). Cases 1 and 3 were from group 1, cases 2 and 4 and patient 2 were from group 2, and patient 1 was from group 3. Parental analysis indicated that frameshift mutations in cases 1 and 2 were absent from the parents (*de novo* mutations), whereas the missense substitution of patient 2 was inherited from phenotypically normal father. The parents of cases 3 and 4 and patient 1 refused molecular studies. All the mutations and the missense substitutions were absent from 100 control subjects.

Prediction of the occurrence of aberrant splicing and NMD

The two frameshift mutations and the nonsense mutation were predicted to influence neither exonic splice enhancers nor splice donor and acceptor sites (Supplemental Tables 2 and 3). Furthermore, the two frameshift mutations were predicted to produce the premature termination codons on the mRNA transcribed from the last exon

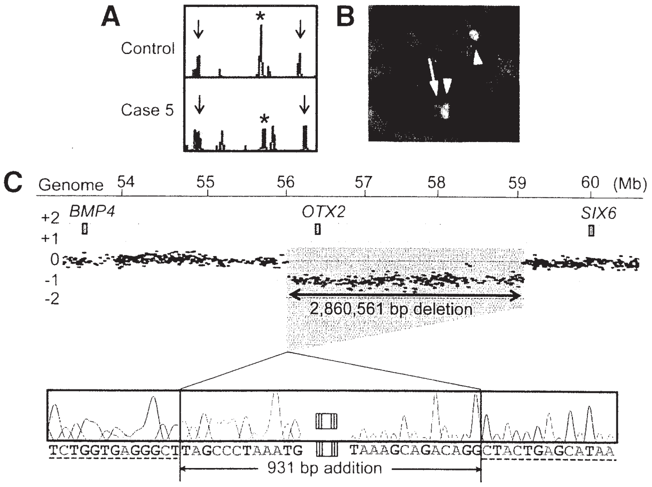
A
Control
Case 5
B
C
Genome 54 55 56 57 58 59 60 (Mb)
BMP4
OTX2
SIX6
+2
+1
0
-1
-2
2,860,561 bp deletion
TCTGGTGAGGGCTTAGCCCTAAATG TAAAGCAGACAGGCTACTGAGCATAA
931 bp addition

FIG. 2. Deletion analysis in case 5. A, MLPA analysis. The *red asterisk* indicates peaks for the *OTX2* exon 4, and the *black arrows* indicate control peaks. The *red peaks* indicate the internal size markers. Deletion of the MLPA probe binding site is indicated by the reduced peak height. B, FISH analysis. The probe for *OTX2* detects only a *single red signal* (an *arrow*), whereas the RP11-566I2 BAC probe identifies *two green signals* (*arrowheads*). C, Oligoarray CGH analysis and direct sequencing of the deletion junction. The deletion is 2,860,561 bp in physical size (shaded in *gray*) and is associated with an addition of a 931-bp segment (highlighted in *yellow*). The normal sequences flanking the microdeletion are indicated with *dashed underlines*.

5, indicating that the frameshift mutations as well as the nonsense mutation had the property to escape NMD (Supplemental Fig. 1).

Identification of a microdeletion

A heterozygous microdeletion affecting *OTX2* was indicated by MLPA and confirmed by FISH in case 5 of group 1 (Fig. 2, A and B). Oligoarray CGH delineated an approximately 2.9-Mb deletion, and sequencing of the fusion point showed that the microdeletion was 2,860,561 bp in physical size (56,006,531–58,867,091 bp on the NC_000014.7) and was associated with an addition of a complex 931-bp segment consisting of the following structures (cen → tel): 2 bp (TA) insertion → 895 bp sequence identical with that in a region just centromeric to the microdeletion (55, 911, 347–55, 912, 241 bp) → 1 bp (C) insertion → 33-bp sequence identical with that within the deleted region (58, 749, 744–58, 749, 776 bp) (Fig. 2C). Repeat sequences were absent around the break points. This microdeletion was not detected in DNA from the parents.

Functional studies of the wild-type and mutant OTX2 proteins

Western blot analysis detected wild-type OTX2 protein of 31.6 kDa and mutant OTX2 proteins of 11.5 kDa (p.K74fsX103), 9.7 kDa (p.A72fsX86), and 15.4 kDa (p.G188X) (Fig. 3A). The molecular masses were as predicted from the mutations. The band intensity was comparable between the wild-type OTX2 protein and the p.G188X-OTX2 protein and was faint for the p.K74fsX103-OTX2 and p.A72fsX86-OTX2 proteins.

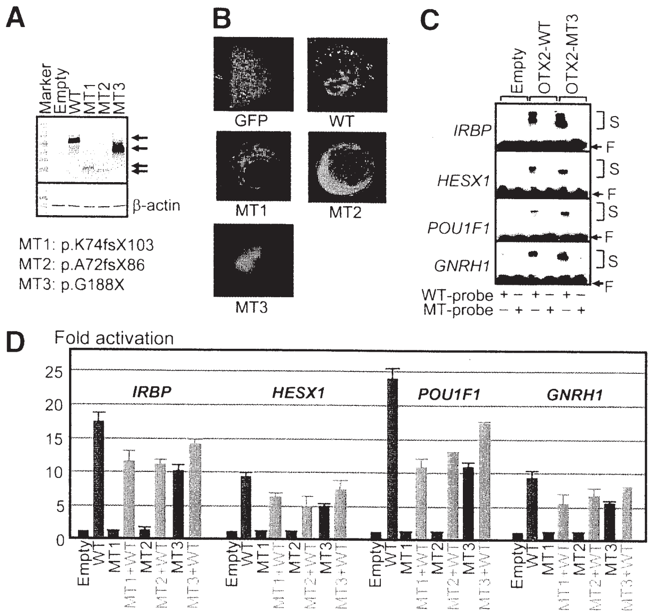

FIG. 3. Functional studies. A, Western blot analysis. Both WT and MT1-MT3 OTX2 proteins are detected with different molecular masses (*arrows*). WT, Wild type; MT1, p.K74fsX103; MT2, p.A72fsX86; and MT3, p.G188X. B, Subcellular localization analysis. Whereas green fluorescent protein (GFP) alone is diffusely distributed throughout the cell, the GFP-fused WT-OTX2 and MT3-OTX2 proteins localize to the nucleus. By contrast, the GFP-fused MT1-OTX2 and MT2-OTX2 proteins are incapable of localizing to the nucleus. C, DNA binding analysis using the wild-type (WT) and mutated (MT) probes derived from the promoters of *IRBP*, *HESX1*, *POU1F1*, and *GNRH1*. The symbols (+) and (−) indicate the presence and absence of the corresponding probes, respectively. Both WT and MT3 OTX2 proteins bind to the WT but not the MT probes. For the probe derived from the *IRBP* promoter, two shifted bands are found for both WT-OTX2 and MT3-OTX2 proteins as reported previously (17). S, Shifted bands; F, free probes. D, Transactivation analysis, using the promoter sequences of *IPBP*, *HESX1*, *POU1F1*, and *GNRH1*. The results are expressed using the mean and SD. The *black*, *blue*, *red*, and *green bars* indicate the data of the empty expression vectors (0.6 μg), expression vectors with WT *OTX2* cDNA (0.6 μg), expression vectors with MT1-MT3 *OTX2* cDNAs (0.6 μg), and the mixture of expression vectors with WT (0.3 μg) and those with MT1-MT3 *OTX2* cDNAs (0.3 μg), respectively; thus, the same amount of expression vectors has been used for each assay.

Subcellular localization analysis showed that the p.G188X-OTX2 protein localized to the nucleus as did the wild-type OTX2 protein, whereas the p.K74fsX103-OTX2 and p.A72fsX86-OTX2 proteins were incapable of localizing to the nucleus (Fig. 3B). The results were consistent with those of the Western blot analysis because nuclear extracts were used for the Western blotting, with some probable contamination of cytoplasm.

DNA binding analysis revealed that the p.G188X-OTX2 protein with nuclear localizing capacity bound to the wild-type OTX2 binding sites within the four promoters examined, including the *GNRH1* promoter, but not to the mutated OTX2 binding sites (Fig. 3C). The band shift

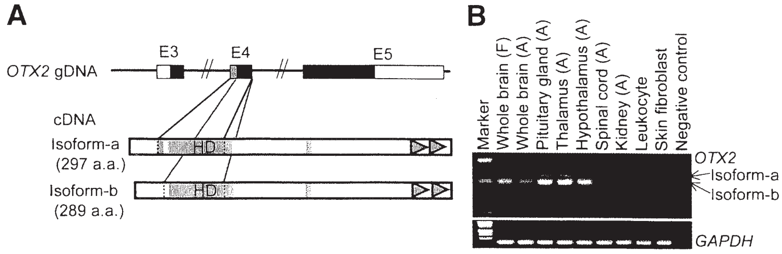

FIG. 4. PCR-based human cDNA library screening for *OTX2* (35 cycles). A, Schematic representation of the *OTX2* isoform-a (NM_21728.2) and isoform-b (NM_172337.1). Because of the two alternative splice acceptor sites at the boundary between intron 3 and exon 4, isoform-a carries eight amino acids (shown in *gray*) in the vicinity of the HD, whereas isoform-b is lacking the eight amino acids. B, PCR amplification data. *OTX2* is clearly expressed in the pituitary and hypothalamus, with isoform-b being the major product. *GAPDH* has been used as an internal control. F, Fetus; A, adult.

was more obvious for the wild-type OTX2 protein than for the p.G188X-OTX2 protein, consistent with the difference in the molecular masses.

Transactivation analysis showed that the wild-type OTX2 protein had transactivation activities for the four promoters examined including the *GNRH1* promoter, whereas the p.K74fsX103-OTX2 and p.A72fsX86-OTX2 proteins had virtually no transactivation function, and the p.G188X-OTX2 protein had reduced (~50%) transactivation activities (Fig. 3D). The three mutant OTX2 proteins had no dominant-negative effects. In addition, the two missense p.A245V-OTX2 and p.T178S-OTX2 proteins had apparently normal transactivation activities with no dominant-negative effect (Supplemental Fig. 2).

PCR-based expression analysis of *OTX2*

OTX2 expression was identified in the pituitary and the hypothalamus as well as in the brain and the thalamus but not detected in the spinal cord, kidney, leukocytes, and skin fibroblasts (Fig. 4). The isoform-b lacking the eight amino acids was predominantly expressed.

Clinical findings in *OTX2* mutation-positive patients

Clinical data are summarized in Table 1 (*left part*). Anophthalmia and/or microphthalmia was present in cases 1–5. Developmental delay was obvious in cases 1 and 3–5, whereas it was obscure in case 2 because of the young age. Prenatal growth was normally preserved in cases 1–5, whereas postnatal growth was compromised in cases 1, 3, and 5. Cases 1 and 5 had IGHD, and case 3 had CPHD (Table 2); furthermore, cases 1, 3, and 5 had pituitary hypoplasia (PH) and/or ectopic posterior pituitary (EPP) (Supplemental Fig. 3). Case 3 showed no pubertal development at 15 yr of age (Tanner pubic hair stage 2 in Japanese boys: 12.5 ± 0.9 yr) (16). Cases 2 and 4 had no discernible pituitary dysfunction and did not receive magnetic resonance imaging examinations. In addition, case 1 had right retractile testis. Patient 1 with p.T178S had CPHD but without ocular anomalies, and patient 2 with p.A245V had bilateral optic nerve hypoplasia and short stature.

Discussion

We identified two frameshift mutations in cases 1 and 2 and a nonsense mutation in unrelated cases 3 and 4. Furthermore, it was predicted that these mutations neither affected splice patterns nor underwent NMD, although direct analysis using mRNA was impossible due to lack of detectable *OTX2* expression in already collected leukocytes as well as skin fibroblasts, which might be available from cases 1–4. Thus, these mutations are predicted to produce aberrant OTX2 proteins *in vivo* that were used in the *in vitro* functional studies. In this context, the functional studies indicated that the two frameshift mutations were amorphic and the nonsense mutation was hypomorphic. The results are consistent with the previous notion that the HD not only has DNA binding capacity but also retains at least a part of nuclear localization signal on its C-terminal portion and the TD primarily resides in the C-terminal region (17) (Fig. 1A). Whereas the two missense substitutions were absent in 100 control subjects, they would be rare normal variations rather than pathological mutations because of the normal transactivation activities with no dominant-negative effect.

We also detected a heterozygous microdeletion involving *OTX2* in case 5 that was not mediated by repeat sequences. This implies the importance of the examination of a microdeletion. Indeed, such a cryptic microdeletion has been identified in multiple genes with the development of MLPA that can serve as a screening method in the detection of microdeletions (18). Whereas the microdeletion of case 5 has removed 16 additional genes (Ensembl Genome Browser, http://www.ensembl.org/), the clinical phenotype of case 5 is explainable by *OTX2* haploinsufficiency alone. Thus, hemizygosity for the 16 genes would not have a major clinical effect, if any.

Furthermore, the present study revealed two findings. First, *OTX2* was expressed in the hypothalamus and had a transactivation function for the *GNRH1* promoter. This implies that *GNRH1* essential for the hypothalamic GnRH secretion is also a target gene of *OTX2*, as has been demonstrated in the mouse (15). Second, the short isoform-b was predominantly identified in the *OTX2* expression-positive tissues. This sug-

TABLE 1. Summary of clinical findings in patients with heterozygous *OTX2* mutations

	Present study					Previous studies[a]			
	Case 1	**Case 2**	**Case 3**	**Case 4**	**Case 5**	**Case 6**	**Case 7**	**Case 8**	**Case 9**
Present age (yr)	3	1	15	10	2	3	6	14	6
Sex	Male	Female	Male	Male	Male	Female	Male	Female	Male
Mutation[b]									
cDNA	c.221_236del	c.214_217del GCACinsCA	c.562G>T	c.562G>T	Whole gene deletion	c.402_403insC	c.674A>G	c.674A>G	c.405_406insCT
Protein	p.K74fsX103	p.A72fsX86	p.G188X	p.G188X	Absent	p. S135fsX136	p.N225S	p.N225S	p.S136fsX178
Function	Severe LOF	Severe LOF	Mild LOF	Mild LOF	Absent	Severe LOF	DN	DN	Severe LOF
Ocular malformation									
Right	AO	MO	MO	MO	MO	AO	N.D.	N.D.	AO
Left	MO	MO	MO	MO	AO	AO	N.D.	N.D.	AO
Developmental delay	+	Uncertain	+	+	+	+	N.D.	N.D.	+
Prenatal growth failure[c]	−	−	−	−	−	−	N.D.	N.D.	−
Birth length (cm) (SDS)	46.5 (−1.2)	48.3 (±0)	50 (+0.5)	49 (±0)	47.9 (−0.5)	50 (+0.6)	N.D.	N.D.	49.5 (+0.2)
Birth weight (kg) (SDS)	2.77 (−0.5)	3.22 (+0.6)	3.62 (+1.5)	3.23 (+0.5)	2.96 (−0.1)	3.16 (+0.2)	N.D.	N.D.	3.49 (+1.2)
Birth OFC (cm) (SDS)	32.5 (−0.7)	34 (+0.7)	N.E.	32.5 (−0.7)	31.5 (−1.4)	33.7 (+0.6)	N.D.	N.D.	N.D.
Postnatal growth failure[c]	+	−	+	−	+	+	+	+	+
Present height (cm) (SDS)	76.9 (−3.3)[d]	73.2 (±0)	114.0 (−4.1)[e]	130.8 (−1.5)	78.1 (−2.4)	85.0 (−3.3)	N.D.	N.D.	81.8 (−5.3)[f]
Present weight (kg) (SDS)	8.9 (−2.6)[d]	8.3 (−0.4)	16.8 (−2.4)[e]	23.2 (−1.6)	9.9 (−1.4)	10.1 (−2.6)	N.D.	N.D.	10.7 (−2.5)[f]
Present OFC (cm) (SDS)	N.E.	N.E.	N.E.	N.E.	N.E.	46 (−1.9)	N.D.	N.D.	47.2 (−2.7)[f]
Paternal height (cm) (SDS)[c]	160 (−1.9)	168 (−0.5)	178 (+1.2)	167 (−0.7)	163 (−1.3)	170 (±0)	178 (+0.3)	188 (+1.8)	N.D.
Maternal height (cm) (SDS)[c]	150 (−1.6)	151 (−1.3)	166 (+1.5)	165 (+1.4)	170 (+2.2)	155 (−0.6)	158 (−0.8)	168 (+0.7)	N.D.
Affected pituitary hormones	GH	No	GH, TSH, PRL, LH, FSH	No	GH	GH	GH, TSH, ACTH, LH, FSH	GH, TSH, ACTH, LH, FSH	GH, TSH, ACTH, LH, FSH
MRI findings									
Pituitary hypoplasia	+	N.E.	+	N.E.	+	−	+	+	+
EPP	+	N.E.	+	N.E.	−	−	+	−	+
Other features	Retractile testis (R)			Seizure		Cleft palate			Chiari malformation

SDS, SD score; OFC, occipitofrontal head circumference; MRI, magnetic resonance imaging; LOF, loss of function; DN, dominant negative; AO, anophthalmia; MO, microphthalmia; N.D., not described; N.E., not examined; PRL, prolactin; R, right.

[a] Case 6, Dateki *et al.* (8); cases 7 and 8, Diaczok *et al.* (9); case 9, Tajima *et al.* (10); [b] the cDNA and protein numbes are based on the human *OTX2* isoform-b (GenBank accession no. NM_172337.1), and the A of the ATG encoding the initiator methionine residue is denoted position +1; thus, the description of the mutations in cases 7–9 is different from that reported by Diaczok *et al.* (9) and Tajima *et al.* (10); [c] assessed by the age- and sex-matched Japanese growth standards (27) (cases 1–6 and 9 and their parents) or by the American growth standards (28) (the parents of cases 7 and 8); [d] at 2 yr 4 months of age before GH treatment; [e] at 10 yr of age before GH treatment; [f] at 4 yr of age before GH treatment.

TABLE 2. Blood hormone values in cases 1–5 with heterozygous *OTX2* mutations

Patient		**Case 1**		**Case 2**		**Case 3**		**Case 4**		**Case 5**	
Sex (age at examination)		**Male (2 yr)**		**Female (1 yr)**		**Male (14 yr)**		**Male (10 yr)**		**Male (2 yr)**	
	Stimulus (dose)	**Basal**	**Peak**	**Basal**	**Peak**	**Basal**	**Peak**	**Basal**	**Peak**	**Basal**	**Peak**
GH (ng/ml)	Insulin (0.1 U/kg)[a]	1.9^b	$\mathbf{4.0}^b$	3.3^b	N.E.	0.8^b	$\mathbf{1.3}^b$	12.1^b	N.E.	0.5^c	$\mathbf{9.0}^c$
	Arginine (0.5 g/kg)									1.1^c	$\mathbf{7.0}^c$
	L-dopa (10 mg/kg)	1.5^b	$\mathbf{3.8}^b$			0.3^b	$\mathbf{1.0}^b$				
LH (mIU/ml)	GnRH (100 μg/m^2)	0.1	1.7	0.1	N.E.	2.3^d	**4.5**	0.4	N.E.	0.1	3.1
FSH (mIU/ml)	GnRH (100 μg/m^2)	1.0	6.2	3.7	N.E.	1.3^d	**6.3**	1.1	N.E.	1.5	9.9
TSH (μU/ml)	TRH (10 μg/kg)	4.2	23.8	1.1	N.E.	0.2	**1.9**	1.1	N.E.	5.2	19.5
Prolactin (ng/ml)	TRH (10 μg/kg)	17.9	34.5	N.E.	N.E.	5.5	**8.3**	9.1	N.E.	10.43	88.8
ACTH (pg/ml)	Insulin (0.1 U/kg)	31	195	N.E.	N.E.	24		N.E.	N.E.	41	222
Cortisol (μg/dl)[d]	Insulin (0.1 U/kg)	12.7		9.4	N.E.	19.4		N.E.	N.E.	25.4	39.2
IGF-I (ng/ml)		**8**		65	N.E.	**5**		214	N.E.	48	
Testosterone (ng/dl)		N.E.		N.E.	N.E.	**45**		<5	N.E.	N.E.	
Free T_4 (ng/dl)		1.32		1.17	N.E.	**0.87**		1.15	N.E.	1.17	
Free T_3 (pg/ml)		2.91		3.24	N.E.	**1.94**		3.92	N.E.	4.54	

The conversion factor to the SI unit: GH, 1.0 (μg/liter); LH, 1.0 (IU/liter); FSH, 1.0 (IU/liter); TSH, 1.0 (mIU/liter); prolactin, 1.0 (μg /liter); ACTH, 0.22 (pmol/liter); cortisol, 27.59 (nmol/liter); IGF-I, 0.131 (nmol/liter); testosterone, 0.035 (nmol/liter); free T_4, 12.87 (pmol/liter); and free T_3, 1.54 (pmol/liter). Hormone values have been evaluated by the age- and sex-matched Japanese reference data (29, 30); low hormone data are *boldfaced*. Blood sampling during the provocation tests: 0, 30, 60, 90, and 120 min. N.E., Not examined.

[a] Sufficient hypoglycemic stimulations were obtained during all the insulin provocation tests; [b] GH was measured using the recombinant GH standard, and the peak GH values of 6 and 3 ng/ml are used as the cutoff values for partial and severe GH deficiency, respectively; [c] GH was measured by the classic RIA, and the peak GH values of 10 and 5 ng/ml were used as the cutoff values for partial and severe GH deficiency; [d] Obtained at 0800–0900 h.

gests that the biological functions of *OTX2* are primarily contributed by the short isoform-b.

Clinical features of cases 1–5 are summarized in Table 1, together with those of the previously reported *OTX2* mutation-positive patients examined for detailed pituitary function. Here four patients with cytogenetically recognizable deletions involving *OTX2* are not included (19–22) because the deletions appear to have removed a large number of genes including *BMP4* and/or *SIX6* (Fig. 2B) that can be relevant to pituitary development and/or function (1, 23).

Several points are noteworthy for the clinical findings. First, although cases 1–5 in this study had anophthalmia and/or microphthalmia, ocular phenotype has not been described in cases 7 and 8 identified by *OTX2* mutation analysis in 50 patients with hypopituitarism (9). Whereas no description of a phenotype would not necessarily indicate the lack of the phenotype, *OTX2* mutations may specifically affect pituitary function at least in several patients. This would not be unexpected because several *OTX2* mutation-positive patients are free from ocular anomalies (6).

Second, pituitary phenotype is variable and independent of the *in vitro* function data. This would be explained by the notion that haploinsufficiency of developmental genes is usually associated with a wide range of penetrance and expressivity depending on other genetic and environmental factors (24), although the actual underlying factors remain to be identified. In this regard, because direct mRNA analysis was not performed, it might be possible that the mutations have not produced the predicted aberrant protein and, consequently, *in vitro* function data do not necessarily reflect the *in vivo* functions. Even if this is the case, the quite different pituitary phenotype between cases 3 and 4 with the same mutation would argue for the notion that pituitary phenotype is independent of the residual OTX2 function.

Third, cases 1, 3, 5, and 6–9 with pituitary dysfunction have IGHD or CPHD involving GH, and show the combination of preserved prenatal growth and compromised postnatal growth characteristic of GH deficiency (25). This suggests that GH is the most vulnerable pituitary hormone in *OTX2* mutations. Consistent with this, previously reported patients with ocular anomalies and *OTX2* mutations also frequently exhibit short stature (6, 8). Thus, pituitary function studies are recommended in patients with ocular anomalies and postnatal short stature to allow for appropriate hormone therapies including GH treatment for short stature, cortisol supplementation at a stress period, T_4 supplementation to protect the developmental deterioration, and sex steroid supplementation to induce secondary sexual characteristics. Furthermore, *OTX2* mutation analysis is also recommended in such patients.

Lastly, PH and/or EPP is present in patients with IGHD and CPHD, except for case 6 with IGHD. In this regard, the following findings are noteworthy: 1) heterozygous loss-of-function mutations of *HESX1* are associated with a wide phenotypic spectrum including CPHD, IGHD, and apparently normal phenotype and often cause PH and

EPP, whereas homozygous *HESX1* mutations usually lead to CPHD as well as PH and EPP (2); 2) heterozygous loss-of-function mutations of *POU1F1* usually permit apparently normal pituitary phenotype, whereas homozygous loss-of-function mutations and heterozygous dominant-negative mutations usually result in GH, TSH, and prolactin deficiencies and often cause PH but not EPP (2); and 3) heterozygous *GNRH1* frameshift mutation are free from discernible phenotype, whereas homozygous *GNRH1* mutations result in isolated hypogonadotropic hypogonadism with no abnormal pituitary structure (26). Collectively, overall pituitary phenotype may primarily be ascribed to reduced *HESX1* expression, although reduced *POU1F1* and *GNRH1* expressions would also play a certain role, and there may be other target genes of *OTX2*.

In summary, the results imply that *OTX2* mutations are associated with variable pituitary phenotype, with no genotype-phenotype correlations, and that *OTX2* can transactivate *GNRH1* as well as *HESX1* and *POU1F1*. Further studies will serve to clarify the role of *OTX2* in the pituitary development and function.

Acknowledgments

We thank the patients and parents for participating in this study. We also thank Dr. Nicola Ragge and Dr. David J Bunyan for the MLPA probe sequence of *OTX2*.

Address all correspondence and requests for reprints to: Dr. T. Ogata, Department of Endocrinology and Metabolism, National Research Institute for Child Health and Development, 2-10-1 Ohkura, Setagaya, Tokyo 157-8535, Japan. E-mail: tomogata@nch.go.jp.

This work was supported by Grants-in-Aid for Young Scientists (B-21791025) from the Ministry of Education, Culture, Sports, Science, and Technology and Grants for Child Health and Development (20C-2); Research on Children and Families (H21-005); and Research on Measures for Intractable Diseases (H21-043) from the Ministry of Health, Labor, and Welfare.

Disclosure Summary: The authors have nothing to declare.

References

1. **Cohen LE, Radovick S** 2002 Molecular basis of combined pituitary hormone deficiencies. Endocr Rev 23:431–442
2. **Kelberman D, Dattani MT** 2007 Hypopituitarism oddities: congenital causes. Horm Res 68(Suppl 5):138–144
3. **Vieira TC, Boldarine VT, Abucham J** 2007 Molecular analysis of PROP1, PIT1, HESX1, LHX3, and LHX4 shows high frequency of PROP1 mutations in patients with familial forms of combined pituitary hormone deficiency. Arq Bras Endocrinol Metab 51:1097–1103
4. **Hever AM, Williamson KA, van Heyningen V** 2006 Developmental malformations of the eye: the role of *PAX6*, *SOX2* and *OTX2*. Clin Genet 69:459–470
5. **Courtois V, Chatelain G, Han ZY, Le Novère N, Brun G, Lamonerie T** 2003 New Otx2 mRNA isoforms expressed in the mouse brain. J Neurochem 84:840–853
6. **Ragge NK, Brown AG, Poloschek CM, Lorenz B, Henderson RA, Clarke MP, Russell-Eggitt I, Fielder A, Gerrelli D, Martinez-Barbera JP, Ruddle P, Hurst J, Collin JR, Salt A, Cooper ST, Thompson PJ, Sisodiya SM, Williamson KA, Fitzpatrick DR, van Heyningen V, Hanson IM** 2005 Heterozygous mutations of *OTX2* cause severe ocular malformations. Am J Hum Genet 76:1008–1022
7. **Wyatt A, Bakrania P, Bunyan DJ, Osborne RJ, Crolla JA, Salt A, Ayuso C, Newbury-Ecob R, Abou-Rayyah Y, Collin JR, Robinson D, Ragge N** 2008 Novel heterozygous OTX2 mutations and whole gene deletions in anophthalmia, microphthalmia and coloboma. Hum Mutat 29:E278–E283
8. **Dateki S, Fukami M, Sato N, Muroya K, Adachi M, Ogata T** 2008 OTX2 mutation in a patient with anophthalmia, short stature, and partial growth hormone deficiency: functional studies using the IRBP, HESX1, and POU1F1 promoters. J Clin Endocrinol Metab 93:3697–3702
9. **Diaczok D, Romero C, Zunich J, Marshall I, Radovick S** 2008 A novel dominant-negative mutation of OTX2 associated with combined pituitary hormone deficiency. J Clin Endocrinol Metab 93: 4351–4359
10. **Tajima T, Ohtake A, Hoshino M, Amemiya S, Sasaki N, Ishizu K, Fujieda K** 2009 OTX2 loss of function mutation causes anophthalmia and combined pituitary hormone deficiency with a small anterior and ectopic posterior pituitary. J Clin Endocrinol Metab 94: 314–319
11. **Cartegni L, Chew SL, Krainer AR** 2002 Listening to silence and understanding nonsense: exonic mutations that affect splicing. Nat Rev Genet 3:285–298
12. **Strachan T, Read AP** 2004 Instability of the human genome: mutation and DNA repair. In: Human molecular genetics. 3rd ed. London and New York: Garland Science; 334–337
13. **Holbrook JA, Neu-Yilik G, Hentze MW, Kulozik AE** 2004 Nonsense-mediated decay approaches the clinic. Nat Genet 36:801–808
14. **Schouten JP, McElgunn CJ, Waaijer R, Zwijnenburg D, Diepvens F, Pals G** 2002 Relative quantification of 40 nucleic acid sequences by multiplex ligation-dependent probe amplification. Nucleic Acids Res 30:e57
15. **Kelley CG, Lavorgna G, Clark ME, Boncinelli E, Mellon PL** 2000 The Otx2 homeoprotein regulates expression from the gonadotropin-releasing hormone proximal promoter. Mol Endocrinol 14:1246–1256
16. **Matsuo N** 1993 Skeletal and sexual maturation in Japanese children. Clin Pediatr Endocrinol 2(Suppl):1–4
17. **Chatelain G, Fossat N, Brun G, Lamonerie T** 2006 Molecular dissection reveals decreased activity and not dominant-negative effect in human OTX2 mutants. J Mol Med 84:604–615
18. **den Dunnen JT, White SJ** 2006 MLPA and MAPH: sensitive detection of deletions and duplications. Curr Protoc Hum Genet Chapter 7, Unit 7.14
19. **Bennett CP, Betts DR, Seller MJ** 1991 Deletion 14q (q22q23) associated with anophthalmia, absent pituitary, and other abnormalities. J Med Genet 28:280–281
20. **Elliott J, Maltby EL, Reynolds B** 1993 A case of deletion 14(q22.1→q22.3) associated with anophthalmia and pituitary abnormalities. J Med Genet 30:251–252
21. **Lemyre E, Lemieux N, Décarie JC, Lambert M** 1998 Del(14)(q22.1q23.2) in a patient with anophthalmia and pituitary hypoplasia. Am J Med Genet 77:162–165
22. **Nolen LD, Amor D, Haywood A, St Heaps L, Willcock C, Mihelec M, Tam P, Billson F, Grigg J, Peters G, Jamieson RV** 2006 Deletion at 14q22–23 indicates a contiguous gene syndrome comprising anophthalmia, pituitary hypoplasia, and ear anomalies. Am J Med Genet A 140:1711–1718

23. **Zhu X, Lin CR, Prefontaine GG, Tollkuhn J, Rosenfeld MG** 2005 Genetic control of pituitary development and hypopituitarism. Curr Opin Genet Dev 15:332–340
24. **Fisher E, Scambler P** 1994 Human haploinsufficiency— one for sorrow, two for joy. Nat Genet 7:5–7
25. **Parks JS, Felner EI** 2007 Hypopituitarism. In: Kliegman RM, Behrman RE, Jenson HB, Stanton BF, eds. Nelson textbook of pediatrics. 18th ed. Philadelphia: Saunders Elsevier; 2293–2299
26. **Bouligand J, Ghervan C, Tello JA, Brailly-Tabard S, Salenave S, Chanson P, Lombès M, Millar RP, Guiochon-Mantel A, Young J** 2009 Isolated familial hypogonadotropic hypogonadism and a GNRH1 mutation. N Engl J Med 360:2742–2748
27. **Suwa S, Tachibana K, Maesaka H, Tanaka T, Yokoya S** 1992 Longitudinal standards for height and height velocity for Japanese children from birth to maturity. Clin Pediatr Endocrinol 1:5–13
28. **Kuczmarski RJ, Ogden CL, Guo SS, Grummer-Strawn LM, Flegal KM, Mei Z, Wei R, Curtin LR, Roche AF, Johnson CL** 2002 2000 CDC growth charts for the United States: methods and development. Vital Health Stat 11 246:1–190
29. **Japan Public Health Association** 1996 Normal biochemical values in Japanese children (in Japanese). Tokyo: Sanko Press
30. **Inada H, Imamura T, Nakajima R** 2002 Manual of endocrine examination for children (in Japanese). Osaka: Medical Review

ORIGINAL ARTICLE

Endocrine Research—Brief Report

Mutation and Gene Copy Number Analyses of Six Pituitary Transcription Factor Genes in 71 Patients with Combined Pituitary Hormone Deficiency: Identification of a Single Patient with *LHX4* Deletion

Sumito Dateki, Maki Fukami, Ayumi Uematsu, Masayuki Kaji, Manami Iso, Makoto Ono, Michiyo Mizota, Susumu Yokoya, Katsuaki Motomura, Eiichi Kinoshita, Hiroyuki Moriuchi, and Tsutomu Ogata

Department of Endocrinology and Metabolism (S.D., M.F., M.I., T.O.), National Research Institute for Child Health and Development, Tokyo 157-8535, Japan; Department of Pediatrics (S.D., K.M., E.K., H.M.), Nagasaki University Graduate School of Biomedical Sciences, Nagasaki 852-8501, Japan; Division of Endocrinology and Metabolism (A.U., M.K), Shizuoka Children's Hospital, Shizuoka 232-8555, Japan; Department of Pediatrics and Developmental Biology (M.O.), Tokyo Medical and Dental University Graduate School of Medical and Dental Sciences, Tokyo 113-8519, Japan; Department of Pediatrics (M.M.), Faculty of Medicine, Kagoshima University, Kagoshima 890-8544, Japan; Department of Medical Subspecialties (S.Y.), National Children's Medical Center, Tokyo 157-8535, Japan

Context: Mutations of multiple transcription factor genes involved in pituitary development have been identified in a minor portion of patients with combined pituitary hormone deficiency (CPHD). However, copy number aberrations involving such genes have been poorly investigated in patients with CPHD.

Objective: We aimed to report the results of mutation and gene copy number analyses in patients with CPHD.

Subjects and Methods: Seventy-one Japanese patients with CPHD were examined for mutations and gene copy number aberrations affecting *POU1F1*, *PROP1*, *HESX1*, *LHX3*, *LHX4*, and *SOX3* by PCR-direct sequencing and multiplex ligation-dependent probe amplification. When a deletion was indicated, it was further studied by fluorescence *in situ* hybridization, oligoarray comparative genomic hybridization, and serial sequencing for long PCR products encompassing the deletion junction.

Results: We identified a *de novo* heterozygous 522,009-bp deletion involving *LHX4* in a patient with CPHD (GH, TSH, PRL, LH, and FSH deficiencies), anterior pituitary hypoplasia, ectopic posterior pituitary, and underdeveloped sella turcica. We also identified five novel heterozygous missense substitutions (p.V201I and p.H387P in *LHX4*, p.T63M and p.A322T in *LHX3*, and p.V53L in *SOX3*) that were assessed as rare variants by sequencing analyses for control subjects and available parents and by functional studies and *in silico* analyses.

Conclusions: The results imply the rarity of abnormalities affecting the six genes in patients with CPHD and the significance of the gene copy number analysis in such patients. ***(J Clin Endocrinol Metab* 95: 4043–4047, 2010)**

ISSN Print 0021-972X ISSN Online 1945-7197
Printed in U.S.A.
Copyright © 2010 by The Endocrine Society
doi: 10.1210/jc.2010-0150 Received January 20, 2010. Accepted May 13, 2010.
First Published Online June 9, 2010

Abbreviations: CGH, Comparative genomic hybridization; CPHD, combined pituitary hormone deficiency; ESE, exonic splice enhancer; FISH, fluorescence *in situ* hybridization; HPA, hypothalamic-pituitary-adrenal; MLPA, multiplex ligation-dependent probe amplification.

Pituitary development and function depends on spatially and temporally controlled expression of multiple transcription factor genes such as *POU1F1*, *PROP1*, *HESX1*, *LHX3*, *LHX4*, *SOX3*, and *OTX2* (1–3). Mutations of these genes are usually associated with combined pituitary hormone deficiency (CPHD), although they sometimes lead to isolated GH deficiency (1–3). However, mutations of these genes have been found only in a minor portion of patients with CPHD (2–6). Thus, although multiple genes would remain to be identified in CPHD, a certain fraction of mutations may have been overlooked in these known genes. In this regard, because previous studies have primarily been performed with PCR-direct sequencing for coding exons (4–6), gene copy number aberrations (deletions and duplications) affecting such genes, as well as pathological mutations in noncoding regions, may remain undetected in patients with CPHD. Indeed, microdeletions of *PROP1* and *LHX3* and microduplications of *SOX3* have been identified in a few patients with CPHD (7–9). Thus, we performed sequence and gene copy number analyses for six pituitary transcription factor genes in Japanese patients with CPHD.

Patients and Methods

Patients

We studied 71 Japanese patients with various types of CPHD (39 males and 32 females; age 1–43 yr). In all the patients, *OTX2* mutations and gene copy number aberrations have been excluded previously (3).

Primers and probes

The primers and probes used are summarized in Supplemental Table 1 (published on The Endocrine Society's Journals Online web site at http://jcem.endojournals.org).

Sequence analysis

This study was approved by the Institutional Review Board Committee at the National Center for Child Health and Development. After obtaining written informed consent, leukocyte genomic DNA samples of the 71 patients were amplified by PCR for the all coding exons and their flanking splice sites of *POU1F1*, *PROP1*, *HESX1*, *LHX3*, *LHX4*, and *SOX3*. Subsequently, the PCR products were subjected to direct sequencing on a CEQ 8000 autosequencer (Beckman Coulter, Fullerton, CA). To confirm a heterozygous substitution, the corresponding PCR products were subcloned with a TOPO TA cloning kit (Invitrogen, Carlsbad, CA), and normal and mutant alleles were sequenced separately. The GenBank sequence data at NCBI (http://www.ncbi.nlm.nih.gov/genbank) were used as references. For controls, DNA samples of 100 Japanese healthy adults were used with permission.

Functional studies

Functional studies were performed for an *LHX4* missense variant (for details, see Supplemental Methods). In brief, we constructed expression vectors containing wild-type and variant *LHX4* cDNAs and a luciferase reporter vector containing the *POU1F1* promoter sequence with an LHX4-binding site (10). Subsequently, transactivation analysis was performed with dual-luciferase reporter assay system (Promega, Madison, WI) using COS1 cells.

In silico analyses

The conservation status of substituted wild-type amino acid residues was investigated using the UniGene data at NCBI. The possibility that identified substitutions could cause aberrant splicing was examined by ESE finder release 3.0 for the prediction of exonic splice enhancers (ESEs) (http://rulai.cshl.edu/cgi-bin/tools/ESE3/esefinder.cgi) (11) and by the program at Berkeley *Drosophila* Genome Project for the prediction of splice donor and accepter sites (http://www.fruitfly.org/seq_tools/splice.html) (12).

Gene copy number analysis

Muitlplex ligation-dependent probe amplification (MLPA) (13) was performed as a screening of a possible gene copy number alteration (deletion and duplication) in all 71 patients, using a commercially available MLPA probe mix (P236) (MRC-Holland, Amsterdam, The Netherlands) for all coding exons of *POU1F1*, *PROP1*, *HESX1*, *LHX3*, and *LHX4*, together with originally designed probes for *SOX3*. The procedure was as described in the manufacturer's instructions. To confirm a deletion, fluorescence *in situ* hybridization (FISH) was performed with a long PCR product. To indicate an extent of a deletion, oligoarray comparative genomic hybridization (CGH) was carried out with 1x244K Human Genome Array (catalog no. G4411B; Agilent Technologies, Santa Clara, CA), according to the manufacturer's protocol. Finally, to characterize a deletion, long PCR was performed with primer pairs flanking the deleted region, and the PCR product was subjected to direct sequencing using serial sequence primers. The deletion size and the junction structure were determined by comparing the obtained sequences with the reference sequences at NCBI Database (NC_000014.7), and additional deleted genes were examined with Ensembl Database (http://www.ensembl.org/). The presence or absence of repeat sequences around the breakpoints was examined with Repeatmasker (http://www.repeatmasker.org).

Results

Identification of five missense variants

We identified five novel heterozygous missense substitutions, *i.e.* p.T63M (c.188C→T) and p.A322T (c.964G→A) in *LHX3* (GenBank accession number NM_178138), p.V201I (c.601G→A) and p.H387P (c.1160A→C) in *LHX4* (NM_033343), and p.V53L (c.157G→C) in *SOX3* (NM_005634). These substitutions were found in different patients. No other mutations or novel substitutions were identified in the six genes examined. In the 100 control subjects, *LHX4*-p.H387P was detected in four subjects and *SOX3*-p.V53L in three subjects, whereas *LHX3*-p.T63M, *LHX3*-p.A322T, and *LHX4*-p.V201I were absent. Furthermore, sequencing of

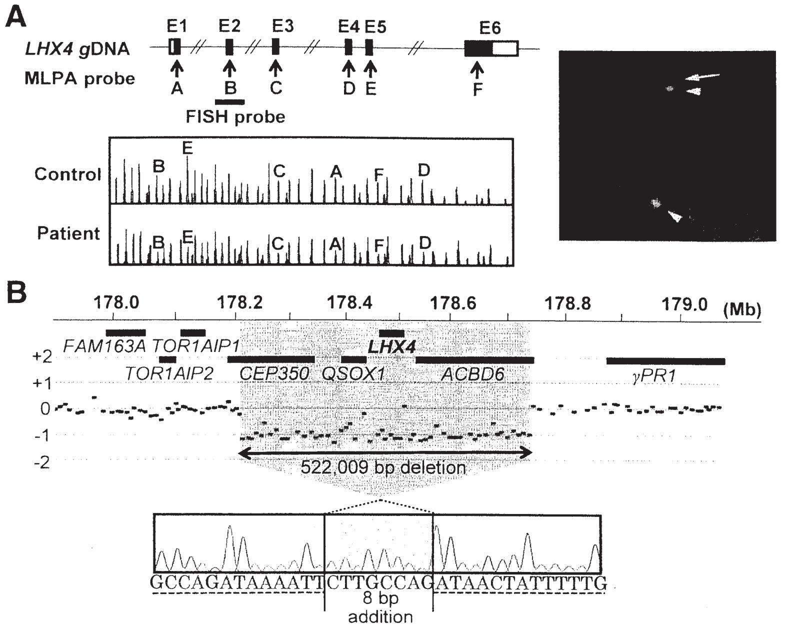

FIG. 1. Gene copy number analysis. Panel A, MLPA and FISH analyses. The *black and white boxes* on genomic DNA (gDNA) denote the coding regions on exons 1–6 (E1–E6) and the untranslated regions, respectively. The sites examined by MLPA probes (A–F) are indicated by *arrows*, and the region identified by the 5305-bp FISH probe is shown by a *thick horizontal line*. In MLPA analysis, the peaks for the sites A–F are reduced in the patient. The *red* peaks indicate the internal size markers. In FISH analysis, the *red* signal is derived from the probe for *LHX4*, and the *green* signals are derived from chromosome 1 centromere control probe (Cytocell, Cambridge, UK) used as an internal control. The probe for *LHX4* is labeled with digoxigenin and detected by rhodamine antidigoxigenin, and the control probe is labeled with biotin and detected by avidin conjugated to fluorescein isothiocyanate. Panel B, Oligoarray CGH analysis and direct sequencing of the deletion junction. The deletion is 522,009 bp in physical size (*shaded in gray*) and is associated with an addition of an 8-bp segment of unknown origin (*highlighted in yellow*). The normal sequences flanking the microdeletion are indicated with *dashed underlines*.

parental samples revealed *LHX3*-p.T63M and *LHX3*-p.A322T in the phenotypically normal mother and father, respectively; parental analysis was refused for *LHX4*-p.V201I, *LHX4*-p.H387P, and *SOX3*-p.V53L. Thus, four missense variants except for *LHX4*-p.V201I were found in healthy controls or parents. For *LHX4*-p.V201I, functional studies showed a normal transactivation function for the *POU1F1* promoter, with no dominant-negative effect (Supplemental Fig. 1). *In silico* analyses indicated that the V201 and the H387 residues in *LHX4* and the A322 residue in *LHX3* were well conserved, whereas the T63 in *LHX3* and the V53 in *SOX3* were poorly conserved (Supplemental Table 2). Furthermore, it was predicted that *LHX4*-V201I and *LHX4*-H387P were unlikely to influence ESEs, whereas *LHX3*-T63M and *LHX3*-A322T might affect ESEs (Supplemental Table 3). None of the missense variants were predicted to influence splice sites (Supplemental Table 4).

Identification of a microdeletion involving *LHX4*

A heterozygous deletion involving *LHX4* was indicated by MLPA and confirmed by FISH (Fig. 1A). Oligoarray CGH and sequencing of the fusion point showed that the deletion was 522,009 bp in physical size and was associated with an addition of an 8-bp segment of unknown origin (Fig. 1B). There were no repeat sequences around the deletion breakpoints. The deletion also affected *CEP350*, *QSOX1*, and *ACBD6*. This microdeletion was absent from the parents.

Patient with the microdeletion

This Japanese female patient was born at 40 wk gestation after an uncomplicated pregnancy and delivery. At birth, her length was 48.0 cm (−0.2 SD), her weight 2.59 kg (−1.0 SD), and her head circumference 33 cm (−0.1 SD). She had transient respiratory distress and hypoglycemia in the early neonatal period. Furthermore, biochemical studies for prolonged jaundice indicated central hypothyroidism at 1 month of age (Table 1). Thus, she was placed on thyroid hormone replacement therapy.

At 1 yr 6 months of age, she was referred to us because of severe short stature. Her height was 64.5 cm (−5.1 SD), and her weight was 6.2 kg (−2.8 SD). Endocrine studies at that time revealed severe GH and prolactin deficiencies (Table 1). Her karyotype was 46,XX in all 50 lymphocytes examined. Recombinant human GH therapy (0.175 mg/kg·wk) was started at 1 yr 8 months of age, showing a remarkable effect. Brain magnetic resonance imaging at 5 yr of age delineated anterior pituitary hypoplasia with a small cystic lesion, ectopic posterior pituitary, and underdeveloped sella turcica (Supplemental Fig. 2). At 11 yr of age, a GnRH test was performed due to lack of pubertal signs, revealing gonadotropin deficiencies (Table 1). Thus, sex steroid replacement therapy was started at 13 yr of age. She had no episode of adrenal insufficiency, with normal blood ACTH and cortisol values at yearly examinations. A CRH stimulation test at 17 yr of age also showed an apparently normal hypothalamic-pituitary-adrenal (HPA) function (Table 1). On the last examination at 17 yr old, she measured 148.7 cm (−1.8 SD), weighed 45.6 kg (−0.9 SD), and manifested full pubertal development. She had no developmental retardation.

The nonconsanguineous parents and the three brothers were clinically normal. The father was 164 cm (−1.2 SD) tall, and the mother was 155 cm (−0.6 SD) tall.

TABLE 1. Blood hormone values of the patient with *LHX4* deletion

	Stimulus (dosage)	1 month, basal	1.5 yr Basal	1.5 yr Peak	11 yr Basal	11 yr Peak	17 yr Basal	17 yr Peak
GH (ng/ml)	GHRH (1 mg/kg)		0.2	**1.2**				
	Arginine (0.5 g/kg)		0.1	**0.2**				
	L-Dopa (10 mg/kg)		0.1	**0.1**				
LH (mIU/ml)	GnRH (100 mg/m^2)		<0.5		0.3	**0.8**		
FSH (mIU/ml)	GnRH (100 mg/m^2)		0.5		1.3	**1.6**		
TSH (mU/ml)	TRH (10 mg/kg)	3.5	2.3[a]	**3.9**[a]				
Prolactin (ng/ml)	TRH (10 mg/kg)		**<1.0**	**<1.0**				
ACTH (pg/ml)[b]	CRH (2 mg/kg)		24.6		26.4		26.1	118.7
Cortisol (μg/dl)[b]	CRH (2 mg/kg)		17.5		10.6		15.7	37.82
IGF-I (ng/ml)			**9**					
Free T_4 (ng/dl)		**0.6**	**1.1**[a]					
Estradiol (pg/ml)					**<15**			

The conversion factors to the SI unit are as follows: GH 1.0 (μg/liter), LH 1.0 (IU/liter), FSH 1.0 (IU/liter), TSH 1.0 (mIU/liter), prolactin 1.0 (μg/liter), ACTH 0.22 (pmol/liter), cortisol 27.59 (nmol/liter), IGF-I 0.131 (nmol/liter), free T_4 12.87 (pmol/liter), and estradiol 3.671 (pmol/liter). Hormone values have been evaluated by the age- and sex-matched Japanese reference data; low hormone data are in *bold*. Blood sampling during the provocation tests were done at 0, 30, 60, 90, and 120 min.

[a] Examined under T_4 supplementation therapy.

[b] Obtained at 0800 h.

Discussion

We performed sequence and gene copy number analyses for all coding exons of six previously known genes in 71 patients with CPHD, although noncoding regions were not examined. Consequently, we could identify only a single patient with a heterozygous microdeletion involving *LHX4*. This indicates the rarity of abnormalities affecting the six genes in patients with CPHD and, at the same time, the significance of the gene copy number analysis in such patients. In this regard, because gene copy number aberrations have been found for multiple genes including microdeletions of *PROP1* and *LHX3* and microduplications of *SOX3* (7–9, 14, 15), this implies that gene copy number aberrations should be screened in genetic diagnosis.

Several matters are noteworthy for the clinical and molecular findings of the patient with the microdeletion involving *LHX4*. First, the HPA function was preserved normally at 17 yr of age. However, ACTH deficiency has often been identified in the previously reported patients with heterozygous intragenic loss-of-function mutations of *LHX4* (Supplemental Table 5), and the HPA function often deteriorates with age in patients with CPHD (2). Thus, careful follow-up is necessary for the HPA function of this patient. Second, the microdeletion has affected three additional genes. In this context, the pituitary phenotype of this patient remains within the clinical spectrum of patients with *LHX4* mutations (Supplemental Table 5), and there was no discernible extrapituitary phenotype. Thus, hemizygosity for the three genes would not have a major clinical effect, if any. Third, the deletion breakpoints resided on nonrepeat sequences, and the fusion point was associated with an addition of an 8-bp segment of unknown origin. This indicates that the deletion has been produced by nonhomologous end joining, *i.e.* an aberrant breakage and re-union between nonhomologous sequences (16).

We also identified five novel heterozygous missense substitutions. In this regard, the data obtained from sequencing analysis in control subjects and available parents, functional studies, and *in silico* analyses argue against the five missense substitutions being a disease-causing pathological mutation, although the possibility that they might function as a susceptibility factor for the development of CPHD remains tenable. In particular, *LHX4*-p.V201I, which was absent from 100 control subjects and affected the well-conserved V201 residue, may have been erroneously regarded as a pathological mutation, unless additional studies were performed. Indeed, *LHX4*-p.V201I exerted no predictable effect on the splicing pattern and had a normal transactivation activity in the used system, although transactivation function may be variable depending on the used promoters and cells (17). Such rare variants with an apparently normal function have also been reported previously (3, 18). Thus, whereas *in vitro* experimental data and *in silico* prediction data may not precisely reflect *in vivo* functions, it is recommended to perform such studies for novel substitutions, especially missense substitutions.

In summary, the results imply the rarity of pathological abnormalities in the previously known genes in patients with CPHD and the significance of the gene copy number analysis in such patients. Thus, the causes of CPHD remain elusive in most patients, and additional studies are required to clarify the underlying factors for the development of CPHD.

Acknowledgments

We thank the patients and the parents for participating in this study. We also thank Dr. Takizawa and Dr. Morita for participating in medical care of the reported patients.

Address all correspondence and requests for reprints to: Dr. T. Ogata, Department of Endocrinology and Metabolism, National Research Institute for Child Health and Development, 2-10-1 Ohkura, Setagaya, Tokyo 157-8535, Japan. E-mail: tomogata@nch.go.jp.

This work was supported by Grants for Child Health and Development (20C-2) and Research on Children and Families (H21-005) from the Ministry of Health, Labor, and Welfare and by Grants-in-Aid for Young Scientists (B) (21791025) from the Ministry of Education, Culture, Sports, Science, and Technology, Japan.

Disclosure Summary: All authors report no conflicts of interest.

References

1. **Cohen LE, Radovick S** 2002 Molecular basis of combined pituitary hormone deficiencies. Endocr Rev 23:431–442
2. **Kelberman D, Rizzoti K, Lovell-Badge R, Robinson IC, Dattani MT** 2009 Genetic regulation of pituitary gland development in human and mouse. Endocr Rev 30:790–829
3. **Dateki S, Kosaka K, Hasegawa K, Tanaka H, Azuma N, Yokoya S, Muroya K, Adachi M, Tajima T, Motomura K, Kinoshita E, Moriuchi H, Sato N, Fukami M, Ogata T** 2010 Heterozygous orthodenticle homeobox 2 mutations are associated with variable pituitary phenotype. J Clin Endocrinol Metab 95:756–764
4. **Coya R, Vela A, Pérez de Nanclares G, Rica I, Castaño L, Busturia MA, Martul P; GEDPIT group** 2007 Panhypopituitarism: genetic versus acquired etiological factors. J Pediatr Endocrinol Metab 20:27–36
5. **Mehta A, Hindmarsh PC, Mehta H, Turton JP, Russell-Eggitt I, Taylor D, Chong WK, Dattani MT** 2009 Congenital hypopituitarism: clinical, molecular and neuroradiological correlates. Clin Endocrinol (Oxf) 71:376–382
6. **Reynaud R, Gueydan M, Saveanu A, Vallette-Kasic S, Enjalbert A, Brue T, Barlier A** 2006 Genetic screening of combined pituitary hormone deficiency: experience in 195 patients. J Clin Endocrinol Metab 91:3329–3336
7. **Abrão MG, Leite MV, Carvalho LR, Billerbeck AE, Nishi MY, Barbosa AS, Martin RM, Arnhold IJ, Mendonca BB** 2006 Combined pituitary hormone deficiency (CPHD) due to a complete PROP1 deletion. Clin Endocrinol (Oxf) 65:294–300
8. **Pfaeffle RW, Savage JJ, Hunter CS, Palme C, Ahlmann M, Kumar P, Bellone J, Schoenau E, Korsch E, Brämswig JH, Stobbe HM, Blum WF, Rhodes SJ** 2007 Four novel mutations of the *LHX3* gene cause combined pituitary hormone deficiencies with or without limited neck rotation. J Clin Endocrinol Metab 92:1909–1919
9. **Woods KS, Cundall M, Turton J, Rizotti K, Mehta A, Palmer R, Wong J, Chong WK, Al-Zyoud M, El-Ali M, Otonkoski T, Martinez-Barbera JP, Thomas PQ, Robinson IC, Lovell-Badge R, Woodward KJ, Dattani MT** 2005 Over- and underdosage of SOX3 is associated with infundibular hypoplasia and hypopituitarism. Am J Hum Genet 76:833–849
10. **Machinis K, Amselem S** 2005 Functional relationship between *LHX4* and *POU1F1* in light of the *LHX4* mutation identified in patients with pituitary defects. J Clin Endocrinol Metab 90:5456–5462
11. **Cartegni L, Chew SL, Krainer AR** 2002 Listening to silence and understanding nonsense: exonic mutations that affect splicing. Nat Rev Genet 3:285–298
12. **Strachan T, Read AP** 2004 Instability of the human genome: mutation and DNA repair. In: Human molecular genetics. 3rd ed. London and New York: Garland Science; 334–337
13. **Schouten JP, McElgunn CJ, Waaijer R, Zwijnenburg D, Diepvens F, Pals G** 2002 Relative quantification of 40 nucleic acid sequences by multiplex ligation-dependent probe amplification. Nucleic Acids Res 30:e57
14. **Desviat LR, Pérez B, Ugarte M** 2006 Identification of exonic deletions in the PAH gene causing phenylketonuria by MLPA analysis. Clin Chim Acta 373:164–167
15. **Fukami M, Dateki S, Kato F, Hasegawa Y, Mochizuki H, Horikawa R, Ogata T** 2008 Identification and characterization of cryptic *SHOX* intragenic deletions in three Japanese patients with Léri-Weill dyschondrosteosis. J Hum Genet 53:454–459
16. **Shaw CJ, Lupski JR** 2004 Implications of human genome architecture for rearrangement-based disorders: the genomic basis of disease. Hum Mol Genet 13:R57–R64
17. **Ito M, Achermann JC, Jameson JL** 2000 A naturally occurring steroidogenic factor-1 mutation exhibits differential binding and activation of target genes. J Biol Chem 275:31708–31714
18. **Castinetti F, Saveanu A, Reynaud R, Quentien MH, Buffin A, Brauner R, Kaffel N, Albarel F, Guedj AM, El Kholy M, Amin M, Enjalbert A, Barlier A, Brue T** 2008 A novel dysfunctional *LHX4* mutation with high phenotypical variability in patients with hypopituitarism. J Clin Endocrinol Metab 93:2790–2799

The IG-DMR and the *MEG3*-DMR at Human Chromosome 14q32.2: Hierarchical Interaction and Distinct Functional Properties as Imprinting Control Centers

Masayo Kagami[1], Maureen J. O'Sullivan[2], Andrew J. Green[3,4], Yoshiyuki Watabe[5], Osamu Arisaka[5], Nobuhide Masawa[6], Kentarou Matsuoka[7], Maki Fukami[1], Keiko Matsubara[1], Fumiko Kato[1], Anne C. Ferguson-Smith[8], Tsutomu Ogata[1]*

1 Department of Endocrinology and Metabolism, National Research Institute for Child Health and Development, Tokyo, Japan, 2 Department of Pathology, School of Medicine, Our Lady's Children's Hospital, Trinity College, Dublin, Ireland, 3 National Center for Medical Genetics, University College Dublin, Our Lady's Hospital, Dublin, Ireland, 4 School of Medicine and Medical Science, University College, Dublin, Ireland, 5 Department of Pediatrics, Dokkyo University School of Medicine, Tochigi, Japan, 6 Department of Pathology, Dokkyo University School of Medicine, Tochigi, Japan, 7 Department of Pathology, National Center for Child Health and Development, Tokyo, Japan, 8 Department of Physiology, Development and Neuroscience, University of Cambridge, Cambridge, United Kingdom

Abstract

Human chromosome 14q32.2 harbors the germline-derived primary *DLK1-MEG3* intergenic differentially methylated region (IG-DMR) and the postfertilization-derived secondary *MEG3*-DMR, together with multiple imprinted genes. Although previous studies in cases with microdeletions and epimutations affecting both DMRs and paternal/maternal uniparental disomy 14-like phenotypes argue for a critical regulatory function of the two DMRs for the 14q32.2 imprinted region, the precise role of the individual DMR remains to be clarified. We studied an infant with upd(14)pat body and placental phenotypes and a heterozygous microdeletion involving the IG-DMR alone (patient 1) and a neonate with upd(14)pat body, but no placental phenotype and a heterozygous microdeletion involving the *MEG3*-DMR alone (patient 2). The results generated from the analysis of these two patients imply that the IG-DMR and the *MEG3*-DMR function as imprinting control centers in the placenta and the body, respectively, with a hierarchical interaction for the methylation pattern in the body governed by the IG-DMR. To our knowledge, this is the first study demonstrating an essential long-range imprinting regulatory function for the secondary DMR.

Citation: Kagami M, O'Sullivan MJ, Green AJ, Watabe Y, Arisaka O, et al. (2010) The IG-DMR and the *MEG3*-DMR at Human Chromosome 14q32.2: Hierarchical Interaction and Distinct Functional Properties as Imprinting Control Centers. PLoS Genet 6(6): e1000992. doi:10.1371/journal.pgen.1000992

Editor: Wolf Reik, The Babraham Institute, United Kingdom

Received December 29, 2009; **Accepted** May 19, 2010; **Published** June 17, 2010

Copyright: © 2010 Kagami et al. This is an open-access article distributed under the terms of the Creative Commons Attribution License, which permits unrestricted use, distribution, and reproduction in any medium, provided the original author and source are credited.

Funding: This work was supported by grants from the Ministry of Health, Labor, and Welfare; from the Ministry of Education, Science, Sports and Culture; and from Takeda Science Foundation. The funders had no role in study design, data collection and analysis, decision to publish, or preparation of the manuscript.

Competing Interests: The authors have declared that no competing interests exist.

* E-mail: tomogata@nch.go.jp

Introduction

Human chromosome 14q32.2 carries a cluster of protein-coding paternally expressed genes (*PEGs*) such as *DLK1* and *RTL1* and non-coding maternally expressed genes (*MEGs*) such as *MEG3* (alias, *GTL2*), *RTL1as* (*RTL1* antisense), *MEG8*, *snoRNAs*, and *microRNAs* [1,2]. Consistent with this, paternal uniparental disomy 14 (upd(14)pat) results in a unique phenotype characterized by facial abnormality, small bell-shaped thorax, abdominal wall defects, placentomegaly, and polyhydramnios [2,3], and maternal uniparental disomy 14 (upd(14)mat) leads to less-characteristic but clinically discernible features including growth failure [2,4].

The 14q32.2 imprinted region also harbors two differentially methylated regions (DMRs), i.e., the germline-derived primary *DLK1-MEG3* intergenic DMR (IG-DMR) and the postfertilization-derived secondary *MEG3*-DMR [1,2]. Both DMRs are hypermethylated after paternal transmission and hypomethylated after maternal transmission in the body, whereas in the placenta the IG-DMR alone remains as a DMR and the *MEG3*-DMR is rather hypomethylated [1,2]. Furthermore, previous studies in cases with upd(14)pat/mat-like phenotypes have revealed that epimutations (hypermethylation) and microdeletions affecting both DMRs of maternal origin cause paternalization of the 14q32.2 imprinted region, and that epimutations (hypomethylation) affecting both DMRs of paternal origin cause maternalization of the 14q32.2 imprinted region, while microdeletions involving the DMRs of paternal origin have no effect on the imprinting status [2,5–8]. These findings, together with the notion that parent-of-origin specific expression patterns of imprinted genes are primarily dependent on the methylation status of the DMRs [9], argue for a critical regulatory function of the two DMRs for the 14q32.2 imprinted region, with possible different effects between the body and the placenta.

However, the precise role of individual DMR remains to be clarified. Here, we report that the IG-DMR and the *MEG3*-DMR show a hierarchical interaction for the methylation pattern in the body, and function as imprinting control centers in the placenta and the body, respectively. To our knowledge, this is the first study demonstrating not only different roles between the primary and secondary DMRs at a single imprinted region, but also an essential regulatory function for the secondary DMR.

Author Summary

Genomic imprinting is a process causing genes to be expressed in a parent-of-origin specific manner—some imprinted genes are expressed from maternally inherited chromosomes and others from paternally inherited chromosomes. Imprinted genes are often located in clusters regulated by regions that are differentially methylated according to their parental origin. The human chromosome 14q32.2 imprinted region harbors the germline-derived primary *DLK1-MEG3* intergenic differentially methylated region (IG-DMR) and the postfertilization-derived secondary *MEG3*-DMR, together with multiple imprinted genes. Perturbed dosage of these imprinted genes, for example in patients with paternal and maternal uniparental disomy 14, causes distinct phenotypes. Here, through analysis of patients with microdeletions recapitulating some or all of the uniparental disomy 14 phenotypes, we show that the IG-DMR acts as an upstream regulator for the methylation pattern of the *MEG3*-DMR in the body but not in the placenta. Importantly, in the body, the *MEG3*-DMR functions as an imprinting control center. To our knowledge, this is the first study demonstrating an essential function for the secondary DMR in the regulation of multiple imprinted genes. Thus, the results provide a significant advance in the clarification of underlying epigenetic features that can act to regulate imprinting.

Results

Clinical reports

We studied an infant with upd(14)pat body and placental phenotypes (patient 1) and a neonate with upd(14)pat body, but no placental, phenotype (patient 2) (Figure 1). Detailed clinical features of patients 1 and 2 are shown in Table 1. In brief, patient 1 was delivered by a caesarean section at 33 weeks of gestation due to progressive polyhydramnios despite amnioreduction at 28 and 30 weeks of gestation, whereas patient 2 was born at 28 weeks of gestation by a vaginal delivery due to progressive labor without discernible polyhydramnios. Placentomegaly was observed in patient 1 but not in patient 2. Patients 1 and 2 were found to have characteristic face, small bell-shaped thorax with coat hanger appearance of the ribs, and omphalocele. Patient 1 received surgical treatment for omphalocele immediately after birth and mechanical ventilation for several months. At present, she is 5.5 months of age, and still requires intensive care including oxygen administration and tube feeding. Patient 2 died at four days of age due to massive intracranial hemorrhage, while receiving intensive care including mechanical ventilation. The mother of patient 1 had several non-specific clinical features such as short stature and obesity. The father of patient 1 and the parents of patient 2 were clinically normal.

Sample preparation

We isolated genomic DNA (gDNA) and transcripts (*mRNAs*, *snoRNAs*, and *microRNAs*) from fresh leukocytes of patients 1 and the parents of patients 1 and 2, from fresh skin fibroblasts of patient 2, and from formalin-fixed and paraffin-embedded placental samples of patient 1 and similarly treated pituitary and adrenal samples of patient 2 (although multiple body tissues were available in patient 2, useful gDNA and transcript samples were not obtained from other tissues probably due to drastic postmortem degradation). We also made metaphase spreads from leukocytes and skin fibroblasts. For comparison, we obtained control samples from fresh normal adult leukocytes, neonatal skin fibroblasts, and placenta at 38 weeks of gestation, and from fresh leukocytes of upd(14)pat/mat patients and formalin-fixed and paraffin-embedded placenta of a upd(14)pat patient [2,3].

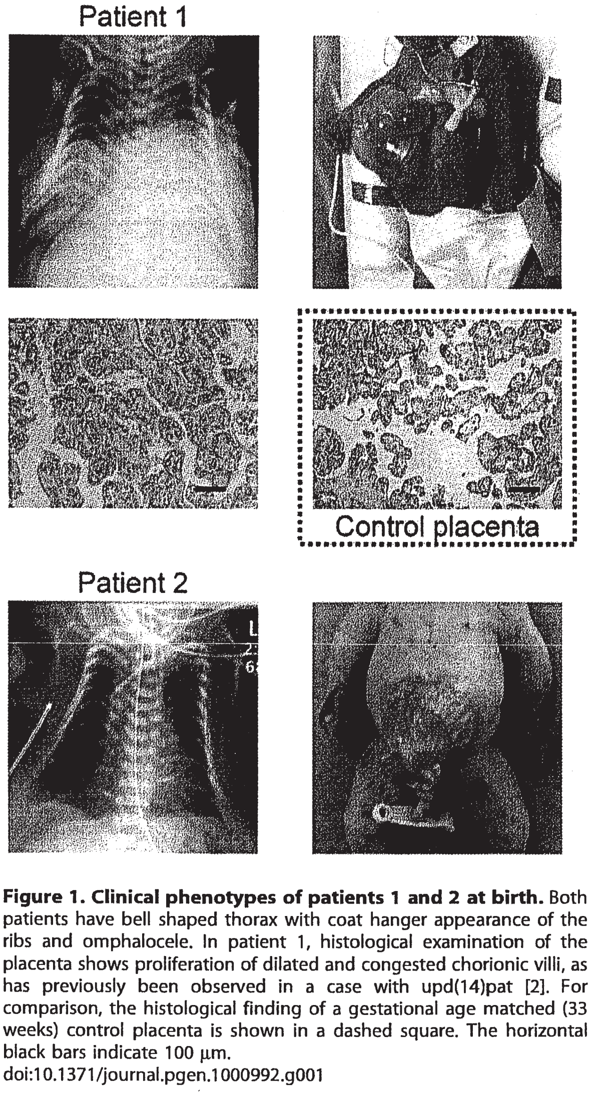

Figure 1. Clinical phenotypes of patients 1 and 2 at birth. Both patients have bell shaped thorax with coat hanger appearance of the ribs and omphalocele. In patient 1, histological examination of the placenta shows proliferation of dilated and congested chorionic villi, as has previously been observed in a case with upd(14)pat [2]. For comparison, the histological finding of a gestational age matched (33 weeks) control placenta is shown in a dashed square. The horizontal black bars indicate 100 μm.
doi:10.1371/journal.pgen.1000992.g001

Structural analysis of the imprinted region

We first examined the structure of the 14q32.2 imprinted region (Figure 2). Upd(14) was excluded in patients 1 and 2 as well as in the mother of patient 1 by microsatellite analysis (Table S1), and FISH analysis for the two DMRs identified a familial heterozygous deletion encompassing the IG-DMR alone in patient 1 and her mother and a *de novo* heterozygous deletion encompassing the *MEG3*-DMR alone in patient 2 (Figure 2). The microdeletions were further localized by SNP genotyping for 70 loci (Table S1) and quantitative real-time PCR (q-PCR) analysis for four regions around the DMRs (Figure S1A), and serial direct sequencing for the long PCR products harboring the deletion junctions successfully identified the fusion points of the microdeletions in patient 1 and her mother and in patient 2 (Figure 2). According to the NT_026437 sequence data at the NCBI Database (Genome Build 36.3) (http://preview.ncbi.nlm.nih.gov/guide/), the deletion

Table 1. Clinical features in patients 1 and 2.

	Patient 1	Patient 2	Upd(14)pat (n = 20)[c]
Present age	5.5 months	Deceased at 4 days	0–9 years
Sex	Female	Female	Male:Female = 9:11
Karyotype	46,XX	46,XX	
Pregnancy and delivery			
Gestational age (weeks)	33	28	28–37
Delivery	Caesarean	Vaginal	Vaginal:Caesarean = 6:7
Polyhydramnios	Yes	No	20/20 (<28)[d]
Amnioreduction (weeks)	2× (28, 30)	No	6/6
Placentomegaly	Yes	No	10/10
Growth pattern			
Prenatal growth failure	No	No	1/13
Birth length (cm)	43 (WNR)[a]	34 (WNR)[a]	
Birth weight (kg)	2.84 (>90 centile)[a]	1.32 (WNR)[a]	
Postnatal growth failure	Yes	...	5/6
Present stature (cm)	56.3 (−3.0 SD)[b]	...	
Present weight (kg)	5.02 (−3.0 SD)[b]	...	
Characteristic face			
Frontal bossing	No	Yes	5/7
Hairy forehead	Yes	Yes	9/10
Blepharophimosis	Yes	No	14/15
Depressed nasal bridge	Yes	Yes	13/13
Anteverted nares	Yes	No	6/10
Small ears	Yes	Yes	11/12
Protruding philtrum	Yes	No	15/15
Puckered lips	No	No	3/10
Micrognathia	Yes	Yes	11/12
Thoracic abnormality			
Bell-shaped thorax	Yes	Yes	17/17
Mechanical ventilation	Yes	Yes	17/17
Abdominal wall defect			
Diastasis recti	...	...	15/17
Omphalocele	Yes	Yes	2/17[e]
Others			
Short webbed neck	Yes	Yes	14/14
Cardiac disease	No	Yes (PDA)	5/10
Inguinal hernia	No	No	2/6
Coxa valga	Yes	No	3/4
Joint contractures	Yes	No	8/10
Kyphoscoliosis	No	No	4/7
Extra features		Hydronephrosis (bilateral)	

WNR: within the normal range; SD: standard deviation; and PDA: patent ductus arteriosus.

a Assessed by the gestational age- and sex-matched Japanese reference data from the Ministry of Health, Labor, and Welfare (http://www.e-stat.go.jp/SG1/estat/GL02020101.do).

b Assessed by the age- and sex-matched Japanese reference data..

c In the column summarizing the clinical features of 20 patients with upd(14)pat, the denominators indicate the number of cases examined for the presence or absence of each feature, and the numerators represent the number of cases assessed to be positive for that feature; thus, the differences between the denominators and the numerators denote the number of cases evaluated to be negative for that feature (adopted from reference [2]).

d Polyhydramnios has been identified by 28 weeks of gestation.

e Omphalocele is present in two cases with upd(14)pat and in two cases with epimutations [2].

doi:10.1371/journal.pgen.1000992.t001

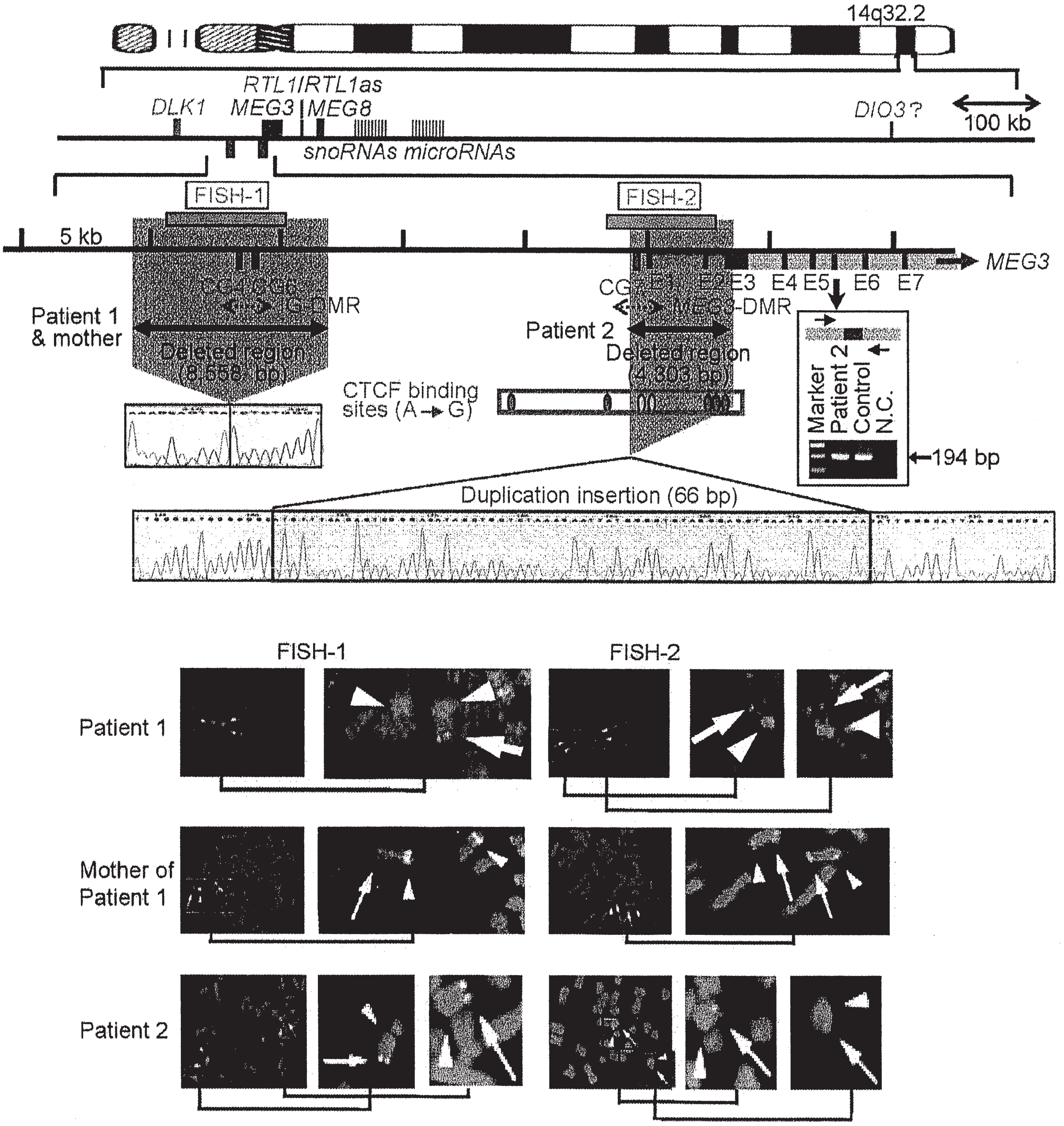
14q32.2
RTL1/RTL1as
DLK1
MEG3
MEG8
DIO3?
100 kb
snoRNAs microRNAs
FISH-1
FISH-2
5 kb
MEG3
CG4 CG6
IG-DMR
CG7
E1 E2 E3 E4 E5 E6 E7
MEG3-DMR
Patient 1
& mother
Deleted region
(8,558 bp)
Patient 2
Deleted region
(4,303 bp)
CTCF binding
sites (A→G)
Marker
Patient 2
Control
N.C.
194 bp
Duplication insertion (66 bp)
FISH-1
FISH-2
Patient 1
Mother of
Patient 1
Patient 2

Figure 2. Physical map of the 14q32.2 imprinted region and the deleted segments in patient 1 and her mother and in patient 2 (shaded in gray). *PEGs* are shown in blue, *MEGs* in red, and the IG-DMR (CG4 and CG6) and the *MEG3*-DMR (CG7) in green. It remains to be clarified whether *DIO3* is a *PEG*, although mouse *Dio3* is known to be preferentially but not exclusively expressed from a paternally derived chromosome [35]. For *MEG3*, the isoform 2 with nine exons (red bars) and eight introns (light red segment) is shown (Ensembl; http://www.ensembl.org/index.html). Electrochromatograms represent the fusion point in patient 1 and her mother, and the fusion point accompanied by insertion of a 66 bp segment (highlighted in blue) with a sequence identical to that within *MEG3* intron 5 (the blue bar) in patient 2. Since PCR amplification with primers flanking the 66 bp segment at *MEG3* intron 5 has produced a 194 bp single band in patient 2 as well as in a control subject (shown in the box), this indicates that the 66 bp segment at the fusion point is caused by a duplicated insertion rather than by a transfer from intron 5 to the fusion point (if the 66 bp is transferred from the original position, a 128 bp band as well as a 194 bp band should be present in patient 2) (the marker size: 100, 200, and 300 bp). In the FISH images, the red signals (arrows) have been identified by the FISH-1 probe and the FISH-2 probe, and the light green signals (arrowheads) by the RP11-566I2 probe for 14q12 used as an internal control. The faint signal detected by the FISH-2 probe in patient 2 is consistent with the preservation of a ~1.2 kb region identified by the centromeric portion of the FISH-2 probe.

doi:10.1371/journal.pgen.1000992.g002

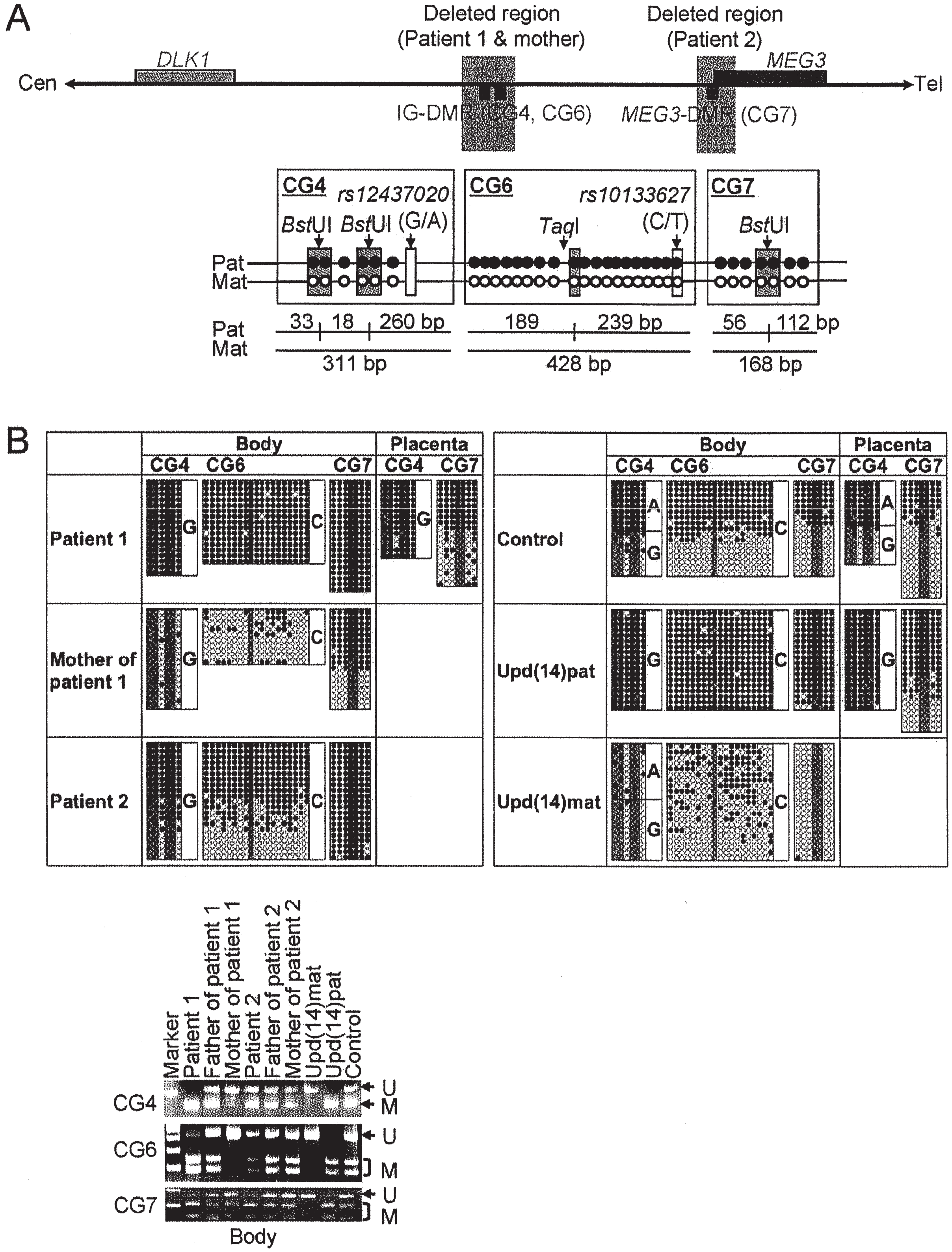
A
Deleted region (Patient 1 & mother)
Deleted region (Patient 2)
DLK1
MEG3
Cen
Tel
IG-DMR (CG4, CG6)
MEG3-DMR (CG7)
CG4
rs12437020
BstUI
BstUI
(G/A)
CG6
rs10133627
TaqI
(C/T)
CG7
BstUI
Pat
Mat
33
18
260 bp
311 bp
189
239 bp
428 bp
56
112 bp
168 bp
B
Body
Placenta
CG4
CG6
CG7
Patient 1
Mother of patient 1
Patient 2
Control
Upd(14)pat
Upd(14)mat
A
G
C
Marker
Patient 1
Father of patient 1
Mother of patient 1
Patient 2
Father of patient 2
Mother of patient 2
Upd(14)mat
Upd(14)pat
Control
U
M
Body

Figure 3. Methylation analysis of the IG-DMR (CG4 and CG6) and the *MEG3*-DMR (CG7). Filled and open circles indicate methylated and unmethylated cytosines at the CpG dinucleotides, respectively. (A) Structure of CG4, CG6, and CG7. Pat: paternally derived chromosome; and Mat:

maternally derived chromosome. The PCR products for CG4 (311 bp) harbor 6 CpG dinucleotides and a G/A SNP (*rs12437020*), and are digested with *Bst*UI into three fragment (33 bp, 18 bp, and 260 bp) when the cytosines at the first and the second CpG dinucleotides and the fourth and the fifth CpG dinucleotides (indicated with orange rectangles) are methylated. The PCR products for CG6 (428 bp) carry 19 CpG dinucleotides and a C/T SNP (*rs10133627*), and are digested with *Taq*I into two fragment (189 bp and 239 bp) when the cytosine at the 9th CpG dinucleotide (indicated with an orange rectangle) is methylated. The PCR products for CG7 harbor 7 CpG dinucleotides, and are digested with *Bst*UI into two fragment (56 bp and 112 bp) when the cytosines at the fourth and the fifth CpG dinucleotides (indicated with orange rectangles) are methylated. These enzymes have been utilized for combined bisulfite restriction analysis (COBRA). (B) Methylation analysis. Upper part shows bisulfite sequencing data. The SNP typing data are also denoted for CG4 and CG6. The circles highlighted in orange correspond to those shown in Figure 3A. The relatively long CG6 was not amplified from the formalin-fixed and paraffin-embedded placental samples, probably because of the degradation of genomic DNA. Note that CG4 is differentially methylated in a control placenta and is massively hypermethylated in a upd(14)pat placenta, whereas CG7 is rather hypomethylated in a upd(14)pat placenta as well as in a control placenta. Lower part shows COBRA data. U: unmethylated clone specific bands (311 bp for CG4, 428 bp for CG6, and 168 bp for CG7); and M: methylated clone specific bands (260 bp for CG4, 239 bp and 189 bp for CG6, and 112 bp and 56 bp for CG7). The results reproduce the bisulfite sequencing data, and delineate normal findings of the father of patient 1 and the parents of patient 2.
doi:10.1371/journal.pgen.1000992.g003

size was 8,558 bp (82,270,449–82,279,006 bp) for the microdeletion in patient 1 and her mother, and 4,303 bp (82,290,978–82,295,280 bp) for the microdeletion in patient 2. The microdeletion in patient 2 also involved the 5′ part of *MEG3* and five of the seven putative CTCF binding sites A–G [10], and was accompanied by insertion of a 66 bp sequence duplicated from *MEG3* intron 5 (82,299,727–82,299,792 bp on NT_026437). Direct sequencing of the exonic or transcribed regions detected no mutation in *DLK1*, *MEG3*, and *RTL1*, although several cDNA polymorphisms (cSNPs) were identified (Table S1). Oligoarray comparative genomic hybridization identified no other discernible structural abnormality (Figure S1B).

Methylation analysis of the two DMRs and the seven putative CTCF binding sites

We next studied methylation patterns of the previously reported IG-DMR (CG4 and CG6) and *MEG3*-DMR (CG7) (Figure 3A) [2], using bisulfite treated gDNA samples. Bisulfite sequencing and combined bisulfite restriction analysis using body samples revealed a hypermethylated IG-DMR and *MEG3*-DMR in patient 1, a hypomethylated IG-DMR and differentially methylated *MEG3*-DMR in the mother of patient 1, and a differentially methylated IG-DMR and hypermethylated *MEG3*-DMR in patient 2, and bisulfite sequencing using placental samples showed a hypermethylated IG-DMR and rather hypomethylated *MEG3*-DMR in patient 1 (Figure 3B).

We also examined methylation patterns of the seven putative CTCF binding sites by bisulfite sequencing (Figure 4A). The sites C and D alone exhibited DMRs in the body and were rather hypomethylated in the placenta (Figure 4B), as observed in CG7. Furthermore, to identify an informative SNP(s) pattern for allele-specific bisulfite sequencing, we examined a 349 bp region encompassing the site C and a 356 bp region encompassing the site D as well as a 300 bp region spanning the previously reported three SNPs near the site D, in 120 control subjects, the cases with upd(14)pat/mat, and patients 1 and 2 and their parents. Consequently, an informative polymorphism was identified for a novel G/A SNP near the site D in only a single control subject, and the parent-of-origin specific methylation pattern was confirmed (Figure 4C). No informative SNP was found in the examined region around the site C, and no other informative SNP was identified in the two examined regions around the site D, with the previously known three SNPs being present in a homozygous condition in all the subjects analyzed.

Expression analysis of the imprinted genes

Finally, we performed expression analyses, using standard reverse transcriptase (RT)-PCR and/or q-PCR analysis for multiple imprinted genes in this region (Figure 5A–5C). For leukocytes, weak expression was detected for *MEG3* and *SNORD114-29* in a control subject and the mother of patient 1 but not in patient 1. For skin fibroblasts, although all *MEGs* but no *PEGs* were expressed in control subjects, neither *MEGs* nor *PEGs* were expressed in patient 2. For placentas, although all imprinted genes were expressed in control subjects, *PEGs* only were expressed in patient 1. For the pituitary and adrenal of patient 2, *DLK1* expression alone was identified.

Expression pattern analyses using informative cSNPs revealed monoallelic *MEG3* expression in the leukocytes of the mother of patient 1 (Figure 5D), and biparental *RTL1* expression in the placenta of patient 1 (no informative cSNP was detected for *DLK1*) and biparental *DLK1* expression in the pituitary and adrenal of patient 2 (*RTL1* was not expressed in the pituitary and adrenal) (Figure 5E), as well as maternal *MEG3* expression in the control leukocytes and paternal *RTL1* expression in the control placentas (Figure S2). Although we also attempted q-PCR analysis, precise assessment was impossible for *MEG3* in the mother of patient 1 because of faint expression level in leukocytes and for *RTL1* in patient 1 and *DLK1* in patient 2 because of poor quality of mRNAs obtained from formalin-fixed and paraffin-embedded tissues.

Discussion

The data of the present study are summarized in Figure 6. Parental origin of the microdeletion positive chromosomes is based on the methylation patterns of the preserved DMRs in patients 1 and 2 and the mother of patient 1 as well as maternal transmission in patient 1. Loss of the hypomethylated IG-DMR of maternal origin in patient 1 was associated with epimutation (hypermethylation) of the *MEG3*-DMR in the body and caused paternalization of the imprinted region and typical upd(14)pat body and placental phenotypes, whereas loss of the hypomethylated *MEG3*-DMR of maternal origin in patient 2 permitted normal methylation pattern of the IG-DMR in the body and resulted in maternal to paternal epigenotypic alteration and typical upd(14)pat body, but no placental, phenotype. In this regard, while a 66 bp segment was inserted in patient 2, this segment contains no known regulatory sequence [11] or evolutionarily conserved element [12] (also examined with a VISTA program, http://genome.lbl.gov/vista/index.shtml). Similarly, while no control samples were available for pituitary and adrenal, the previous study in human subjects has shown paternal *DLK1* expression in adrenal as well as monoallelic *DLK1* and *MEG3* expressions in various tissues [11]. Furthermore, the present and the previous studies [2] indicate that this region is imprinted in the placenta as well as in the body. Thus, these results, in conjunction with the finding that the IG-DMR remains as a DMR and the *MEG3*-DMR exhibits a non-DMR in the placenta [2], imply the following: (1) the IG-DMR functions hierarchically as an upstream regulator for the methylation pattern of the *MEG3*-DMR on the maternally inherited chromosome in the body, but not in the placenta; (2) the hypomethylated

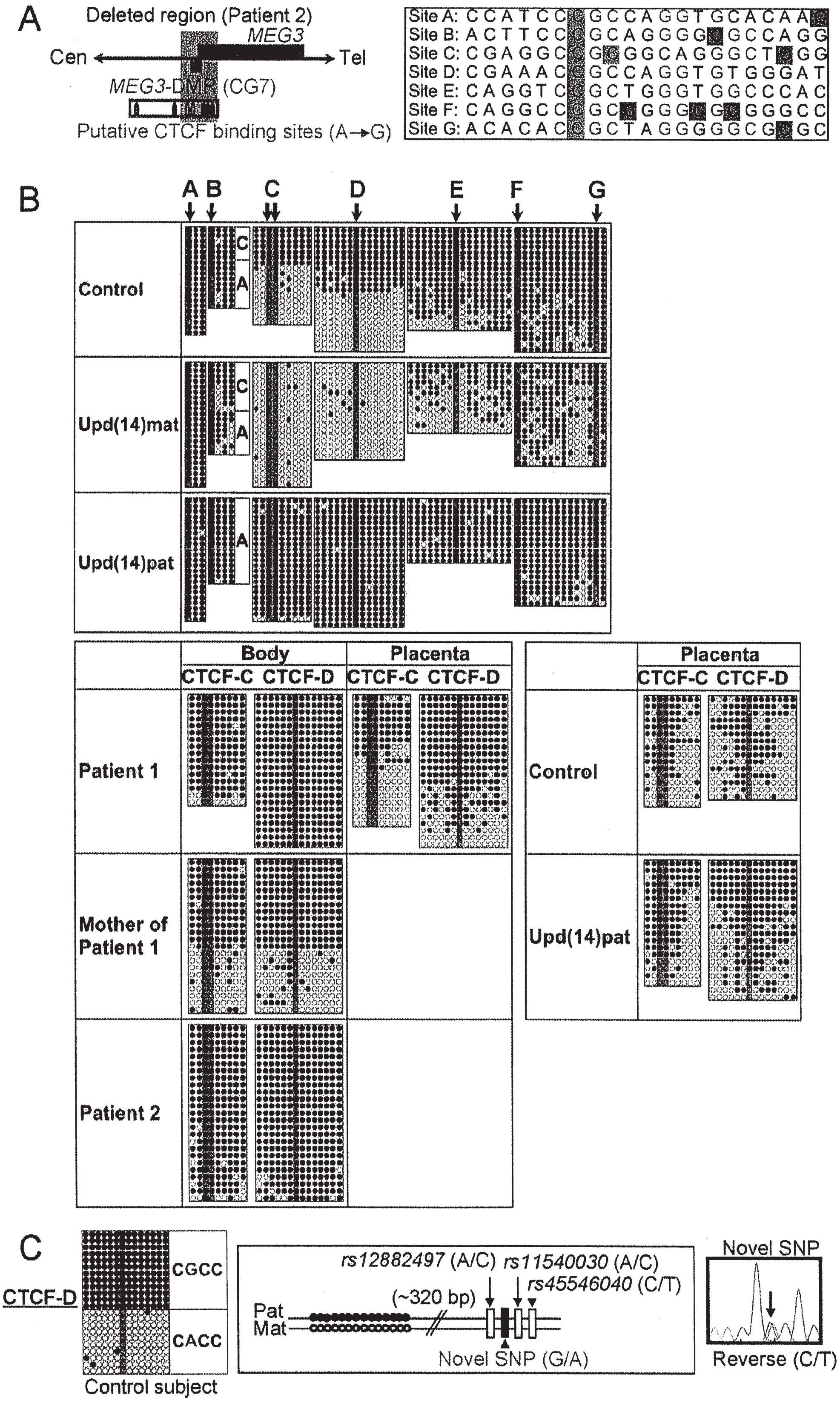
A
Deleted region (Patient 2)
MEG3
Cen
Tel
MEG3-DMR (CG7)
Putative CTCF binding sites (A→G)
Site A: C C A T C C C G C C A G G T G C A C A A C
Site B: A C T T C C C G C A G G G G C G C C A G G
Site C: C G A G G C C G C G G C A G G G C T C G G
Site D: C G A A A C C G C C A G G T G T G G G A T
Site E: C A G G T C C G C T G G G T G G C C C A C
Site F: C A G G C C C G C C G G G C G C G G G C C
Site G: A C A C A C C G C T A G G G G G C G C G C
B
A B C D E F G
Control
Upd(14)mat
Upd(14)pat
C
A
Body
Placenta
CTCF-C CTCF-D
Patient 1
Mother of Patient 1
Patient 2
Control
C
CTCF-D
CGCC
CACC
Control subject
rs12882497 (A/C)
rs11540030 (A/C)
rs45546040 (C/T)
(~320 bp)
Pat
Mat
Novel SNP (G/A)
Novel SNP
Reverse (C/T)

Figure 4. Methylation analysis of the putative CTCF protein binding sites A–G. (A) Location and sequence of the putative CTCF binding sites. In the left part, the sites C and D are painted in yellow and the remaining sites in purple. In the right part, the consensus CTCF binding motifs are shown in red letters; the cytosine residues at the CpG dinucleotides within the CTCF binding motifs are highlighted in blue, and those outside the CTCF binding motifs are highlighted in green [10]. (B) Methylation analysis. Upper part shows bisulfite sequencing data, using leukocyte genomic DNA samples. Since PCR products for the site B contain a C/A SNP (*rs11627993*), genotyping data are also indicated. The circles highlighted in blue correspond to those shown in Figure 4A. The sites C and D exhibit clear DMRs. Lower part indicates the results of the sites C and D using leukocyte and/or placental genomic DNA samples. The findings are similar to those of CG7. (C) Allele-specific methylation pattern of the CTCF binding site D. A novel G/A SNP has been identified in a single control subject, as shown on a reverse chromatogram delineating a C/T SNP pattern, while the previously reported three SNPs were present in a homozygous condition. Methylated and unmethylated clones are associated with the "G" and the "A" alleles, respectively.
doi:10.1371/journal.pgen.1000992.g004

MEG3-DMR functions as an essential imprinting regulator for both *PEGs* and *MEGs* in the body; and (3) in the placenta, the hypomethylated IG-DMR directly controls the imprinting pattern of both *PEGs* and *MEGs*. These notions also explain the epigenotypic alteration in the previous cases with epimutations or microdeletions affecting both DMRs (Figure S3).

It remains to be clarified how the IG-DMR and the *MEG3*-DMR interact hierarchically in the body. However, the present data, together with the previous findings in cases with epimutations [2,5–8], imply that *MEG3*-DMR can remain hypomethylated only in the presence of a hypomethylated IG-DMR and is methylated when the IG-DMR is deleted or methylated irrespective of the parental origin. Furthermore, mouse studies have suggested that the methylation pattern of the postfertilization-derived *Gtl2*-DMR (the mouse homolog for the *MEG3*-DMR) is dependent on that of the germline-derive IG-DMR [13]. Thus, a preferential binding of some factor(s) to the unmethylated IG-DMR may cause a conformational alteration of the genomic structure, thereby protecting the methylation of the *MEG3*-DMR.

It also remains to be elucidated how the IG-DMR and the *MEG3*-DMR regulate the expression of both *PEGs* and *MEGs* in the placenta and the body, respectively. For the *MEG3*-DMR, however, the CTCF binding sites C and D may play a pivotal role in the imprinting regulation. The methylation analysis indicates that the two sites reside within the *MEG3*-DMR, and it is known that the CTCF protein with versatile functions preferentially binds to unmethylated target sequences including the sites C and D [10,14–16]. In this regard, all the *MEGs* in this imprinted region can be transcribed together in the same orientation and show a strikingly similar tissue expressions pattern [1,12], whereas *PEGs* are transcribed in different directions and are co-expressed with *MEGs* only in limited cell-types [1,17]. It is possible, therefore, that preferential CTCF binding to the grossly unmethylated sites C and D activates all the *MEGs* as a large transcription unit and represses all the *PEGs* perhaps by influencing chromatin structure and histone modification independently of the effects of expressed *MEGs*. In support of this, CTCF protein acts as a transcriptional activator for *Gtl2* (the mouse homolog for *MEG3*) in the mouse [18].

Such an imprinting control model has not been proposed previously. It is different from the CTCF protein-mediated insulator model indicated for the *H19*-DMR and from the non-coding RNA-mediated model implicated for several imprinted regions including the KvDMR1 [19]. However, the KvDMR1 harbors two putative CTCF binding sites that may mediate non-coding RNA independent imprinting regulation [20], and the imprinting control center for Prader-Willi syndrome [21] also carries three CTCF binding sites (examined with a Search for CTCF DNA Binding Sites program, http://www.essex.ac.uk/bs/molonc/spa.html). Thus, while each imprinted region would be regulated by a different mechanism, a CTCF protein may be involved in the imprinting control of multiple regions, in various manners.

This imprinted region has also been studied in the mouse. Clinical and molecular findings in wildtype mice [1,22,23], mice with PatDi(12) (paternal disomy for chromosome 12 harboring this imprinted region) [13,24,25], and mice with targeted deletions for the IG-DMR (ΔIG-DMR) [22,26] and for the *Gtl2*-DMR (Δ*Gtl2*-DMR) [27] are summarized in Table 2. These data, together with human data, provide several informative findings. First, in both the human and the mouse, the IG-DMR is differentially methylated in both the body and the placenta, whereas the *MEG3*/*Gtl2*-DMR is differentially methylated in the body and exhibits non-DMR in the placenta. Second, the IG-DMR and the *MEG3*/*Gtl2*-DMR show a hierarchical interaction on the maternally derived chromosome in both the human and the mouse bodies. Indeed, the *MEG3*/*Gtl2*-DMR is epimutated in patient 1 and mice with maternally inherited ΔIG-DMR, and the IG-DMR is normally methylated in patient 2 and mice with maternally inherited Δ*Gtl2*-DMR. Third, the function of the IG-DMR is comparable between human and mouse bodies and different between human and mouse placentas. Indeed, patient 1 has upd(14)pat body and placental phenotypes, whereas mice with the ΔIG-DMR of maternal origin have PatDi(12)-compatible body phenotype and apparently normal placental phenotype. It is likely that imprinting regulation in the mouse placenta is contributed by some mechanism(s) other than the methylation pattern of the IG-DMR, such as chromatin conformation [22,28,29].

Unfortunately, however, the data of Δ*Gtl2*-DMR mice appears to be drastically complicated by the retained neomycin cassette in the upstream region of *Gtl2*. Indeed, it has been shown that the insertion of a *lacZ* gene or a neomycin gene in the similar upstream region of *Gtl2* causes severely dysregulated expression patterns and abnormal phenotypes after both paternal and maternal transmissions [30,31], and that deletion of the inserted neomycin gene results in apparently normal expression patterns and phenotypes after both paternal and maternal transmissions [31]. (In this regard, although a possible influence of the inserted 66 bp segment can not be excluded formally in patient 2, phenotype and expression data in patient 2 are compatible with simple paternalization of the imprinted region.) In addition, since the apparently normal phenotype in mice homozygous for Δ*Gtl2*-DMR is reminiscent of that in sheep homozygous for the callipyge mutation [32], a complicated mechanism(s) such as the polar overdominance may be operating in the Δ*Gtl2*-DMR mice [33]. Thus, it remains to be clarified whether the *MEG3*/*Gtl2*-DMR has a similar or different function between the human and the mouse.

Two points should be made in reference to the present study. First, the proposed functions of the two DMRs are based on the results of single patients. This must be kept in mind, because there might be a hidden patient-specific abnormality or event that might explain the results. For example, the abnormal placental phenotype in patient 1 might be caused by some co-incidental aberration, and the apparently normal placenta in patient 2 might be due to mosaicism with grossly preserved *MEG3*-DMR in the placenta and grossly deleted *MEG3*-DMR in the body. Second,

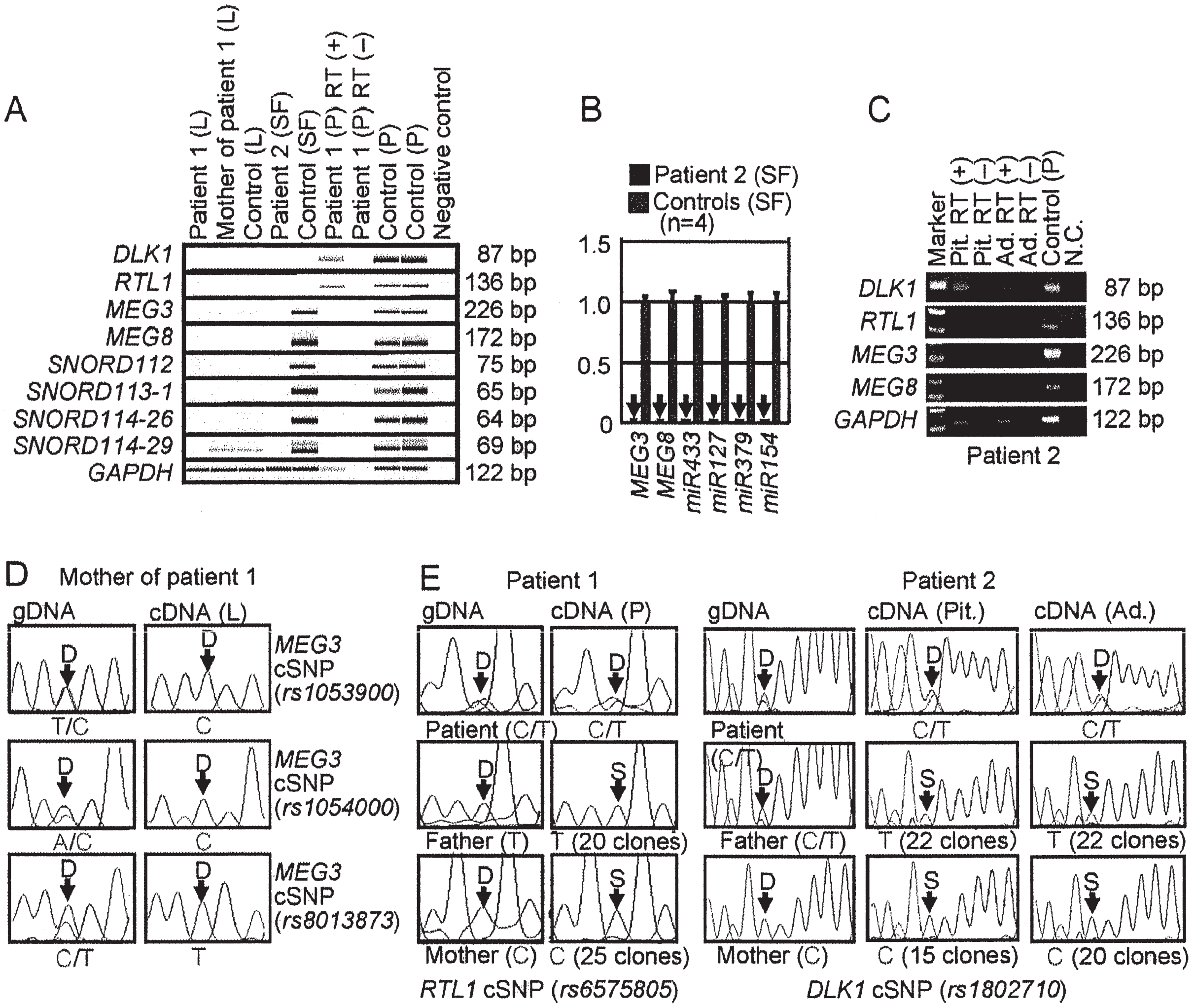

Figure 5. Expression analysis. (A) Reverse transcriptase (RT)-PCR analysis. L: leukocytes; SF: skin fibroblasts; and P: placenta. The relatively weak *GAPDH* expression for the formalin-fixed and paraffin-embedded placenta of patient 1 indicates considerable mRNA degradation. Since a single exon was amplified for *DLK1* and *RTL1*, PCR was performed with and without RT for the placenta of patient 1, to exclude the possibility of false positive results caused by genomic DNA contamination. (B) Quantitative real-time PCR (q-PCR) analysis of *MEG3*, *MEG8*, and *miRNAs*, using fresh skin fibroblasts (SF) of patient 2 and four control neonates. Of the examined *MEGs*, *miR433* and *miR127* are encoded by *RTL1as*. (C) RT-PCR analysis for the formalin-fixed and paraffin-embedded pituitary (Pit.) and the adrenal (Ad.) in patient 2. The bands for *DLK1* are detected in the presence of RT and undetected in the absence of RT, thereby excluding contamination of genomic DNA. (D) Monoallelic *MEG3* expression in the leukocytes of the mother of patient 1. The three cSNPs are present in a heterozygous status in gDNA and in a hemizygous status in cDNA. D: direct sequence. (E) Biparental *RTL1* expression in the placenta of patient 1 and biparental *DLK1* expression in the pituitary and adrenal of patient 2. D: direct sequence; and S: subcloned sequence. In patient 1, genotyping of *RTL1* cSNP (*rs6575805*) using gDNA indicates maternal origin of the "C" allele and paternal origin of the "T" allele, and sequencing analysis using cDNA confirms expression of maternally as well as paternally derived *RTL1*. Similarly, in patient 2, genotyping of *DLK1* cSNP (*rs1802710*) using gDNA denotes maternal origin of the "C" allele and paternal origin of the "T" alleles, and sequencing analysis using cDNA confirms expression of maternally as well as paternally inherited *DLK1*.
doi:10.1371/journal.pgen.1000992.g005

the clinical features in the mother of patient 1 such as short stature and obesity are often observed in cases with upd(14)mat (Table S2). However, the clinical features are non-specific and appear to be irrelevant to the microdeletion involving the IG-DMR, because loss of the paternally derived IG-DMR does not affect the imprinted status [2,26]. Indeed, *MEG3* in the mother of patient 1 showed normal monoallelic expression in the presence of the differentially methylated *MEG3*-DMR. Nevertheless, since the upd(14)mat phenotype is primarily ascribed to loss of functional *DLK1* (Figure S3B) [2,34], it might be possible that the microdeletion involving the IG-DMR has affected a *cis*-acting regulatory element for *DLK1* expression (for details, see Note in the legend for Table S2). Further studies in cases with similar microdeletions will permit clarification of these two points.

In summary, the results show a hierarchical interaction and distinct functional properties of the IG-DMR and the *MEG3*-DMR in imprinting control. Thus, this study provides significant advance in the clarification of mechanisms involved in the imprinting regulation at the 14q32.2 imprinted region and the development of upd(14) phenotype.

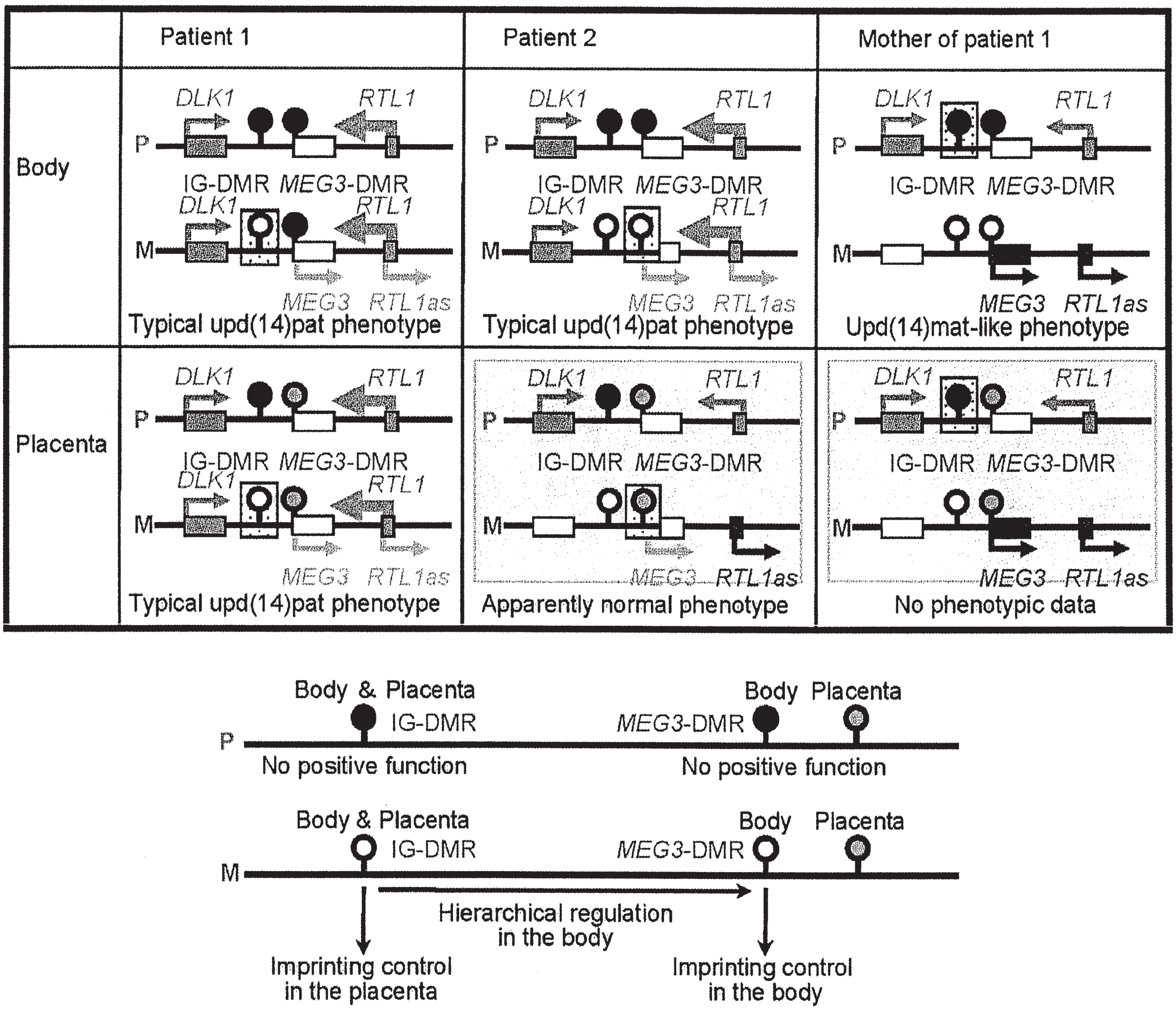
Patient 1
Patient 2
Mother of patient 1
Body
Placenta
DLK1
RTL1
P
M
IG-DMR
MEG3-DMR
MEG3
RTL1as
Typical upd(14)pat phenotype
Upd(14)mat-like phenotype
Apparently normal phenotype
No phenotypic data
Body & Placenta
Body
Placenta
No positive function
Hierarchical regulation in the body
Imprinting control in the placenta
Imprinting control in the body

Figure 6. Schematic representation of the observed and predicted methylation and expression patterns. Deleted regions in patients 1 and 2 and the mother of patient 1 are indicated by stippled rectangles. P: paternally derived chromosome; and M: maternally derived chromosome. Representative imprinted genes are shown; these genes are known to be imprinted in the body and the placenta [2] (see also Figure S2). Placental samples have not been obtained in patient 2 and the mother of patient 1 (highlighted with light green backgrounds). Thick arrows for *RTL1* in patients 1 and 2 represent increased *RTL1* expression that is ascribed to loss of functional microRNA-containing *RTL1as* as a repressor for *RTL1* [26,36–38]; this phenomenon has been indicated in placentas with upd(14)pat and in those with an epimutation and a microdeletion involving the two DMRs (Figure S3A and S3C) [2]. *MEG3* and *RTL1as* that are disrupted or predicted to have become silent on the maternally derived chromosome are written in gray. Filled and open circles represent hypermethylated and hypomethylated DMRs, respectively; since the *MEG3*-DMR is rather hypomethylated and regarded as non-DMR in the placenta [2] (see also Figure 3), it is painted in gray.
doi:10.1371/journal.pgen.1000992.g006

Materials and Methods

Ethics statement

This study was approved by the Institutional Review Board Committees at National Center for Child health and Development, University College Dublin, and Dokkyo University School of Medicine, and performed after obtaining written informed consent.

Primers

All the primers utilized in this study are summarized in Table S3.

Sample preparation

For leukocytes and skin fibroblasts, genomic DNA (gDNA) samples were extracted with FlexiGene DNA Kit (Qiagen), and RNA samples were prepared with RNeasy Plus Mini (Qiagen) for *DLK1, MEG3, RTL1, MEG8* and *snoRNAs*, and with mirVana miRNA Isolation Kit (Ambion) for *microRNAs*. For paraffin-embedded tissues including the placenta, brain, lung, heart, liver, spleen, kidney, bladder, and small intestine, gDNA and RNA samples were extracted with RecoverAll Total Nucleic Acids Isolation Kit (Ambion) using slices of 40 μm thick. For fresh control placental samples, gDNA and RNA were extracted using ISOGEN (Nippon Gene). After treating total RNA samples with

Table 2. Clinical and molecular findings in wild-type and PatDi(12) mice and mice with maternally inherited ΔIG-DMR and Δ*Gtl2*-DMR.

	Wildtype	PatDi(12)	ΔIG-DMR (~4.15 kb)^{a}	Δ*Gtl2*-DMR (~10 kb)^{b}
				Neomycin cassette (+)
<Body>				
Phenotype	Normal	Abnormal^{c}	PatDi(12) phenotype^{c}	Normal at birth Lethal by 4 weeks
Methylation pattern				
IG-DMR	Differential	Methylated	Methylated^{d}	Differential
Gtl2-DMR	Differential	Methylated	Epimutated^{e}	Methylated^{d}
Expression pattern				
Pegs	Monoallelic	Increased (~2x)	Biparental Increased (2x or 4.5x)^{f}	Grossly normal
Megs	Monoallelic	Absent	Absent	Decreased (<0.2~0.5x)^{g}
<Placenta>				
Phenotype	Normal	Placentomegaly	Apparently normal	Not determined
Methylation pattern				
IG-DMR	Differential	Methylated	Not determined	Not determined
Gtl2-DMR	Non-DMR	Non-DMR	Not determined	Not determined
Expression pattern				
Pegs	Monoallelic	Not determined	Increased (1.5~1.8x)^{g}	Decreased (0.5~0.85x)^{g}
Megs	Monoallelic	Not determined	Decreased (0.6~0.8x)^{g}	Decreased (<0.1~1.0)^{g}
Remark			Paternal transmission^{h}	Paternal transmission^{i} Biparental transmission^{j}

a The deletion size is smaller than that of patient 1 and her mother in this study, especially at the centromeric region.
b The microdeletion also involves *Gtl2*, and the deletion size is larger than that of patient 2 in this study.
c Body phenotype includes bell-shaped thorax with rib anomalies, distended abdomen, and short and broad neck.
d Hemizygosity for the methylated DMR of paternal origin.
e Hypermethylation of the maternally derived DMR.
f 2x *Dlk1* and *Dio3* expression levels and 4.5x *Rtl1* expression level. The markedly elevated *Rtl1* expression level is ascribed to a synergic effect between activation of the usually silent *Rtl1* of maternal origin and loss of functional microRNA-containing *Rtl1as* as a repressor for *Rtl1* [26,36–38].
g The expression level is variable among examined tissues and examined genes.
h The ΔIG-DMR of paternal origin has permitted normal *Gtl2*-DMR methylation pattern, intact imprinting status, and normal phenotype in the body (no data on the placenta).
i The Δ*Gtl2*-DMR of paternal origin is accompanied by normal methylation pattern of the IG-DMR and variably reduced *Pegs* expression and increased *Megs* expression in the body, and has yielded severe growth retardation accompanied by perinatal lethality.
j The homozygous mutants have survived and developed into fertile adults, despite rather altered expression patterns of the imprinted genes.
doi:10.1371/journal.pgen.1000992.t002

DNase, cDNA samples for *DLK1, MEG3, MEG8*, and *snoRNAs* were prepared with oligo(dT) primers from 1 µg of RNA using Superscript III Reverse Transcriptase (Invitrogen), and those for *microRNAs* were synthesized from 300 ng of RNA using TaqMan MicroRNA Reverse Transcription Kit (Applied Biosystems). For *RTL1*, cDNA samples were synthesized with *RTL1*-specific primers that do not amplify *RTL1as*. Control gDNA and cDNA samples were extracted from adult leukocytes and neonatal skin fibroblasts purchased from Takara Bio Inc. Japan, and from a fresh placenta of 38 weeks of gestation. Metaphase spreads were prepared from leukocytes and skin fibroblasts using colcemide (Invitrogen).

Structural analysis

Microsatellite analysis and SNP genotyping were performed as described previously [2]. For FISH analysis, metaphase spreads were hybridized with a 5,104 bp FISH-1 probe and a 5,182 bp FISH-2 probe produced by long PCR, together with an RP11-566I2 probe for 14q12 used as an internal control [2]. The FISH-1 and FISH-2 probes were labeled with digoxigenin and detected by rhodamine anti-digoxigenin, and the RP11-566I2 probe was labeled with biotin and detected by avidin conjugated to fluorescein isothiocyanate. For quantitative real-time PCR analysis, the relative copy number to RNaseP (catalog No: 4316831, Applied Biosystems) was determined by the Taqman real-time PCR method using the probe-primer mix on an ABI PRISM 7000 (Applied Biosystems). To determine the breakpoints of microdeletions, sequence analysis was performed for long PCR products harboring the fusion points, using serial forward primers on the CEQ 8000 autosequencer (Beckman Coulter). Direct sequencing was also performed on the CEQ 8000 autosequencer. Oligoarray comparative genomic hybridization was performed with 1×244K Human Genome Array (catalog No: G4411B) (Agilent Technologies), according to the manufacturer's protocol.

Methylation analysis

Methylation analysis was performed for gDNA treated with bisulfite using the EZ DNA Methylation Kit (Zymo Research). After PCR amplification using primer sets that hybridize both methylated and unmethylated clones because of lack of CpG dinucleotides within the primer sequences, the PCR products were digested with appropriate restriction enzymes for combined bisulfite restriction analysis. For bisulfite sequencing, the PCR products were subcloned with TOPO TA Cloning Kit (Invitrogen) and subjected to direct sequencing on the CEQ 8000 autosequencer.

Expression analysis

Standard RT-PCR was performed for *DLK1*, *RTL1*, *MEG3*, *MEG8*, and *snoRNAs* using primers hybridizing to exonic or transcribed sequences, and one µl of PCR reaction solutions was loaded onto Gel-Dye Mix (Agilent). Taqman real-time PCR was carried out using the probe-primer mixtures (assay No: Hs00292028 for *MEG3* and Hs00419701 for *MEG8*; assay ID: 001028 for *miR433*, 000452 for *miR127*, 000568 for *miR379*, and 000477 for *miR154*) on the ABI PRISM 7000. Data were normalized against *GAPDH* (catalog No: 4326317E) for *MEG3* and *MEG8* and against *RNU48* (assay ID: 0010006) for the remaining *miRs*. The expression studies were performed three times for each sample.

To examine the imprinting status of *MEG3* in the leukocytes of the mother of patient 1, direct sequence data for informative cSNPs were compared between gDNA and cDNA. To analyze the imprinting status of *RTL1* in the placental sample of patient 1 and that of *DLK1* in the pituitary and adrenal samples of patient 2, RT-PCR products containing exonic cSNPs informative for the parental origin were subcloned with TOPO TA Cloning Kit, and multiple clones were subjected to direct sequencing on the CEQ 8000 autosequencer. Furthermore, *MEG3* expression pattern was examined using leukocyte gDNA and cDNA samples from multiple normal subjects and leukocyte gDNA samples from their mothers, and *RTL1* expression pattern was analyzed using gDNA and cDNA samples from multiple fresh normal placentas and leukocyte gDNA from the mothers.

Supporting Information

Figure S1 Structural analysis. (A) Quantitative real-time PCR analysis (q-PCR) for four regions (q-PCR-1-4) in patient 2. The q-PCR-1 and q-PCR-2 regions are present in two copies whereas q-PCR-3 and q-PCR-4 regions are present in a single copy in patient 2. The four regions are present in two copies in the parents and a control subject, in a single copy in the two previously reported patients with microdeletions involving the examined regions (Deletion-1 and Deletion-2 are case 2 and case 3 in Kagami et al. [2], respectively), and in three copies in a hitherto unreported case with 46,XX,der(17)t(14;17)(q32.2;p13)pat who have three copies of the 14q32.2 imprinted region. Since the microsatellite locus *D14S985* is present in two copies (Table S1) and the *MEG3*-DMR is deleted (Figure 2) in patient 2, this has served to localize the breakpoints. (B) Oligoarray comparative genomic hybridization for a ~1 Mb imprinted region. All the signals remain within the normal range (-1 SD ~ +1 SD) (shaded in light blue) in patients 1 and 2.

Found at: doi:10.1371/journal.pgen.1000992.s001 (1.17 MB TIF)

Figure S2 Expression analysis. (A) Maternal *MEG3* expression in the leukocytes of normal subjects. Genotyping has been performed for three cSNPs using genomic DNA (gDNA) and cDNA of leukocytes from control subjects and gDNA samples of their mothers, indicating that both maternally and non-maternally (paternally) derived alleles are delineated in the gDNA, whereas maternally inherited alleles alone are identified in cDNA. These three cSNPs have also been studied in the mother of patient 1 (Figure 5D). (B) Paternal *RTL1* expression in the placenta of a normal subject. Genotyping has been carried out for *RTL1* cSNP using gDNA and cDNA samples of a fresh placenta and gDNA sample from the mother, showing that both maternally and non-maternally (paternally) derived alleles are delineated in the gDNA, whereas a non-maternally (paternally) inherited allele alone is detected in cDNA. This cSNP has also been examined in the placenta of patient 1 (Figure 5E). Furthermore, the results confirm that the primers utilized in this study have amplified *RTL1*, but not *RTL1as*.

Found at: doi:10.1371/journal.pgen.1000992.s002 (0.39 MB TIF)

Figure S3 Schematic representation of the observed and predicted methylation and expression patterns in previously reported cases with upd(14)pat/mat-like phenotypes and in normal and upd(14)pat/mat subjects. For the explanations of the illustrations, see the legend for Figure 6. Previous studies have indicated that (1) Epimutation-1, Deletion-1, Deletion-2, and Deletion-3 lead to maternal to paternal epigenotypic alteration; (2) Epimutation-2 results in paternal to maternal epigenotypic alteration; and (3) Deletion-4 and Deletion-5 have no effect on the epigenotypic status [2,5–8,26]. (A) Cases with typical or mild upd(14)pat phenotype. Epimutation-1: Hypermethylation of the IG-DMR and the *MEG3*-DMR of maternal origin in the body, and that of the IG-DMR of maternal origin in the placenta (the *MEG3*-DMR is rather hypomethylated in the placenta) (cases 6–8 in Kagami et al. [2]). Deletion-1: Microdeletion involving *DLK1*, the two DMRs, and *MEG3* on the maternally inherited chromosome (case 2 in Kagami et al. [2]). Deletion-2: Microdeletion involving *DLK1*, the two DMRs, *MEG3*, *RTL1*, and *RTL1as* on the maternally inherited chromosome (cases 3 and 5 in Kagami et al. [2]). Deletion-3: Microdeletion involving the two DMRs, *MEG3*, *RTL1*, and *RTL1as* on the maternally inherited chromosome (case 4 in Kagami et al. [2]). These findings are explained by the following notions: (1) Epimutation (hypermethylation) of the normally hypomethylated IG-DMR of maternal origin directly results in paternalization of the imprinted region in the placenta and indirectly leads to paternalization of the imprinted region in the body via epimutation (hypermethylation) of the usually hypomethylated *MEG3*-DMR of maternal origin. Thus, the epimutation (hypermethylation) is predicted to have impaired the IG-DMR as the primary target, followed by the epimutation (hypermethylation) of the *MEG3*-DMR after fertilization; (2) Loss of the hypomethylated *MEG3*-DMR of maternal origin leads to paternalization of the imprinted region in the body; and (3) Loss of the hypomethylated IG-DMR of maternal origin results in paternalization of the imprinted region in the placenta. Furthermore, epigenotype-phenotype correlations imply that the severity of upd(14)pat phenotype is primarily determined by the *RTL1* expression dosage rather than the *DLK1* expression dosage [2]. (B) Cases with upd(14)mat-like phenotype. Epimutation-2: Hypomethylation of the IG-DMR and the *MEG3*-DMR of paternal origin (Temple et al. [5], Buiting et al. [6], Hosoki et al. [7], and Zechner et al. [8]). Deletion-4: Microdeletion involving *DLK1*, the two DMRs, and *MEG3* on the paternally inherited chromosome (cases 9 and 10 in Kagami et al. [2]). Deletion-5: Microdeletion involving *DLK1*, the two DMRs, *MEG3*, *RTL1*, and *RTL1as* on the paternally inherited chromosome (case 11 in Kagami et al. [2] and patient 3 in Buiting et al. [6]). These findings are consistent with the following notions: (1) Epimutation (hypomethylation) of the normally hypermethylated IG-DMR of paternal origin directly results in maternalization of the imprinted region in the placenta and indirectly leads to maternalization of the imprinted region in the body through epimutation (hypomethylation) of the usually hypermethylated *MEG3*-DMR of paternal origin. Thus, epimutation (hypomethylation) is predicted to have affected the IG-DMR

as the primary target, followed by the epimutation (hypomethylation) of the *MEG3*-DMR after fertilization; and (2) Loss of the hypermethylated DMRs of paternal origin has no effect on the imprinting status [2,26], so that upd(14)mat-like phenotype is primarily ascribed to the additive effects of loss of functional *DLK1* and *RTL1* from the paternally derived chromosome (the effects of loss of *DIO3* appears to be minor, if any [2,35]). Although the *MEGs* expression dosage is predicted to be normal in Deletion-4 and Deletion-5 and doubled in Epimutation-2 as well as in upd(14)mat, it remains to be determined whether the difference in the *MEGs* expression dosage has major clinical effects or not. (C) Normal and upd(14)pat/mat subjects.

Found at: doi:10.1371/journal.pgen.1000992.s003 (2.72 MB TIF)

Table S1 The results of microsatellite and SNP analyses.

Found at: doi:10.1371/journal.pgen.1000992.s004 (0.19 MB DOC)

Table S2 Clinical features in the mother of patient 1.

Found at: doi:10.1371/journal.pgen.1000992.s005 (0.09 MB DOC)

Table S3 Primers utilized in the present study.

Found at: doi:10.1371/journal.pgen.1000992.s006 (0.14 MB DOC)

Author Contributions

Conceived and designed the experiments: MK ACFS TO. Performed the experiments: MK MF KM FK. Analyzed the data: MK TO. Contributed reagents/materials/analysis tools: MJO AJG YW OA NM KM TO. Wrote the paper: TO.

References

1. da Rocha ST, Edwards CA, Ito M, Ogata T, Ferguson-Smith AC (2008) Genomic imprinting at the mammalian Dlk1-Dio3 domain. Trends Genet 24: 306–316.
2. Kagami M, Sekita Y, Nishimura G, Irie M, Kato F, et al. (2008) Deletions and epimutations affecting the human 14q32.2 imprinted region in individuals with paternal and maternal upd(14)-like phenotypes. Nat Genet 40: 237–242.
3. Kagami M, Yamazawa K, Matsubara K, Matsuo N, Ogata T (2008) Placentomegaly in paternal uniparental disomy for human chromosome 14. Placenta 29: 760–761.
4. Kotzot D (2004) Maternal uniparental disomy 14 dissection of the phenotype with respect to rare autosomal recessively inherited traits, trisomy mosaicism, and genomic imprinting. Ann Genet 47: 251–260.
5. Temple IK, Shrubb V, Lever M, Bullman H, Mackay DJ (2007) Isolated imprinting mutation of the DLK1/GTL2 locus associated with a clinical presentation of maternal uniparental disomy of chromosome 14. J Med Genet 44: 637–640.
6. Buiting K, Kanber D, Martín-Subero JI, Lieb W, Terhal P, et al. (2008) Clinical features of maternal uniparental disomy 14 in patients with an epimutation and a deletion of the imprinted DLK1/GTL2 gene cluster. Hum Mutat 29: 1141–1146.
7. Hosoki K, Ogata T, Kagami M, Tanaka T, Saitoh S (2008) Epimutation (hypomethylation) affecting the chromosome 14q32.2 imprinted region in a girl with upd(14)mat-like phenotype. Eur J Hum Genet 16: 1019–1023.
8. Zechner U, Kohlschmidt N, Rittner G, Damatova N, Beyer V, et al. (2009) Epimutation at human chromosome 14q32.2 in a boy with a upd(14)mat-like clinical phenotype. Clin Genet 75: 251–258.
9. Li E, Beard C, Jaenisch R (1993) Role for DNA methylation in genomic imprinting. Nature 366: 362–365.
10. Rosa AL, Wu YQ, Kwabi-Addo B, Coveler KJ, Reid Sutton V, et al. (2005) Allele-specific methylation of a functional CTCF binding site upstream of MEG3 in the human imprinted domain of 14q32. Chromosome Res 13: 809–818.
11. Wylie AA, Murphy SK, Orton TC, Jirtle RL (2000) Novel imprinted DLK1/GTL2 domain on human chromosome 14 contains motifs that mimic those implicated in IGF2/H19 regulation. Genome Res 10: 1711–1718.
12. Tierling S, Dalbert S, Schoppenhorst S, Tsai CE, Oliger S, et al. (2007) High-resolution map and imprinting analysis of the Gtl2-Dnchc1 domain on mouse chromosome 12. Genomics 87: 225–235.
13. Takada S, Paulsen M, Tevendale M, Tsai CE, Kelsey G, et al. (2002) Epigenetic analysis of the Dlk1-Gtl2 imprinted domain on mouse chromosome 12: implications for imprinting control from comparison with Igf2-H19. Hum Mol Genet 11: 77–86.
14. Ohlsson R, Renkawitz R, Lobanenkov V (2001) CTCF is a uniquely versatile transcription regulator linked to epigenetics and disease. Trends Genet 17: 520–527.
15. Hark AT, Schoenherr CJ, Katz DJ, Ingram RS, Levorse JM, et al. (2000) CTCF mediates methylation-sensitive enhancer-blocking activity at the H19/Igf2 locus. Nature 405: 486–489.
16. Kanduri C, Pant V, Loukinov D, Pugacheva E, Qi CF, et al. (2000) Functional association of CTCF with the insulator upstream of the H19 gene is parent of origin-specific and methylation-sensitive. Curr Biol 10: 853–856.
17. da Rocha ST, Tevendale M, Knowles E, Takada S, Watkins M, et al. (2007) Restricted co-expression of Dlk1 and the reciprocally imprinted non-coding RNA, Gtl2: implications for cis-acting control. Dev Biol 306: 810–823.
18. Wan LB, Pan H, Hannenhalli S, Cheng Y, Ma J, et al. (2008) Maternal depletion of CTCF reveals multiple functions during oocyte and preimplantation embryo development. Development 135: 2729–2738.
19. Ideraabdullah FY, Vigneau S, Bartolomei MS (2008) Genomic imprinting mechanisms in mammals. Mutat Res 647: 77–85.
20. Fitzpatrick GV, Pugacheva EM, Shin JY, Abdullaev Z, Yang Y, et al. (2007) Allele-specific binding of CTCF to the multipartite imprinting control region KvDMR1. Mol Cell Biol 27: 2636–2647.
21. Horsthemke B, Wagstaff J (2008) Mechanisms of imprinting of the Prader-Willi/Angelman region. Am J Med Genet A 146A: 2041–2052.
22. Lin SP, Coan P, da Rocha ST, Seitz H, Cavaille J, et al. (2007) Differential regulation of imprinting in the murine embryo and placenta by the Dlk1-Dio3 imprinting control region. Development 134: 417–426.
23. Coan PM, Burton GJ, Ferguson-Smith AC (2005) Imprinted genes in the placenta–a review. Placenta 26 Suppl A: S10–20.
24. Georgiades P, Watkins M, Surani MA, Ferguson-Smith AC (2000) Parental origin-specific developmental defects in mice with uniparental disomy for chromosome 12. Development 127: 4719–4728.
25. Takada S, Tevendale M, Baker J, Georgiades P, Campbell E, et al. (2000) Delta-like and gtl2 are reciprocally expressed, differentially methylated linked imprinted genes on mouse chromosome 12. Curr Biol 10: 1135–1138.
26. Lin SP, Youngson N, Takada S, Seitz H, Reik W, et al. (2003) Asymmetric regulation of imprinting on the maternal and paternal chromosomes at the Dlk1-Gtl2 imprinted cluster on mouse chromosome 12. Nat Genet 35: 97–102.
27. Takahashi N, Okamoto A, Kobayashi R, Shirai M, Obata Y, et al. (2009) Deletion of Gtl2, imprinted non-coding RNA, with its differentially methylated region induces lethal parent-origin-dependent defects in mice. Hum Mol Genet 18: 1879–1888.
28. Lewis A, Mitsuya K, Umlauf D, Smith P, Dean W, et al. (2004) Imprinting on distal chromosome 7 in the placenta involves repressive histone methylation independent of DNA methylation. Nat Genet 36: 1291–1295.
29. Umlauf D, Goto Y, Cao R, Cerqueira F, Wagschal A, et al. (2004) Imprinting along the Kcnq1 domain on mouse chromosome 7 involves repressive histone methylation and recruitment of Polycomb group complexes. Nat Genet 36: 1296–1300.
30. Sekita Y, Wagatsuma H, Irie M, Kobayashi S, Kohda T, et al. (2006) Aberrant regulation of imprinted gene expression in Gtl2lacZ mice. Cytogenet. Genome Res 113: 223–229.
31. Steshina EY, Carr MS, Glick EA, Yevtodiyenko A, Appelbe OK, et al. (2006) Loss of imprinting at the Dlk1-Gtl2 locus caused by insertional mutagenesis in the Gtl2 5′ region. BMC Genet 7: 44.
32. Charlier C, Segers K, Karim L, Shay T, Gyapay G, et al. (2001) The callipyge mutation enhances the expression of coregulated imprinted genes in cis without affecting their imprinting status. Nat Genet 27: 367–369.
33. Georges M, Charlier C, Cockett N (2003) The callipyge locus: evidence for the trans interaction of reciprocally imprinted genes. Trends Genet 19: 248–252.
34. Moon YS, Smas CM, Lee K, Villena JA, Kim KH, et al. (2002) Mice lacking paternally expressed Pref-1/Dlk1 display growth retardation and accelerated adiposity. Mol Cell Biol 22: 5585–5592.
35. Tsai CE, Lin SP, Ito M, Takagi N, Takada S, et al. (2002) Genomic imprinting contributes to thyroid hormone metabolism in the mouse embryo. Curr Biol 12: 1221–1226.
36. Sekita Y, Wagatsuma H, Nakamura K, Ono R, Kagami M, et al. (2008) Role of retrotransposon-derived imprinted gene, Rtl1, in the feto-maternal interface of mouse placenta. Nat Genet 40: 243–248.
37. Seitz H, Youngson N, Lin SP, Dalbert S, Paulsen M, et al. (2003) Imprinted microRNA genes transcribed antisense to a reciprocally imprinted retrotransposon-like gene. Nat Genet 34: 261–262.
38. Davis E, Caiment F, Tordoir X, Cavaillé J, Ferguson-Smith A, et al. (2005) RNAi-mediated allelic trans-interaction at the imprinted Rtl1/Peg11 locus. Curr Biol 15: 743–749.

Downloaded from jmg.bmj.com on August 18, 2010 - Published by group.bmj.com

JMG Online First, published on August 3, 2010 as 10.1136/jmg.2010.079343

Parthenogenetic chimaerism/mosaicism with a Silver-Russell syndrome-like phenotype

K Yamazawa,[1,2] K Nakabayashi,[3] M Kagami,[1] T Sato,[1] S Saitoh,[4] R Horikawa,[5] N Hizuka,[6] T Ogata[1]

► Additional figures, tables and an appendix are published online only. To view these files, please visit the journal online (http://jmg.bmj.com).

[1]Departments of Endocrinology and Metabolism, National Research Institute for Child Health and Development, Tokyo, Japan
[2]Department of Physiology, Development & Neuroscience, University of Cambridge, Cambridge, UK
[3]Maternal-Fetal Biology, National Research Institute for Child Health and Development, Tokyo, Japan
[4]Department of Pediatrics, Hokkaido University Graduate School of Medicine, Sapporo, Japan
[5]Division of Endocrinology and Metabolism, National Children's Hospital, Tokyo, Japan
[6]Department of Medicine, Institute of Clinical Endocrinology, Tokyo Women's Medical University, Tokyo, Japan

Correspondence to
Dr Tsutomu Ogata, Department of Endocrinology and Metabolism, National Research Institute for Child Health and Development, 2-10-1 Ohkura, Setagaya, Tokyo 157-8535, Japan; tomogata@nch.go.jp

Received 20 March 2010
Revised 6 May 2010
Accepted 8 May 2010

UNLOCKED

This paper is freely available online under the BMJ Journals unlocked scheme, see http://jmg.bmj.com/site/about/unlocked.xhtml

ABSTRACT

Introduction We report a 34-year-old Japanese female with a Silver-Russell syndrome (SRS)-like phenotype and a mosaic Turner syndrome karyotype (45,X/46,XX).

Methods/Results Molecular studies including methylation analysis of 17 differentially methylated regions (DMRs) on the autosomes and the *XIST*-DMR on the X chromosome and genome-wide microsatellite analysis for 96 autosomal loci and 30 X chromosomal loci revealed that the 46,XX cell lineage was accompanied by maternal uniparental isodisomy for all chromosomes (upid(AC)mat), whereas the 45,X cell lineage was associated with biparentally derived autosomes and a maternally derived X chromosome. The frequency of the 46,XX upid(AC)mat cells was calculated as 84% in leukocytes, 56% in salivary cells, and 18% in buccal epithelial cells.

Discussion The results imply that a parthenogenetic activation took place around the time of fertilisation of a sperm missing a sex chromosome, resulting in the generation of the upid(AC)mat 46,XX cell lineage by endoreplication of one blastomere containing a female pronucleus and the 45,X cell lineage by union of male and female pronuclei. It is likely that the extent of overall (epi)genetic aberrations exceeded the threshold level for the development of SRS phenotype, but not for the occurrence of other imprinting disorders or recessive Mendelian disorders.

Although a mammal with maternal uniparental disomy for all chromosomes (upd(AC)mat) is incompatible with life because of genomic imprinting,[1] a mammal with a upd(AC)mat cell lineage could be viable in the presence of a co-existing normal cell lineage. In the human, Strain *et al*[2] have reported 46,XX peripheral blood cells with maternal uniparental isodisomy for all chromosomes (upid(AC)mat) in a 1.2-year-old phenotypically male patient with aggressive behaviour, hemifacial hypoplasia and normal birth weight. Because of the 46,XX disorders of sex development, detailed molecular studies were performed, revealing the presence of a normal 46,XY cell lineage in a vast majority of skin fibroblasts and a upid(AC)mat 46,XX cell lineage in nearly all blood cells. In addition, although the data are insufficient to draw a definitive conclusion, Horike *et al*[3] have also identified 46,XX peripheral blood cells with possible upd(AC)mat in a phenotypically male patient through methylation analyses for plural differentially methylated regions (DMRs) in 11 patients with Silver–Russell syndrome (SRS)-like phenotype. This patient was found to have a normal 46,XY cell lineage and a triploid 69,XXY cell lineage in skin fibroblasts.

However, such patients with a upd(AC)mat cell lineage remain extremely rare, and there is no report describing a human with such a cell lineage in the absence of a normal cell lineage. Here, we report a female patient with a upid(AC)mat 46,XX cell lineage and a non-upd 45,X cell lineage who was identified through genetic screenings of 103 patients with SRS-like phenotype.

MATERIALS AND METHODS

Case report

This Japanese female patient was conceived naturally and born at 40 weeks of gestation by a normal vaginal delivery. At birth, her length was 44.0 cm (−3.1 SD), her weight 2.1 kg (−2.9 SD) and her occipitofrontal head circumference (OFC) 30.5 cm (−2.3 SD). The parents and the younger brother were clinically normal (the father died from a traffic accident).

At 2 years of age, she was referred to us because of growth failure. Her height was 77.7 cm (−2.5 SD), her weight 8.45 kg (−2.6 SD) and her OFC 43.5 cm (−2.5 SD). Physical examination revealed several SRS-like somatic features such as triangular face, right hemihypoplasia and bilateral fifth finger clinodactyly. She also had developmental retardation, with a developmental quotient of 56. Endocrine studies for short stature were normal as were radiological studies. Cytogenetic analysis using lymphocytes indicated a low-grade mosaic Turner syndrome (TS) karyotype, 45,X[3]/46,XX[47]. Thus, a screening of TS phenotype[4] was performed, detecting horseshoe kidney but no body surface features or cardiovascular lesion. Chromosome analysis was repeated at 6 and 32 years of age using lymphocytes, revealing a 45,X[8]/46,XX[92] karyotype and a 45,X[12]/46,XX[88] karyotype, respectively. On the last examination at 34 years of age, her height was 125.0 cm (−6.2 SD), her weight 37.5 kg (−2.0 SD) and her OFC 51.2 cm (−2.8 SD). She was engaged in a simple work and was able to get on her daily life for herself.

Sample preparation

This study was approved by the Institutional Review Board Committees at National Center for Child health and Development. After obtaining written informed consent, genomic DNA was extracted from leukocytes of the patient, the mother and the brother and from salivary cells, which comprise ∼40% of buccal epithelial cells and ∼60% of leukocytes,[5] of the patient. Lymphocyte metaphase spreads and leukocyte RNA were also

Copyright Article author (or their employer) 2010. Produced by BMJ Publishing Group Ltd under licence.

Downloaded from jmg.bmj.com on August 18, 2010 - Published by group.bmj.com

obtained from the patient. Leukocytes of healthy adults and patients with imprinting disorders were utilised for controls.

Primers and probes

The primers utilised in this study are summarised in supplementary methods and supplementary tables 1—3.

DMR analyses

We first performed bio-combined bisulfite restriction analysis (COBRA)[6] and bisulfite sequencing of the *H19*-DMR (A) on chromosome 11p15.5 by the previously described methods[7] and methylation-sensitive PCR analysis of the *MEST*-DMR (A) on chromosome 7q32.2 by the previously described methods[8] with minor modifications (the methylated and unmethylated allele-specific primers were designed to yield PCR products of different sizes, and the PCR products were visualised on the 2100 Bioanalyzer (Agilent, Santa Clara, California, USA)). This was because hypomethylation (epimutation) of the normally methylated *H19*-DMR of paternal origin and maternal uniparental disomy 7 are known to account for 35—65% and 5—10% of SRS patients, respectively.[9] [10] In addition, fluorescence in situ hybridisation (FISH) analysis was performed with a ~84-kb RP5-998N23 probe containing the *H19*-DMR (BACPAC Resources Center, Oakland, California, USA). We also examined multiple other DMRs by bio-COBRA. The ratio of methylated clones (the methylation index) was calculated using peak heights of digested and undigested fragments on the 2100 Bioanalyzer using 2100 expert software.

Genome-wide microsatellite analysis

Microsatellite analysis was performed for 96 autosomal loci and 30 X chromosomal loci. The segment encompassing each locus was PCR-amplified, and the PCR product size was determined on the ABI PRISM 310 autosequencer using GeneScan software (Applied Biosystems, Foster City, California, USA).

PCR analysis for Y chromosomal loci

Standard PCR was performed for six Y chromosomal loci. The PCR products were electrophoresed using the 2100 Bioanalyzer.

Expression analysis

Quantitative real-time reverse transcriptase PCR analysis was performed for three paternally expressed genes (*IGF2*, *SNRPN* and *ZAC1*) and four maternally expressed genes (*H19*, *MEG3*, *PHLDA2* and *CDKN1C*) that are known to be variably (usually weakly) expressed in leukocytes (UniGene, http://www.ncbi.nlm.nih.gov/sites/entrez?db=unigene), using an ABI Prism 7000 Sequence Detection System (Applied Biosystems). *TBP* and *GAPDH* were utilised as internal controls.

RESULTS

DMR analyses

In leukocytes, the bio-COBRA indicated severely hypomethylated *H19*-DMR, and bisulfite sequencing combined with *rs2251375* SNP typing for 30 clones revealed maternal origin of 29 hypomethylated clones and non-maternal (paternal) origin of a single methylated clone in this patient (figure 1A). Thus, the marked hypomethylation of the *H19*-DMR was caused by predominance of maternally derived clones rather than hypomethylation of the *H19*-DMR of paternal origin. FISH analysis for 100 lymphocyte metaphase spreads excluded an apparent deletion of the paternally derived *H19*-DMR or duplication of the maternally derived *H19*-DMR (Supplementary figure 1). Methylation-sensitive PCR amplification for the *MEST*-DMR delineated a major peak for the methylated allele and a minor peak for the unmethylated allele (figure 1B). This also indicated the predominance of maternally derived clones and the co-existence of a minor portion of paternally derived clones. Furthermore, autosomal DMRs invariably exhibited markedly abnormal methylation patterns consistent with predominance of maternally inherited DMRs, whereas the methylation index of the *XIST*-DMR on the X chromosome remained within the female reference range (figure 1C). The abnormal methylation patterns were less obvious in salivary cells (thus, in buccal epithelial cells) than in leukocytes, except for the methylation index for the *XIST*-DMR that mildly exceeded the female reference range (figure 1A—C).

Microsatellite analysis

Major peaks consistent with maternal uniparental isodisomy and minor peaks of non-maternal (paternal) origin were identified for at least one locus on each autosome, with the minor peaks of non-maternal origin being more obvious in salivary cells than in leukocytes (figure 1D and supplementary table 4). Furthermore, the frequency of the upid(AC)mat cells was calculated as 84% in leukocytes, 56% in salivary cells and 18% in epithelial buccal cells, using the area under curves for the maternally and the non-maternally inherited peaks (supplementary note). Such minor peaks of non-maternal origin were not detected for all the 30 X chromosomal loci examined.

PCR analysis for Y chromosomal loci

PCR amplification failed to detect any trace of Y chromosome-specific bands in leukocytes and salivary cells (Supplementary figure 2).

Expression analysis

Expression analysis using control leukocytes indicated that, of the seven examined genes, *SNRPN* expression alone was strong enough to allow for a precise assessment (Supplementary figure 3). *SNRPN* expression was extremely low in this patient (figure 1E).

DISCUSSION

These results imply that this patient had a upid(AC)mat 46,XX cell lineage and a non-upd 45,X cell lineage. Indeed, methylation patterns of the *XIST*-DMR is explained by assuming that the two X chromosomes in the upid(AC)mat cells undergo random X-inactivation and that 45,X cells with the methylated *XIST*-DMR on a single active X chromosome[11] are relatively prevalent in buccal epithelial cells. Furthermore, lack of non-maternally derived minor peaks for microsatellite loci on the X chromosome is explained by assuming that the two X chromosomes in the upid(AC)mat cells and the single X chromosome in the 45,X cells are derived from a common X chromosome of maternal origin, with no paternally derived sex chromosome. It is likely, therefore, that a parthenogenetic activation took place around the time of fertilisation of a sperm missing a sex chromosome, resulting in the generation of the 46,XX cell lineage with upid (AC)mat by endoreplication (the replication of DNA without the subsequent completion of mitosis) of one blastomere containing a female pronucleus and the 45,X cell lineage with biparentally derived autosomes and a maternally derived X chromosome by union of male and female pronuclei (figure 2), although it is also possible that a paternally derived sex chromosome was present in the sperm but was lost from the normal

Downloaded from jmg.bmj.com on August 18, 2010 - Published by group.bmj.com

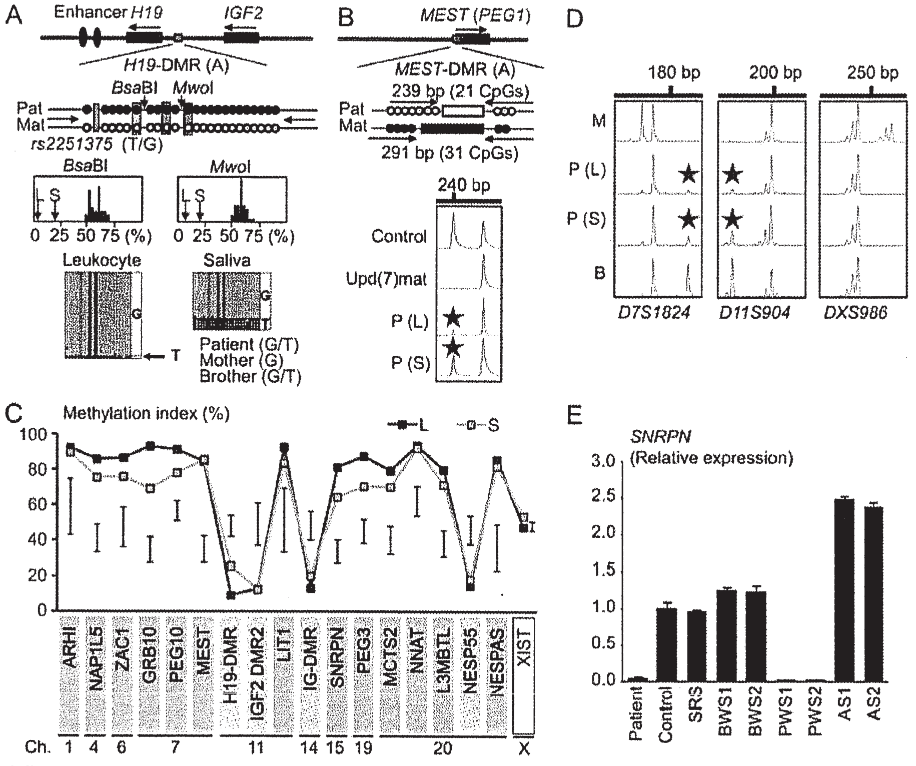

Figure 1 Representative molecular results. Pat, paternally derived allele; Mat, maternally derived allele; P, patient; M, mother; B, brother; L, leukocytes; and S, salivary cells. Filled and open circles in A and B represent methylated and unmethylated cytosine residues at the CpG dinucleotides, respectively. A. Methylation patterns of the *H19*-DMR (A) harbouring 23 CpG dinucleotides and the T/G SNP (*rs2251375*) (a grey box). The PCR products are digested with *Bsa*BI when the cytosine at the sixth CpG dinucleotide (highlighted in yellow) is methylated and with *Mwo*I when the two cytosines at the ninth and the 11th CpG dinucleotides (highlighted in orange) are methylated. For the bio-COBRA data, the black histograms represent the distribution of methylation indices (%) in 50 control participants, and L and S denote the methylation indices for leukocytes and salivary cells of this patient, respectively. For the bisulfite sequencing data, each line indicates a single clone. B. Methylated and unmethylated allele-specific PCR analysis for the *MEST*-DMR (A). In a control participant, the PCR products for methylated and unmethylated alleles are delineated, and the unequal amplification is consistent with a short product being more easily amplified than a long product. In a previously reported patient with upd(7)mat,[8] the methylated allele only is amplified. In this patient, major peaks for the methylated allele and minor peaks for the unmethylated allele (red asterisks) are detected. C. Methylation patterns for the 18 DMRs examined. The DMRs highlighted in blue and pink are methylated after paternal and maternal transmissions, respectively. The black vertical bars indicate the reference data (maximum–minimum) in 20 normal control participants, using leukocyte genomic DNA (for the *XIST*-DMR, 16 female data are shown). D. Representative microsatellite analysis. Minor peaks (red asterisks) have been identified for *D7S1824* and *D11S904* but not for *DXS986* of the patient. Since the peaks for *D7S1824* and *D11S904* are absent in the mother and clearly present in the brother, they are assessed to be of paternal origin. E. Relative expression level (mean ± SD) of *SNRPN* on chromosome 15. The data have been normalised against *TBP*. SRS, an SRS patient with an epimutation (hypomethylation) of the *H19*-DMR; BWS1, a BWS patient with an epimutation (hypermethylation) of the *H19*-DMR; BWS2, a BWS patient with upd(11)pat; PWS1, a PWS patient with upd(15)mat; PWS2, a PWS patient with an epimutation (hypermethylation) of the *SNRPN*-DMR; AS1, an Angelman syndrome (AS) patient with upd(15)pat; and AS2, an AS patient with an epimutation (hypomethylation) of the *SNRPN*-DMR.

cell lineage at the very early developmental stage. Hence, in a strict sense, this patient is neither a chimera resulting from the fusion of two different zygotes nor a mosaic caused by a mitotic error of a single zygote. In this regard, a triploid cell stage is assumed in the generation of a upid(AC)mat cell lineage, and such triploid cells may have been detected in skin fibroblasts of the patient reported by Horike *et al.*[3]

The upid(AC)mat cells accounted for the majority of leukocytes even in adulthood of this patient, despite global negative selective pressure.[12 13] This phenomenon, though intriguing, would not be unexpected in human studies because leukocytes are usually utilised for genetic analyses. Rather, if the upid(AC)mat cells were barely present in leukocytes, they would not have been detected. It is likely, therefore, that upid(AC)mat cells have occupied a relatively large portion of the definitive haematopoietic tissues primarily as a stochastic event. Furthermore, parthenogenetic chimera mouse studies have revealed that parthenogenetic cells are found at a relatively high frequency in some tissues/organs including blood and are barely identified in other tissues/organs such as skeletal muscle and liver.[13] Such a possible tissue-specific selection in favour of the preservation of parthenogenetic cells in the definitive haematopoietic tissues may also be relevant to the predominance of the upid(AC)mat cells in leukocytes. In addition, a reduced growth potential of 45,X cells[14] may also have contributed to the skewed ratio of the two cell lineages.

Clinical features of this patient would be determined by several factors. They include: (1) the ratio of two cell lineages in various tissues/organs, (2) the number of imprinted regions or DMRs relevant to the development of specific imprinting disorders (eg, plural regions/DMRs on chromosomes 7 and 11 for SRS[9 10] and a single region/DMR on chromosome 15 for Prader–Willi syndrome (PWS)),[15] (3) the degree of clinical effects of dysregulated imprinted regions/DMRs (an (epi)dominant effect has been

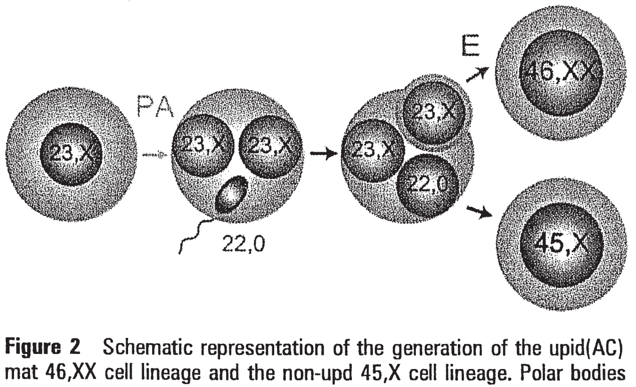

Figure 2 Schematic representation of the generation of the upid(AC)mat 46,XX cell lineage and the non-upd 45,X cell lineage. Polar bodies are not shown. PA, parthenogenetic activation; and E, endoreplication of one blastomere containing a female pronucleus.

Downloaded from jmg.bmj.com on August 18, 2010 - Published by group.bmj.com

assumed for the 11p15.5 imprinted regions including the *IGF2–H19* domain on the basis of SRS or Beckwith–Wiedemann syndrome (BWS) phenotype in patients with multilocus hypomethylation[16] and BWS-like phenotype in patients with a upid (AC)pat cell lineage,[17] a mirror image of a upid(AC)mat cell lineage), (4) expression levels of imprinted genes in upid(AC)mat cells (although *SNRPN* expression of this patient was consistent with upid(AC)mat cells being predominant in leukocytes, complicated expression patterns have been identified for several imprinted genes in androgenetic and parthenogenetic fetal mice, probably because of perturbed *cis*- and *trans*-acting regulatory mechanisms)[18] and (5) unmasking of possible maternally inherited recessive mutation(s) in upid(AC)mat cells.[19] Collectively, it appears that the extent of overall (epi)genetic aberrations exceeded the threshold level for the development of SRS phenotype and horseshoe kidney characteristic of TS[4] but remained below the threshold level for the occurrence of other imprinting disorders or recessive Mendelian disorders.

In summary, we identified a upid(AC)mat 46,XX cell lineage in a woman with an SRS-like phenotype and a 45,X cell lineage accompanied by autosomal haploid sets of biparental origin. This report will facilitate further identification of patients with a upid(AC)mat cell lineage and better clarification of the clinical phenotypes in such patients.

Acknowledgements We thank the patient and her family members for their participation in this study. We also thank Dr. Toshiro Nagai for providing us with blood samples of patients with Prader–Willi syndrome.

Funding This work was supported by grants from the Ministry of Health, Labor, and Welfare and from the Ministry of Education, Science, Sports and Culture.

Competing interests None.

Patient consent Obtained.

Ethics approval This study was conducted with the approval of the Institutional Review Board Committees at National Center for Child health and Development.

Contributors Drs Kazuki Yamazawa (first author) and Kazuhiko Nakabayashi (second author) contributed equally to this work.

Provenance and peer review Not commissioned; externally peer reviewed.

REFERENCES

1. **McGrath J,** Solter D. Completion of mouse embryogenesis requires both the maternal and paternal genomes. *Cell* 1984;**37**:179–83.
2. **Strain L,** Warner JP, Johnston T, Bonthron DT. A human parthenogenetic chimaera. *Nat Genet* 1995;**11**:164–9.
3. **Horike S,** Ferreira JC, Meguro-Horike M, Choufani S, Smith AC, Shuman C, Meschino W, Chitayat D, Zackai E, Scherer SW, Weksberg R. Screening of DNA methylation at the H19 promoter or the distal region of its ICR1 ensures efficient detection of chromosome 11p15 epimutations in Russell–Silver syndrome. *Am J Med Genet Part A* 2009;**149A**:2415–23.
4. **Styne D,** Grumbach M. Puberty: ontogeny, neuroendocrinology, physiology, and disorders. In: Kronenberg H, Melmed M, Polonsky K, Larsen P, eds. *Williams textbook of endocrinology*, 11th edn. Philadelphia: Saunders 2008:969–1166.
5. **Thiede C,** Prange-Krex G, Freiberg-Richter J, Bornhauser M, Ehninger G. Buccal swabs but not mouthwash samples can be used to obtain pretransplant DNA fingerprints from recipients of allogeneic bone marrow transplants. *Bone Marrow Transplant* 2000;**25**:575–7.
6. **Brena RM,** Auer H, Kornacker K, Hackanson B, Raval A, Byrd JC, Plass C. Accurate quantification of DNA methylation using combined bisulfite restriction analysis coupled with the Agilent 2100 Bioanalyzer platform. *Nucleic Acids Res* 2006;**34**:e17.
7. **Yamazawa K,** Kagami M, Nagai T, Kondoh T, Onigata K, Maeyama K, Hasegawa T, Hasegawa Y, Yamazaki T, Mizuno S, Miyoshi Y, Miyagawa S, Horikawa R, Matsuoka K, Ogata T. Molecular and clinical findings and their correlations in Silver–Russell syndrome: implications for a positive role of IGF2 in growth determination and differential imprinting regulation of the IGF2-H19 domain in bodies and placentas. *J Mol Med* 2008;**86**:1171–81.
8. **Yamazawa K,** Kagami M, Ogawa M, Horikawa R, Ogata T. Placental hypoplasia in maternal uniparental disomy for chromosome 7. *Am J Med Genet Part A* 2008;**146A**:514–16.
9. **Abu-Amero S,** Monk D, Frost J, Preece M, Stanier P, Moore GE. The genetic aetiology of Silver–Russell syndrome. *J Med Genet* 2008;**45**:193–9.
10. **Eggermann T,** Eggermann K, Schonherr N. Growth retardation versus overgrowth: Silver–Russell syndrome is genetically opposite to Beckwith–Wiedemann syndrome. *Trends Genet* 2008;**24**:195–204.
11. **Goto T,** Monk M. Regulation of X-chromosome inactivation in development in mice and humans. *Microbiol Mol Biol Rev* 1998;**62**:362–78.
12. **Nagy A,** Sass M, Markkula M. Systematic non-uniform distribution of parthenogenetic cells in adult mouse chimaeras. *Development* 1989;**106**:321–4.
13. **Fundele R,** Norris ML, Barton SC, Reik W, Surani MA. Systematic elimination of parthenogenetic cells in mouse chimeras. *Development* 1989;**106**:29–35.
14. **Verp MS,** Rosinsky B, Le Beau MM, Martin AO, Kaplan R, Wallemark CB, Otano L, Simpson JL. Growth disadvantage of 45, X and 46, X, del(X)(p11) fibroblasts. *Clin Genet* 1988;**33**:277–85.
15. **Horsthemke B,** Wagstaff J. Mechanisms of imprinting of the Prader–Willi/Angelman region. *Am J Med Genet A* 2008;**146A**:2041–52.
16. **Azzi S,** Rossignol S, Steunou V, Sas T, Thibaud N, Danton F, Le Jule M, Heinrichs C, Cabrol S, Gicquel C, Le Bouc Y, Netchine I. Multilocus methylation analysis in a large cohort of 11p15-related foetal growth disorders (Russell Silver and Beckwith Wiedemann syndromes) reveals simultaneous loss of methylation at paternal and maternal imprinted loci. *Hum Mol Genet* 2009;**18**:4724–33.
17. **Wilson M,** Peters G, Bennetts B, McGillivray G, Wu ZH, Poon C, Algar E. The clinical phenotype of mosaicism for genome-wide paternal uniparental disomy: two new reports. *Am J Med Genet Part A* 2008;**146A**:137–48.
18. **Ogawa H,** Wu Q, Komiyama J, Obata Y, Kono T. Disruption of parental-specific expression of imprinted genes in uniparental fetuses. *FEBS Lett* 2006;**580**:5377–84.
19. **Engel E.** A fascination with chromosome rescue in uniparental disomy: Mendelian recessive outlaws and imprinting copyrights infringements. *Eur J Hum Genet* 2006;**14**:1158–69.

RESEARCH LETTER

AMERICAN JOURNAL OF medical genetics PART A

Prenatal Findings of Paternal Uniparental Disomy 14: Delineation of Further Patient

Nobuhiro Suzumori,[1,2]* Tsutomu Ogata,[3] Eita Mizutani,[1,2] Yukio Hattori,[1] Keiko Matsubara,[3] Masayo Kagami,[3] and Mayumi Sugiura-Ogasawara[1]

[1]Department of Obstetrics & Gynecology, Nagoya City University Graduate School of Medicine, Nagoya, Japan

[2]Division of Molecular and Clinical Genetics, Nagoya City University Graduate School of Medicine, Nagoya, Japan

[3]Department of Endocrinology and Metabolism, National Research Institute for Child Health and Development, Tokyo, Japan

Received 5 March 2010; Accepted 2 August 2010

How to Cite this Article:
Suzumori N, Ogata T, Mizutani E, Hattori Y, Matsubara K, Kagami M, Sugiura-Ogasawara M. 2010. Prenatal Findings of Paternal Uniparental Disomy 14: Delineation of Further Patient.
Am J Med Genet Part A 152A:3189–3192.

TO THE EDITOR:

Human chromosome 14q32.2 carries a cluster of imprinted genes including paternally expressed genes such as *DLK1* and *RTL1* and maternally expressed genes such as *MEG3* (alias *GTL2*) and *RTL1as* (*RTL1* antisense), together with the germline-derived intergenic differentially methylated region (IG-DMR) and the postfertilization-derived *MEG3*-DMR [da Rocha et al., 2008; Kagami et al., 2008a]. Consistent with this, paternal uniparental disomy 14 (upd(14)pat) results in a unique phenotype characterized by facial abnormality, small bell-shaped thorax with coat-hanger appearance of the ribs, abdominal wall defects, placentomegaly, and polyhydramnios [Kagami et al., 2008a,b], and maternal uniparental disomy 14 (upd(14)mat) leads to less-characteristic but clinically discernible features including growth failure [Kotzot, 2004; Kagami et al., 2008a].

For upd(14)pat, this condition has primarily been identified by the pathognomonic chest roentgenographic findings that are obtained immediately after birth because of severe respiratory dysfunction [Kagami et al., 2008a]. However, upd(14)pat has also been suspected prenatally by fetal radiological findings suggestive of small thorax and other characteristic findings [Curtis et al., 2006; Yamanaka et al., 2010]. Here, we report on prenatal findings in a hitherto unreported upd(14)pat patient. The results will serve to the prenatal identification of similarly affected patients and appropriate neonatal care including respiratory management.

A 41-year-old gravida 1, para 0 Japanese woman was referred to Nagoya City University Hospital because of polyhydramnios at 24 weeks of gestation. The polyhydramnios was severe and required repeated amnioreduction (1,600 ml at 26 weeks, 1,800 ml at 29 weeks, 2,000 ml at 32 weeks, and 2,100 ml at 35 weeks). The fetal urine volume was normal (5–12 ml per hr). At 28 weeks of gestation, 3D ultrasound studies were performed, delineating dysmorphic face, anteverted nares, micrognathia and small thorax characteristic of upd(14)pat (Fig. 1), although the differential diagnosis included Beckwith–Wiedemann syndrome and several types of skeletal dysplasia. Thereafter, ultrasound studies were weekly carried out, indicating almost normal fetal growth and normal umbilical artery Doppler.

At 37 weeks of gestation, a 2,778 g male infant was delivered by cesarean because of fetal distress. The placenta was 1,384 g (gestational age-matched reference, 510 ± 98 g) [Kagami et al., 2008b]. The patient had severe asphyxia, and immediately received appropriate management including mechanical ventilation for 6 days and nasal directional positive airway pressure at the neonatal intensive care unit. At birth, physical examination revealed hairy forehead, blepharophimosis, depressed nasal bridge, anteverted nares, small ears, protruding philtrum, puckered lips, micrognathia, short webbed neck, joint contractures, and diastasis recti, and roentgenograms showed typical bell-shaped thorax with coat-hanger appearance of the ribs (Fig. 2). Coax valga or kyphoscoliosis was uncertain. Discharge from hospital was 35 days after birth. On the last examination at 8 months of age, the patient

---

*Correspondence to:
Nobuhiro Suzumori, M.D., Ph.D., Division of Molecular and Clinical Genetics, Department of Obstetrics 8601, Japan.
E-mail: og.n.suz@med.nagoya-cu.ac.jp
Published online 24 November 2010 in Wiley Online Library (wileyonlinelibrary.com)
DOI 10.1002/ajmg.a.33719

© 2010 Wiley-Liss, Inc.

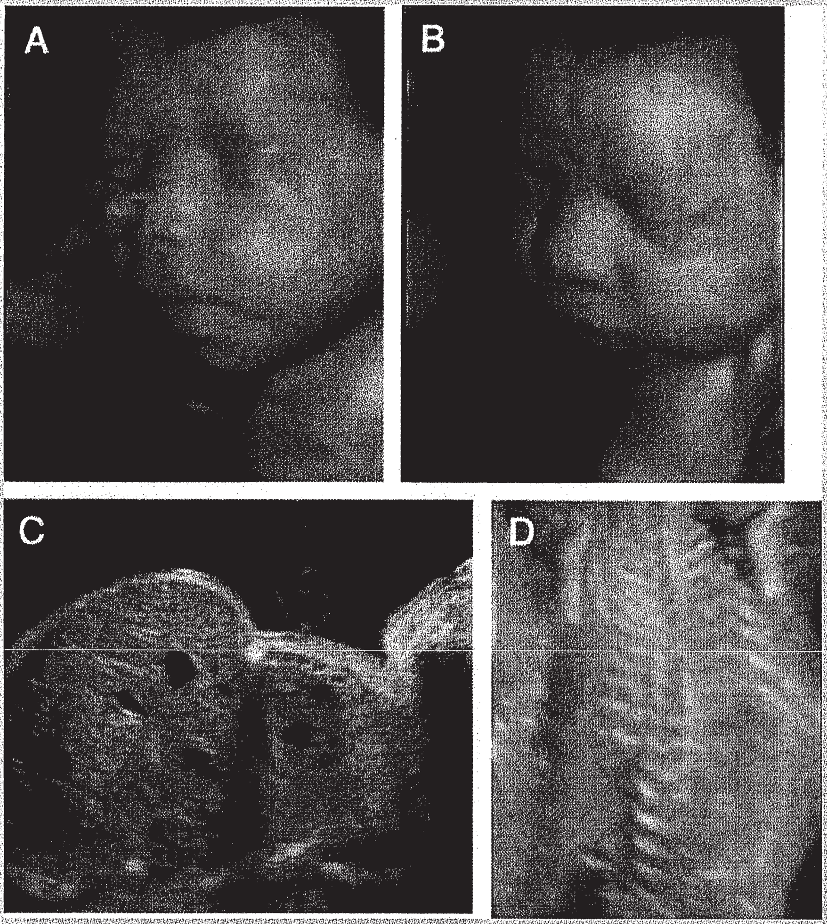

FIG. 1. Prenatal 3D findings at 28 weeks of gestation. A,B: Face appearance with blepharophimosis, depressed nasal bridge, anteverted nares, and micrognathia. C: Small thorax and polyhydramnios. D: Coat-hanger like appearance of the ribs.

required regular oropharyngeal suction and nasogastric tube feeding due to a poor swallowing reflex, and showed developmental delay. At the time of the last evaluation there was no seizure disorder.

To confirm the findings, cytogenetic and molecular studies were performed for the cord blood of the patient by the previously described methods [Kagami et al., 2008a]. This study was approved by the Institutional Review Board Committees at National Center for Child Health and Development and Nagoya City University, and performed after obtaining written informed consent. The karyotype was normal, and metaphase fluorescence in situ hybridization (FISH) analysis with a 202 kb BAC probe containing *DLK1* (RP11-566J3) and a 165 kb BAC probe containing *MG3* and *RTL1/RTL1as* (RP11-123M6) (http://bacpac.-chori.org/) delineated two signals with a similar intensity, respectively. Methylation analysis for bisulfite-treated genomic DNA indicated the presence of paternally derived hypermethylated IG-DMR (CG4 and CG6) and *MEG3*-DMR (CG7) and the absence of maternally derived hypomethylated DMRs. Furthermore, microsatellite analysis was performed using leukocyte genomic DNA of patient and parents, revealing uniparental paternal isodisomy for chromosome 14 (Table I, Fig. 3).

In this patient with molecularly confirmed upd(14)pat, ultrasound studies unequivocally showed typical upd(14)pat phenotypes such as thoracic abnormality and facial dysmorphic features. While this is the first report documenting the facial appearance of the affected fetus, small thorax has been suspected prenatally in five patients with upd(14)pat or epimutations of the IG-DMR and the *MEG3*-DMR, with coat-hanger appearance of the ribs being delineated in one patient [Curtis et al., 2006; Yamanaka et al., 2010]. In this regard, it is notable that polyhydramnios has invariably been identified in upd(14)pat by the second trimester [Kagami et al., 2008a]. It is recommended, therefore, to perform radiological studies for pregnant women with polyhydramnios, to suspect upd(14)pat-compatible clinical features of the fetus. This will permit appropriate counseling and delivery planning at a tertiary

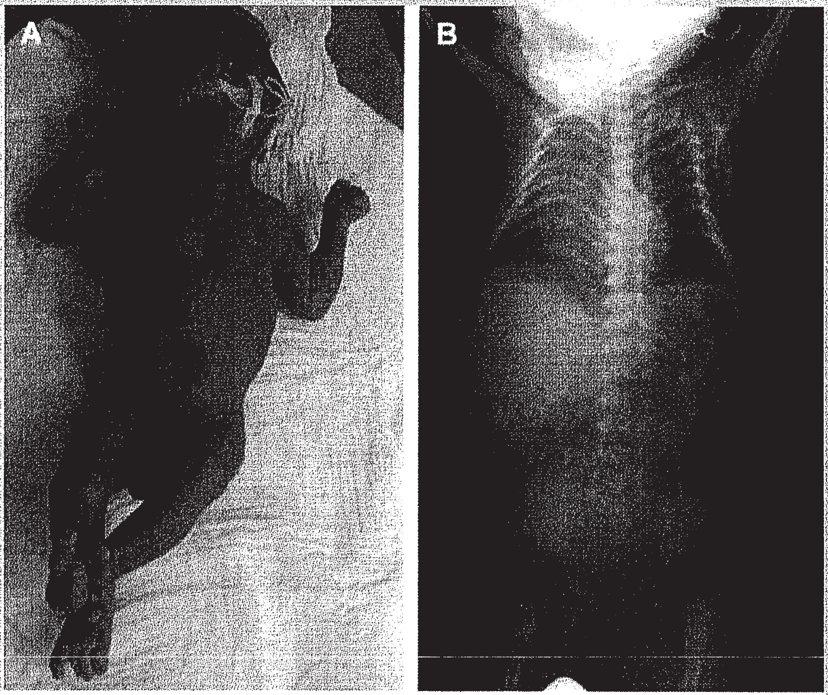

FIG. 2. Postnatal findings at 1 month of age. A: Front view. B: Chest roentgenogram showing bell-shaped thorax with coat-hanger appearance of the ribs.

center with neonatal intensive care as well as pertinent molecular studies using cord blood.

ACKNOWLEDGMENTS

We thank Dr. Saori Kaneko for her assistance in coordinating this research. We also acknowledge the cooperation of the patient's family in allowing us to publish their information.

TABLE I. The Results of Microsatellite Analysis

Locus	Location	Mother	Patient	Father	Assessment
D14S80	14q12	98	98	98	N.I.
D14S608	14q12	200	194	194/210	Isodisomy
D14S588	14q23–24.1	114/126	114	114/122	N.I.
D14S617	14q32.12	139/169	143	143/165	Isodisomy
D14S250	14q32.2	159	159	159/167	N.I.
D14S1006	14q32.2	127/139	127	127/139	N.I.
D14S985	14q32.2	135/137	131	131/133	Isodisomy
D14S1010	14q32.33	134/142	142	142/144	N.I.
D14S1007	14q32.33	119	119	119	N.I.

N.I., not informative.
The Arabic numbers indicate the PCR product sizes in bp.
The imprinted region resides at 14q32.2.
D14S985 is located in the intron of *MEG3*.

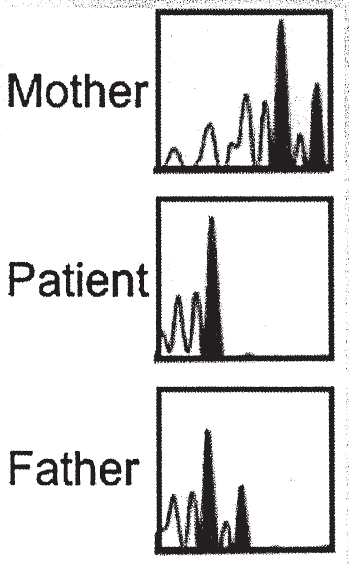

FIG. 3. Microsatellite analysis for *D14S985* residing in the intron of *MEG3*. One of the two peaks in the father is transmitted to the patient, and both of the two peaks in the mother are not inherited by the patient. The PCR fragment size: 135 and 137 bp in the mother, 131 bp in the patient, and 131 and 133 bp in the father. [Color figure can be viewed in the online issue, which is available at wileyonlinelibrary.com]

REFERENCES

Curtis L, Antonelli E, Vial Y, Rimensberger P, Merrer ML, Hinard C, Bottani A, Fokstuen S. 2006. Prenatal diagnostic indicators of paternal uniparental disomy 14. Prenat Diagn 26:662–666.

da Rocha ST, Edwards CA, Ito M, Ogata T, Ferguson-Smith AC. 2008. Genomic imprinting at the mammalian Dlk1-Dio3 domain. Trends Genet 24:306–316.

Kagami M, Sekita Y, Nishimura G, Irie M, Kato F, Okada M, Yamamori S, Kishimoto H, Nakayama M, Tanaka Y, Matsuoka K, Takahashi T, Noguchi M, Tanaka Y, Masumoto K, Utsunomiya T, Kouzan H, Komatsu Y, Ohashi H, Kurosawa K, Kosaki K, Ferguson-Smith AC, Ishino F, Ogata T. 2008a. Deletions and epimutations affecting the human 14q32.2 imprinted region in individuals with paternal and maternal upd(14)-like phenotypes. Nat Genet 40:237–242.

Kagami M, Yamazawa K, Matsubara K, Matsuo N, Ogata T. 2008b. Placentomegaly in paternal uniparental disomy for human chromosome 14. Placenta 29:760–761.

Kotzot D. 2004. Maternal uniparental disomy 14 dissection of the phenotype with respect to rare autosomal recessively inherited traits, trisomy mosaicism, and genomic imprinting. Ann Genet 47: 251–260.

Yamanaka M, Ishikawa H, Saito K, Maruyama Y, Ozawa K, Shibasaki J, Nishimura G, Kurosawa K. 2010. Prenatal findings of paternal uniparental disomy 14: Report of four patients. Am J Med Genet Part A 152A:789–791.

Journal of Human Genetics (2011) 56, 91–93

© 2011 The Japan Society of Human Genetics All rights reserved 1434-5161/11 $32.00

www.nature.com/jhg

SHORT COMMUNICATION

Androgenetic/biparental mosaicism in a girl with Beckwith–Wiedemann syndrome-like and upd(14)pat-like phenotypes

Kazuki Yamazawa[1,5], Kazuhiko Nakabayashi[2], Kentaro Matsuoka[3], Keiko Masubara[1], Kenichiro Hata[2], Reiko Horikawa[4] and Tsutomu Ogata[1]

This report describes androgenetic/biparental mosaicism in a 4-year-old Japanese girl with Beckwith–Wiedemann syndrome (BWS)-like and paternal uniparental disomy 14 (upd(14)pat)-like phenotypes. We performed methylation analysis for 18 differentially methylated regions on various chromosomes, genome-wide microsatellite analysis for a total of 90 loci and expression analysis of *SNRPN* in leukocytes. Consequently, she was found to have an androgenetic 46,XX cell lineage and a normal 46,XX cell lineage, with the frequency of the androgenetic cells being roughly calculated as 91% in leukocytes, 70% in tongue tissues and 79% in tonsil tissues. It is likely that, after a normal fertilization between an ovum and a sperm, the paternally derived pronucleus alone, but not the maternally derived pronucleus, underwent a mitotic division, resulting both in the generation of the androgenetic cell lineage by endoreplication of one blastomere containing a paternally derived pronucleus and in the formation of the normal cell lineage by union of paternally and maternally derived pronuclei. It appears that the extent of overall (epi)genetic aberrations exceeded the threshold level for the development of BWS-like and upd(14)pat-like phenotypes, but not for the occurrence of other imprinting disorders or recessive Mendelian disorders.

Journal of Human Genetics (2011) **56,** 91–93; doi:10.1038/jhg.2010.142; published online 11 November 2010

Keywords: androgenesis; Beckwith–Wiedemann syndrome; mosaicism; upd(14)pat

INTRODUCTION

A pure androgenetic human with paternal uniparental disomy for all chromosomes is incompatible with life because of genomic imprinting.[1,2] However, a human with an androgenetic cell lineage could be viable in the presence of a normal cell lineage. Indeed, an androgenetic cell lineage has been identified in six liveborn individuals with variable phenotypes.[3–7] All the androgenetic cell lineages have a 46,XX karyotype, and this is consistent with the lethality of an androgenetic 46,YY cell lineage.

Here, we report on a girl with androgenetic/biparental mosaicism, and discuss the underlying factors for the phenotypic development.

CASE REPORT

This patient was conceived naturally to non-consanguineous and healthy parents. At 24 weeks gestation, the mother was referred to us because of threatened premature delivery. Ultrasound studies showed Beckwith–Wiedemann syndrome (BWS)-like features,[8] such as macroglossia, organomegaly and umbilical hernia, together with polyhydramnios and placentomegaly. The mother repeatedly received amnioreduction and tocolysis.

She was delivered by an emergency cesarean section because of preterm rupture of membranes at 34 weeks of gestation. Her birth weight was 3730 g (+4.8 s.d. for gestational age), and her length 45.6 cm (+0.7 s.d.). The placenta weighed 1040 g (+7.3 s.d.).[9] She was admitted to a neonatal intensive care unit due to asphyxia. Physical examination confirmed a BWS-like phenotype. Notably, chest roentgenograms delineated mild bell-shaped thorax characteristic of paternal uniparental disomy 14 (upd(14)pat),[10] although coat hanger appearance of the ribs indicative of upd(14)pat was absent (Supplementary Figure 1). She was placed on mechanical ventilation for 2 months, and received tracheostomy, glossectomy and tonsillectomy in her infancy, due to upper airway obstruction. She also had several clinical features occasionally reported in BWS[8] (Supplementary Table 1). Her karyotype was 46,XX in all the 50 lymphocytes analyzed. On the last examination at 4 years of age, she showed postnatal growth failure and severe developmental retardation.

---

[1]Department of Molecular Endocrinology, National Research Institute for Child Health and Development, Tokyo, Japan; [2]Department of Maternal-Fetal Biology, National Research Institute for Child Health and Development, Tokyo, Japan; [3]Division of Pathology, National Medical Center for Children and Mothers, Tokyo, Japan and [4]Division of Endocrinology and Metabolism, National Medical Center for Children and Mothers, Tokyo, Japan
[5]Current address: Department of Physiology, Development & Neuroscience, University of Cambridge, Cambridge, UK.
Correspondence: Dr T Ogata, Department of Molecular Endocrinology, National Research Institute for Child Health and Development, 2-10-1 Ohkura, Setagaya, Tokyo 157-8535, Japan.
E-mail: tomogata@nch.go.jp

Received 9 September 2010; revised 18 October 2010; accepted 22 October 2010; published online 11 November 2010

MOLECULAR STUDIES

This study was approved by the Institutional Review Board Committee at the National Center for Child health and Development, and performed after obtaining informed consent.

Methylation analysis

We first performed bisulfite sequencing for the *H19*-DMR (differentially methylated region) and KvDMR1 as a screening of BWS[11,12] and that for the IG-DMR and the *MEG3*-DMR as a screening of upd(14)pat,[10] using leukocyte genomic DNA. Paternally derived clones were predominantly identified for the four DMRs examined (Figure 1a). We next performed combined bisulfite restriction analysis for multiple DMRs, as reported previously.[13] All the autosomal DMRs exhibited markedly skewed methylation patterns consistent with predominance of paternally inherited clones, whereas the *XIST*-DMR on the X chromosome showed a normal methylation pattern (Figure 1a).

Genome-wide microsatellite analysis

Microsatellite analysis was performed for 90 loci with high heterozygosities in the Japanese population.[14] Major peaks consistent with paternal uniparental isodisomy and minor peaks of maternal origin were identified for at least one locus on each chromosome, with the minor peaks of maternal origin being more obvious in tongue and tonsil tissues than in leukocytes (Figure 1b and Supplementary Table 2). There were no loci with three or four peaks indicative of chimerism. The frequency of the androgenetic cells was calculated as 91% in leukocytes, 70% in tongue cells and 79% in tonsil cells, although the estimation apparently was a rough one (for details, see Supplementary Methods).

Expression analysis

We examined *SNRPN* expression, because *SNRPN* showed strong expression in leukocytes (for details, see Supplementary Data). *SNRPN* expression was almost doubled in the leukocytes of this patient (Figure 1c).

DISCUSSION

These results suggest that this patient had an androgenetic 46,XX cell lineage and a normal 46,XX cell lineage. In this regard, both the androgenetic and the biparental cell lineages appear to have derived from a single sperm and a single ovum, because a single haploid genome of paternal origin and that of maternal origin were identified in this patient by genome-wide microsatellite analysis. Thus, it is likely that after a normal fertilization between an ovum and a sperm, the paternally derived pronucleus alone, but not the maternally derived pronucleus, underwent a mitotic division, resulting both in the generation of the androgenetic cell lineage by endoreplication of

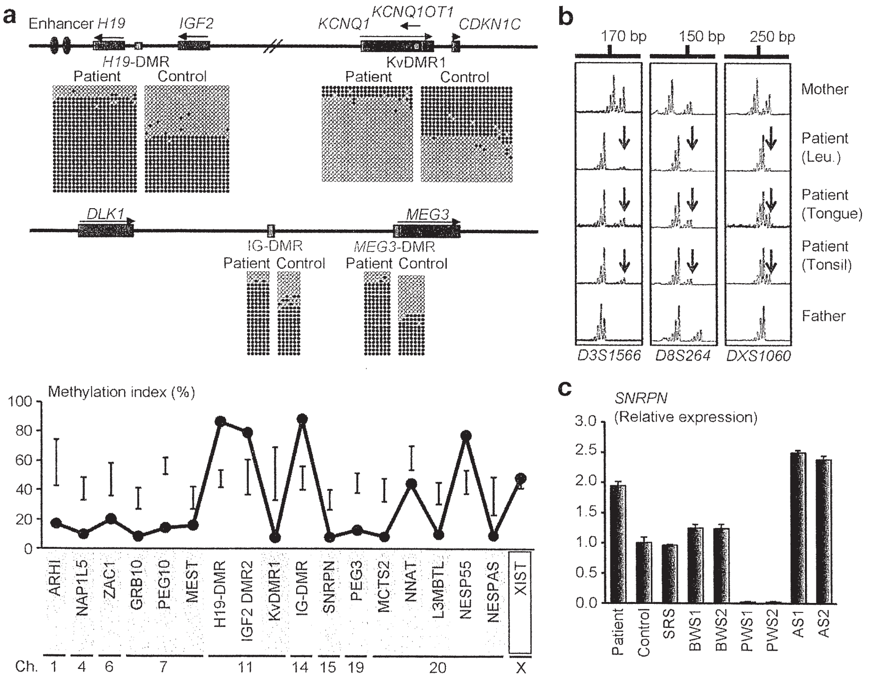

Figure 1 Representative molecular results. (**a**) Methylation analysis. Upper part: Bisulfite sequencing data for the *H19*-DMR and the KvDMR1 on 11p15.5, and those for the IG-DMR and the *MEG3*-DMR on 14q32.2. Each line indicates a single clone, and each circle denotes a CpG dinucleotide; filled and open circles represent methylated and unmethylated cytosines, respectively. Paternally expressed genes are shown in blue, maternally expressed gene in red, and the DMRs in green. The *H19*-DMR, the IG-DMR, and the *MEG3*-DMR are usually methylated after paternal transmission and unmethylated after maternal transmission, whereas the KvDMR1 is usually unmethylated after paternal transmission and methylated after maternal transmission.[10,11] Lower part: Methylation indices (the ratios of methylated clones) obtained from the COBRA analyses for the 18 DMRs. The DMRs highlighted in blue and pink are methylated after paternal and maternal transmissions, respectively. The black vertical bars indicate the reference data (maximum – minimum) in leukocyte genomic DNA of 20 normal control subjects (the *XIST*-DMR data are obtained from 16 control females). (**b**) Representative microsatellite analysis. Major peaks of paternal origin and minor peaks of maternal origin (red arrows) have been identified in this patient. The minor peaks of maternal origin are more obvious in tongue and tonsil tissues than in leukocytes (Leu.). (**c**) Relative expression level (mean ± s.d.) of *SNRPN*. The data are normalized against *TBP*. SRS: an SRS patient with an epimutation (hypomethylation) of the *H19*-DMR; BWS1: a BWS patient with an epimutation (hypermethylation) of the *H19*-DMR; BWS2: a BWS patient with upd(11)pat; PWS1: a Prader-Willi syndrome (PWS) patient with upd(15)mat; PWS2: a PWS patient with an epimutation (hypermethylation) of the *SNRPN*-DMR; AS1: an Angelman syndrome (AS) patient with upd(15)pat; and AS2: an AS patient with an epimutation (hypomethylation) of the *SNRPN*-DMR. The data were obtained using an ABI Prism 7000 Sequence Detection System (Applied Biosystems).

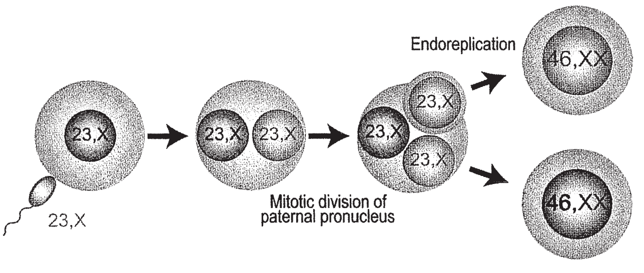

Figure 2 Schematic representation of the generation of the androgenetic/biparental mosaicism. Polar bodies are not shown.

one blastomere containing a paternally derived pronucleus and in the formation of the normal cell lineage by union of paternally and maternally derived pronuclei (Figure 2). This model has been proposed for androgenetic/biparental mosaicism generated after fertilization between a single ovum and a single sperm.[5,15,16] The normal methylation pattern of the *XIST*-DMR is explained by assuming that the two X chromosomes in the androgenetic cell lineage undergo random X-inactivation, as in the normal cell lineage. Furthermore, the results of microsatellite analysis imply that the androgenetic cells were more prevalent in leukocytes than in tongue and tonsil tissues.

A somatic androgenetic cell lineage has been identified in seven liveborn patients including this patient (Supplementary Table 1).[3–7] In this context, leukocytes are preferentially utilized for genetic analyses in human patients, and detailed examinations such as analyses of plural DMRs are necessary to detect an androgenetic cell lineage. Thus, the hitherto identified patients would be limited to those who had androgenetic cells as a predominant cell lineage in leukocytes probably because of a stochastic event and received detailed molecular studies. If so, an androgenetic cell lineage may not be so rare, and could be revealed by detailed analyses as well as examinations of additional tissues in patients with relatively complex phenotypes, as observed in the present patient.

Phenotypic features in androgenetic/biparental mosaicism would be determined by several factors. They include (1) the ratio of two cell lineages in various tissues/organs, (2) the number of imprinted domains relevant to specific features (for example, dysregulation of the imprinted domains on 11p15.5 and 14q32.2 is involved in placentomegaly[9,17]), (3) the degree of clinical effects of dysregulated imprinted domains (an (epi)dominant effect has been assumed for the 11p15.5 imprinted domains[18]), (4) expression levels of imprinted genes in androgenetic cells (although *SNRPN* expression of this patient was consistent with androgenetic cells being predominant in leukocytes, complicated expression patterns have been identified for several imprinted genes in both androgenetic and parthenogenetic fetal mice, probably because of perturbed *cis*- and *trans*-acting regulatory mechanisms[19]) and (5) unmasking of possible paternally inherited recessive mutation(s) in androgenetic cells. Thus, in this patient, it appears that the extent of overall (epi)genetic aberrations exceeded the threshold level for the development of BWS-like and upd(14)pat-like body and placental phenotypes, but remained below the threshold level for the occurrence of other imprinting disorders or recessive Mendelian disorders.

CONFLICT OF INTEREST

The authors declare no conflict of interest.

ACKNOWLEDGEMENTS

This work was supported by grants from the Ministry of Health, Labor, and Welfare, and the Ministry of Education, Science, Sports and Culture.

---

1 Surani, M. A., Barton, S. C. & Norris, M. L. Development of reconstituted mouse eggs suggests imprinting of the genome during gametogenesis. *Nature* **308,** 548–550 (1984).
2 McGrath, J. & Solter, D. Completion of mouse embryogenesis requires both the maternal and paternal genomes. *Cell* **37,** 179–183 (1984).
3 Hoban, P. R., Heighway, J., White, G. R., Baker, B., Gardner, J., Birch, J. M. *et al.* Genome-wide loss of maternal alleles in a nephrogenic rest and Wilms' tumour from a BWS patient. *Hum. Genet.* **95,** 651–656 (1995).
4 Bryke, C. R., Garber, A. T. & Israel, J. Evolution of a complex phenotype in a unique patient with a paternal uniparental disomy for every chromosome cell line and a normal biparental inheritance cell line. *Am. J. Hum. Genet.* **75**(Suppl), 831 (2004).
5 Giurgea, I., Sanlaville, D., Fournet, J. C., Sempoux, C., Bellanne-Chantelot, C. & Touati, G. Congenital hyperinsulinism and mosaic abnormalities of the ploidy. *J. Med. Genet.* **43,** 248–254 (2006).
6 Wilson, M., Peters, G., Bennetts, B., McGillivray, G., Wu, Z. H., Poon, C. *et al.* The clinical phenotype of mosaicism for genome-wide paternal uniparental disomy: two new reports. *Am. J. Med. Genet. Part A* **146A,** 137–148 (2008).
7 Reed, R. C., Beischel, L., Schoof, J., Johnson, J., Raff, M. L. & Kapur, R. P. Androgenetic/biparental mosaicism in an infant with hepatic mesenchymal hamartoma and placental mesenchymal dysplasia. *Pediatr. Dev. Pathol.* **11,** 377–383 (2008).
8 Jones, K. L. *Smith's Recognizable Patterns of Human Malformation* 6th edn. (Elsevier Saunders: Philadelphia, 2006).
9 Kagami, M., Yamazawa, K., Matsubara, K., Matsuo, N. & Ogata, T. Placentomegaly in paternal uniparental disomy for human chromosome 14. *Placenta* **29,** 760–761 (2008).
10 Kagami, M., Sekita, Y., Nishimura, G., Irie, M., Kato, F., Okada, M. *et al.* Deletions and epimutations affecting the human 14q32.2 imprinted region in individuals with paternal and maternal upd(14)-like phenotypes. *Nat. Genet.* **40,** 237–242 (2008).
11 Yamazawa, K., Kagami, M., Nagai, T., Kondoh, T., Onigata, K., Maeyama, K. *et al.* Molecular and clinical findings and their correlations in Silver-Russell syndrome: implications for a positive role of IGF2 in growth determination and differential imprinting regulation of the IGF2-H19 domain in bodies and placentas. *J. Mol. Med.* **86,** 1171–1181 (2008).
12 Weksberg, R., Shuman, C. & Beckwith, J. B. Beckwith-Wiedemann syndrome. *Eur. J. Hum. Genet.* **18,** 8–14 (2010).
13 Yamazawa, K., Nakabayashi, K., Kagami, M., Sato, T., Saitoh, S., Horikawa, R. *et al.* Parthenogenetic chimaerism/mosaicism with a Silver-Russell syndrome-like phenotype. *J. Med. Genet.* **47,** 782–785 (2010).
14 Ikari, K., Onda, H., Furushima, K., Maeda, S., Harata, S. & Takeda, J. Establishment of an optimized set of 406 microsatellite markers covering the whole genome for the Japanese population. *J. Hum. Genet.* **46,** 207–210 (2001).
15 Kaiser-Rogers, K. A., McFadden, D. E., Livasy, C. A., Dansereau, J., Jiang, R., Knops, J. F. *et al.* Androgenetic/biparental mosaicism causes placental mesenchymal dysplasia. *J. Med. Genet.* **43,** 187–192 (2006).
16 Kotzot, D. Complex and segmental uniparental disomy updated. *J. Med. Genet.* **45,** 545–556 (2008).
17 Monk, D., Arnaud, P., Apostolidou, S., Hills, F. A., Kelsey, G., Stanier, P. *et al.* Limited evolutionary conservation of imprinting in the human placenta. *Proc. Natl. Acad. Sci. USA.* **103,** 6623–6628 (2006).
18 Azzi, S., Rossignol, S., Steunou, V., Sas, T., Thibaud, N., Danton, F. *et al.* Multilocus methylation analysis in a large cohort of 11p15-related foetal growth disorders (Russell Silver and Beckwith Wiedemann syndromes) reveals simultaneous loss of methylation at paternal and maternal imprinted loci. *Hum. Mol. Genet.* **18,** 4724–4733 (2009).
19 Ogawa, H., Wu, Q., Komiyama, J., Obata, Y. & Kono, T. Disruption of parental-specific expression of imprinted genes in uniparental fetuses. *FEBS Lett.* **580,** 5377–5384 (2006).

Supplementary Information accompanies the paper on Journal of Human Genetics website (http://www.nature.com/jhg)

Journal of Human Genetics (2011) 56, 94–96
© 2011 The Japan Society of Human Genetics All rights reserved 1434-5161/11 $32.00
www.nature.com/jhg

SHORT COMMUNICATION

Low prevalence of classical galactosemia in Korean population

Beom Hee Lee[1,2,3,6], Chong Kun Cheon[4,6], Jae-Min Kim[2], Minji Kang[2], Joo Hyun Kim[2], Song Hyun Yang[5], Gu-Hwan Kim[2,3], Jin-ho Choi[1] and Han-Wook Yoo[1,2,3]

This study described the clinical and molecular genetic features of classical galactosemia in Korean population to contribute to the insight in the spectrum of galactosemia in the world, as little is known about the spectrum and incidence of galactosemia in Asia. During the 11-year study period, only three Korean children were identified as having classical galactosemia on the basis of the enzymatic and molecular genetic analysis. Asians have been reported to have mutations distinct from those of Caucasians and African Americans, indicating that galactose-1-phosphate uridyltransferase mutations are ethnically diverse. Our three patients had a total of three mutations (c.252+1G > A, p.Q169H and p.E363K), two of which were novel (p.E363K and c.252+1G > A) mutations. Interestingly, c.252+1G > A, which leads to skipping of exon 2, was observed in all three patients (three of six alleles), indicating that this mutation may be common in Koreans with classical galactosemia. Screening for classical galactosemia in 158 126 Korean newborns identified no patient with classical galactosemia. In conclusion, our findings provide further evidence for the ethnic diversity of classical galactosemia, which may be as rare in Koreans as in other Asian populations.

Journal of Human Genetics (2011) **56,** 94–96; doi:10.1038/jhg.2010.152; published online 9 December 2010

Keywords: ethnic divergence; galactosemia; GALT; mutation

Classical galactosemia (OMIM 230400) is caused by a deficiency in galactose-1-phosphate uridyltransferase (GALT; EC2.7.712). Classical galactosemia is characterized by more severe clinical manifestations than the other two types, galactosemia II or III, with newborns usually manifesting symptoms within a few days of birth after milk feeding.[1–3]

The incidence of classical galactosemia in western Europe has been estimated to be between 1:23 000 and 1:89 000.[1,4,5] In Korean newborns, the overall incidence of the three types of galactosemia have been reported to be approximately 1:40 000,[6] but the exact incidence of classical galactosemia is not yet known. Since the first report of a mutation in the *GALT* gene,[7] more than 200 different mutations have been identified with missense mutations being observed most commonly (http://www.hgmd.org).[1,8] The most common mutations in Caucasian and African American populations are p.Q188R and p.S135L, respectively,[9–11] but neither of these mutations have been detected to date in Asian populations. Similarly, Japanese patients have distinct mutations, such as p.V85_N97delinsRfsX8, p.W249X and p.R231H, which have not been observed in Caucasians and African Americans, providing further evidence for genetic heterogeneities among ethnic groups.[1,12,13]

Between March 1999 and May 2010, only three unrelated Korean patients were diagnosed with classical galactosemia at the Asan Medical Center, Seoul, Korea, with the diagnosis of each confirmed by enzyme assays and molecular genetic analysis (Table 1). All patients were identified by neonatal screening program performed at 3–5 days of life. Patients 1 and 2 had neonatal jaundice with slightly increased serum hepatic enzyme concentrations, which was not progressive, whereas patient 3 had clinically deteriorated and showed progressive jaundice and a bleeding tendency, while awaiting the results of screening tests that were reported on the eleventh day after birth (Table 1). Median total plasma galactose concentration was 50 mg per 100 ml (range, 13.5–68.9 mg per 100 ml; normal range <13 mg per 100 ml) and median erythrocyte galactose-1-phosphate concentration was 10.4 mg per 100 ml (range 1.60–62.8 mg per 100 ml; normal range <0.3 mg per 100 ml). The GALT activity was decreased in all patients, ranging from 0.1 to 0.8 umol hr^{-1} per gram hemoglobin (median, 0.3umol hr^{-1} per gram hemoglobin; normal range, 25.7 ± 3.6 umol hr^{-1} per gram hemoglobin) (Table 1). A galactose-restricted diet was effective in decreasing galactose and galactose-1-phosphate concentrations in all patients. The hepatic dysfunction, jaundice and

---

[1]Department of Pediatrics, Asan Medical Center Children's Hospital, University of Ulsan College of Medicine, Seoul, Korea; [2]Genome Research Center for Birth defects and Genetic Diseases, Asan Medical Center Children's Hospital, University of Ulsan College of Medicine, Seoul, Korea; [3]Medical Genetics Clinic and Laboratory, Asan Medical Center Children's Hospital, University of Ulsan College of Medicine, Seoul, Korea; [4]Department of Pediatrics, Genetic and Metabolic Clinic, Children Hospital, Pusan National University, Gyeongnam, South Korea and [5]Green Cross Reference Laboratory, Seoul, Korea

[6]These authors contributed equally to this paper as first authors.

Correspondence: Dr H-W Yoo, Genome Research Center for Birth defects and Genetic Diseases, Asan Medical Center Children's Hospital, University of Ulsan College of Medicine, 388-1 Pungnap-Dong, Songpa-Gu, Seoul 138-736, Korea.
E-mail: hwyoo@amc.seoul.kr

Received 13 September 2010; revised 14 October 2010; accepted 9 November 2010; published online 9 December 2010

CANT1 mutation is also responsible for Desbuquois dysplasia, type 2 and Kim variant

Tatsuya Furuichi,[1,2] Jin Dai,[1] Tae-Joon Cho,[3] Satoru Sakazume,[4] Masahide Ikema,[5] Yoshito Matsui,[6] Gareth Baynam,[7] Toshiro Nagai,[4] Noriko Miyake,[8] Naomichi Matsumoto,[8] Hirofumi Ohashi,[9] Sheila Unger,[10] Andrea Superti-Furga,[10] Ok-Hwa Kim,[11] Gen Nishimura,[12] Shiro Ikegawa[1]

► Additional figures and tables are published online only. To view these files please visit the journal online (http://jmg.bmj.com).

[1]Laboratory of Bone and Joint Diseases, Center for Genomic Medicine, RIKEN, Tokyo, Japan
[2]Laboratory Animal Facility, Research Center for Medical Sciences, Jikei University School of Medicine, Tokyo, Japan
[3]Department of Orthopaedic Surgery, Seoul National University Children's Hospital, Seoul, Korea
[4]Department of Pediatrics, Dokkyo Medical University Kosigaya Hospital, Koshigaya, Japan
[5]Department of Orthopaedic, Nagasaki Prefectural Center of Medicine and Welfare for Children, Nagasaki, Japan
[6]Department of Orthopedic Surgery, University of Toyama, Toyama, Japan
[7]Genetic Services of Western Australia, Princess Margaret Hospital for Children and King Edward Memorial Hospital for Women, Western Australia, Australia
[8]Department of Human Genetics, Yokohama City University Graduate School of Medicine, Yokohama, Japan
[9]Division of Medical Genetics, Saitama Children's Medical Center, Iwatsuki, Japan
[10]Center for Pediatrics and Adolescent Medicine, University of Freiburg, Freiburg, Germany
[11]Department of Radiology, Ajou University Hospital, Suwon, Korea
[12]Department of Pediatric Imaging, Tokyo Metropolitan Children's Medical Center, Futyu, Japan

Correspondence to
Dr Shiro Ikegawa, Laboratory of Bone and Joint Diseases, Center for Genomic Medicine, RIKEN, 4-6-1 Shirokanedai, Minato-ku, Tokyo 108-8639, Japan; sikegawa@ims.u-tokyo.ac.jp

Received 8 May 2010
Revised 30 June 2010
Accepted 3 July 2010

ABSTRACT

Background Desbuquois dysplasia (DD) is a recessively inherited condition characterised by short stature, generalised skeletal dysplasia and advanced bone maturation. DD is both clinically and radiographically heterogeneous, and two subtypes have been distinguished based on the presence (type 1) or absence (type 2) of an accessory metacarpal bone. In addition, an apparently distinct variant without additional metacarpal bone but with short metacarpals and long phalanges (Kim variant) has been described recently. Mutations in the gene that encodes for CANT1 (calcium-activated nucleotidase 1) have been identified in a subset of patients with DD type 1.

Methods A series of 11 subjects with DD from eight families (one type 1, two type 2, five Kim variant) were examined for *CANT1* mutations by direct sequencing of all coding exons and their flanking introns.

Results Eight distinct mutations were identified in seven families (one type 1, one type 2 and all 5 Kim variant): three were nonsense and five were missense. All missense mutations occurred at highly conserved amino acids in the nucleotidase conserved regions of CANT1. Measurement of nucleotidase activity in vitro showed that the missense mutations were all associated with loss-of-function.

Conclusion The clinical-radiographic spectrum produced by *CANT1* mutations must be extended to include DD type 2 and Kim variant. While presence or absence of an additional metacarpal ossification centre has been used to distinguish subtypes of DD, this sign is not a distinctive criterion to predict the molecular basis in DD.

INTRODUCTION

Desbuquois dysplasia (DD; MIM 251450) is a severe skeletal dysplasia inherited in an autosomal recessive manner. DD belongs to the 'multiple dislocation group' in the International Nosology of Genetic Skeletal Disorders.[1] It is characterised clinically by short limb short stature, severe joint laxity with facultative congenital dislocations, flat midface, micrograthia, cleft palate, and progressive scoliosis. The main radiological features include a peculiar 'monkey wrench' or 'Swedish key' appearance of the proximal femur (exaggerated trochanter), hypoplasia of thorax and ilia, mild spondylar dysplasia, and hand abnormalities including an additional ossification centre and advanced bone age.[2]

DD has been considered clinically and radiographically heterogeneous. It has been classified into two types on the basis of the presence (type 1) or absence (type 2) of characteristic hand anomalies, which consist of an extra ossification centre distal to the second metacarpal, delta phalanx, bifid distal thumb phalanx, and dislocation of the interphalangeal joints (figure 1A).[3] DD type 2 is also referred to as the 'normal' hand type because the accessory metacarpal ossification centre is not seen. It only presents with minor changes of the hand, such as malalignment of the interphalangeal joint and brachydactly. More than half of the DD patients belong to this subtype.[3] In addition, we have recently described a new clinical subtype of DD, Kim variant.[4] The hand shape of the variant is apparently normal, thus the patients most closely resemble type 2; however, the radiographic abnormalities in the hands are significant, including short metacarpals and elongated phalanges together with remarkably advanced carpal bone age (figure 1B). Long term follow-up showed that severe precocious osteoarthritis of the hand and spine is a major manifestation of this specific clinical variant.[4]

The apparent phenotypical heterogeneity of DD has been taken to suggest genetic heterogeneity. Thus, the DD gene was localised to a 1.65 Mb interval on chromosome 17q25 by homozygosity mapping using four consanguineous families with DD type 1, while DD with normal hands was believed not to map to this interval.[5 6] Recently, Huber and colleagues searched for mutations in genes in the interval and identified mutations in the calcium activated nucleotidase 1 (*CANT1*) gene.[7] CANT1 is a extracellular protein that functions as a nucleotide tri- and diphosphatase. It preferentially hydrolyses uridine diphosphate (UDP) followed by guanosine diphosphate (GDP), uridine triphosphate (UTP) and adenosine diphosphate (ADP).[8–10]

The function of CANT1 in skeletal formation is unknown. It is expressed in chondrocytes, and chondrocytes from DD type 1 patients with *CANT1* mutations have abnormally distended rough endoplasmic reticulum (ER) implicating CANT1 in chondrocyte ER metabolism.[7] The disease-causing mechanism of *CANT1* mutation is also unclear. The first mutation study reported seven *CANT1* mutations; three are nonsense mutations that are predicted to cause the nonsense mutation mediated RNA decay and one is a homozygous large deletion encompassing 5′-UTR and exon 1 that results in loss of *CANT1* mRNA.[7] These

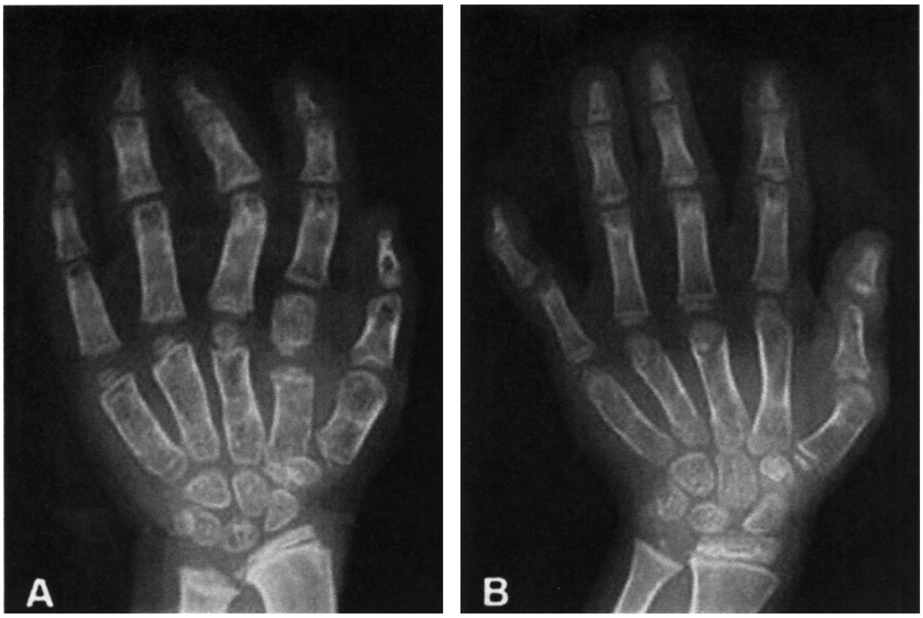

Figure 1 Hand radiographs of Desbuquois dysplasia (DD) type 1 and Kim variant at age 3 years. (A) DD type 1 carrying the homozygous *CANT1* mutation, p.R300C. This girl has been reported previously as family 4.[7] Note the additional ossification centre at the second metacarpal. (B) DD Kim variant (patient 7 in the present study) carrying the compound heterozygous *CANT1* mutations, p.V226M and p.A360D. There is no additional ossification centre. Both patients show precocious carpal ossification.

findings suggest that loss of CANT1 function causes DD. However, functional impact of the missense mutations has not been examined. It is of note that the genetic mapping was done using DD type 1 families, and that all patients in whom *CANT1* mutations were identified had DD type 1.[7] Therefore, it remains to be determined whether *CANT1* is responsible for other types of DD.

To explore further the range of *CANT1* mutations in DD, we searched for *CANT1* mutations in three types (type 1, type 2, Kim variant) of DD patients. We found a total of eight distinct mutations in seven families (type 1, type 2, and all five Kim variant); all were novel. By measuring the CANT1 enzyme activity in vitro, we confirmed that DD results from CANT1 loss of function.

PATIENTS AND METHODS

Patients

DD patients were recruited through the International Skeletal Dysplasia Registry (ISDR) (http://www.csmc.edu/), the European Skeletal Dysplasia Network (ESDN) (http://www.esdn.org/), and the Japanese Skeletal Dysplasia Consortium (JSDC) (http://www.riken.jp/lab-www/OA-team/JSDC/). Clinical criteria for inclusion in the study were prenatal and postnatal growth failure with short limbs, mid-face hypoplasia or round face with flat nasal bridge, joint laxity and foot deformities. Major radiological criteria were Swedish key appearance of the proximal femur, advanced carpo-tarsal ossification, short tubular bones, and hyperphalangy (extra-ossicle between the proximal phalanx and metacarpal of the index finger) in type 1. Minor radiological criteria included hypoplastic lower ilia and vertebral modification, such as coronal clefts or irregular endplates at birth and mild vertebral flattening with round vertebral endplates or normal vertebral bodies in later life. Clinical and radiographic phenotypes of the patients were evaluated by the experts of the organisations and reviewed by the authors (SU, AS-F, OK, and GN).

Eleven patients with DD from eight families were recruited for this study (table 1). Clinical data of patient 1 have been reported previously.[11] Patients 4, 5, 7, and 8 have also been reported previously (as patients 3, 5, 6, and 1, respectively).[4] The study was approved by the ethics committee of RIKEN and participating institutions and informed consent was obtained from all subjects.

Mutation screening

Genomic DNA was extracted from blood by standard procedures or from saliva using Oragene DNA Self-Collection kit (DNA Genotek, Kanata Ontario, Canada). Exon sequences of *CANT1* with their flanking intron sequences were amplified by PCR from genomic DNA. PCR primer sequences and PCR condition are listed in supplemental table 1. PCR products were purified using MinElute PCR purification Kit (Qiagen, Valencia, CA, USA) and sequenced for both strands using an ABI Prism 3730 automated sequencer (PE Biosystems; Foster City, CA, USA). Genomic DNAs from the parents and sibs were sequenced for the corresponding regions.

cDNA cloning and in vitro mutagenesis

The full length *CANT1* cDNA was amplified by PCR using cDNAs prepared from OUMS-27 cells as a template and cloned into pcDNA3.1 (+). The missense mutations were introduced into *CANT1* cDNA by PCR based mutagenesis. The introduced mutations were confirmed by DNA sequencing.

Nucleotidase assay

COS-7 cells were grown to 70–80% confluence in 100 mm culture dishes and were transfected with 6 μg of empty, wild-type or mutant *CANT1* expression vectors using Fugene 6 transfection reagent (Roche Diagnostics, Basel, Switzerland). At 8 h after transfection, cells were transferred to Opti-MEM serum-free media and cultured for 48 h. Buffer exchange in the culture supernatant (10 ml) was performed with ultrafiltration through Amicon Ultra-10K centrifugal filter (Millipore, Billerica, MA, USA) using 50 ml of sterile deionised water and the resulting solution concentrated to 100 ml using VIVASPIN 500, 10000 MWCO (Vivascience, Hanover, Germany). Nucleotidase activities in the purified media were determined by modification of a previous method.[12] Briefly, the purified media were 20 times or 500 times diluted with 40 mM succinate buffer (pH 6.5)

Furuichi T, Dai J, Cho T-J, *et al. J Med Genet* (2010). doi:10.1136/jmg.2010.080226

Table 1 *CANT1* mutations in eight families with Desbuquois dysplasia

Patient ID	Subtype	Consanguinity	Ethnicity	Mutation	
				Paternal	**Maternal**
P1	1	No	Australian Caucasian	c.228_229insC (p.W77LfsX13)	c.671T→C (p.L224P)
P2*	2	Yes	Turkish	c.375G→C (p.W125C)	c.375G→C (p.W125C)
P3	2	Yes	Turkish	(−)	(−)
P4*	Kim variant	Yes	Japanese	c.676G→A (p.V226M)	c.676G→A (p.V226M)
P5	Kim variant	No	Japanese	c.861C→A (p.C287X)	c.676G→A (p.V226M)
P6	Kim variant	No	Japanese	c.676G→A (p.V226M)	c.494T→C (p.M165T)
P7	Kim variant	No	Korean	c.676G→A (p.V226M)	c.1079C→A (p.A360D)
P8*	Kim variant	No	Korean	c.676G→A (p.V226M)	IVS2−9G→A (p.G279VfsX8)

*There are two affected siblings in these families.

containing 4 mM $CaCl_2$, and 2 mM ADP or UDP, and incubated at 37°C for 1 min. The amounts of inorganic phosphate from ADP or UDP in the reaction were measured by a colorimetric molybdenum blue method.

Western blotting

Cell lysate was prepared using M-PER mammalian protein extraction reagents (Pierce, Rockford, IL, USA). Proteins in the cell lysate and the culture supernatant were separated by electrophoresis on SDS-polyacrylamide gels and transferred onto nitrocellulose membranes (Amersham Biosciences, Piscataway, NJ, USA). The primary antibody to CANT1 (Abcam, Cambridge, UK) was used at 1:1000 dilution, and then horseradish peroxidase conjugated anti-rabbit IgG (GE Healthcare, Chalfont St Giles, UK) was used at 1:2000 dilution. Chemiluminescent signals were detected using ECL plus western blotting detection reagents (Amersham).

RESULTS

Identification of *CANT1* mutations

We examined 11 subjects with DD from eight families (one type 1, two type 2, five Kim variant) and identified *CANT1* mutations in seven families, including all of those with DD Kim variant (table 1). Two homozygous mutations, c.375G→C (p.W125C) and c.676G→A (p.V226M), were found in two consanguineous families; others were compound heterozygous mutations. Cosegregation of mutations in the families was confirmed by sequencing genomic DNA of available family members. Altogether, we found eight distinct mutations; two were nonsense (p.W77LfsX13, p.C287X), five were missense (p.W125C, p.M165T, p.L224P, p.V226M, p.A360D), and one was at a splice acceptor site (IVS2−9G→A) (table 1, supplemental figure 1A). All mutations have not been reported so far.

To investigate the effect of IVS2−9G→A on splicing, we extracted RNA from peripheral leucocytes of patient 8. We cloned and sequenced its reverse transcriptase PCR (RT-PCR) products. We identified two distinct subclones: one had a 7 bp insertion between exons 2 and 3 (c.835_836insTTCCCAG) (supplemental figure 1B) and the other had c.676G→A (p.V226M). The former clone indicates that IVS2−9G→A generates a new splice acceptor site (supplemental figure 1C), which is predicted to produce a premature stop codon (p.G279VfsX8).

Among the eight mutations, c.676G→A was found in all families with Kim variant, and the other mutations were found only once. c.676G→A was found in 1/754 Japanese and 1/187 Korean controls in a heterozygous state. The other mutations were not found in approximately 100 ethnically matched controls, or in public sequence variation databases. No mutations were found in one type 2 family. We screened for *DTDST* mutations in this family as previously described,[13] but found no mutation.

CANT1 belongs to the apyrase protein family.[8–10] CANT1 related apyrases have eight highly conserved regions, designated as nucleotidase conserved regions (NCRs) (figure 2).[14] All amino acid residues substituted by the missense mutations in DD patients were located in NCRs and highly conserved among diverse species and related apyrases (figure 2).

Functional characterisation of *CANT1* missense mutations

We evaluated the causality of the *CANT1* missense mutants by measuring their nucleotidase activity. We constructed expression vectors for the missense mutations identified in this study and the common mutation (p.R300C) previously identified,[7] as well as two missense single nucleotide polymorphism (SNPs), p.A323T (rs9903215) and p.G391E (rs34082669) registered in dbSNP database (http://www.ncbi.nlm.nih.gov/snp) (figure 2). In our assay system, the wild-type CANT1 was obviously calcium dependent and preferentially hydrolysed UDP (data not shown), as reported previously.[8 9] Although CANT1 hydrolyses ADP poorly, ADP hydrolysation by soluble apyrases has been reported to be involved in thrombo-regulation.[10] Therefore, we measured nucleotidase activity of the mutants for both UDP and ADP. The activities of all DD mutant proteins were significantly reduced in both assays compared to that of the wild-type protein (figure 3A). The enzymatic activities of the SNP proteins were similar to that of the wild-type protein.

To investigate the stability and secretion of the missense mutant proteins, we checked the over-expressed proteins in cell lysates and culture supernatants by western blot analysis (figure 3B). The band intensities of four DD mutants (p.W125C, p.M165T, p.V226M, p.R300C) and two SNPs were equal to that of the wild-type in both analyses using cell lysates and culture supernatants, indicating that these proteins are stable and can be secreted normally into the culture supernatant. In contrast, the L224P band was drastically reduced in the cell lysate and not detectable in the culture supernatant, suggesting that L224P protein was unstable. An A360D band was at a similar level in the cell lysate but not detectable in the culture supernatant, indicating that A360D mutant could not be secreted into the culture medium. When the plasmid vector backbone was changed to another one, these results for the L224P and A360D mutants were unchanged.

DISCUSSION

We found eight novel *CANT1* mutations in seven of the eight DD families examined (type 1, type 2 and Kim variant). These included both nonsense and missense mutations, and our in vitro study showed the loss of CANT1 enzyme activity in the missense mutants. Therefore, DD is caused by CANT1 deficiency. Our study suggests that CANT1 deficiency may be caused by early degradation and failure of secretion as well as the

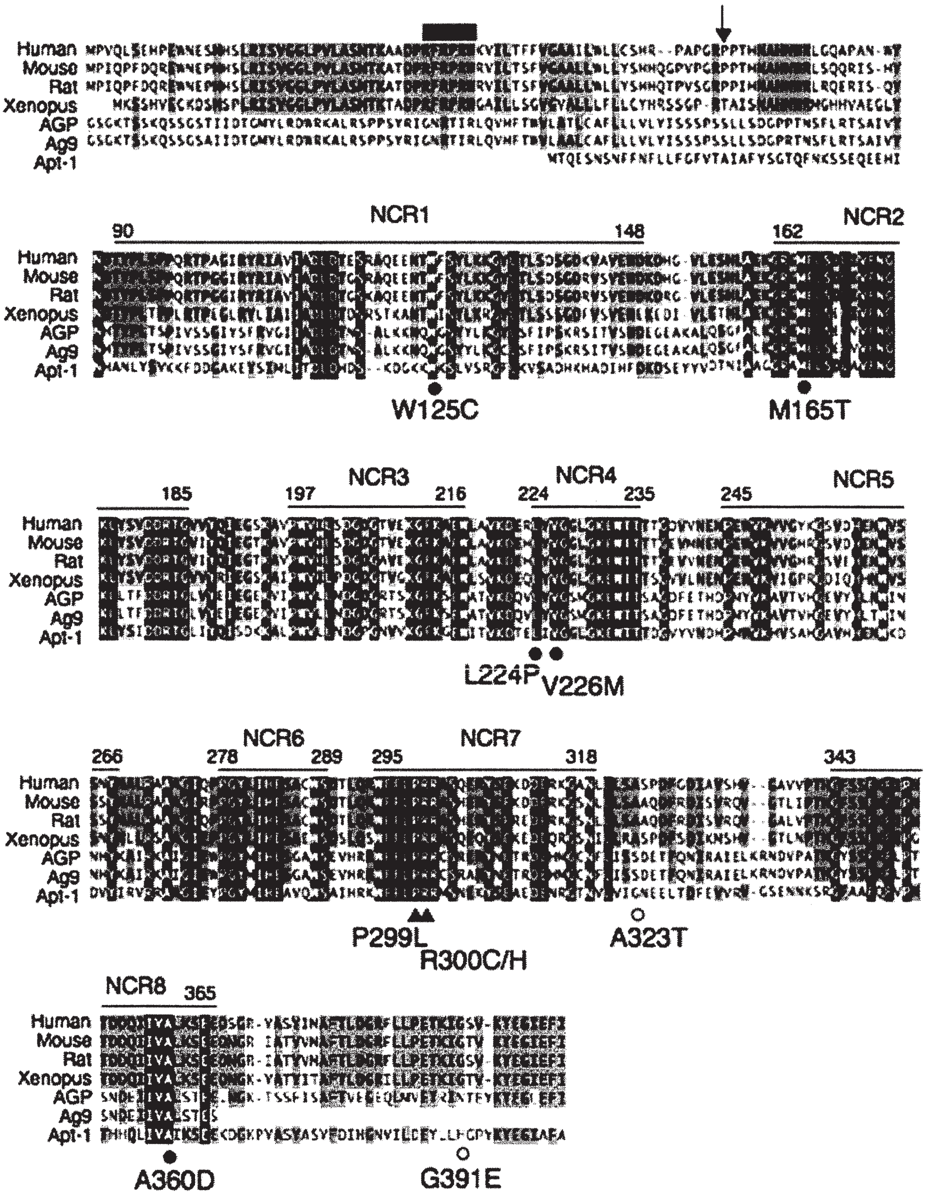

Figure 2 Amino acid sequence alignment of human CANT1 and related apyrase proteins. Residues were shaded to indicate levels of conservation (black shape: complete conservation, grey shape: moderate conservation). Reference sequences: Human (AAH65038.1, *Homo sapiens* CANT1); Mouse (AH200mous03.1, *Mus musculus* CANT1); Rat (NP653355.1, *Rattus norvergicus* CANT1); Xenopus (AAH61377.1, *Xenopus tropicalis* CANT1), AGP (XP_321938.3, *Anopheles gambiae* apyrase); Ag9 (CAC35453, *A gambiae* apyrase); Apt-1 (NP_509283, *Caenrohabditis elegans* apyrase). NCR: nucleotidase conserved region. The numbers show the amino acid positions corresponding to human CANT1. The positions of the missense mutations identified in patients with Desbuquois dysplasia in this study and in a previous study and missense single nucleotide polymorphisms (SNPs) in the public database are indicated by solid circles, solid triangles and open circles, respectively. N-terminal RXR endoplasmic reticulum (ER) retention/retrieval motif of vertebrate CANT1 is represented by a black bar. Predicted signal peptide cleavage site is indicated by an arrow.

decreased enzyme activity secondary to a specific amino acid substitution. Further characterisation of the disease-causing mechanism of the missense mutations is necessary to gain insight into function and metabolism of the CANT1 protein.

The first study reported three distinct missense mutations.[7] Two are recurrent mutations in R300 (R300C/H), and one in the neighbouring amino acid (P299); all are in NCR7. In our study, we found no mutation in this hot spot. All five missense mutations in this study were also in NCRs but were not clustered in a specific region. In contrast, we found a common mutation, V226M, in all five families with Kim variant. Although the previous paper stressed that R300 belongs to a pentad of alternating positively and negatively charged residues (D114, Q284, R300, Q365, and K394) that comprise a network of four salt bridges involved in the catalytic site of CANT1,[7] the missense mutations identified in our study affected none of these residues.

The previous study examined only DD type 1 patients and identified *CANT1* mutations.[7] In this study, we identified *CANT1* mutations in all types of DD, indicating that the clinical–radiographic spectrum of *CANT1* mutations must be extended to include distinct variants of Desbuquois syndrome. The V226M mutation was identified in all patients with DD Kim variant, suggesting that this mutation is necessary for the phenotype. However, because all patients with DD Kim variant in this study were East Asians, it may just reflect that V226M is prevalent among East Asians. Consistent with this hypothesis, the carrier frequency was indeed higher in this population. *CANT1* mutation was not identified in one DD type 2 patient. Furthermore, linkage analysis excluded the possibility that *CANT1* locus is responsible in three inbred DD families without typical hand abnormality (not included in the present study).[6] Those results suggest that there may indeed be genetic heterogeneity in DD type 2. Further accumulation of the knowledge on phenotypes and mutations is required to gain a full picture of the phenotype–genotype association. In particular, diagnostic criteria for DD must now be revised with the knowledge offered by molecular definition. While presence or absence of an additional metacarpal bone has been used to distinguish subtypes of DD, this sign is not a distinctive criterion to predict the molecular basis in DD.

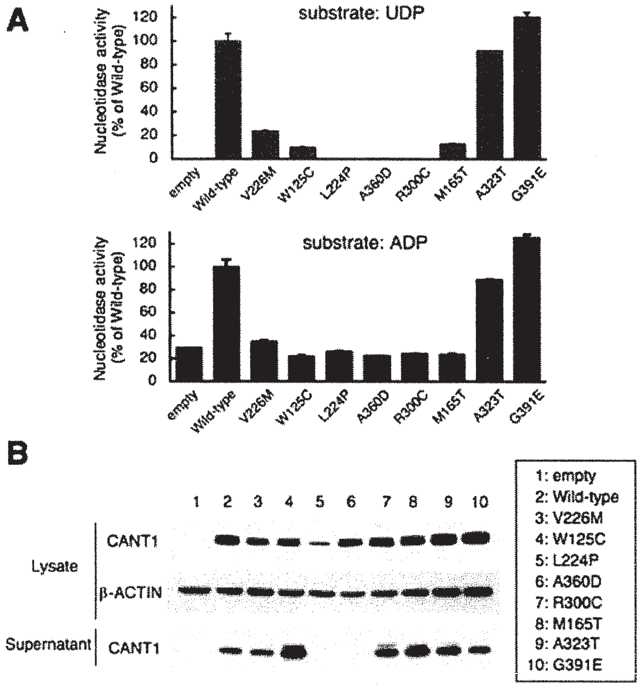

Figure 3 Functional characterisation of CANT1 missense mutations in Desbuquois dysplasia (DD) patients. (A) Nucleotidase activity of CANT1 mutations using uridine diphosphate (UDP) (upper panel) and adenosine diphosphate (ADP) (lower panel) as substrates. COS7 cells were transfected with expression vectors for empty, wild-type and missense mutant CANT1 proteins. The supernatant from the COS7 cells was used to measure the nucleotidase activity. W125C, M165T, L224P, V226M, R300C, A360D: missense mutants identified in DD; A323T, G391E: missense SNPs in the public database. Note that the nucleotidase activities of all DD missense mutants are significantly reduced compared to that of the wild-type protein in both assays. Results are presented as mean±SE (n=4). The same results were obtained from the independent experiments. (B) Western blot analysis for over-expressed CANT1 mutant proteins. Cell lysate and culture supernatant were prepared from COS-7 cells transfected with expression vectors for empty, wild type and missense mutant CANT1 proteins. The membranes with the cell lysates were stripped and re-probed with anti-β-actin antibody as a control. There were no bands for L224P and A360D in the supernatant. The same results were obtained from the independent experiments.

The exact function of CANT1 in humans remains unclear. CANT1 is a member of the apyrase family, which is classified into two groups based on amino acid sequence homology; one is the E-type ATPase family and the other is the family of apyrases cloned from haematophagous arthropods.[10 15 16] CANT1 is classified in the latter group. Apyrases hydrolyse adenosine triphosphate (ATP) and ADP to adenosine monophosphate (AMP). ADP is one of the most important physiological agonists for platelet recruitment, aggregation and plug formation.[17] Haematophagous insects secret apyrases from their salivary gland to hydrolyse ADP, allowing them to feed on the host's blood for an extended time.[18] The endothelial cell plasma membrane apyarase, CD39, an E-type ATPase, has also been implicated in thrombo-regulation.[19] It has been shown that CANT1 has ADPase activity, but relatively low in comparison to its UDPase activity. An alternative hypothesis is that of CANT1 playing a role in making activated sugars available in the ER for synthesis of proteoglycans[7] (see below). In this study, we again showed that CANT1 had ADPase activity and the missense mutants lost this activity (figure 3A). At present, the physiological functions of CANT1 remain to be determined as does the possible role of thrombo-regulation in enchondral ossification and pathogenesis of DD.

Human CANT1 was cloned as a new member of extracellular nucleotidases[8] ; however, mammalian CANT1 proteins have the N-terminus RXR, ER retention/retrial motif and that the over-expressed rat CANT1 preferentially localised to the ER.[9] These findings suggest that CANT1 may exist as membrane bound forms in the ER as well as soluble forms. CANT1 substrates (UDP, GDP, UTP) are involved in several signalling functions including calcium (Ca^{2+}) release, through activation of pyrimidinergic signalling.[20–22] The binding of pyrimidinergic nucleotides (UTP/UDP) to P2Y receptors generates inositol 1,4,5-triphosphate (IP_3) through their coupling to phospholipase C. IP_3 binding to its receptor at the ER surface causes rapid Ca^{2+} release from the ER stores.[21] It has been reported that IP3 receptor dependent Ca^{2+} release from the ER stores is increased during ER stress and plays a critical role in ER stress induced apoptosis.[23] Abnormally distended rough ER containing inclusion bodies was found in the chondrocytes and fibroblasts of DD patients.[7] The abnormality may be related to impaired ER function caused by *CANT1* mutations. The deletion of APY-1, the *Caenrohabditis elegans* homologue of CANT1, sensitised the worms to ER stress and induced defects in pharynx and muscle organisation, leading to a reduced lifespan.[24] Involvement of ER stress response in chondrogenesis and pathology of skeletal dysplasias has been reported.[25 26]

DD shares some phenotypic features with diastrophic dysplasia (OMIM 222600) and recessive Larsen syndrome (OMIM 245600). Both are caused by deficiency of enzymes involved in the metabolism of chondroitin sulfate, an essential component of cartilage matrix. We have previously shown that a functional defect of the solute carrier-35 D1 (SLC35D1) caused a severe skeletal dysplasia in mouse and human.[27 28] SLC35D1 is a nucleotide sugar transporter that transports UDP-N-acetylgalactosamine and UDP-glucronic acid from the cytoplasm into the ER.[29 30] The transported nucleotide sugars are utilised for synthesis of sugar chains of chondroitin sulfate.[27] The resulting UDP is hydrolysed to uridine monophosphate (UMP) by luminal nucleoside diphosphatase, and then UMP is exchanged via the antiporter system for importing further nucleotide sugars.[30] We speculate that CANT1 may work as this luminal nucleoside diphosphatase, thereby being involved in the nucleotide sugar/nucleoside monophosphate antiport system that is essential for cartilage development and functions. CANT1 deficiency might interfere with the availability of nucleotide sugars needed for chondroitin sulfate synthesis.

Key points

- ▶ ***CANT1*** **mutations were identified in seven out of eight Desbuquois dysplasia (DD) families. A total of eight distinct mutations were found; all were hitherto undescribed.**
- ▶ **Mutations were detected in DD type 2 and Kim variant. Thus,** ***CANT1*** **is responsible for more than DD type 1.**
- ▶ **By measuring the CANT1 enzyme activity in vitro, we confirmed that missense mutations resulted in loss of function. Two missense mutations showed abnormal secretion.**
- ▶ **While the presence or absence of an additional metacarpal ossification centre has been used to distinguish subtypes of DD, this sign is not a distinctive criterion to predict the molecular basis in DD.**

Our discovery has extended the phenotypic spectrum of *CANT1* mutations and shown that *CANT1* mutations are responsible not only for DD type 1, but also for type 2 and Kim variant. Further studies are necessary to characterise fully the role of CANT1 in chondrogenesis and identify possible therapeutic targets. On the practical side, mutation analysis of *CANT1* may be warranted in all patients with a diagnostic suspicion of Desbuquois dysplasia, regardless of the specific hand phenotype.

Acknowledgements We are grateful to Dr S Tominaga for her help in this study. We are also grateful to the patients, their family members, and their doctors for participating in the study. This project was supported by grants-in-aids from the Ministry of Education, Culture, Sports and Science of Japan (Contract grant No. 20390408 and No. 21249024), from Research on Child Health and Development (Contract grant No. 20-S-3), from the Ministry of Health, Labour and Welfare of Japan (Measures for Intractable Diseases 046 in 2010), from the Korea Healthcare Technology R&D Project, Ministry for Health, Welfare and Family Affairs, Republic of Korea (No. A080588), from the German Ministry for Education and Research (BMBF contract grant "SKELNET"), from the European Union (FP6, Contract grant "EuroGrow") and from the University of Freiburg. EL and BZ are supported by individual grants from Deutsche Forschungsgemeinschaft (La 1381/1-3). This project was also supported by the European Skeletal Dysplasia Network ESDN (http://www.esdn.org), The University of Freiburg, and the Japanese Skeletal Dysplasia Consortium (http://www.riken.jp/lab-www/OA-team/JSDC/).

Competing interests None declared.

Patient consent Obtained.

Ethics approval This study was conducted with the approval of the Ethics Committee of RIKEN.

Provenance and peer review Not commissioned; externally peer reviewed.

REFERENCES

1. **Superti-Furga A,** Unger S. Nosology and classification of genetic skeletal disorders: 2006 revision. *Am J Med Genet A* 2007;**143**:1–18.
2. **Desbuquois G,** Grenier B, Michel J, Rossignol C. Nanisme chondrodystrophique avec ossification anarchique et polymalformations chez deux soeurs. *Arch Fr Pediatr* 1966;**23**:573–87.
3. **Huber C,** Oules B, Bertoli M, Chami M, Fradin M, Alanay Y, Al-Gazali LI, Ausems MGEM, Bitoun P, Cavalcanti DP, Krebs A, Le Merrer M, Mortier G, Shafeghati Y, Superti-Furga A, Robertson SP, Le Goff C, Muda AO, Paterlini-Brechot P, Munnich A, Cormier-Daire V. Identification of *CANT1* mutations in Desbuquois dysplasia. *Am J Hum Genet* 2009;**85**:706–10.
4. **Faivre L,** Cormier-Daire V, Eliott AM, Field F, Munnich A, Maroteaux P, Le Merrer M, Lachman R. Desbuquois dysplasia, a reevaluation with abnormal and "normal" hands: radiographic manifestations. *Am J Med Genet A* 2004;**124**:48–53.
5. **Kim OH,** Nishimura G, Song HR, Matsui Y, Sakazume S, Yamada M, Narumi Y, Alanay Y, Unger S, Cho TJ, Park SS, Ikegawa S, Meinecke P, Superti-Furga A. A variant of Desbuquois dysplasia characterized by advanced carpal bone age, short metacarpals, and elongated phalanges: report of seven cases. *Am J Med Genet A* 2010;**152**:875–85.
6. **Faivre L,** Le Merrer M, Al-Gazali LI, Ausems MGEM, Bitoun P, Bacq D, Maroteaux P, Munnich A, Cormier-Daire V. Homozygosity mapping of a Desbuquois dysplasia locus to chromosome 17q25.3. *J Med Genet* 2003;**40**:282–4.
7. **Faivre L,** Le Merrer M, Zerres K, Ben Hariz M, Scheffer D, Young ID, Maroteaux P, Munnich A, Cormier-Daire V. Clinical and genetic heterogeneity in Desbuquois dysplasia. *Am J Med Genet A* 2004;**128**:29–32.
8. **Smith TM,** Hicks-Berger CA, Kim S, Kirley TL. Cloning, expression, and characterization of a soluble calcium-activated nucleotidase, a human enzyme belonging to a new family of extracellular nucleotidases. *Arch Biochem Biophys* 2002;**406**:105–15.
9. **Failer BU,** Braun N, Zimmermann H. Cloning, expression, and functional characterization of a Ca^{2+}-dependent endoplasmic reticulum nucleoside diphosphatase. *J Bio Chem* 2002;**40**:36978–86.
10. **Smith TM,** Kirley TL. The calcium activated nucleotidases: a diverse family of soluble and membrane associated nucleotide hydrolyzing enzymes. *Purinergic Signal* 2006;**2**:327–33.
11. **Baynam G,** Kiraly-Borri C, Goldblatt J, Dickinson JE, Jevon GP, Overkov A. A recurrence of a hydrop lethal skeletal dysplasia showing similarity to Desbuquois dysplasia and a proposed new sign: the Upsilon sign. *Am J Med Genet A* 2010;**152**:966–9.
12. **Traverso-cori A,** Chaimovich H, Cori O. Kinetic studies and properties of potato apyrase. *Arch Biochem Biophys* 1965;**109**:173–84.
13. **Maeda K,** Miyamoto Y, Sawai H, Karniski LP, Nakashima E, Nishimura G, Ikegawa S. A compound heterozygote harboring novel and recurrent *DTDST* mutations with intermediate phenotype between atelosteogenesis type II and diastrophic dysplasia. *Am J Med Genet A* 2006;**140**:1143–7.
14. **Yang M,** Kirley TL. Site-directed mutagenesis of human soluble calcium-activated nucleotidase 1 (hSCAN-1): identification of residues essential for enzyme activity and the Ca^{2+}-induced conformational change. *Biochemistry* 2004;**43**:9185–94.
15. **Plesner L.** Ecto-ATPases: identification and functions. *Int Rev Cytol* 1995;**158**:141–214.
16. **Valenzuela JG,** Charlab R, Galperin MY, Ribeiro JM. Purification, cloning, and expression of an apyrase from the bed bug cimex lectularis. A new type of nucleotide-bindind enzyme. *J Biol Chem* 1998;**273**:30583–90.
17. **Benoit P,** Dogne JM. Platelet ADP-receptors and their antagonists. *Mini Rev Med Chem* 2003;**3**:145–8.
18. **Ribeiro JM,** Francischetti IM. Role of arthropod saliva in blood feeding: sialome and post-sialome perspectives. *Annu Rev Entomol* 2003;**48**:73–88.
19. **Marcus AJ,** Broekman MJ, Drosopoulos JH, Islam N, Alyonycheva TN, Safier LB, Hajjar KA, Posnett DN, Schoenborn MA, Schooley KA, Gayle RB, Maliszewski CR. The endothelial cell ecto-ADPase responsible for inhibition of platelet function is CD39. *J Clin Invest* 1997;**99**:1351–60.
20. **Abbracchio MP,** Burnstock G, Boeynaems JM, Barnard EA, Boyer JL, Kennedy C, Knight GE, Fumagalli M, Gachet C, Jacobson KA, Weisman GA. International Union of Pharmacology LVIII: update on the P2Y G protein-coupled nucleotide receptors: from molecular mechanisms and pathophysiology to therapy. *Pharmacol Rev* 2006;**58**:281–341.
21. **Clapham DE.** Calcium signaling. *Cell* 2007;**131**:1047–58.
22. **Lecca D,** Ceruti S. Uracil nucleotides: from metabolic intermediates to neuroprotection and neuroinflammation. *Biochem Pharmacol* 2008;**75**:1869–81.
23. **Li G,** Mongillo M, Chin KT, Harding H, Ron D, Marks AR, Tabas I. Role of ERO1-alpha-mediated stimulation of inositol 1,4,5-triphosphate receptor activity in endoplasmic reticulum stress-induced apoptosis. *J Cell Biol* 2009;**186**:783–92.
24. **Uccelletti D,** Pascoli A, Farina F, Alberti A, Mancini P, Hirschberg CB, Palleschi C. APY-1, a novel Caenorhabditis elegans apyrase involved in unfolded protein response signalling and stress responses. *Mol Biol Cell* 2008;**19**:1337–45.
25. **Saito A,** Hino S, Murakami T, Kanemoto S, Kondo S, Saitoh M, Nishimura R, Yoneda T, Furuichi T, Ikegawa S, Ikawa M, Okabe M, Imaizumi K. Regulation of endoplasmic reticulum stress response by a BBF2H7-mediated Sec23a pathway is essential for chondrogenesis. *Nat Cell Biol* 2009;**11**:1197–204.
26. **Rajpar MH,** McDermott B, Kung L, Eardley R, Knowles L, Heeran M, Thornton DJ, Wilson R, Bateman JF, Poulsom R, Arvan P, Kadler KE, Briggs MD, Boot-Handford RP. Targeted induction of endoplasmic reticulum stress induces cartilage pathology. *PLoS Genet* 2009;**5**:e1000691.
27. **Hiraoka S,** Furuichi T, Nishimura G, Shibata S, Yanagishita M, Rimoin DL, Superti-Furga A, Nikkels PG, Ogawa M, Katsuyama K, Toyoda H, Kinoshita-Toyoda A, Ishida N, Isono K, Sanai Y, Cohn DH, Koseki H, Ikegawa S. Nucleotide-sugar transporter SLC35D1 is critical to chondroitin sulfate synthesis in cartilage and skeletal development in mouse and human. *Nat Med* 2007;**13**:1363–7.
28. **Furuichi T,** Kayserili H, Hiraoka S, Nishimura G, Ohashi H, Aslanger AD, Koseki H, Cohn DH, Superti-Furga A, Unger S, Ikegawa S. Identification of loss-of-function mutations of *SLC35D1* in patients with Schneckenbecken dysplasia, but not with other severe spondylodysplastic dysplasias group diseases. *J Med Genet* 2009;**46**:562–8.
29. **Muraoka M,** Kawakita M, Ishida N. Molecular characterization of human UDP-glucuronic acid/UDP-N-acetylgalactosamine transporter, a novel nucleotide sugar transporter with dual substrate specificity. *FEBS Lett* 2001;**495**:87–93.
30. **Ishida N,** Kawakita M. Molecular physiology and pathology of the nucleotide sugar transporter family (SLC35). *Pflugers Arch* 2004;**447**:768–75.